The role of the second messenger cyclic di-GMP in *Bacillus subtilis*

DISSERTATION

zur Erlangung des Doktorgrades
der Naturwissenschaften
(Dr. rer. nat.)

dem
Fachbereich Chemie
der Philipps-Universität Marburg
vorgelegt von

Patricia Bedrunka, M. Sc.
geboren in Kłodzko, Polen

Marburg an der Lahn,
Juni 2017

Vom Fachbereich Chemie der Philipps-Universität Marburg (Hochschulkennziffer 1180) als Dissertation am _____. _____. _____ angenommen.

Erstgutachter:	Prof. Dr. Peter L. Graumann Fachbereich Chemie, Philipps-Universität Marburg
Zweitgutachter:	Dr. Gert Bange Fachbereich Chemie, Philipps-Universität Marburg
Tag der Disputation:	14.08.2017

Die Untersuchungen zur vorliegenden Dissertation wurden in der Zeit vom Januar 2013 bis Januar 2017 unter der Leitung von Herrn Prof. Dr. Peter L. Graumann an der Philipps-Universität Marburg (LOEWE Zentrum für synthetische Mikrobiologie, SYNMIKRO) durchgeführt.

EIDESSTATTLICHE ERKLÄRUNG

(gemäß § 10, Abs. 1 der Promotionsordnung der Mathematisch-Naturwissenschaftlichen Fachbereiche und des Medizinischen Fachbereichs für seine mathematisch-naturwissenschaftlichen Fächer der Philipps-Universität Marburg vom 15.07.2009)

Ich versichere, dass ich meine vorgelegte Dissertation:

"The role of the second messenger cyclic di-GMP in *Bacillus subtilis*"

selbst und ohne fremde Hilfe verfasst, nicht andere als die in ihr angegebenen Quellen oder Hilfsmittel benutzt, alle vollständig oder sinngemäß übernommenen Zitate als solche gekennzeichnet sowie die Dissertation in der vorliegenden oder einer ähnlichen Form noch bei keiner anderen in- oder ausländischen Hochschule anlässlich eines Promotionsversuches oder zu anderen Prüfungszwecken eingereicht habe.

Ort, Datum Patricia Bedrunka

SUMMARY

The bacterial second messenger c-di-GMP represents an integral key regulator in the control of bacterial motility and biofilm formation. In this context, an increase in intracellular c-di-GMP production correlates with a sessile lifestyle, whereas low c-di-GMP levels favor planktonic cell behavior. Intracellular c-di-GMP levels are controlled by the antagonistic activity of c-di-GMP specific synthetases (diguanylate cyclases, DGCs) and hydrolases (phosphodiesterases, PDEs). Bacteria contain diverse c-di-GMP binding receptors/effectors, which exert the regulatory functions of this signaling molecule.

A given bacterial genome typically encodes several paralogous copies of DGCs and PDEs. This lead to the question of how cells cope with such a multiplicity of signaling components and guarantee that specificity within certain signaling modules is mediated. Two general models for signal specificity through functional sequestration are currently discussed: the so-called *local* and *global pool* signaling hypotheses. Spatially sequestering the signal (pool) in multi-protein complexes at distinct cellular site may result in highly specific signaling pathways. Temporal and/ or conditional separation through differential expression and activation of DGCs/ PDEs/ output systems respectively, could have a distinct impact on the global c-di-GMP pool.

This work investigates the role of c-di-GMP and its players in the Gram-positive model organism *B. subtilis*, which possesses a relatively small c-di-GMP signaling equipment. In particular, the obtained findings define a novel c-di-GMP signaling pathway regulating the production of an unknown exopolysaccharide (EPS) and furthermore imply that local and global signaling pools potentially operate in *B. subtilis* to regulate motility and exopolysaccharide production.

The proposed c-di-GMP receptor YdaK resides in the putative EPS synthesis operon *ydaJKLMN*. Artificial YdaJ-N induction results in strongly altered colony biofilms, increased Congo Red staining and provokes furthermore cell clumping, which provides indirect evidence of EPS production. The putative EPS synthase components YdaM/ YdaN and YdaK co-localize to clusters predominantly at the cell poles and are statically positioned at this subcellular site, suggesting that exopolysaccharide production takes place at distinct sites of the membrane. The potential glycosyl hydrolase YdaJ is not essential for the generation of the above-described

phenotypes, whereas the presence of YdaK is required, implying an involvement of the second messenger c-di-GMP.

To approach the potential regulation of exopolysaccharide production through c-di-GMP via YdaK, different combinations of overexpression and deletion mutants of the operon and of *dgc* genes, respectively, were generated. Importantly, the presence of *dgcK* was shown to be indispensable for the production of the unknown EPS, thereby revealing a new function for one of the three known DGC enzymes. DgcK and YdaK partially co-localize to the same subcellular positions at the cell membrane implying close proximity of these players, which strongly suggests that YdaK receives its activation signal directly from the spatially close DgcK in agreement with the *local pool* hypothesis.

The cytoplasmic DgcP synthetase can complement for DgcK only upon overproduction, while the third c-di-GMP synthetase, DgcW, seems not to be part of the signaling pathway. Removal of the regulatory EAL domain from DgcW reveals a distinct function in biofilm formation. Therefore, our study is compatible with the *local pool signaling* hypothesis, but shows that in case of the *yda* operon, this can easily be overcome by overproduction of non-cognate DGCs, indicating that global pools can also confer signals to this regulatory circuit. Furthermore, indications are provided within this study that all three DGCs might cooperate in inhibition of motility via the c-di-GMP receptor DgrA indicating that DgrA depends on globally elevated c-di-GMP levels.

ZUSAMMENFASSUNG

Der bakterielle sekundäre Botenstoff c-di-GMP repräsentiert einen integralen Schlüsselregler in der Kontrolle der bakteriellen Motilität und der Biofilmbildung. In diesem Zusammenhang korreliert eine Zunahme der intrazellulären c-di-GMP-Produktion mit einer sessilen Lebensweise, während niedrige c-di-GMP-Spiegel planktonisches Zellverhalten begünstigen. Die intrazelluläre c-di-GMP-Menge wird durch die antagonistische Aktivität von c-di-GMP-spezifischen Synthetasen (Diguanylatzyklasen, DGCs) und Hydrolasen (Phosphodiesterasen, PDEs) gesteuert. Bakterien besitzen verschiedene c-di-GMP-Bindungsrezeptoren/ Effektoren, welche die regulatorischen Funktionen dieses Signalmoleküls ausüben.

Ein gegebenes bakterielles Genom kodiert typischerweise mehrere paralogische Kopien von DGCs und PDEs. Dies führt zu der Frage, wie Zellen mit einer solchen Vielzahl von Signalkomponenten zurechtkommen und garantieren, dass Spezifität innerhalb bestimmter Signalmodule vermittelt wird. Zwei allgemeine Modelle für die Signalspezifität durch funktionelle Sequestrierung werden derzeit diskutiert: die sogenannten lokalen und globalen Pool-Signal-Hypothesen. Die räumliche Sequestrierung des Signals (Pool) in Multi-Protein-Komplexe an einer bestimmten zellulären Stelle kann zu hochspezifischen Signalwegen führen. Die zeitliche und/ oder konditionale Trennung durch differentielle Expression und Aktivierung von DGCs/PDEs/ Output-Systemen könnte einen deutlicheren Einfluss auf den globalen c-di-GMP-Pool haben.

Die vorliegende Arbeit untersucht die Rolle von c-di-GMP und seinen Spielern im Gram-positiven Modellorganismus *B. subtilis*, welcher eine relativ kleine c-di-GMP-Signalausrüstung aufweist. Insbesondere definieren die erhaltenen Erkenntnisse einen neuen c-di-GMP-Signalweg, der die Produktion eines unbekannten Exopolysaccharids (EPSs) reguliert. Darüber hinaus implizieren die erhaltenen Ergebnisse, dass lokale und globale Signalpools potentiell in *B. subtilis* operieren, um Motilität und EPS-Produktion zu regulieren.

Der vorgeschlagene c-di-GMP-Rezeptor YdaK ist in dem putativen EPS-Operon *ydaJKLMN* kodiert. Eine künstliche YdaJ-N Induktion führt zu stark veränderten Kolonie-Biofilmen, einer erhöhten Kongo-Rot-Färbung und provoziert darüber hinaus Zellverklumpungen. Diese Beobachtungen liefern indirekte Beweise für die Produktion eines EPSs. Die mutmaßlichen EPS-Synthasekomponenten YdaM/ YdaN und YdaK co-lokalisieren vorwiegend an den Zellpolen als Cluster und sind an diesen subzellulären Stellen statisch

positioniert. Dies deutet darauf hin, dass die EPS-Produktion an bestimmten Positionen der Membran stattfindet. Die potentielle Glykosylhydrolase YdaJ ist für die Erzeugung der oben beschriebenen Phänotypen nicht essentiell, während die Anwesenheit von YdaK erforderlich ist, was auf eine Beteiligung des sekundären Botenstoffs c-di-GMP hindeutet.

Um die potenzielle Regulierung der EPS-Produktion durch c-di-GMP über YdaK zu untersuchen, wurden unterschiedliche Kombinationen von Überexpressions- und Deletionsmutanten des Operons bzw. von *dgc* Genen erzeugt. Wichtig ist, dass die Anwesenheit von *dgcK* für die Herstellung des unbekannten EPSs unentbehrlich war und damit eine neue Funktion für eines der drei bekannten DGC-Enzyme enthüllt wurde. DgcK und YdaK co-lokalisieren partiell an den gleichen subzellulären Positionen der Zellmembran. Dies impliziert eine direkte Nähe der Spieler und deutet in Übereinstimmung mit der lokalen Poolhypothese darauf hin, dass YdaK sein Aktivierungssignal direkt von der räumlich nahen DgcK erhält.

Die zytoplasmatische DgcP-Synthetase kann DgcK durch Überproduktion komplementieren, während die dritte c-di-GMP-Synthetase, DgcW, nicht Teil des Signalweges zu sein scheint. Eine Entfernung der regulatorischen EAL-Domäne von DgcW zeigt eine andere Funktion im Bezug auf Biofilmbildung auf. Daher ist diese Studie kompatibel mit der lokalen Pool-Signal-Hypothese, zeigt aber, dass im Falle des Yda-Operons dies leicht durch Überproduktion von nicht-verwandten DGCs überwunden werden kann, sodass globale Pools vermutlich auch Signale an diese regulatorische Schaltung vermitteln können. Darüber hinaus werden in dieser Studie Hinweise vorgelegt, dass alle drei DGCs an der Hemmung der Motilität über den c-di-GMP-Rezeptor DgrA beteiligt sein könnten, was darauf hinweist, dass DgrA von global erhöhten c-di-GMP Konzentrationen abhängt.

CONTENTS

TABLE OF FIGURES

INTRODUCTION

ARTICLES

ARTICLE I

ARTICLE II

UNPUBLISHED RESULTS

DISCUSSION

1 INTRODUCTION

1.1 Biofilms

"The number of these animalcules in the scurf of a man's teeth are so many that I believe they exceed the number of men in a kingdom."

Antoni van Leeuwenhoek, 1684

In the late 17th century, the famous microscopy and microbiology pioneer Antoni van Leeuwenhoek (1632-1723) described a vast accumulation of organisms (*animalcules*) in his dental plaque in a report to the Royal Society of London (Dobell, 1960). Today, we know van Leeuwenhoek was referring to a phenomenon called the formation of microbial biofilms (BFs; Høiby, 2014). Biofilms are multicellular microbial communities found to be associated to almost every existing natural and artificial surface or interface. The highly differentiated community members are embedded in an extracellular matrix (ECM) of their own synthesis, which enables the generation of spatially organized three-dimensional (3-D) structures (Costerton *et al.*, 1987; 1995). Within these tissue-like structures, the ECM is generally composed of exopolysaccharide (EPS), proteins and nucleic acids. ECM components play a major role in ensuring the mechanical integrity of the community, while simultaneously reserving nutrients and offering physical protection against environmental cues (Branda *et al.*, 2005, Flemming & Wingender, 2010). The increased fitness of BF-associated organisms suggests that the collective association of microbes likely represents their prevailing lifestyle whereas the planktonic mode is rather regarded as a transient life period during translocation from one habitat to another in order to occupy a new ecological niche or location for example (Watnick & Kolter, 2000, Davey & O´Toole, 2000).

Particularly BF-associated bacteria can exhibit a profoundly different physiology than an equivalent free-floating population revealing increased resistance to antibiotics, tolerance to various exogenous stress conditions and the host immune response (Anderson & O´ Toole, 2008; Høiby *et al.*, 2010; McKew *et al.*, 2011). It is estimated that bacterial BFs are responsible for 65-80 % of human infections and therefore cause major problems in the public health systems worldwide (Sauer *et al.*, 2007; Joo & Otto, 2012). Due to their clinical relevance, studies of

bacterial BFs have initially mainly focused on Gram-negative, pathogenic bacteria resulting in the establishment of model systems for bacterial BF formation. For example, the opportunistic pathogen *Pseudomonas aeruginosa* is amongst the best-studied bacteria with respect to BF formation, and is primarily known for its ability to colonize and infect lungs of patients who suffer from cystic fibrosis (Vlamakis *et al.*, 2013; Monds & O´ Toole, 2009). Despite being critical in medical settings and industrial biofouling, BF formation can also be beneficial in terms of plant growth promotion and waste water treatment for instance (Morikawa, 2006; Farra *et al.*, 2014).

1.1.1 BFs in the laboratory

On account of their high complexity in natural settings, research on bacterial BF formation widely focuses on experimental model systems investigating single-species communities grown under simplified and reproducible conditions (Mielich-Süss & Lopez, 2014). Several different strategies have been developed allowing the artificial generation and observation of BFs in the laboratory (**Fig. 1.1**). The majority of genetic studies traditionally investigates static BF growth at air-liquid interfaces, known as pellicles, or on solid agar surfaces establishing macroscopically complex architectures, often referred to as macro-colony BFs (**Fig. 1.1**; Haussler & Fuqua, 2013; Limoli *et al.*, 2015; Franklin *et al.*, 2015).

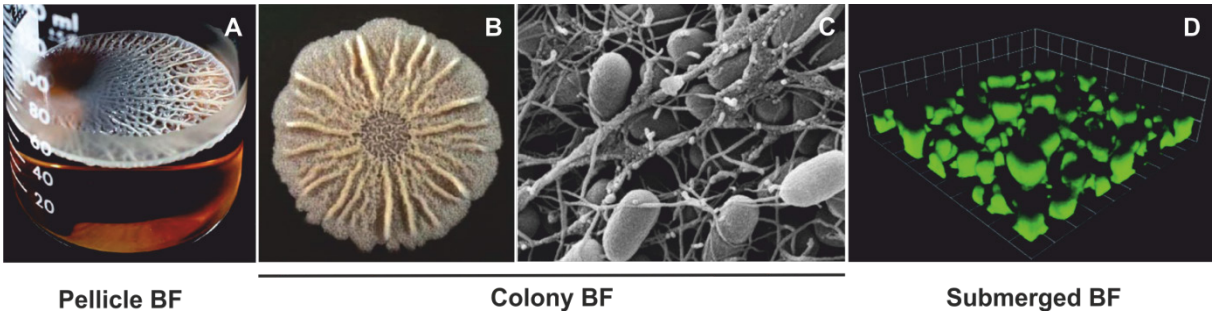

Fig. 1.1. Laboratory approaches to study bacterial BF formation
(**A**) Statically cultured *Bacillus subtilis* at an air-liquid interface forms pellicles. Image adapted from Branda *et al.*, 2001. (**B**) Example of a colony BF formed by *B. subtilis* on solid BF promoting medium (López *et al.*, 2010). (**C**) High-resolution SEM image of an *Escherichia coli* macro-colony cross-section revealing a mixture of cellulose sheets and flagella interconnecting individual cells. Micrograph adapted from Serra *et al.*, 2013. (**D**) CSLM analysis of submerged communities generated by fluorescently labelled *P. aeruginosa* cells. Micrograph adapted from Banin *et al.*, 2005.

The morphology of bacterial macro-colony BFs can vary fundamentally especially in terms of shape and texture among different species and even among different isolates of the same species (Mielich-Süss & Lopez, 2014; Richter *et al.*, 2014). For many decades and especially in the early days of microbiology, bacterial colonies have been a practical object to classify and characterize bacteria and their BF development (Kaufmann & Schaible, 2005; Branda *et al.*, 2005). Emerging from the interplay between environmental signals and diverse genetic circuits, expanding macro-colony BFs may display different topological structures including the formation of *concentric rings*, *radially oriented ridges* and *elaborated wrinkles* as observed in *Escherichia coli* (Serra *et al.*, 2013). The formation of these so-called *wrinkled*, *rugose* or *rdar* (for red, dry and rough) morphotypes depends to a great extent on the synthesis of ECM component and a variety of different studies could demonstrate a clear correlation between the ability to produce those and the level of morphological complexity (Haussler & Fuqua, 2013; Anwar *et al.*, 2014; Zhang *et al.*, 2016). Despite visual inspections of whole macro-colonies using different ECM dyes such as Congo Red and Calcofluor (Solano *et al.*, 2002; Friedmann & Kolter, 2003), the micro-anatomy of those bacterial BFs can be further visualized at the cellular level by scanning electron microscopy (SEM) or by confocal scanning laser microscopy (CSLM) of cross-sections (compare **Fig. 1.1**).

Another form of laboratory BFs is represented by surface-attached communities on submerged solid surfaces of microtiter plates or of microfluidic cell advices (Franklin *et al.*, 2015; Branda *et al.*, 2005). The use of flow cell systems coupled with analysis through CSLM allows the formation of BFs under highly controlled conditions and enables a non-invasive observation of their maturation. Submerged BFs have been intensively used to study the spatial and temporal aggregation behavior of bacteria. These results allowed the creation of the below described model of bacterial BF formation (see **Fig. 1.2**).

BF formation is widely assumed as a developmental process resulting from a temporal sequence of highly coordinated stages. The broad developmental phases, encompassing attachment to a surface, BF maturation and BF dispersal, appear to be conserved among a wide range of bacteria although molecular mechanisms governing BF formation can differ greatly between different species (Sauer *et al.*, 2007; Stoodley *et al.*, 2002; Kaplan, 2010). During the process of BF maturation, bacteria undergo various cellular differentiation processes (**Fig. 1.2**). The main developmental step is the transition from a single motile stage to a sessile multicellular phase representing the initiation of BF formation (attachment). Upon BF-favoring conditions such as nutrient availability, individual motile cells localize and initially attach reversibly to a carrier surface. Following an irreversible binding to the surface, attached cells subsequently proliferate and aggregate into micro-colonies through the concomitant secretion of ECM components. The following step includes the further growth of micro-colonies into 3-D

structures (maturation phase). In the final stage of BF development, single motile cells detach from the BF and disperse into the environment. BF dispersal represents an essential step of the developmental cycle contributing mainly to bacterial survival and potential disease transmission (Kaplan, 2010).

In the following, this study will focus on macro-colony BFs established by mono-species populations of the soil-dwelling bacterium *Bacillus subtilis*, which has emerged as an alternative model organism for BF formation of rhizobacteria.

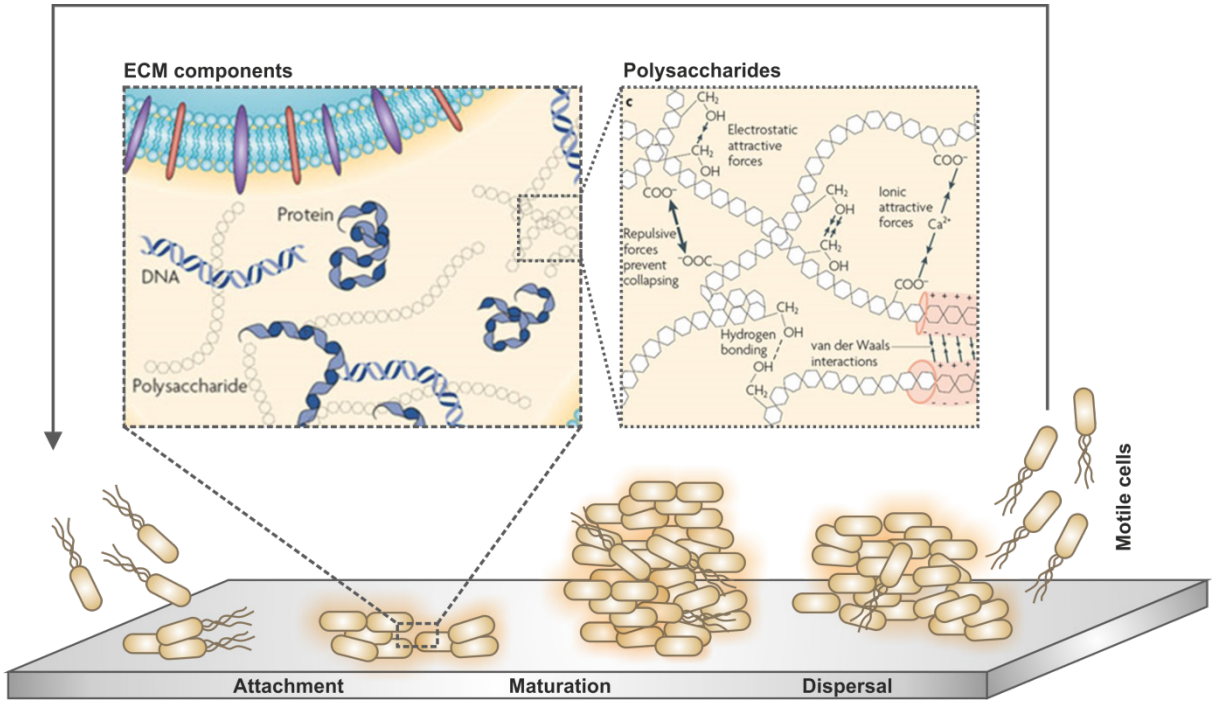

Fig. 1.2. Schematic representation of bacterial BF development and ECM components
Submerged BF formation on a solid surface comprises three major stages. The first stage involves initial and irreversible attachment representing the early development of BF formation, followed by the second stage: maturation of BF architecture. This stage is characterized by the production of extracellular polymers, mainly of polysaccharides, proteins and DNA that are heterogeneously distributed and entangled between single cells (upper panels, adapted from Flemming & Wingender, 2010). ECM components (polysaccharides) associate by weak physicochemical interactions including hydrogen bonds, van der Waals forces and electrostatic interactions thereby ensuring ECM stability. BF dispersal represents the final stage, where cells are released from the community to colonize new areas. Figure adapted and modified after Stoodley *et al.*, 2002 and Suchanek, 2016.

1.2 BF formation in *Bacillus subtilis*

Like many natural environments, soil is a heterogeneous and nutrient-poor habitat where microbial growth parameters such as carbon availability, fluctuate greatly (Williams, 1985; Paul & Clark, 1989). Therefore, soil-living bacteria are usually confronted with lack of nutrients (Davey & O´ Toole, 2000). The rhizosphere, a term describing the plant-root surface and the immediate surrounding area of roots (Hiltner, 1904; York *et al.*, 2016), constitutes an important ecological niche for microorganisms, where nutrients are more readily available as a consequence of rhizodeposition (Dennis *et al.*, 2010). Plant root exudations comprise a huge diversity of organic compounds such as sugars and amino acids, originating from diverse sources such as sloughed-off cells for instance. Availability of these compounds within the rhizosphere enables microbial proliferation and the formation of structured microbial BFs, which are in turn beneficial for the plants. Plant-associated bacteria like *Bacillus* spp. for example, are becoming increasingly important in agricultural settings serving as natural alternatives to chemical pesticides due to their ability to stimulate plant growth and to suppress pathogenic bacteria and fungi (Vlamakis *et al.*, 2013).

The rod-shaped *B. subtilis* is a non-pathogenic, Gram-positive model organism belonging to the phylum of firmicutes. It has been intensively studied particularly in terms of bacterial chromosome replication and cell differentiation processes from the dawn of microbiology. Already in 1877, Ferdinand Cohn (1828-1898) has described the characteristic features of *B. subtilis* including spore development, the transition between single and filamentous cells and its ability to form pellicles in static cultures (McLoon *et al.*, 2011). At the beginning of the 21st century, Branda and others (2001) have recognized the ability of the undomesticated *B. subtilis* strain NCIB3610 to produce apart from pellicles, *thick* and *structurally complicated* colony BFs, on semi-solid agar medium which promotes the expression of genes required for ECM production (compare **Fig. 1.1**). In the same year, it has been also demonstrated that domesticated *B. subtilis* (strain JH642) can form submerged BFs on abiotic surfaces (Hamon & Lazazzera, 2001). Due to their practicable handling, further studies concerning *B. subtilis* BF formation mainly focused on pellicle and colony BFs as experimental model systems, although an increasing number of studies started to investigate *in situ* plant root colonization or to use of flow cell advices (Allard-Massicotte *et al.*, 2016; Humphries *et al.*, 2017). In all experimental systems, formation of *B. subtilis* BFs requires the differentiation of an isogenic progenitor population into subpopulations of functionally distinct, coexisting cell types and the production ECM components, which are shared with the entire community (Cairns *et al.*, 2014). The complexity of BF morphology can vary to a high extend and depends on the experimental settings, but much more importantly: the

individual *B. subtilis* strain (Mielich-Süss & Lopez, 2014 McLoon *et al.*, 2011). Laboratory strains such as *B. subtilis* PY79 and 168 for example form fragile and unstructured pellicle and colony communities respectively as a consequence of domestication.

1.2.1 ECM components in *B. subtilis* BFs

The establishment of all types of robust *B. subtilis* BFs substantially depends on the secretion of ECM components, but their composition can vary greatly among different isolates. Undomesticated *B. subtilis* strains produce ECM components, which exhibit a wide range of sizes (MWs range: 0.6 to 128 kDa) and chemical properties (Marvasi *et al.*, 2010; Omoike & Chorover, 2004).

The major ECM component secreted by undomesticated *B. subtilis* NCIB3610 is a chemically poorly characterized exopolysaccharide, which is synthesized by the products of the fifteen gene long *epsA-O* operon whose expression is ensured by a mechanism termed processive riboantitermination (Irnov & Winkler, 2010; Artsimovitch, 2010). Mutations of most of the genes within this cluster result in defective BFs lacking the characteristic complex morphologies (Roux *et al.*, 2015). So far, the specific function of the corresponding gene products has not been studied in detail, with a few exceptions. EpsB and EpsA establish a putative tyrosine kinase/ modulator couple and are both required for BF formation (Gerwig *et al.*, 2014; Elsholz *et al.*, 2014), but little is known concerning the identity of phosphorylated downstream targets (Gerwig & Stülke, 2014; Cairns *et al.*, 2014). The best-characterized protein encoded by the *epsA-O* operon, EpsE, exhibits a dual function in EPS synthesis as a glycosyltransferase and in motility inhibition as a proposed flagellar clutch (Guttenplan *et al.*, 2010). EpsE is thought to ensure motility block when exopolysaccharide production is initiated through a direct interaction with the flagellar motor switch protein FliG thereby prohibiting the generation of torgue. Within the *epsA-O* cluster, the *epsHIJK* locus has been proposed to encode proteins able to synthesize the conserved bacterial exopolysaccharide poly-*N*-acetylglucosamine that may function as a scaffold and anchoring substrate for polysaccharides produced by other *epsA-O* encoded proteins (Roux *et al.*, 2015). The exact molecular composition of the polysaccharide synthesized by this complex machinery is however still unknown and requires further systematic investigations especially because its nature apparently depends on substrate availability (Cairns *et al.*, 2014; Roux *et al.*, 2015).

In addition to the EPS produced by the gene products of *epsA-O*, various *B. subtilis* strains are able to synthesize Levan, a prominent structural extracellular polymeric substance consisting of β-(2–6) linked D-fructose molecules with branching β-(2–1) units (Marvasi *et al.*, 2010; Benigar

et al., 2014). Its synthesis occurs extracellularly by the action of secreted (SacB) levansucrase using sucrose as a substrate (Shimotsu & Henner, 1986; Méndez-Lorenzo *et al.*, 2015). Although this EPS is not essential for BF formation *in vitro*, it can partially compensate for the absence of the *epsA-O* cluster and may contribute to BF development of *B. subtilis* in nature (Dogsa *et al.*, 2013). Besides the two structural ECM components described above, some wild type isolates including *B. subtilis* B-1 and *B. subtilis* (natto) synthesize the extracellular substance poly-*γ*-glutamic acid (PGA). PGA is an anionic, viscous polymer, which might play a role in the sorption of ions and/or charged molecules (Candela & Fouet, 2006; Marvasi *et al.*, 2010). However, PGA synthesized by the gene products of *pgsBCA* in *B. subtilis* is not required for colony- or pellicle BF establishment (Branda *et al.*, 2006).

In addition to structural EPS, *B. subtilis* BFs contain various extracellular protein components. The synthesis of amyloid-like fiber structures accomplished by proteins encoded within the *tapA-sipW-tasA* operon is essential for *B. subtilis* BF formation in some, but not in all experimental set ups (Hamon *et al.*, 2004; Branda *et al.*, 2004, 2006; Romero *et al.*, 2010). Amyloids consist of fibers and are characterized by a quaternary structure in which parallel sheets are enriched and arranged perpendicular to the axis of the fiber exhibiting great robustness and stability (Fowler *et al.*, 2007; Romero & Kolter, 2014). The amyloid-like fibers of *B. subtilis* are mainly composed of TasA proteins, whereas TapA is required to anchor those to the cell surface and SipW is involved in processing and proper secretion of both components (Stöver & Driks, 1999; Chai *et al.*, 2013). Deletions of respective genes in the operon lead to a reduced formation of robust and rugose colony BFs, suggesting that TasA reconstitutes a connection network for cells embedded in the ECM and may furthermore contribute to the formation of *aerial structures* (*fruiting bodies*) harboring sporulating cells (Stöver & Driks, 1999; Romero *et al.*, 2010), but the precise role of TasA is still unknown.

The proper development of structured *B. subtilis* BFs depends furthermore on the secretion of the hydophobin BslA, which functions synergistically with both TasA and the BF essential EPS described above. BslA is a small amphiphilic protein with a hydrophobic cap that is able to form an organized protein layer at the surface of the community thereby not only providing liquid repellency but also allowing the assembly of amyloid-like fibers and EPS (Ostrowski *et al.*, 2011; Kobayashi & Iwano, 2012; Hobley *et al.*, 2013).

1.2.2 Pellicle and colony BF development of *B. subtilis*

In standing liquid cultures, the process of pellicle BF formation starts with the migration of single cells to the air-liquid interface with the contribution of flagellum-based motility, chemotaxis and oxygen sensing (Hölscher *et al.*, 2015). Planktonic cells switch to the sessile state through the downregulation of flagellar gene expression while simultaneously upregulating genes required for ECM production. In general, this switch can be driven by different external cues such as low oxygen levels (Kolodkin-Gal *et al.*, 2013) and surface adherence (Cairns *et al.*, 2013). Sessile cells begin to proliferate at the air-liquid interphase as non-motile cell chains (Branda *et al.*, 2001). Through the repression of cell wall hydrolases (autolysins) and secretion of ECM components, cell filaments arrange and adhere to each other in a parallel manner. These bundles evolve to a complex reticular structure as the pellicle grows including the formation of aerial substructures serving as preferential sporulation sites (compare **Fig. 1.3A**; Branda *et al.*, 2001; Kobayashi, 2007; Vlamakis *et al.*, 2013).

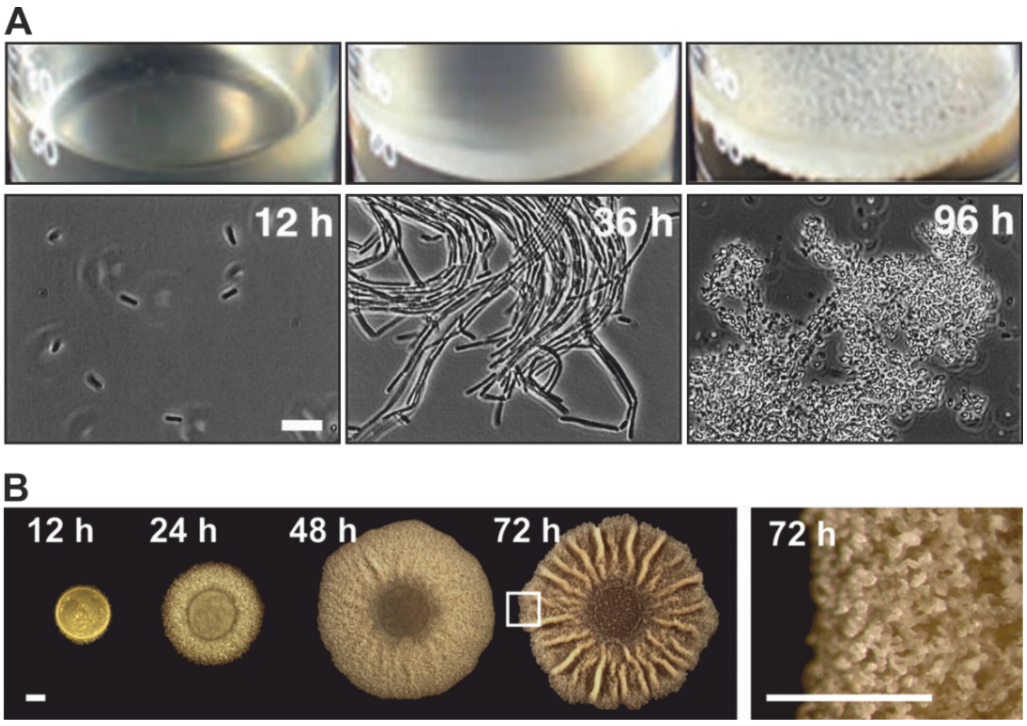

Fig. 1.3. Pellicle and colony development of undomesticated *B. subtilis* NCIB3610
(**A**) Photographs of *B. subtilis* NCIB3610 pellicle formation (upper panel) and phase contrast micrographs (lower panel) of corresponding cell types present at the depicted time points. Bar: 5 µm. Images adapted from Branda *et al.*, 2001 and Lemon *et al.*, 2008. (**B**) Top view of colony BF development. The magnified panel depicts aerial structures harboring sporulating cells. Bars: 1 mm. Adapted from Vlamakis *et al.*, 2008.

Colony BFs of *B. subtilis* exhibit similar cell differentiation and spatial organization patterns as pellicle BFs, yet little is known about the initial developmental stages of colony establishment. A recent study though, has followed colony development of domesticated *B. subtilis* PY79 from a single progenitor cell demonstrating that the early stages of colony development exhibit characteristic morphological patterns (Mamou *et al.*, 2016). This includes the formation of leading cell chains, which are preferentially arranged in a Y-shape and derive from the colony center. These so-called Y-arms extend in multiple directions serving as guiding cells for the determination of the future colony size and architecture. Cells in the center further divide and propagate in bundles possibly with the help of nanotubes (Dubey *et al.*, 2016) leading to central thickening and colony expansion until the boarders defined by the leader cells are reached. Whether undomesticated *B. subtilis* strains also occupy a territory via leader cells prior to an extensive central growing phase potentially coordinated by nanotubes, needs to be further elucidated.

When cultures of *B. subtilis* NCIB3610 are applied on a BF-promoting medium surface, motile cells subsequently proliferate and start to produce ECM components. Continued growth and cell differentiation processes lead to horizontal BF expansion and maturation (see **Fig. 1.3B**). This includes the development of branching wrinkles originating from the inoculation area across the surface within a few days of incubation. Wrinkles form as a consequence of localized cell death patterns and exopolysaccharide production (Asally *et al.*, 2012). Cell death locally reduces the thickness of the BF and in combination with community expansion and the production of ECM components, which physically restrict cells, mechanical (compressive) forces are spatially focused (see **Fig. 1.4A**; Asally *et al.*, 2012; Persat *et al.*, 2015). This contributes to vertical buckling of the colony structure and consequently to initiation of wrinkle formation offering the community several advantages. Wrinkles generate a network of channels exhibiting high permeability to liquid flow thereby facilitating nutrient availability and circulation especially for cells in the center which are deprived of nutrients (Wilking *et al.*, 2013). Additionally, wrinkled morphology of colony BFs increases their surface-to-volume ratio which is thought to serve as an adaptation process providing increased accessibility to oxygen (Dietrich *et al.*, 2013; Kolodkin-Gal *et al.*, 2013).

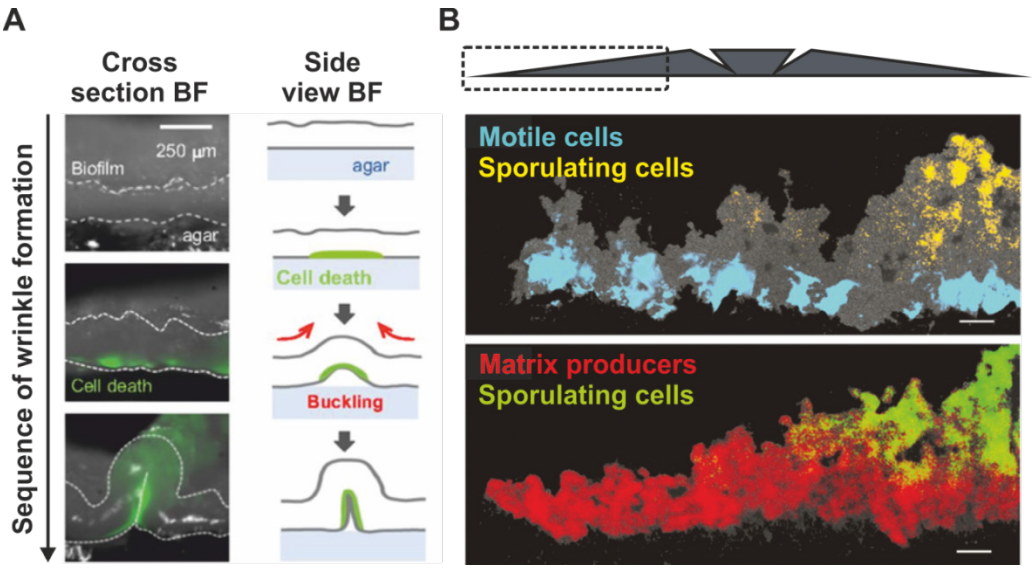

Fig. 1.4. Colony development: wrinkle formation and differentiation into distinct cell types

(**A**) Wrinkle formation correlates with areas of localized cell death and results in the generation of fluid channels by matrix buckling. Left panel: fluorescence microscopy of cross-sections in which dead cells appear green (Sytox® Green nucleic acid stain). Right panel: schematic representation. Figure adapted from Asally *et al.*, 2012. (**B**) Fluorescence microscopy of macro-colony (48 h) thin-sections revealing distinct distributions of different cell types. The corresponding colonies originate from cultures harboring a dual reporter system. Bars: 50 µm. Figure adapted and modified from Vlamakis *et al.*, 2008.

1.2.3 Regulatory networks governing cell differentiation processes during BF formation in *B. subtilis*

Following the activation of different genetic programs, cells encased in a mature BF differentiate into subpopulations exhibiting distinct spatiotemporal distribution patterns (**Fig. 1.4B**; Vlamakis *et al.*, 2008). Early in BF formation, the colony community mainly consists of motile cells, which are located at the BF surface. Upon BF maturation a portion of this subpopulation moves to the bottom layer and borders of the colony whereas the majority of cells differentiates into ECM producers and expands throughout the entire colony. In the late stages of colony BF formation, matrix producers are mainly positioned at the edges of the colony and a new subpopulation of sporulating cells arises primarily from former matrix producing subpopulations. The regulatory network governing the control of cell differentiation within the community encompasses three key transcriptional regulators: Spo0A, DegU and ComA. Their activation is mediated through

phosphorylation by specific sets of histidine kinases (Kovács, 2016). Each regulator controls a specific subset of genes thereby determining the differentiation pathway into a specific cell fate (Lopez & Kolter, 2010). Cell motility is guaranteed when these regulators are in the non-phosphorylated state (Lopez & Kolter, 2010). In the presence of different environmental cues, activation of these key players occurs and results in a decrease of the motile population and favored differentiation into other cell types. The following differentiation programs are not mutually exclusive to any specialized cell-type or subpopulation, but rather overlap in contrast to planktonic cells, which are only present when none of the programs is active (Mielich-Süss & Lopez, 2014).

The master regulator Spo0A controls the expression of about 120 genes (Molle *et al.*, 2003) and is activated by phosphorylation of a single aspartate residue via a multicomponent phosphor-relay including five different sensor kinases (KinA-E) and the phosphor-transferring proteins Spo0F and Spo0B (Burbulys *et al.*, 1991; Fabret *et al.*, 1999). The level of phosphorylated Spo0A (Spo0A~P) in the cell is subject to different regulatory mechanisms that are governed by networks consisting of the above mentioned kinases and diverse phosphatases, which respond to environmental and physiological signals (Ohlsen *et al.*, 1994; Perego *et al.*, 1996). Gradual increase in the intracellular concentration of Spo0A~P facilitates the expression of distinct developmental gene sets thereby defining if a cell differentiates into an ECM producer and/ or enters the sporulation pathway for example (Grau *et al.*, 2015). In response to low activation of Spo0A~P (intermediate levels) involving i.e. the kinases KinC and KinD, cells differentiate into ECM producers whereas spore development is induced at high concentrations mainly due to the activation of KinA and KinB (Kovács, 2016). The activity of KinD, proposed to represent the major kinase involved in BF formation (McLoon *et al.*, 2011), has been shown to be triggered by glycerol and manganese (Shemesh & Chai, 2013) and by increasing osmotic pressure for example (Rubinstein *et al.*, 2012).

Following activation of Spo0A, Spo0A~P regulates directly or indirectly two parallel pathways of antirepression (**Fig. 1.5**). In motile cells AbrB and SinR are active transcription repressors of the *epsA-O* and *tapA-sipW-tasA* operons as well as of *bslA* (indirect) thereby preventing matrix gene expression and thus BF formation. In order to switch from the planktonic to the sessile state, the action of these repressors needs to be antagonized. At certain threshold levels, Spo0A~P triggers the production of two anti-repressors: AbbA and SinI. Interaction between the respective repressor and its corresponding antirepressor (AbrA/ AbbA and SinR/ SinI respectively) leads to repressor inactivation and consequently derepression of matrix gene expression is facilitated (Cairns *et al.*, 2014).

The formation of the SinI-SinR protein-protein complex inactivates SinR and allows furthermore the expression of a second SinR-antagonist called SlrR, whose encoding gene itself is under the negative control of SinR (Chu *et al.*, 2008). The derepression of *slrR* through inactivation of SinR, results in high SlrR levels that acts subsequently in two ways on SinR. SlrR and SinR form a tight complex thereby rendering the ability of SinR to repress *slrR* and matrix gene expression. Additionally SlrR re-purposes SinR activity upon high SlrR levels as the SinR-SlrR hetero-dimer represses motility and autolysin genes (Norman *et al.*, 2013; Newman *et al.*, 2013). In this case SinR functions as a co-repressor for SlrR thereby controlling the switch between the motile and sessile lifestyle (Chai *et al.*, 2010).

Similarly to Spo0A, also the level of the pleiotropic regulator DegU~P dictates which cell-type manifest within a developing BF (Dahl *et al.*, 1991; Cairns *et al.*, 2014; Marlow *et al.*, 2014; Kovács, 2016). The histidine kinase DegS and the aspartate response regulator DegU constitute a two component system controlling swimming and swarming motility, genetic competence (Dubnau *et al.*, 1994), exoprotease production (Marlow *et a*l., 2014), production of PGA (Stanley & Lazazzera, 2005) and indirectly also the production of the hydrophobin BslA (Verhamme *et al.*, 2007; Murray *et al.*, 2009; Cairns *et al.*, 2014).

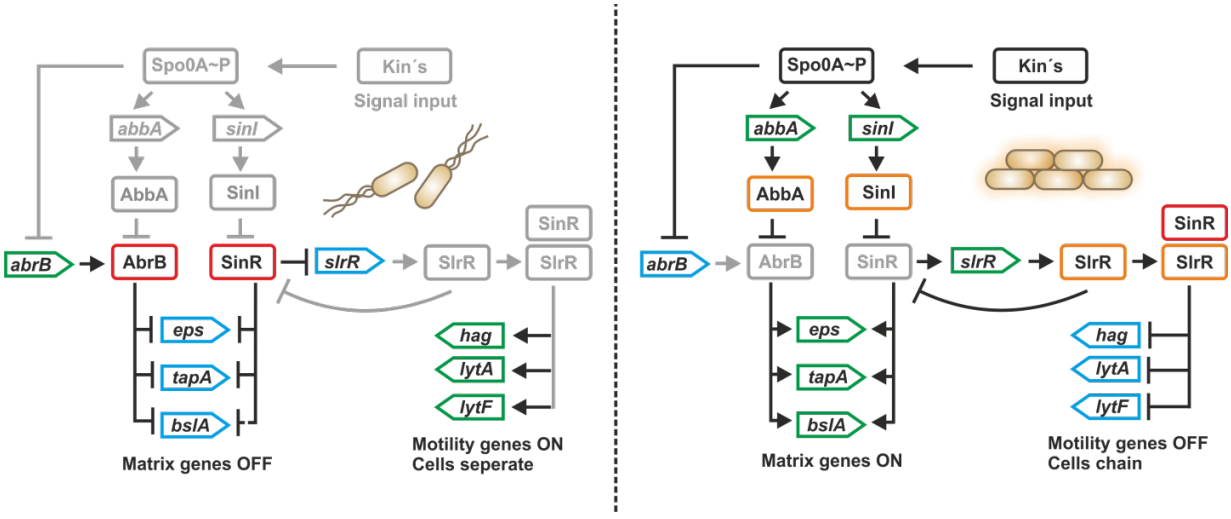

Fig. 1.5. Regulatory circuits governing the motile to sessile switch in *B. subtilis*
Scheme of selected regulatory pathways controlling gene expression during (**A**) planktonic and (**B**) sessile growth. Rectangles indicate proteins and pentagons single genes and gene clusters respectively. Repression mechanisms are indicated by T-bars, activation by arrows. Active gene expression is depicted in green and blue represents absence of gene transcription. Transcriptional repressors are depicted in red and their corresponding anti-repressors in orange. Grey colored pathways are inactive. For a detailed description see chapter **1.2.3**. Figure adapted and modified after: Cairns *et al.*, 2014.

1. 3 Signal transduction via cyclic nucleotides

Signal transduction via cyclic nucleotide-based second messengers represents a key element in all three domains of life. In these systems intra- and extracellular signals (*first messengers*) are perceived by specific receptors, which do not directly interact with downstream regulators, but instead affect the intracellular concentration of specific diffusible molecules. These so-called *second messengers* ultimately amplify and convert the perceived signal into a cellular response through an interaction with different cellular targets including proteins and RNA molecules (Lodish *et al.*, 2000).

Since the discovery of the two important eukaryotic second messengers cyclic adenosine 3',5'-monophosphate (cAMP, Rall & Sutherland, 1958; Sutherland & Rall, 1958) and cyclic guanosine 3',5'-monophosphate (cGMP, Ashman *et al.*, 1963), mediating for instance the effect of hormones and light to regulate vasodilatory effects and vision respectively (Beavo & Brunton, 2002), research on cyclic nucleotide-based second messengers has expanded drastically. Almost at the same time, the presence of cAMP in prokaryotes was confirmed revealing its todays best-known target CRP (cAMP receptor protein or catabolite repressor protein), a transcriptional regulator that permits the utilization of alternative sugars (Makman & Sutherland, 1965, Ullmann & Monod, 1968). This second messenger regulates various other processes such as motility and virulence in bacteria and the corresponding synthesizing enzymes, adenylate cyclases (AC), are even more diverse than their eukaryotic orthologs building up five structurally distinct classes (Bahzu & Danchin, 1994; Linder & Schultz, 2003), although some organisms do not contain ACs, such as *Bacillus subtilis*.

Newly upcoming nucleotide-based second messengers such as c-di-AMP (Luo & Helmann, 2012; Corrigan & Gründling, 2013), c-AMP-GMP (Davies *et al.*, 2012; Nelson *et al.*, 2015) and c-GMP-AMP (Civril *et al.*, 2013) lead to the questions of how cells cope with such a multiplicity of signaling pathways via diverse second messengers and guarantee that specificity within these systems is mediated. One answer to this contains likely a combination of various different spatio-temporal regulatory circuits sensing different external signals and acting on distinct transcriptional, translational and posttranslational levels. Currently, several studies are lifting the lid on the selectivity and control exerted by cAMP in eukaryots (reviewed in Cooper & Tabbasum, 2014). Its synthesizing enzymes ACs appear to be the center of highly organized and dynamic micro-domains. Spatial proximity of second messenger metabolizing proteins, effectors and targets may be also essential for bacterial second messenger signaling cascades, in particular for highly complex nucleotide signaling networks as suggested for the c-di-GMP pathways in various bacterial species (Kulasakara *et al.*, 2006; Hengge, 2009; Dahlstrom *et al.*, 2015, 2016).

1.3.1 The second messenger c-di-GMP

Bis-(3',5')-cyclic dimeric guanosine monophosphate (c-di-GMP) was originally identified as an allosteric activator molecule of the cellulose synthase in *Gluconacetobacter xylinus* (Ross *et al.* 1987) and in *Agrobacterium tumefaciens* (Amikam & Benziman, 1989). Over the years, the ubiquitous occurrence of this second messenger in members of all major bacterial phyla has been recognized and its regulatory function in bacterial processes including especially BF formation, motility, virulence and cell cycle progression could be demonstrated particularly in Gram-negative bacteria like *E. coli* (Weber *et al.*, 2006, Boehm *et al.*, 2009) *P. aeruginosa* (Kulasakara *et al.*, 2006; Lee *et al.*, 2007), *Vibrio cholerae* (Tischler & Camilli, 2004) and *Caulobacter crescentus* (Lori *et al.*, 2015). Generally, low levels of c-di-GMP are thought to favor motility and single cell behavior whereas increased concentrations of c-di-GMP are associated with surface attachment and BF formation (Simm *et al.*, 2004; reviewed in Hengge, 2009; Römling *et al.*, 2013; Jenal *et al.*, 2017).

Intracellular levels of c-di-GMP are modulated in response to internal and environmental cues which is achieved through the coordinated activity of two antagonistic enzyme families (**Fig. 1.6**). C-di-GMP is synthesized by diguanylate cyclases (DGCs) harboring a conserved GGDEF domain, from two molecules GTP and is degraded by specific phosphodiesterases (PDEs) containing either a conserved EAL or HD-GYP domain. These domains are named after their amino acid active site motifs that have been demonstrated to be conserved and essential for the corresponding catalytic action (Ausmees *et al.* 2001; Simm *et al.*, 2004). The majority of GGDEF and EAL domains are associated with a variety of different N-terminal sensory domains, including most commonly PAS (PER/ARNT/SIM), GAF (c**G**MP-specific phosphodi-esterases, **a**denylyl cyclases and **F**hlA) and REC (CheY-homologous receiver domain) domains that are able to affect the activation/ inactivation of the corresponding downstream domain, thereby connecting extra- and intracellular signals to c-di-GMP synthesis or degradation (Galperin *et al.*, 2001, Galperin, 2004, Römling *et al.*, 2013).

The synthesis of c-di-GMP requires the cooperative action of two GGDEF domains. These are arranged in an antiparallel manner where each monomer binds one GTP molecule to form an active site at the dimer interface resulting in the formation of two intermolecular phosphodiester linkages and pyrophosphate release (Wassmann *et al.*, 2007; De *et al.*, 2009; Schirmer, 2016). The formation of homodimers can be facilitated in a signal-dependent manner through amino-terminal accessory domains such as REC domains, which dimerize following phosphorylation (Paul *et al.*, 2007). Another mechanism, which affects GGDEF domain activity, involves allosteric product inhibition through a four-residue motif called autoinhibitory I-site. I-sites are formed by the arginine and aspartic acids of the conserved 'RxxD' motif located

upstream of the active site motif [GG(D/E)EF] and both separated by a five amino acid linker. Binding of c-di-GMP to the I-site prevents overconsumption of the substrate, non-physiological accumulation of this second messenger and potentially maintains c-di-GMP in defined concentration areas (Christen *et al.*, 2006; Dahlstrom *et al.*, 2016).

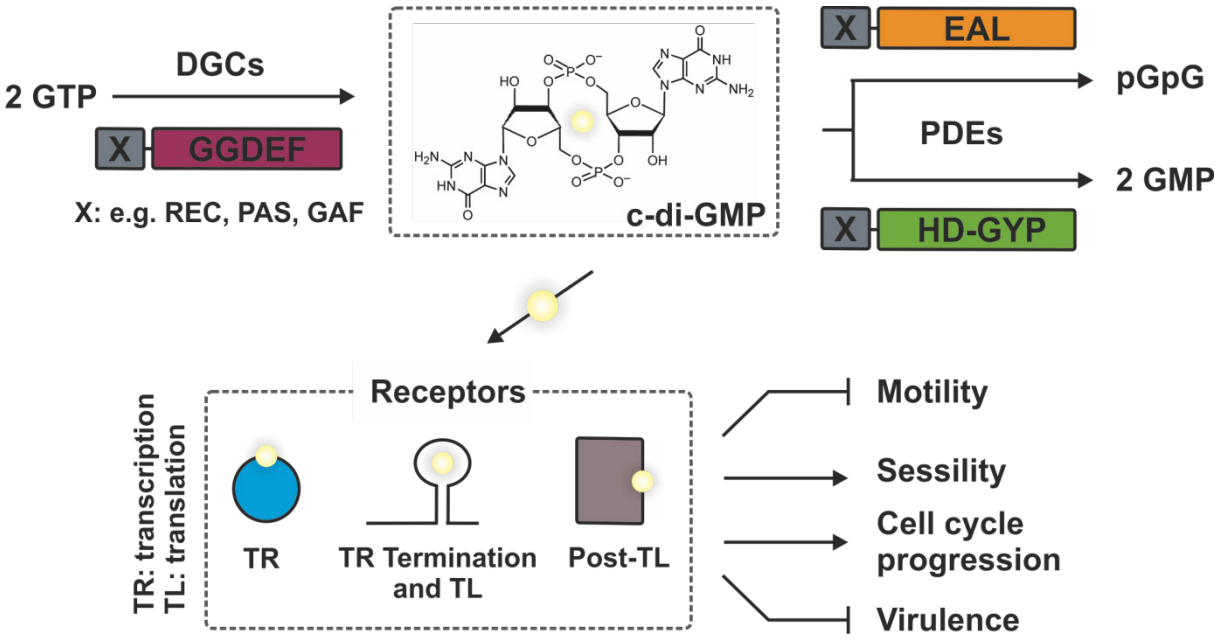

Fig. 1.6. Model of c-di-GMP signaling
C-di-GMP is synthesized and hydrolyzed by diguanylate cyclases (DGCs) and phosphodiesterases (PDEs) respectively. "X" indicates putative sensory domains. C-di-GMP exerts its control on diverse bacterial processes through binding to different kinds of receptors including proteins and riboswitches. Figure adapted and modified after Krasteva *et al.*, 2012 and Conner *et al.*, 2017.

Breakdown of c-di-GMP is mediated by two types of c-di-GMP specific PDEs (see also above). EAL-type PDEs also operate as dimers and catalyze the opening of the cyclic nucleotide through hydrolysis of one phosphodiester bond giving rise to the linear dinucleotide 5′-phosphoguanylyl-(3′,5′)-guanosine (pGpG), a nanoRNA molecule whose degradation to two molecules of GMP by oligoribonucleases is required for the termination of c-di-GMP signaling in *P. aeruginosa* (Orr *et al.*, 2015) and which has been proposed to be capable of exerting control on gene expression (Goldman *et al.*, 2011, Römling *et al.*, 2013). In contrast to EAL-domain PDEs, the unrelated HD-GYP PDEs are less abundant and are capable of complete c-di-GMP hydrolysis into GMP in a one-step reaction (Bellini *et al.*, 2014).

Genomic analysis of bacterial genomes revealed that GGDEF domains are frequently combined with one of their antagonizing domains (EAL- and HD-GYP domains) in the same polypeptide chain (Römling *et al.*, 2013). In these scenarios both domains can be enzymatically active, but differentially regulated by distinct extra- and/- or intracellular signals resulting in a prevalent activity (synthesis or hydrolysis of c-di-GMP) of these multi-domain proteins (Tarutina *et al.*, 2006; Hull *et al.*, 2012). Besides bifunctional enzymes, the majority of GGDEF-EAL or GGDEF-HD-GYP tandem domain proteins harbor at least one inactive domain. In this case, the inactive domain, mostly characterized by degenerated active site motifs, has acquired a regulatory function including substrate binding but not processing or an involvement in protein-protein or protein-RNA interactions for example (Christen *et al.*, 2005; Navarro *et al.*, 2009; Römling *et al.*, 2013).

1.3.2 C-di-GMP effectors

In order to transduce environmental and/- or intracellular signals into a cellular response, c-di-GMP binds to a range of effectors such as protein and RNA, involved in a variety of cellular functions. At the mechanistic level, c-di-GMP allosterically regulates the activity of enzymes and proteins. Moreover, it regulates gene expression either through the modulation of transcription factors or by direct interaction with riboswitches (Valentini and Filloux, 2016).

Using bioinformatics approaches the widely distributed PilZ domain [consensus $RxxxRx_{20\text{-}30}$ (D/N) x (S/A) xxG] was identified as the first c-di-GMP receptor type (Amikam & Galperin, 2006, Pratt *et al.*, 2007; Shin *et al.*, 2011). These domains frequently exist as stand-alone domain proteins and are by far the most prevalent c-di-GMP binding proteins (Römling *et al.*, 2013). It is widely hypothesized that free-standing PilZ domains primarily function as adaptors by binding their interaction partner in a c-di-GMP dependent manner (Habazettl *et al.*, 2011; Xu *et al.*, 2016). PilZ domains combined with N-terminal so-called YcgR-N domains are able to negatively regulate bacterial motility via the interaction with flagella components upon c-di-GMP binding such as YcgR from *E. coli* and *S. enterica* (Ryjenkov *et al.*, 2006; Paul *et al.*, 2010; Boehm *et al.*, 2010) and DgrA from *C. crescentus* and *B. subtilis* (Christen *et al.*, 2007; Chen *et al.*, 2012; Gao *et al.*, 2013). Additionally, PilZ domains are associated to regulatory or enzymatic domains among them also type 2 glycosyltransferases as BcsA (Ross *et al.*, 1991), which is post-translationally and allosterically activated by its c-di-GMP-bound PilZ domain to enable cellulose synthesis in *G. xylinus* (Ross *et al.* 1987) and *R. sphaeroides* (Morgan *et al.*, 2013).

Besides PilZ proteins, transcription factors such as FleQ (Hickman *et al.*, 2008; Baraquet *et al.*, 2012) and BldD (Tschowri *et al.*, 2014) and c-di-GMP responsive riboswitches (Sudarsan *et al.*, 2008; Kulshina *et al.*, 2009; Bordeleau *et al.*, 2015), enzymatically inactive (degenerated) GGDEF and EAL domains have been reported to constitute another major classes of c-di-GMP effectors. These domains have lost their enzymatic activity to synthesize or hydrolyze c-di-GMP, but maintained the ability to bind the second messenger and to act as c-di-GMP output effectors (Newell *et al.*, 2009; Ozaki *et al.*, 2014).

1.3.3 Biosynthesis of prokaryotic EPSs and regulatory mechanisms via c-di-GMP

The assembly and export strategies of bacterial EPS synthesis are currently categorized into three distinct biosynthetic mechanisms: the Wzx/Wzy-dependent pathway, the ATP-binding cassette (ABC)-transporter dependent system, and the so called synthase-dependent pathway (reviewed in Schmid *et al.*, 2015). Another strategy is represented by EPS that are extracellularly synthesized through the activity of cell-surface linked glycosyltransferases. Wzx/ Wzy-dependent and ABC-transporter dependent systems both use cytosolic sugar nucleotides as activated precursors and lipid acceptors/ carriers at the cytoplasmic face of the membrane on which the initial polysaccharide chain is assembled. In Wzx/Wzy-dependent systems individual repeat units are synthesized and transported across the membrane via Wzx (flippase), following polymerization by the polymerase Wzy in the periplasm (Marczak *et al.*, 2013; Baker *et al.*, 2015). Contrarily, in ABC-transporter dependent systems, synthesis of the entire polysaccharide is terminated in the cytoplasm prior to export (Willis and Whitfield, 2013). Synthase-dependent pathways are characterized by the presence of a membrane-embedded glycosyltransferase with dual function: simultaneous synthesis/ polymerization and export of the polymer (Hubbard *et al.*, 2012; Whitney and Howell, 2013). Especially synthase-dependent and Wzx/Wzy-dependent EPS machineries have been reported to be widely controlled by c-di-GMP (Pérez-Mendoza & Sanjuán, 2016) and the underlying transcriptional and post-translational control mechanisms have been intensively studied in model organisms such as *E. coli* and *P. aeruginosa* for example.

In *P. aeruginosa* three major c-di-GMP output effectors including FleQ, PelD and Alg44 are involved in the regulation of different EPS synthesizing machineries (Wolska *et al.*, 2016). The AAA+ ATPase FleQ is a transcriptional regulator, which does not harbor a PilZ domain in contrast to Alg44, but its ATPase activity is subjected to competitive inhibition by c-di-GMP at high concentrations (Arora *et al.*, 1997; Matsuyama *et al.*, 2016). FleQ is the master activator of

flagellar gene expression at low intracellular c-di-GMP levels and acts as a repressor of the EPS operons *pslA-L* and *pelA-G* under these conditions (Baraquet *et al.*, 2012). This repression is relieved upon high c-di-GMP levels (Baraquet & Harwood, 2013). The Pseudomonas *pelA-G* operon is not only regulated at the transcriptional level via c-di-GMP but also post-translationally, which is mediated by the operon encoded TM protein PelD (Liang, 2015). PelD displays besides four TMH, a cytosolic GAF and non-enzymatic GGDEF domain (Whitney *et al.*, 2012). The positively charged so-called Pel EPS is composed of partially deacetylated N-acetylgalactosamine and N-acetylglucosamine molecules (Jennings *et al.*, 2015). Its synthesis depends highly on the conserved allosteric I-site motif within the degenerated GGDEF domain of PelD that has been demonstrated to bind dimeric self-intercalating c-di-GMP with low affinity (K_D = 1-2 μM; Whitney *et al.*, 2012).

Similarly, the firmicute *Listeria monocytogenes* contains a machinery that is post-translationally regulated by an enzymatically inactive GGDEF TM-protein that functions as a c-di-GMP receptor (PssE). The polysaccharide consists of a β-1,4-linked N-acetylmannosamine chain decorated with terminal α-1,6-linked galactose molecules and is synthesized by the products of the *pssA-E* gene cluster (Köseoglu *et al.*, 2015). The GGDEF domain of PssE binds c-di-GMP (K_D ~ 0.8 μM) presumably via its conserved I-site motif (Chen *et al.*, 2014). Activation of EPS synthesis is thought to be governed through a c-di-GMP mediated interaction between PssE and the putative glycosyltransferase PssC. Furthermore, it has been hypothesized that PssE may utilize local c-di-GMP pools generated by two spatially associated membrane DGCs (Köseoglu *et al.*, 2015).

PssE, PelD, the glycosyltransferase BcsA and the membrane-anchored PilZ domain protein Alg44 belong to a group of c-di-GMP receptors that are able to regulate EPS synthesis post-translationally through an activation of their corresponding associated glycosyl transferases although applying presumably different activation mechanisms (Whitney *et al.*, 2012; Moradali *et al.*, 2015; 2017). Alg44 acts as a co-polymerase for the alginate synthesizing subunit Alg8. Alginates are linear EPSs consisting of variable amounts of β-1,4-linked β-D-mannuronic acid and of its epimer α-L-guluronic acid. Both Alg44 and Alg8 constitute the alginate polymerase, which is activated through c-di-GMP binding to the PilZ domain of Alg44 (Maharaj 1993; Remminghorst & Rehm 2006; Moradari *et al.*, 2017).

The genome of *P. aeruginosa* encodes for 33 GGDEF domain proteins, but only a small subset has been demonstrated to influence the production of the above-described EPS. For example, the alginate biosynthesis machinery is activated by the membrane protein MucR which constitutes a hybrid GGDEF/EAL domain protein (Hay *et al.*, 2009; Li *et al.*, 2013), but also by the GGDEF-domain protein SadC (Schmidt *et al.*, 2016). C-di-GMP production by these

enzymes is presumably triggered by different environmental signals resulting in the generation of localized c-di-GMP concentrations through direct interaction or close vicinity of the corresponding DGCs with their downstream c-di-GMP receptor Alg44 (Wang *et al.*, 2015). Likewise, Pel biosynthesis is hypothesized to be controlled by local c-di-GMP pools produced by the DGCs WspR, RoeA, YfiN and SadC (Liang, 2015).

1.4 C-di-GMP signaling in *B. subtilis*

B. subtilis (compare to: **1.2**) possesses a functional c-di-GMP signaling system, which is known to participate in motility control (Chen *et al.*, 2012; Gao *et al.*, 2013). In contrast to *B. thuringiensis*, where c-di-GMP synthesis has been demonstrated to be essential for BF formation including the master DGC CdgF (Fagerlund *et al.*, 2016), *B. subtilis* can form robust colony and pellicle BFs independently of c-di-GMP signaling components under standard laboratory conditions (Chen *et al.*, 2012; Gao *et al.*, 2013). *B. subtilis* harbors a concise set of c-di-GMP metabolizing enzymes consisting of three active DGCs (DgcK/ YhcK, DgcP/ YtrP and DgcW/ YkoW) and one major PDE (PdeH/ YuxH).

Additionally, three c-di-GMP effector/ receptor proteins have been proposed including the YcgR-paralog DgrA (YpfA), the degenerated GGDEF domain protein YdaK and the inactive EAL domain protein YkuI (**Fig. 1.7**).

The physiological concentrations of c-di-GMP in this organism during different growth conditions have not been explored in detail yet. So far, two independent studies have investigated the intracellular pools of c-di-GMP in *B. subtilis*. Gao *et al.*, (2013) were unable to detect the second messenger during vegetative growth in standard rich medium (limit of detection: 50 pg/ µl). In contrast, analysis performed by Diethmaier *et al.*, (2014) revealed a concentration of approximately 35 ng c-di-GMP per mg of protein using sporulation medium suggesting that c-di-GMP levels rise at the onset of stationary phase as reported for other bacterial species such as *E. coli* (Sommerfeldt *et al.*, 2009). This idea is further supported by the following findings. The -35 and -10 promoter regions of the PDE gene *pdeH* harbor the respective consensus sequences of σ^A-dependent promoters indicating that *pdeH* is constitutively transcribed during vegetative growth as σ^A is the primary housekeeping σ-factor in *B. subtilis* (Weinrauch *et al.*, 1989; Chen *et al.*, 2012; Johnston *et al.*, 2009). By this means, c-di-GMP levels are presumably kept low during vegetative growth due to the c-di-GMP degrading activity of PdeH, which has been proven (Gao *et al.*, 2013). Most notably, *pdeH* expression declines in the course of sporulation (Nicolas *et al.*, 2012) and is under the negative control of the master regulator Spo0A~P (Molle *et al.*, 2003;

Fuijta *et al.*, 2005), further linking c-di-GMP signaling towards stationary phase and BF formation and/ or sporulation (Chen *et al.*, 2012; Purcell & Tamayo, 2016). In contrast to several known PDEs, PdeH harbors no signaling-sensing domain which would allow for post-translational regulation of PDE activity. Hence, it was postulated that PdeH is mainly regulated at the level of gene expression (Chen *et al.*, 2012), which furthermore indicates a global role of PdeH in this signaling system. Noteworthy, PdeH harbors an N-terminal EAL domain and additionally a C-terminally located HD-domain, predicted to have a metal-dependent phosphohydrolase activity (Aravind and Koonin, 1998). It remains to be clarified whether the EAL domain is solely responsible for c-di-GMP degradation or whether both domains are required for the breakdown.

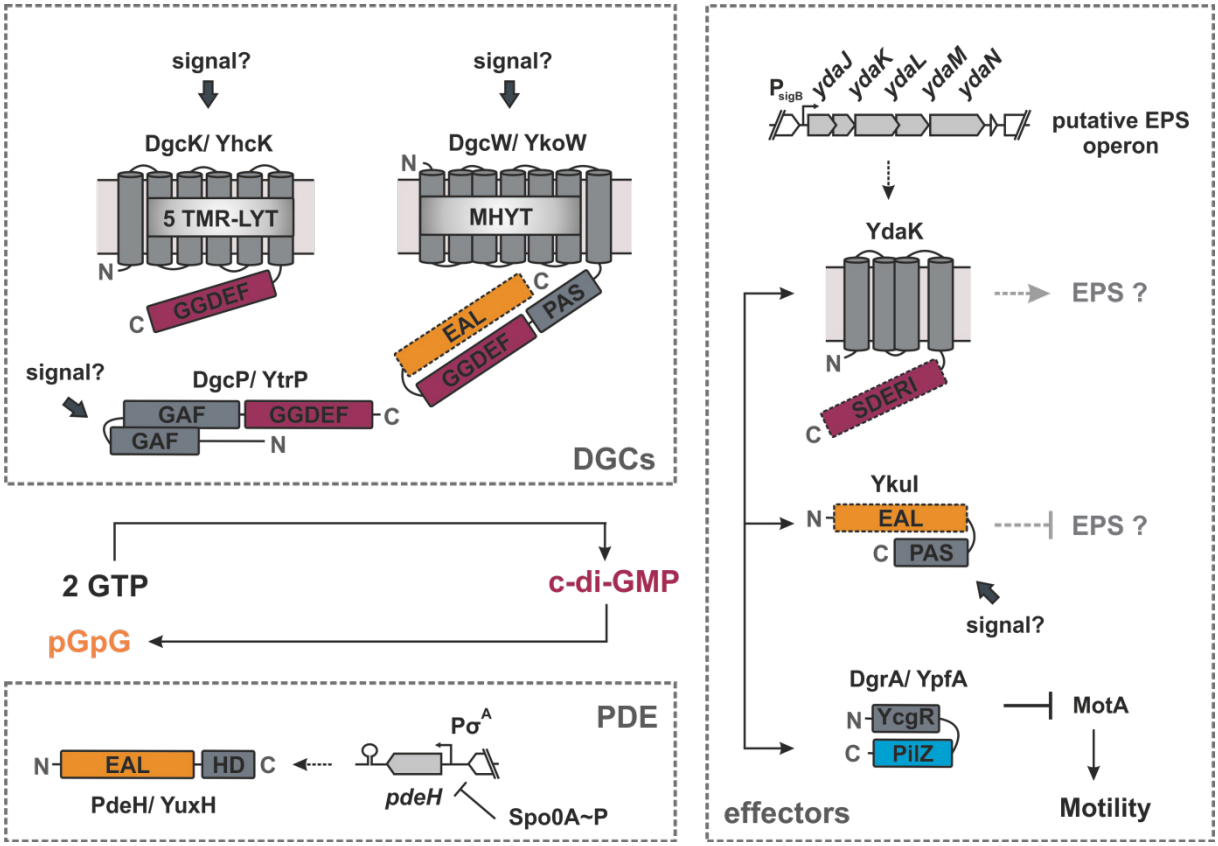

Fig. 1.7. C-di-GMP signaling components in *B. subtilis*
B. subtilis harbors three active DGCs with so far unknown cellular outputs despite c-di-GMP synthesis. PdeH is the only known active PDE in *B. subtilis* and known to be regulated on the transcriptional level by the before introduced master regulator Spo0A (compare to: **1.2.3**). C-di-GMP is known to inhibit motility behavior through the conserved PilZ domain protein DgrA. The degenerated GGDEF domain protein YdaK and the inactive EAL domain protein YkuI are hypothesized to function as receptors potentially involved in EPS synthesis. Color code for schematic representation of protein domains: putative soluble signaling domains and TM domains (grey), GGDEF domains (purple), EAL domains (orange), PilZ domain (blue). Dashed lines indicate inactive protein domains (YdaK, YkuI). In case of DgcW, the EAL domain activity has not been tested so far in *vitro*.

1.4.1 C-di-GMP mediated motility inhibition via DgrA

Although undetectable in vegetative wild type cells, elevated intracellular c-di-GMP levels could be achieved either by deletion of the sole PDE gene *pdeH* or by an artificial overproduction of one of the 3 active DGCs DgcK, DgcP or DgcW (Chen *et al.*, 2012; Gao *et al.*, 2013). Consistent with c-di-GMP signaling principles in Gram-negative bacteria, cells exhibited motility inhibition under these circumstances. The transient inhibition of swarming motility was attributed to the presence of only one gene encoding the PilZ-domain protein DgrA. DgrA is a paralog of *E. coli* YcgR and was shown to bind c-di-GMP *in vitro* (K_D = 11 nM) and to directly inhibit motility through protein-protein interactions with the flagellum motor component MotA (Chen *et al.*, 2012; Gao *et al.*, 2013). Using GST pulldown assays and subsequent MS-analysis, further potential c-di-GMP and/ or DgrA targets could be detected including MotA and MotB, the flagellin subunit (Hag) and the surfactin biosynthesis proteins (SrfAA, SrfAB, and SrfAC; Chen *et al.*, 2012).

Notably, transient inhibition of swarming motility by DgrA was observed upon elevated intracellular c-di-GMP levels, but also upon *dgrA* overexpression without artificially altering the levels of intracellular c-di-GMP (Chen *et al.*, 2012). When *dgrA* was constitutively expressed upon *pdeH* deletion, swarming motility was not only transiently blocked but almost completely suppressed suggesting different levels of *dgrA* expression under swarming conditions (Gao *et al.*, 2013). In addition to its negative effect on swarming behavior, overproduced DgrA also inhibited swimming behavior of *B. subtilis* as suggested by light microscopic analysis (Chen *et al.*, 2012).

Likewise, deletion of *dgrA* resulted in slightly altered BF morphologies reflected by accelerated wrinkle development and delayed disassembly of pellicles (Chen *et al.*, 2012).

1.4.2 Diguanylate cyclases in *B. subtilis*

While an increased concentration of c-di-GMP concentrations correlates with reduced motility, neither DGC deletion mutants including single- and triple mutations, nor any overexpression strain was altered in terms of BF formation (Chen *et al.*, 2012; Gao *et al.*, 2013). However, the c-di-GMP synthesizing activity of all three predicted DGCs could be confirmed through *in vivo* and *in vitro* analysis (Gao et al., 2013).

Two out of three DGCs (DgcK, DgcW) in *B. subtilis* harbor predicted N-terminal transmembrane domains constituting putative signaling domains. DgcK (formerly YhcK) is a putative TM protein with a C-terminal cytosolic GGDEF domain. Together with the phosphorelay sensor kinase LytS, DgcK was selected as representative putative sensor protein of

the 5TMR-LYT family (for 5 transmembrane receptors of the LytS-YhcK Type, PF07694). Members of this family display a conserved membrane-spanning domain encompassing 5 TM helices that constitute a putative sensory domain (Anantharaman & Aravind, 2003). Their function is not clear yet. LytS-type proteins combine the 5 TM-domain with cytoplasmic GAF and histidine kinase domains, whereas in YhcK-type proteins the 5 TM domain is associated with GGDEF domains. In the closely related *B.* cereus group, the ortholog protein CdgA (32 % amino acid identity, 98 % sequence coverage) has been demonstrated to have a mild positive effect on BF formation upon overproduction, while revealing pronounced negative effects on cytotoxicity *in vitro* (Fagerlund *et al.*, 2016). In *L. monocytogenes*, DgcA and DgcB positively regulate the production of an EPS, but also in this case the sensory functions of these YhcK-type proteins remained unexplored (Chen *et al.*, 2014; Koseoglu *et al.*, 2015).

Interestingly, *dgcW* belongs to SigD regulon and is co-transcribed with various chemotaxis genes including *yoaH*, *mcpB* and *mcpA* (Nicolas *et al.*, 2012; SubtiWiki). The encoded protein displays a similar domain arrangement as MucR from *P. aeruginosa* (Hay *et al.*, 2009; Li *et al.* 2013). Bioinformatics predictions of DgcW (formerly YkoW) revealed the presence of an N-terminal so-called MHYT domain harboring seven predicted membrane-spanning helices, that are proposed to sense diatomic gases (O_2, CO or NO) through conserved residues that may coordinate copper ions (Galperin *et al.*, 2001, Li *et al.*, 2013). However, under standard laboratory and anaerobic conditions by means of either nitrate respiration or glucose fermentation, that would require oxygen sensing, deletion of *dgcW* has no effect on bacterial growth (Galperin *et al.*, 2001). DgcW is further predicted to contain an additional PAS sensory domain, located between the TM-domain MHYT and the cytoplasmic GGDEF and EAL domains. *In vitro* analysis of the GGDEF domain revealed elevated c-di-GMP levels when the adjacent PAS domain was included implying also a potential stimulatory activity of this sensory domain in *vivo* (Gao *et al.,* 2013). The artificial overproduction of full-length DgcW resulted in increased cellular c-di-GMP levels. Therefore, it was concluded that DgcW primarily possesses DGC activity, despite that the adjacent EAL domain may function as a negative regulator of the GGDEF domain, as *in vivo* experiments and sequence analysis indicate (Gao *et al.*, 2013). Notably, sequence analysis revealed, in contrast to the GGDEF domains of DgcK and DgcP, a degenerated RxxD I-site motif within the GGDEF domain of DgcW (PxxG) which supports the view of the EAL domain as a negative regulatory element of the GGDEF domain. Overproduction of DgcW in wild-type background resulted in detectable c-di-GMP levels, but particularly increased in a quadruple mutant lacking all GGDEF domain proteins (Gao *et al.*, 2013), which implies a potential cross-talk between those in *B. subtilis*.

The third DGC encoded in the genome of *B. subtilis*, DgcP, reported to be an active diguanylate cyclase *in vivo* and *in vitro* (Gao *et al.*, 2013), lacks transmembrane domain receptors but harbors two predicted N-terminal GAF sensory domains (SMART) which have been shown to stimulate the activity of the adjacent C-terminal GGDEF domain *in vitro* (Gao *et al.*, 2013). GAF domains are prominent regulatory input domains of DGCs such as REC and PAS domains and they are able to bind small molecules such as cAMP and cGMP (Charbonneau *et al.*, 1990; Biswas *et al.*, 2015). Although specific for distinct, widely unknown signals, the various kinds of input domains are commonly linked to catalytic GGDEF output domains via a protruding helical segment that forms a parallel coiled coil with its symmetry mate (Schirmer, 2016). The input domains and the stalk are proposed to function as dimerization modules in order to regulate the quaternary structure and activity of GGDEF proteins in a signal-induced manner (Schirmer, 2016), a mechanism that could also apply for DgcP. DgcP has no counterpart in the *B. cereus* group, but it seems to be conserved in the *B. subtilis* group. Distinct cellular functions could not be assigned to DgcP, neither to the other two above described DGCs.

1.4.3 The potential c-di-GMP output effectors YkuI and YdaK

Apart from the motility inhibitor DgrA, two other proteins (YkuI and YdaK) have been hypothesized to serve as c-di-GMP effectors in *B. subtilis* including a potentially inactive EAL-domain and a degenerated GGDEF domain protein. Both c-di-GMP targets do not contribute to motility inhibition upon increased second messenger levels as demonstrated by Gao and co-workers (2013) and may therefore exhibit distinct functions in *B. subtilis*.

YkuI is a canonical EAL-domain protein that harbors all critical residues constituting this family. The protein has been structurally characterized in its apo- and c-di-GMP-bound states (Minasov *et al.*, 2009). However, its concrete functional role *in vivo* remained controversial. Despite its capability to bind the second messenger, YkuI surprisingly did not exhibit PDE activity towards c-di-GMP *in vitro*. Consequently, it is now widely considered as a c-di-GMP output effector (Minasov *et al.*, 2009). Structural analysis of YkuI documented a TIM- (triose-phosphate isomerase) barrel fold as the basic constituent of c-di-GMP-specific PDEs (Römling *et al.*, 2013). Furthermore, Minasov and coworkers argued that YkuI contains, in contrast to active EAL domain proteins, a degenerated β5-α5 loop, which results in a nonproductive arrangement of active site residues and thus in an inability to degrade c-di-GMP (Minasov *et al.*, 2009; Rao *et al.*, 2009). Noteworthy, YkuI harbors besides the N-terminal located EAL domain an adjacent C-terminal domain that resembles PAS-fold. Both domains are connected through a long linker

helix and participate in the formation of a tight homodimer. The pocket-like C-terminal domain has the potential to accommodate a ligand and may therefore also function as a signaling domain affecting the quaternary structure and potentially also the catalytic activity towards c-di-GMP (Minasov *et al.*, 2009). Hence, it still remains to be determined whether the putative sensory domain functions as a signal input domain to affect c-di-GMP binding and potentially hydrolysis by the EAL domain or as an output domain upon c-di-GMP binding to the EAL-domain altering its conformation (Wolfe and Visick, 2010). Very recently, YkuI has been implicated to control zinc homeostasis in *B. subtilis* (Chandrangsu and Helmann, 2016). Inactivation of *ykuI* and of the *fla-che* operon conferred resistance to high Zn (II) concentrations and it was hypothesized that these disruptions restrict the access of zinc presumably by increasing ECM production based on the following arguments. While not reported for *B. subtilis* YkuI, the ortholog protein CdgJ (55 % amino acid identity, 99 % sequence coverage) harboring a degenerated EAL domain, positively influences BF formation in *B. cereus* (Fagerlund *et al.*, 2016). However, the above described findings rather point towards a negative regulatory function of YkuI on ECM production in *B. subtilis*.

The main actor of this study, YdaK, is a predicted TM protein, bearing a soluble C-terminal GGDEF domain that is catalytically inactive due to its degenerated active site motif (Gao *et al.*, 2013). As described above (**1.3.2**), degenerated EAL- and GGDEF- domains can participate as c-di-GMP binding proteins in different signaling pathways. Indeed, binding of c-di-GMP to the soluble GGDEF domain has been demonstrated *in vitro* occurring only at high c-di-GMP concentrations as verified by isothermal titration calorimetry (ITC). This binding is presumably mediated by the conserved I-site motif present in the GGDEF domain (Gao *et al.*, 2013). In contrast to all other c-di-GMP signaling related genes in *B. subtilis*, *ydaK* locates in a transcriptional unit *ydaJKLMN* that has not been characterized functionally so far (at the beginning of this study). Bioinformatics predictions of the corresponding protein components suggest that these proteins resemble a polysaccharide synthesizing machinery potentially linking c-di-GMP and BF formation in *B. subtilis*, which has been undervalued so far.

1.5 Aims of research

The second messenger c-di-GMP has been under extensive investigation for the last three decades, and a comprehensive view of its function particularly in the course of bacterial lifestyle orchestration in Gram-negative model organisms such as *E. coli* and *P. aeruginosa* has been established. In comparison, only few studies have investigated the function of c-di-GMP in Gram-positive bacteria. The major aim of this work was to gain more detailed insights into the function of c-di-GMP in the Gram-positive model organism *B. subtilis* and into the subcellular localization of involved components.

2 ARTICLES

Personal contribution to published work:

The majority of this work has been published in two articles:

Article I

Patricia Bedrunka and Peter L. Graumann, 2017

Subcellular clustering of a putative c-di-GMP-dependent exopolysaccharide machinery affecting macro-colony architecture in *Bacillus subtilis*. Environmental Microbiology Reports, 9: 211–222.

Article II

Patricia Bedrunka and Peter L. Graumann, 2017

New functions and subcellular localization patterns of c-di-GMP components (GGDEF domain proteins) in *B. subtilis*. Frontiers in Microbiology, 8: 794.

I designed and carried out all experiments. Furthermore, I wrote the majority of both manuscripts, created all figures and tables and revised the manuscripts during the publishing process.

I greatly acknowledge the always helpful support from my supervisor Prof. Dr. Peter Graumann, furthermore from Dr. Felix Dempwolff (confocal microscopy), Dr. Thomas Rösch (preparation of Fig. S3; Article I) and Dr. Gert Bange (comments on both manuscripts). Prof. Dr. Alexander Böhm, who passed away in 2012, inspired this work.

2.1 Article I

Subcellular clustering of a putative c-di-GMP-dependent exopolysaccharide machinery affecting macro-colony architecture in *Bacillus subtilis*.

2.1.1 Abstract

The structure of bacterial biofilms is predominantly established through the secretion of extracellular polymeric substances (EPS). We show that *Bacillus subtilis* contains an operon (*ydaJ-N*) whose induction leads to increased Congo Red staining of biofilms and strongly altered biofilm architecture, suggesting that it mediates the production of an unknown exopolysaccharide. Supporting this idea, overproduction of YdaJKLMN leads to cell clumping during exponential growth in liquid culture, and also causes colony morphology alterations in wild type cells, as well as in a mutant background lacking the major exopolysaccharide of *B. subtilis*. The first gene product of the operon, YdaJ, appears to modify the overproduction effects, but is not essential for cell clumping or altered colony morphology, while the presence of the c-di-GMP receptor YdaK is required, suggesting an involvement of the second messenger c-di-GMP. YdaM, YdaN and YdaK co-localize to clusters predominantly at the cell poles and are statically positioned at this subcellular site, similar to other exopolysaccharide machinery components in other bacteria. Our analysis reveals that *B. subtilis* contains a static subcellular assembly of an EPS machinery that affects cell aggregation and biofilm formation.

2.1.2 Introduction

In natural environments, microbes are predominantly organized in sessile multicellular communities called biofilms (Costerton *et al.*, 1995; Shapiro, 1998). These assemblages consist of distinct subpopulations of specialized cells which exhibit spatial and temporal organization during their coexistence within the community that is encapsulated by a protective extracellular matrix (ECM). In the process of biofilm development for instance, a fraction of the population differentiates into matrix-producing cells in response to external and internal signals (Stewart and Franklin, 2008; Vlamakis *et al.*, 2013). The extracellular matrix synthesized by those specialized cells, consists of extracellular polymeric substances (EPS), encompassing mainly polysaccharide, proteins and nucleic acids and can account for 90 % of the biomass (Flemming and Wingender, 2010). Extracellular matrix components are indispensable for biofilm formation and conservation as their nature determines the physicochemical and biological qualities of a biofilm and ensures the structural and functional integrity of the community.

Undomesticated strains of the Gram-positive soil-dwelling bacterium *Bacillus subtilis* such as NCIB3610, are able to form floating biofilms at air-liqiud interfaces (pellicles), structured colony biofilms on semi-solid agar surfaces and are furthermore capable of colonizing plant roots (Branda *et al.*, 2001; Cairns *et al.*, 2014). Laboratory strains such as 168 and PY79 have largely lost the ability to spread on semi solid agar and to form biofilms as a consequence of domestication (Zeigler *et al.*, 2008; McLoon *et al.*, 2011).

The formation of those complex surface-associated communities depends substantially on the synthesis and secretion of EPS including predominantly the major protein components TasA/TapA which is proposed to constitute an amyloid fibre network (Branda *et al.*, 2006; Romero *et al.*, 2010), the surface-active protein BslA, considered as a bacterial hydrophobin (Kobayashi and Iwano, 2012; Hobley *et al.*, 2013) and particularly exopolysaccharides.

Several studies have demonstrated the importance of the 15 gene-long *epsA-O* cluster concerning biofilm formation in *B. subtilis in vitro* and *in planta* (Marvasi *et al.*, 2010). The chemical composition of the polysaccharide produced by the products of this operon apparently depends on growth conditions/substrate availability and needs to be further clarified (Cairns *et al.*, 2014; Roux *et al.*, 2015).

Furthermore, *B. subtilis* is able to synthesize the exopolysacharide levan, a homopolymer of fructose, via the *epsA-O* adjacent *sacB-yveB-yveA* operon (Dogsa *et al.*, 2013) and the extracellular amino acid polymer γ-polyglutamate (Morikawa *et al.*, 2006; Scoffone *et al.*, 2013).

In this study, we address the question whether an additional putative exopolysaccharide synthesis operon (*ydaJKLMN*) contributes to ECM- and thus biofilm formation in *B. subtilis*

under laboratory conditions. Most interestingly, the second gene product YdaK encodes for a putative c-di-GMP receptor (Chen *et al.*, 2012; Gao *et al.*, 2013) indicating a new function of this second messenger in *B. subtilis*.

The second messenger bis-(3'–5')-cyclic dimeric guanosine monophosphate (c-di-GMP) is a key regulator in the transition between motile and non-motile lifestyles of bacteria (Hengge, 2009). Generally, increased levels of c-di-GMP promote sessile lifestyle and biofilm formation, whereas motility and single cell behavior is inhibited under these circumstances (Simm *et al.*, 2004; Jenal and Malone, 2006). The synthesis and hydrolysis of c-di-GMP is mediated by two sets of enzymes. It is synthesized by diguanylate cyclases (DGCs), which harbor a conserved GGDEF domain, from two molecules GTP and is degraded by specific phosphodiesterases (PDEs) containing either a conserved EAL or HD-GYP domain, giving rise to the linear dinucleotide 5′-phosphoguanylyl-(3′,5′)-guanosine (pGpG).

The GGDEF domain of the transmembrane protein YdaK carries a degenerated GG(D/E)EF signature motif (SDERI) and was shown to be deficient in c-di-GMP synthesis. However, the 4 TM protein is able to bind c-di-GMP with moderate affinity via its soluble C-terminal GGDEF domain, likely at the so called I-site (signature motif RxxD, allosteric product inhibition site in active DGCs) but it is incapable of modulating swarming motility as demonstrated for DgrA, a conserved PilZ-domain c-di-GMP receptor (Chen *et al.*, 2012; Gao *et al.*, 2013).

Because c-di-GMP is known as a transcriptional and posttranslational regulator of different bacterial exopolysaccharide machineries (Liang, 2015), we were interested whether YdaK as a degenerated GGDEF-TM protein would be able to exert control over genes encoded within the same operon, as PelD from *P. aeuruginosa* (Lee *et al.*, 2007; Liang, 2015) and PssE from *L. monocytogenes* (Chen *et al.*, 2014; Koseoglu *et al.*, 2015). We were also interested in testing the subcellular localization of the products of the *yda* operon. Bacterial exopolysaccharide machineries or components of these have been reported to localize to the cell poles for several species including *A. tumefaciens* (Xu *et al.*, 2013), *E. coli* (Le Quere and Ghigo, 2009) and *S. coelicolor* (Xu *et al.*, 2008). Additionally, the components of the polyketide bacillaene synthase cluster at a single site within *B. subtilis* cells (Straight *et al.*, 2007) showing that multicomponent enzyme complexes can cluster and form an enzymatic megacomplex.

2.1.3 Results

2.1.3.1 The *ydaJKLMN* operon in *B. subtilis* encodes for a putative exopolysaccharide synthesis operon and contains a gene, *ydaK*, encoding a potential c-di-GMP binding protein

The potential c-di-GMP receptor YdaK is encoded within a transcriptional unit, harboring four additional genes called *ydaJ*, *ydaL*, *ydaM* and *ydaN*. Condition-dependent transcription profiles (tiling microarray data obtained by Nicolas *et al.*, 2012) of single genes of the cluster and of its 5´ upstream region (**Fig. S1**) revealed co-transcription of these genes under various different laboratory conditions, implying that these genes are under the control of the same promotor. The corresponding genes were assigned to the SigB regulon (alternative stress sigma factor in *B. subtilis*), which is reflected in the upregulated transcription of *ydaJKLMN* elements upon stress treatment such as heat, ethanol and high salt, and in the upregulation during germination and notably also during exponentially growth in rich medium supplemented with glucose (Nicolas *et al.*, 2012).

It is interesting to note that the *yda* operon is absent from the genome of laboratory *B. subtilis* strain PY79, because it is part of an approximately 17 kb-long deletion occurring in this domesticated strain (Zeigler *et al.*, 2008). The reason for this deletion, encompassing the *yda* operon and 8 further open reading frames, is unknown. However, the genomes of the strains *B. subtilis* 168 and NCIB3610 do encode this operon.

Based on bioinformatic analysis of the corresponding elements (for a detailed description see supplementary material **Text S1** and **Fig. S2A**), we hypothesize that the *ydaJKLMN* operon codes for an exopolysaccharide machinery, which is upregulated during exponential growth and various stress conditions and may be regulated by the second messenger c-di-GMP.

2.1.3.2 Overexpression of *ydaJKLMN* or of *ydaKLMN* leads to increased staining of Congo Red

Deletion or overproduction of YdaK alone had no observable effects under laboratory conditions concerning biofilm formation and motility in *B. subtilis* (Gao *et al.*, 2013). In order to provoke a detectable cellular output by means of extracellular matrix production, we opted to overexpress the entire *ydaJKLMN* unit in three *B. subtilis* strains individually: in the laboratory strain *B. subtilis* 168, in its biofilm-proficient ancestor NCIB3610 and in a biofilm-deficient (*epsH*-mutant derived from strain NCIB3610 (*epsH*::*tet*, strain DS9259). Extracellular matrix production

was examined by Congo Red (CR) staining and by visual inspection of biofilm formation of *B. subtilis* macro colonies, as reported previously for different bacterial species (Robledo *et al.*, 2008; Romero *et al.*, 2010). Additionally, we wondered whether YdaJ, product of the first gene within the operon and putative extracellularly-acting endoglucanase, is required for the predicted function (ECM production). Its homolog PssZ (28 % identity, BlastP) is dispensable for extracellular polysaccharide synthesis, mediated by the PssABCDE machinery in *L. monocytogenes* (Koseoglu *et al.*, 2015). Considering this, we decided to generate two constructs mediating the overexpression of the entire transcriptional unit and of a *ydaJ*-lacking variant at the native locus respectively. We used the integrative vector pSG1164 (Lewis and Marston, 1999) and cloned the 5´ end of *ydaJ* or of *ydaK,* respectively, under the control of the plasmid-encoded xylose promotor, resulting in recombinant plasmids pSG1164-PB53 (P_{xylT}*ydaJKLMN*) and pSG1164-PB55 (P_{xylT}*ydaJKLMN*). These constructs were inserted into the respective *B. subtilis* genomes by Campbell-like recombination (Campbell *et al.*, 1977). The resulting strains carry a partial gene of *ydaJ* or of *ydaK,* respectively, and the whole *ydaJKLMN* operon or the operon lacking full-length *ydaJ* under the control of the xylose-dependent promoter (see experimental procedure **Text S2** and **Fig. S2C**).

The property of Congo Red accumulation on solid medium has been frequently associated with the production of extracellular matrix components, such as amyloid fibers or cellulose, in various Gram negative and positive bacteria (Friedman and Kolter, 2004; Solano *et al.*, 2009; Chen *et al.*, 2014). Interestingly, we found that both overexpression mutants are able to accumulate CR to a visually greater extent than wild type cells (**Fig. 1A**). The laboratory strain 168 exhibits no CR-binding and reveals flat and less structured colony morphology in comparison to both overproduction strains. Colonies carrying the plasmid pSG1164-PB53 (strain 168-PB53, P_{xylT}*ydaJKLMN*) and pSG1164-PB55 (strain 168-PB55, P_{xylT}*ydaKLMN*) respectively, display a strikingly distinct morphology on CR agar plates containing the inducer xylose compared to the non-induced colonies.

Overexpression of *ydaJKLMN* (168-PB53) as well as of *ydaKLMN* (168-PB55) results in the formation of red irregularly branched wrinkles in the center of the colony, and overall enhanced CR-binding, especially at the outlines of the inoculation area, which indicates a significant difference in extracellular matrix composition between the parental wild type and both overproduction strains. Those wrinkled phenotypes do not occur on indicator plates without xylose (**Fig. 1A**).

Wrinkled colony morphology and CR-binding has been linked to cell aggregation phenotypes in Gram-negative and positive bacteria (Solano *et al.*, 2009; Koseoglu *et al.*, 2015). We could also observe such aggregation effects (**Fig. 1A**, **Fig. S3**), which we quantified by

spectrophotometry determining the OD_{600} of induced cultures after 90 min of settling (**Fig. S3**). Both overproduction strains, 168-PB53 (P_{xyl}-*ydaJKLMN*) and 168-PB55 (P_{xyl}-*ydaJKLMN*), showed a significant decrease in optical density compared to wild type *B. subtilis* 168 cells, reflecting increased levels of aggregation, although the level of aggregation was visibly enhanced when only *ydaKLMN* (168-PB55) was overexpressed, in comparison to *ydaJKLMN* (168-PB53) overexpression (**Fig. 1A**, **Fig. S3**).

Because an overexpression of *ydaKLMN* missing *ydaJ* coding for a putative glycosyl hydrolase (GH8), resulted in a similar CR binding phenotype as the overexpression of the complete operon, we conclude that the gene product of *ydaJ* is not involved in the synthesis of the unknown polysaccharide but possibly in a post-polymerization modification reaction similar to that of PssZ in *L. monocyotogenes*, which acts outside of the bacterial cell membrane and is not essential for EPS production (Koseoglu *et al.*, 2015). This is further supported by the observation that an overexpression of *ydaJ* from the ectopic *amyE* locus along with an overexpression of *ydaKLMN* (original locus) results in enhanced CR binding, but wrinkle formation and aggregation was completely abolished (strain 168-PB55+15, **Fig 1A**). We speculate that YdaJ partially degrades or modifies the putative exopolysaccharide produced by YdaKLMN.

2.1.3.3 Overexpression of *ydaJKLMN* or of *ydaKLMN* alters morphology of *B. subtilis* macro-colonies on biofilm-promoting medium

Next, we wondered whether an overexpression of *ydaJKLMN* or of *ydaKLMN* alters the morphology of biofilm colonies of the undomesticated wild type strain NCIB3610 known to exhibit "multicellular" behavior by forming robust and complex macro colonies on a biofilm-inducing solid medium (MSgg, minimal salts with glycerol and glutamate, Branda *et al.*, 2001). In order to investigate the role of *ydaJKLMN* in terms of biofilm formation, the two above-described recombinant plasmids pSG1164-PB53 and pSG1164-PB55 were introduced into the *B. subtilis* NCIB3610 genome individually (strains NCIB3610-PB53, -PB55) and biofilm formation was assessed using solid MSgg medium supplemented with CR/CB in the presence or absence of xylose. Additionally, we included a NCIB3610-derived *ydaK* deletion mutant DS9289 (Gao *et al.*, 2013) in our study. Representative images of the corresponding strains are depicted in **Fig. 1B**.

In good agreement with previous observations, the wild type strain displayed complex macro colony architecture (Asally *et al.*, 2012), which was not altered by the addition of xylose under these conditions. The overexpression of *ydaJKLMN* (NCIB3610-PB53, P_{xyl}-*ydaJKLMN*) resulted in an inhibited surface spreading behavior and additionally in the formation of an elevated and extended central ring structure stained with CR/CB, similar to that seen in the 168 background

(**Fig. 1A**). This reduced colony expansion phenotype was even more pronounced in macro colonies that overproduced the machinery lacking the putative glycosyl hydrolase YdaJ (strain NCIB3610-PB55; P_{xyl}-*ydaKLMN*; **Fig. 1B**). Furthermore, a different wrinkle pattern in the initial central inoculum area can be observed displaying more crowded, irregular and thick ridges, compared to the wild type strain and the overproduction strain NCIB3610-PB53 (P_{xyl}-*ydaJKLMN*). While an overproduction causes strong phenotypes on biofilm-promoting medium, the deletion of one component, such as *ydaK,* has only very mild effects (**Fig. 2B**, strain DS9289, Δ*ydaK*), as already previously reported by Gao *et al.*, 2013, suggesting a minor role of the *ydaJKLMN* operon with respect to biofilm formation under standard laboratory conditions.

2.1.3.4 Overexpression of *ydaKLMN* results in wrinkle formation and CR-staining in an *epsH* deficient biofilm mutant

The production of exopolysaccharides and other extracellular matrix components is crucial for the development of biofilms in many bacterial species. This is also true for the undomesticated *B. subtilis* strain NCIB3610, which harbors besides the *ydaJKLMN* cluster a 15-gene polysaccharide operon (*epsA-O*), encoding (at least partially) an EPS biosynthetic machinery that is thought to synthesize the extracellular compound poly-N-acetylglucosamine. This machinery is responsible for complex colony architecture (Branda *et al.*, 2001; Branda *et al.*, 2006; Nagorska *et al.*, 2010; Roux *et al.*, 2015). A deletion of *epsH* (strain DS9259, *epsH*::*tet*) results in flat and fragile macro colonies lacking the structural characteristics of wild type colonies (**Fig. 1C**, Chan *et al.*, 2014).

We investigated if and how overexpression of *ydaJKLMN* or of *ydaKLMN* effects biofilm formation in an *epsH* mutant background. For this reason, both overexpression constructs (pSG1164-PB53 and pSG1164-PB55) were introduced separately into the genome of an NCIB3610-derived *epsH* mutant and biofilm formation on solid MSgg medium was monitored 72 h post-inoculum in the presence and absence of 0.1 % xylose. As presented in **Fig. 1C**, an overexpression of the full length version *ydaJKLMN* (DS9259-PB53, *epsH*::*tet*, P_{xyl}-*ydaJKLMN*), resulted in an unstructured macro colony, similar to the parental strain (*epsH*::*tet*, DS9259, Chan *et al.*, 2014). However, colonies harboring the pSG1164-PB53 construct (DS9259-PB53) revealed a noticeably different surface, a confined colony outline and a reduction in colony size in comparison to the *epsH* mutant, which exhibits small extensions at the periphery. In contrast to this, overexpression of *ydaKLMN* lacking *ydaJ* caused wrinkled colony architecture, encompassing the formation of thick CR-accumulating wrinkles located around the center of the macro colony (DS9259-PB55, *epsH*::*tet*, P_{xyl}-*ydaKLMN*). The formation of these pronounced wrinkles in the absence of YdaJ accompanied by a reduction in colony size in the wild type backgrounds 168 and

NCIB3610, respectively, reinforces a role of YdaJ in remodeling the putative extracellular sugar chains, synthesized most likely by the putative synthase-complex YdaM/YdaN, to form regular structures and to ensure structural integrity of the macro colony.

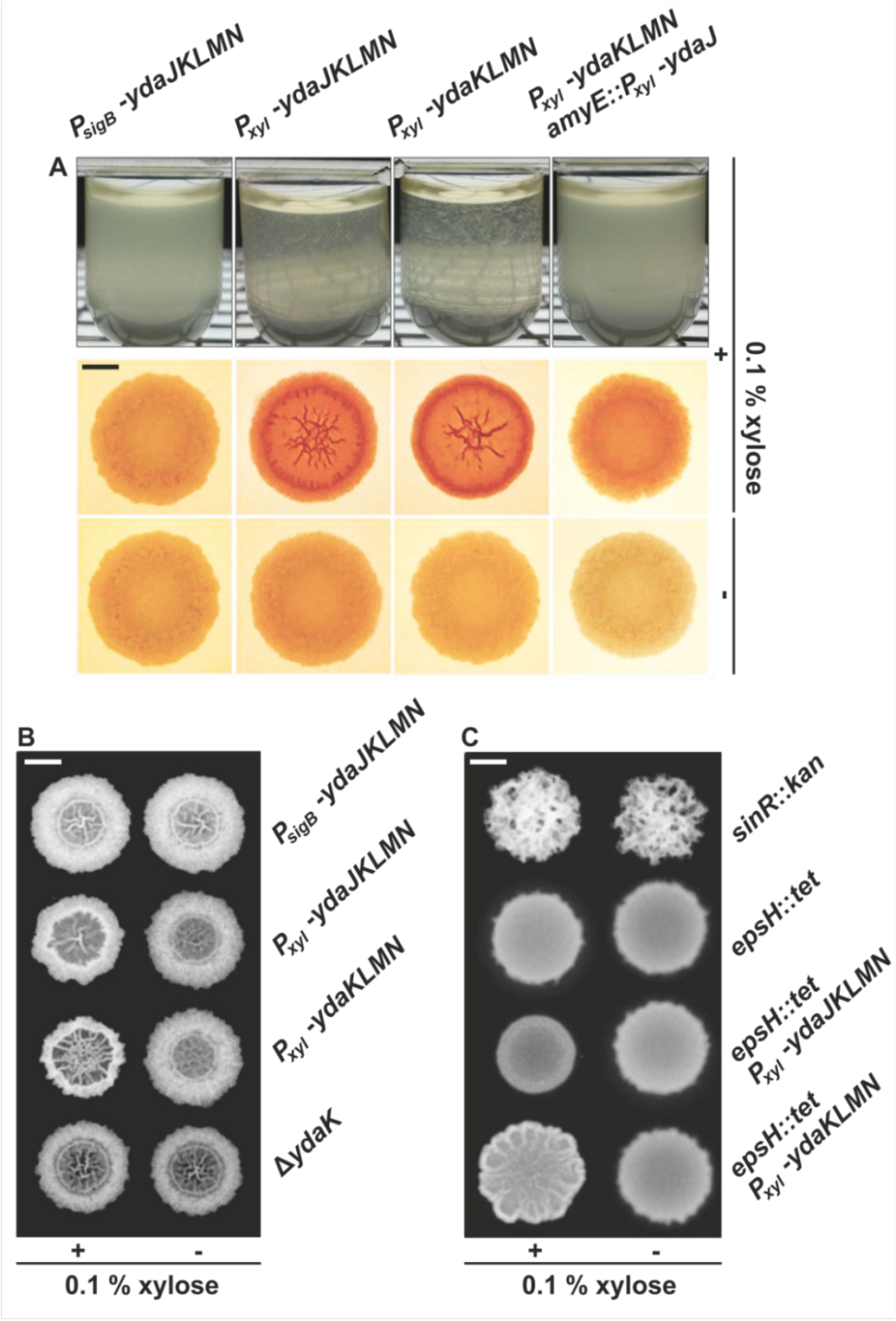

Fig. 1. Congo Red staining, aggregative behavior and biofilm surface architecture of macro-colonies overexpressing the putative exopolysaccharide operon variants *ydaJKLMN* and *ydaKLMN* in different genomic *B. subtilis* backgrounds
(**A**) Exopolysaccharide-dependent *B. subtilis* 168 cell-aggregation in liquid LB medium supplemented with 0.1 % (w/v) xylose and CR-binding of macro-colonies of parental WT *B. subtilis* 168 and strains carrying integrated overexpression constructs as illustrated in **Fig. S2**:

WT *B. subtilis* 168 (**I**. P_{sigB}-*ydaJKLMN*), 168-PB53 (**II**. P_{xyl}-*ydaJKLMN)*, 168-PB55 (**III**. P_{xyl}-*ydaKLMN*) and 168-PB55+PB15 (**IV**. P_{xyl}-*ydaKLMN*; *amyE*::P_{xyl}-*ydaJ*). Individual clones of WT 168 and the indicated overproduction strains were grown in LB to mid-log phase and spotted on indicator plates supplemented with or without 0.1 % (w/v) xylose, CR 40 µg/ml, CB 20 µg/ml, following an incubation of 24 h at 37 °C before imaging colony morphology. Scale bar: 2.5 mm (**B**) Effect of *ydaJKLMN*/ *ydaKLMN* overexpression and *ydaK* deletion on colony surface architectures of *B. subtilis* NCIB3610 using biofilm-promoting medium. An aliquot of exponentially growing cells was washed once in MSgg liquid medium and incubated for additional 30 min in MSgg at 37 °C before spotting the indicated strains on MSgg agar plates [+/- 0.1 % (w/v) xylose, 20 µg/ml CR & CB] followed by an incubation of 72 h at 25 °C. Strains: WT *B. subtilis* NCIB3610 (P_{sigB}-*ydaJKLMN*), NCIB3610-PB53 (P_{xyl}-*ydaJKLMN*), NCIB3610-PB55 (P_{xyl}-*ydaKLMN*), NCIB3610-DS9289 (Δ*ydaK*, Gao *et al.*, 2013). Scale bar represents 5 mm. (**C**) Effect of *ydaJKLMN*/ *ydaKLMN* overexpression on colony surface architecture in a NCIB3610-derived *epsH* biofilm deficient mutant using the biofilm-promoting medium MSgg. Strains: *sin*R::*kan* (DS859, Blair *et al.*, 2008; reflects overproduction of *epsA-O* derived exopolysaccharide), *epsH*::*tet* (DS9259, Chan *et al.*, 2014), DS9259-PB53 (*epsH*::*tet*; P_{xyl}-*ydaJKLMN*), DS9259-PB55 (*epsH*::*tet*; P_{xyl}-*ydaKLMN*). Experimental setup as described in (**B**). Scale bar: 5 mm.

2.1.3.5 The putative c-di-GMP receptor YdaK is essential for the formation of the *ydaJKLMN*-related putative extracellular matrix component in *B. subtilis* 168 and NCIB3610

In order to examine the potential YdaK dependence of the putative EPS machinery, we included a third overexpression construct in our study (pSG1164-PB56), which upon integration enables only the overexpression of the last 3 genes *ydaLMN*, whereas *ydaJK* are not expressed due to an inserted frame shift mutation in the pSG1164-PB56 construct. As illustrated in **Fig. 2AB**, an overexpression of *ydaLMN* in *B. subtilis* 168 and NCIB3610 (fourth column, strains 168/NCIB3610-PB56, P_{xyl}-*ydaLMN*) resulted in similar phenotypes regarding CR-binding, cell aggregation and biofilm formation as observed for the corresponding parental wild type strains indicating that the unknown EPS is not synthesized in the absence of YdaK.

To verify this idea, we performed complementation assays using the overproduction strains *B. subtilis* 168/NCIB3610-PB56 (P_{xyl}-*ydaLMN*), and introduced a full-length copy of *ydaK* under the control of an IPTG-inducible promotor and a xylose dependent-promoter driving *ydaLMN*, respectively, at the *amyE* locus (strains 168-PB56+XG003/ PB16: P_{xyl}-*ydaLMN*; *amyE*::P_{IPTG}-*ydaK*/ *amyE*::P_{xyl}-*ydaK*). Expression of the ectopic *ydaK* gene upon addition of xylose (**Fig. 2A**, fifth column, P_{xyl}-*ydaLMN*; *amyE*::P_{xyl}-*ydaK*) or IPTG (**Fig. 2C**, third column, P_{xyl}-*ydaLMN*; *amyE*::P_{IPTG}-*ydaK*), restored CR-binding, wrinkle formation and cell aggregation of strain 168-PB55 overexpressing *ydaKLMN* from the original locus (**Fig. 2A**, third column, P_{xyl}-

ydaKLMN), in contrast to the control strain which harbors a *yfp* gene at the *amyE* locus (strain 168-PB56+pSG1193, P_{xyl}-*ydaLMN*; *amyE*::P_{xyl}-*yfp*).

Consistent with these results, a stable introduction of *ydaK* into the genome of *B. subtilis* NCIB3610-PB56 and its expression (strain NCIB3610-PB56+PB16, P_{xyl}-*ydaLMN*; *amyE*::P_{xyl}-*ydaK*) also resulted in an altered biofilm development and formation, similar to that observed for strain NCIB3610-PB55 (**Fig. 2B**, P_{xyl}-*ydaKLMN*), which leads to the conclusion that the putative c-di-GMP receptor YdaK is essential for the synthesis of the unknown *ydaJKLMN*-related EPS in both *B. subtilis* backgrounds, and probably acts as an activating factor.

YdaK contains four transmembrane (-TM) α-helices and binds c-di-GMP via its soluble degenerated GGDEF domain. We wondered whether removal of the four TM-helices would influence the activity of YdaK reflected by CR binding of *B. subtilis* macro colonies. We therefore investigated an additional complementation strain, which contains a truncated version of *ydaK,* encoding for the soluble (degenerated) GGDEF domain at the *amyE* site under the control a xylose-inducible promotor, using the 168-PB56 background (**Fig. 2C**, fourth column, P_{xyl}-*ydaLMN*; *amyE*::P_{xyl}-$ydaK_{ggdef}$). The colony morphology of this strain (168-PB56+PB68) resembled that of wild type *B. subtilis* 168 and its derivative 168-PB56 (P_{xyl}-*ydaLMN*) and failed to restore the CR-binding wrinkled phenotype of strain 168-PB55 (P_{xyl}-*ydaKLMN*) indicating that YdaK needs to be embedded into the membrane via its TM domain in order to accomplish its biological function.

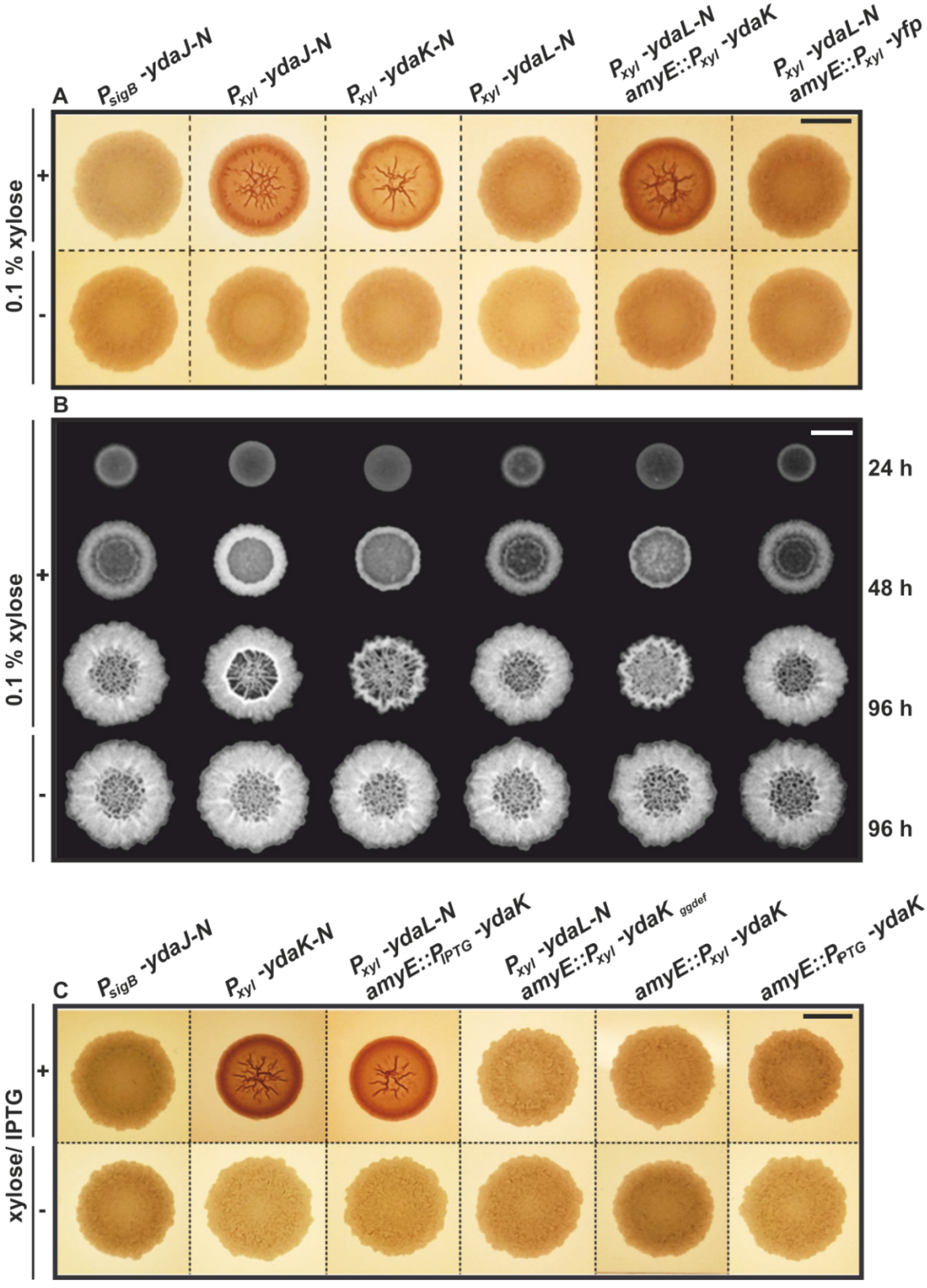

Fig. 2. The synthesis of the *ydaJKLMN*-related unknown EPS depends on the presence of the potential c-di-GMP receptor and 4TM protein YdaK in *B. subtilis*

(**A**) CR-staining of wild type strain *B. subtilis* 168 (P_{sigB}-*ydaJKLMN*) and its derivatives *B. subtilis* 168-PB53 (P_{xyl}-*ydaJKLMN)*, 168-PB55 (P_{xyl}-*ydaKLMN)*, 168-PB56 (P_{xyl}-*ydaLMN*), 168-PB56+ PB16 (P_{xyl}-*ydaLMN*; *amyE*::P_{xyl}-*ydaK*), 168-PB56+pSG1193NLMV (P_{xyl}-*ydaLMN*; *amyE*::P_{xyl}-*yfp*). Experimental as described above. (**B**) Top view of *B. subtilis* biofilm morphology on MSgg solid

medium at different time points for wild type strain NCIB3610 (DK1042), the overproduction mutant strains NCIB3610-PB53 (*P_{xyl}-ydaJKLMN)*, -PB55 (*P_{xyl}-ydaKLMN)*, -PB56 (*P_{xyl}-ydaLMN*) and the complementation strains NCIB3610-PB56+PB16 (*P_{xyl}-ydaLMN*; *amyE*::*P_{xyl}-ydaK*) and NCIB3610-PB56+pSG1193NLMV (*P_{xyl}-ydaLMN*; *amyE*::*P_{xyl}-yfp*). Experimental setup as described above. (**C**) CR-binding phenotypes of the parental WT *B. subtilis* 168 (*P_{sigB}-ydaJKLMN*) and strains carrying integrated overexpression constructs pPB55 (*P_{xyl}-ydaKLMN*), pPB56+ pXG003 (*P_{xyl}ydaLMN*; *amyE*::*P_{IPTG}-ydaK*), pPB56+pPB68 (*P_{xyl}-ydaLMN*; *amyE*::*P_{xyl}-ydaK$_{ggdef}$*), pPB16 (*amyE*::*P_{xyl}-ydaK*) and pXG003 (*amyE*::*P_{IPTG}-ydaK*; Gao *et al.*, 2013) respectively. Scale bars represent 5 mm. Note: this figure is originally published in greyscale**.**

2.1.3.6 A functional YdaK-YFP fusion forms static subcellular clusters

Next, we wondered whether YdaK would be uniformly distributed around the cell membrane or whether it would cluster to specific sites. To investigate the subcellular localization of the putative c-di-GMP receptor YdaK via fluorescence microscopy (**Fig. 3ABD**), we first constructed a strain harboring a translational C-terminal YdaK-mVenus-YFP fusion, encoded at the original gene locus and expression of this fusion is driven by the natural promotor of the *ydaJ-N* operon in the *B. subtilis* 168 background (168-PB10*, P_{sigB}-ydaK-mVenus-yfp*).

Prior to the investigation of protein localization, we tested whether the fusion protein was biologically active (**Fig. 3C**). Because a deletion of any of the *ydaJKLMN* components has no obvious phenotype, we applied the same complementation assay as illustrated in **Fig. 2**, using strain 168-PB56 that overexpresses *ydaLMN* upon addition of xylose as a background to introduce a construct encoding *ydaK-mV-yfp* at the ectopic *amyE*-site under the control of *Pxyl* (168-PB56+PB57*, P_{xyl}-ydaLMN; amyE*::*P_{xyl}-ydaK-mVenus-yfp*). In contrast to the expression of a N-terminal mV-YFP-YdaK fusion, the expression of ectopic *ydaK-mV-yfp* together with an overexpression of *ydaLMN* resulted in a similar CR-binding phenotype as observed for the untagged version (strain 168-PB56+PB16, *P_{xyl}-ydaLMN; amyE*::*P_{xyl}-ydaK*, compare **ii)** & **iv)** in **Fig. 3C**) demonstrating that a C-terminal YFP-fusion can functionally replace the wild type protein.

YdaK-mV-YFP fusions, expressed under native circumstances, localized mostly as a single focus at the lateral cell membrane, but also as bright parallel double or single foci next to or directly at the cell poles in exponentially growing cells (**Fig. 3AB**). We noticed that only a subset (18.5 +/- 1.3 %, n= 1500) of cells exhibited fluorescent signals, suggesting that the expression of the *yda* operon occurs in only a subpopulation of cells. Overproduction of C-terminal CFP- or YFP fusions encoded *in trans* (amylase locus) under the control of an artificial promotor, resulted in a similar localization pattern upon addition of 0.1 % (w/v) xylose (**Fig. 3D**, strain 168-PB24, *amyE*::*P_{xyl}-ydaK-cfp*) as observed in case of YdaK-mVenus-YFP expressed from

the endogenous locus (**Fig. 3A**, strain 168-PB10). Overproduction lead to an increased number of cells displaying foci (94.1 +/- 1.1 %, n=400), and also in the number of foci per cells (62 % of cells displayed 3 foci, only 5 % in case of strain 168-PB10; n = 200); foci retained a preference of localization close to the cell poles and septa.

In summary, we show that the c-di-GMP effector YdaK forms static clusters at distinct sites of the cell membrane indicating that EPS production mediated by the YdaJ-N machinery may take place at single sites within the membrane of growing *B. subtilis* cells.

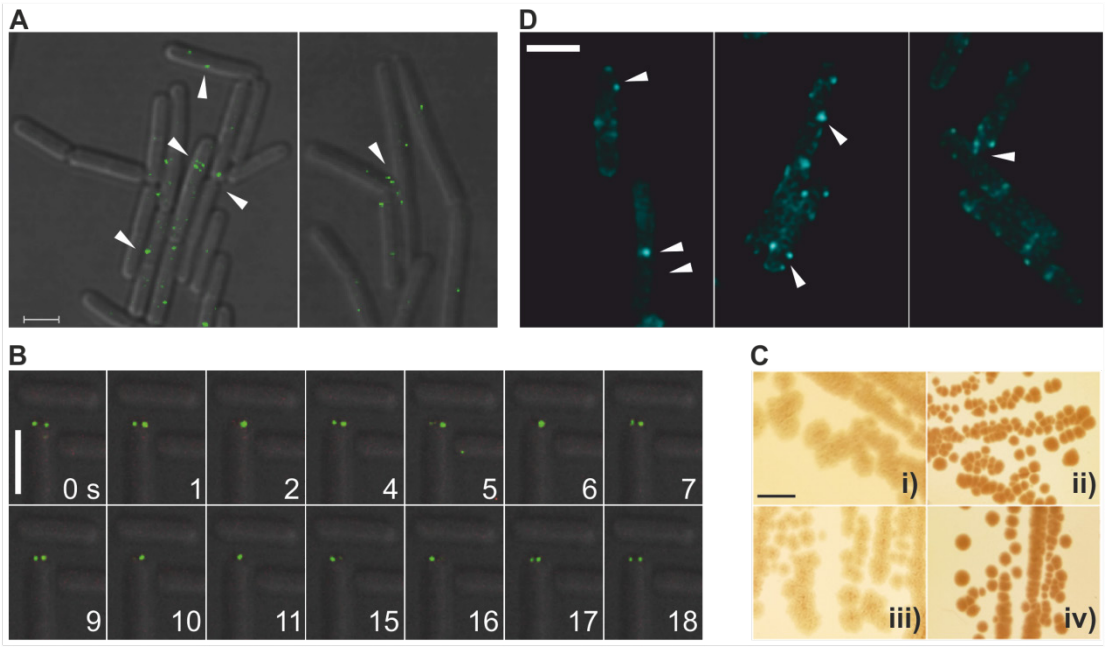

Fig. 3. Subcellular localization and dynamics of the putative c-di-GMP receptor YdaK during exponential growth in live *B. subtilis* 168 cells using confocal fluorescence microscopy

(**A**) Exponentially growing cells expressing *ydaK-mV-yfp* from the original locus in the presence of 0.1 % (w/v) xylose to ensure transcription of downstream genes (strain 168-PB10). Overlay of Normarski DIC and YFP-fluorescence. Bar: 2 µm (**B**) Corresponding time-lapse microscopy experiment of YdaK-mVenus-YFP. Images were captured at the time points (seconds) indicated inside the panels. Bar: 2 µm (**C**) Verification of YdaK-mV-YFP functionality by CR-staining in the presence of 0.1 % (w/v) xylose **i**) WT *B. subtilis* 168 (P_{sigB}-*ydaJKLMN*) **ii**) 168-PB56+PB16 (P_{xyl}-*ydaLMN*; *amyE*::P_{xyl}-*ydaK*) **iii**) 168-PB56+pSG1193NLMV (P_{xyl}-*ydaLMN*; *amyE*::P_{xyl}-*mV-yfp*) **iv**) 168-PB56+PB57 (P_{xyl}-*ydaLMN*; *amyE*::P_{xyl}-*ydaK-mV-yfp*). Bar: 5 mm (**D**) Mid-exponential-phase *B. subtilis* 168 cells expressing *ydaK-cfp* the amylase locus, 45 min after induction with 0.1 % (w/v) xylose (strain 168-PB24). Bar: 2 µm. Note: this figure is originally published in greyscale**.**

2.1.3.7 Components encoded within the *ydaJKLMN* operon co-localize to distinct sites of the cell membrane

We also localized other components encoded within the putative exopolysaccharide operon *ydaJKLMN*. Most fusions showed very low signals, which could only be resolved by using TIRF microscopy. We tagged each protein C-terminally with mV-YFP produced under the control of its original promoter. The plasmid-internal xylose-driven promoter ensured transcription of downstream genes. In case of YdaJ and YdaL fusions, we were not able to detect any membrane localization most likely due to missfolding of YFP outside the cytoplasm since the C-termini of the corresponding proteins are predicted to be outside. Localization attempts using mCherry as a fluorophore resulted in membrane localization but poor signal to noise ratios (data not shown). However, C-terminal YdaM-mV-YFP (**Fig. 4B**, strain 168-PB13, *ydaM-mV-yfp*) and YdaN-mV-YFP (**Fig. 4C**, strain 168-PB14, *ydaN-mV-yfp*) fusions resembled the pattern of YdaK-mV-YFP (strain 168-PB10) localization (**Fig. 4A**, left panels, snapshots) as well as the temporal behavior in exponentially growing 168 cells as presented in **Fig. 4** (right panels). Again, only a subset of around 20 % of cells (n=1400) displayed YdaM-mV-YFP and YdaN-mV-YFP signals, respectively. Time lapse microscopy over a period of 8 sec (continuous illumination with 515 nm, 100 ms intervals) of all three fusions revealed predominantly static localization of foci, at the same, mostly polar cellular positions (**Fig. 4ABC**, right panels; maximum intensity projections MIP and corresponding kymographs). Interestingly, polar localization of bacterial exopolysaccharide producing machineries components has been reported for several bacterial species including *A. tumefaciens* (Xu *et al*., 2013), *E. coli* (Le Quere and Ghigo, 2009) and *S. coelicolor* (Xu *et al*., 2008).

Based on the observation of similar localization patterns, we wondered whether YdaK, YdaM and YdaN co-localize at the preferred cell regions. Using two different fluorophores and a 515 nm/445nm dual band filter, we found that 64.3 +/- 3.3 % of cells which expressed *ydaM-mV-yfp* from its original promotor and *ydaK-cfp* from the ectopic *amyE* locus displaced both signals (**Fig. 5A**), revealing predominant co-localization of both fusion proteins (n = 250, strain 168-PB13+24, *ydaM-mV-yfp; amyE*::P_{xyl}-*ydaK-cfp*). N-terminal mCerulean-YdaM (original locus) fusions also co-localized with C-terminal YdaK-mV-YFP fusions (ectopic locus) in 52.1 +/- 2.6 % of total cell counted (n=300, **Fig. 5B**, strain 168-PB93+PB57, P_{xyl}-*mcerulean-ydaM*; *amyE*::P_{xyl}-*ydaK-mV-yfp*). Additionally, we observed co-localization events between the putative exopolysaccharide synthase components mCerulean-YdaM (original locus) and YdaN-m-YFP (ectopic locus) in 57.8 +/- 4.3 % of cells displaying both foci (**Fig. 5C**, strain 168-PB93+PB96, P_{xyl}-*mcerulean-ydaM*; *amyE*::P_{xyl}-*ydaN-mV-yfp*).

In toto, we provide evidence that the putative EPS-synthase components YdaM and YdaN and the essential potential c-di-GMP receptor YdaK form static subcellular assemblies that localize preferentially at the bacterial cell poles and septa, similar to other bacterial exopolysaccharide machineries.

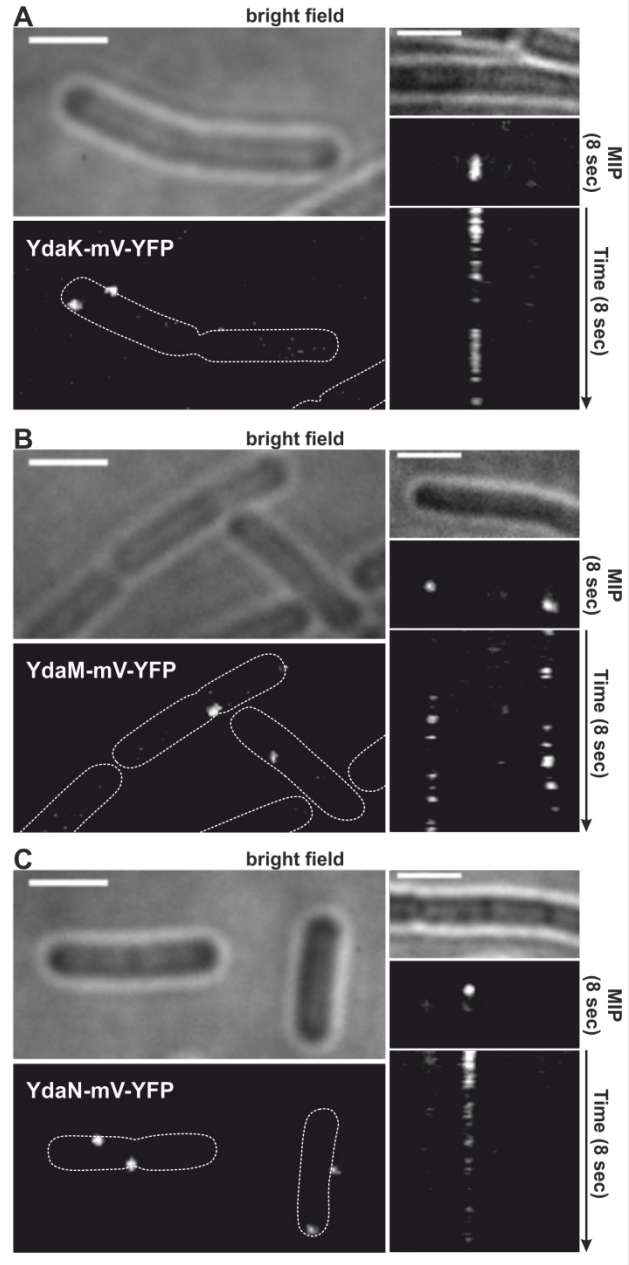

Fig. 4. Subcellular localization of components of the putative YdaJ-N exopolysaccharide machinery

Fluorescence microscopy of endogenously expressed *ydaK-mV-yfp* (**A**), *ydaM-mV-yfp* (**B**) and *ydaN-mV-yfp* (**C**) in exponentially growing *B. subtilis* 168 cells and corresponding bright field images (left panel). Right panel: maximum intensity projections (MIP) from timelapse microscopy and kymographs showing the motion of individual particles over time. Strains: 168-PB10 (*ydaK-mV-yfp*), -PB13 (*ydaM-mV-yfp*), - PB14 (*ydaN-mV-yfp*). Data are representatives of two biolgical replicates. Bars: 2 μm.

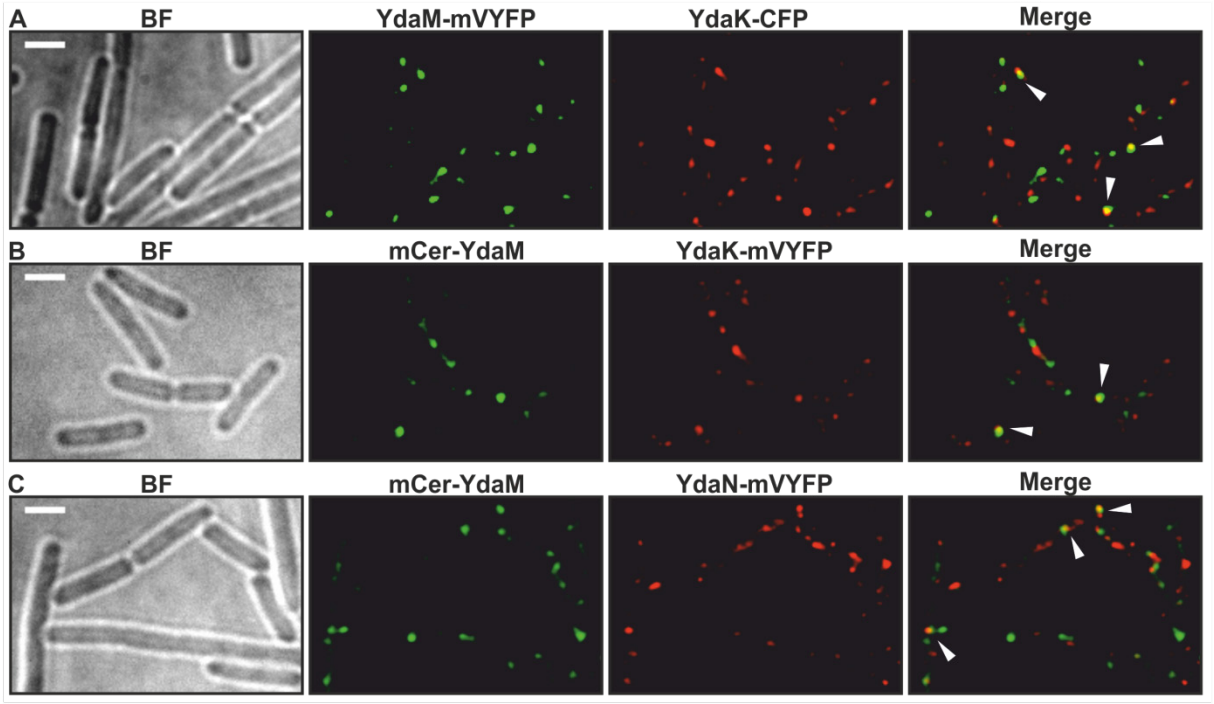

Fig. 5. Simultaneous localization of the potential c-di-GMP receptor YdaK and associated putative polysaccharide synthase components YdaM and YdaN
(**A**) Exponential *B. subtilis* 168 cells producing YdaM-mV-YFP (original locus and promotor, false colored green) and YdaK-CFP (ectopic locus, xylose-inducible promotor, false colored red). Triangles in the overlays of corresponding pictures (right panels) indicate colocalization or close proximity of foci. Strain: 168-PB10+PB24. (**B**) Colocalization of mCerulean-YdaM (original locus, xylose-inducible promotor, false colored green) and YdaK-mV-YFP (ectopic locus, xylose-inducible promotor, false colored red). Strain: 168-PB93+PB57. (**C**) Colocalization of mCerulean-YdaM (original locus, xylose-inducible promotor, false colored green) and YdaN-mV-YFP (ectopic locus, xylose-inducible promotor, false colored red). Strain: 168-PB93+PB96. Scale bars: 2 μm; BF: brightfield

2.1.4 Discussion

The chemical composition of exopolysaccharide polymers produced by the soil bacterium *Bacillus subtilis* is presumably dependent on substrate availability and is currently mainly attributed to two transcriptional units: *epsA-O* & *sacB-yveB-yveA* (Branda *et al.*, 2001; Chai *et al.*, 2012; Dogsa *et al.*, 2013). Our work suggests that *B. subtilis* possesses a third EPS operon, which must be taken into consideration in further studies regarding EPS production of exponential or stationary *B. subtilis* cultures. The most likely function of the *ydaJKLMN* operon is the synthesis of an exopolysaccharide, because in addition to the effect of increased CR binding and wrinkle formation (plus reduced spreading diameter of colonies) during biofilm formation, induction of the operon leads to cell clumping during exponential growth. In spite of our best efforts, we have not found the exact physiological role of the *yda* operon. The transcriptional unit is assigned to the *B. subtilis* σ^B- regulon (Nicolas *et al.*, 2012), but deletion mutants did not reveal any phenotype in biofilm formation or stress resistance, and overproducing the operon did not increase e.g. ethanol stress resistance (data not shown). We can therefore only speculate that the putative exopolysaccharide provides stress resistance under specific stress conditions, and/or under extreme stress, or under unknown conditions.

However, using complementation strains and CR binding assays of *B. subtilis* macro colonies, we show that *ydaK* expression is essential for the activation of the putative exopolysaccharide synthesizing components. YdaK contains four predicted N-terminal transmembrane helices and a soluble degenerate GGDEF domain, which is not able to synthesize but is able to bind the second messenger c-di-GMP with moderate affinity (dissociation constant 1.1 μM), most likely at the so-called I-site (Gao *et al.*, 2013). The role of c-di-GMP, known to be a positive regulator of ECM production, during *B. subtilis* biofilm formation has been addressed by two recent studies (Chen *et al.*, 2012; Gao *et al.* 2013).

No obvious consequence on biofilm formation by changes in intracellular c-di-GMP was observed, whereas high c-di-GMP resulted in motility inhibition via the conserved PilZ-domain protein DgrA (dissociation constant 11.0 nM). Interestingly, Gao *et al.* were unable to detect c-di-GMP in WT cells indicating very low concentrations under their growth conditions (limit of detection 50 pg/μL). Low intracellular c-di-GMP concentrations do not necessarily exclude the potential of c-di-GMP to activate a corresponding low-affinity receptor such as YdaK. The "local signaling/pool" hypothesis i.a. proposes spatial proximity of c-di-GMP metabolizing proteins, effectors and targets producing small localized specific concentrations as suggested in several studies (Merritt *et al.*, 2010; Dahlstrom *et al.*, 2015). Therefore, *B. subtilis* may employ a c-di-GMP signaling network for the regulation of the *yda* operon via a degenerated GGDEF – TM protein

to positively regulate extracellular matrix formation and thus possibly biofilm formation. *B. subtilis* harbors a minimalistic set of three diguanylate cyclases: DgcK, DgcP and DgcW, which can potentially contribute to the c-di-GMP pool utilized by YdaK and/ or serve as interaction partners in order to activate EPS production. In this study, we provide a new tool to study the role of c-di-GMP during biofilm formation in the model organism *B. subtilis*.

Importantly, we observed the formation of subcellular clusters (usually one per cell) of YdaK, YdaM and YdaN at distinct sites (with an enrichment at the cell poles) of exponentially growing *B. subtilis* cells using fluorescence microscopy. The clusters showed static localization, possibly because the synthetase components are anchored within the cell membrane (as predicted by bioinformatics tools, see supplementary material). Co-localization events of YdaM/YdaK and YdaM/ YdaN fluorescent fusions support the idea that subcellular localization at the cell membrane might be important for facilitating protein-protein interactions. This idea is further supported by the observation that a YdaK variant lacking the TM domain is unable to support the activity of the other Yda proteins.

In summary, our observations of clustered components of a putative exopolysaccharide machinery reveal that the concept of enzymatic subcellular assemblies within the membrane of enzymes whose product is secreted is wide spread, and *B. subtilis* contains at least two of such assemblies, the YdaJKLMN machinery and the bacillaene synthase cluster (Straight *et al.*, 2007). It will be highly interesting to further investigate which c-di-GMP pathway activates the Yda proteins, and how the assembly is restricted to a single site within the cell membrane of a bacterium.

2.1.5 Acknowledgments

We would like to thank Luise Kleine Borgmann from the Gurol Süel laboratory (UCSD) for the Biofilm protocol, Felix Dempwolff (now University of Indiana) for help with confocal microscopy and for helpful discussions. Thomas Rösch (University of Marburg) helped with Fig S3, Daniel Kearns and Charles Dann III (University of Indiana, USA) provided strains, which is gratefully acknowledged. Gert Bange (SYNMIKRO, Marburg) provided helpful comments on the manuscript. This work was supported by the state of Hessen (LOEWE program, SYNMIKRO), and by the University of Marburg.

2.1.6 References

Asally, M., Kittisopikul, M., Rue, P., Du, Y., Hu, Z., Cagatay, T. *et al.* (2012) Localized cell death focuses mechanical forces during 3D patterning in a biofilm. *Proc Natl Acad Sci U S A* **109**: 18891-18896.

Branda, S.S., Gonzalez-Pastor, J.E., Ben-Yehuda, S., Losick, R., and Kolter, R. (2001) Fruiting body formation by *Bacillus subtilis*. *Proc Natl Acad Sci U S A* **98**: 11621-11626.

Branda, S.S., Chu, F., Kearns, D.B., Losick, R., and Kolter, R. (2006) A major protein component of the *Bacillus subtilis* biofilm matrix. *Mol Microbiol* **59**: 1229-1238.

Cairns, L.S., Hobley, L., and Stanley-Wall, N.R. (2014) Biofilm formation by *Bacillus subtilis*: new insights into regulatory strategies and assembly mechanisms. *Mol Microbiol* **93**: 587-598.

Campbell, A., Berg, D.E., Botstein, D., Lederberg, E.M., Novick, R.P., Starlinger, P., and Szybalski, W. (1977) Nomenclatur of transposable elements in prokaryotes In *DNA Insertion Elements, Plasmids and Episomes*. Bukhari, A.I., Shapiro, J.A., and Adhya, S.L. (eds): Cold Spring Harbor, New York, pp. 15-22.

Chai, Y., Beauregard, P.B., Vlamakis, H., Losick, R., and Kolter, R. (2012) Galactose metabolism plays a crucial role in biofilm formation by *Bacillus subtilis*. *MBio* **3**: e00184-00112.

Chan, J.M., Guttenplan, S.B., and Kearns, D.B. (2014) Defects in the flagellar motor increase synthesis of poly-gamma-glutamate in *Bacillus subtilis*. *J Bacteriol* **196**: 740-753.

Chen, L.H., Koseoglu, V.K., Guvener, Z.T., Myers-Morales, T., Reed, J.M., D'Orazio, S.E. *et al.* (2014) Cyclic di-GMP-dependent signaling pathways in the pathogenic Firmicute *Listeria monocytogenes*. *PLoS Pathog* **10**: e1004301.

Chen, Y., Chai, Y., Guo, J.H., and Losick, R. (2012) Evidence for cyclic Di-GMP-mediated signaling in *Bacillus subtilis*. *J Bacteriol* **194**: 5080-5090.

Costerton, J.W., Lewandowski, Z., Caldwell, D.E., Korber, D.R., and Lappin-Scott, H.M. (1995) Microbial biofilms. *Annu Rev Microbiol* **49**: 711-745.

Dahlstrom, K.M., Giglio, K.M., Collins, A.J., Sondermann, H., and O'Toole, G.A. (2015) Contribution of physical interactions to signaling specificity between a diguanylate cyclase and its effector. *MBio* **6**: e01978-01915.

Dogsa, I., Brloznik, M., Stopar, D., and Mandic-Mulec, I. (2013) Exopolymer diversity and the role of levan in *Bacillus subtilis* biofilms. *PLoS One* **8**: e62044.

Flemming, H.C., and Wingender, J. (2010) The biofilm matrix. *Nat Rev Microbiol* **8**: 623-633.

Friedman, L., and Kolter, R. (2004) Genes involved in matrix formation in *Pseudomonas aeruginosa* PA14 biofilms. *Mol Microbiol* **51**: 675-690.

Gao, X., Mukherjee, S., Matthews, P.M., Hammad, L.A., Kearns, D.B., and Dann, C.E., 3rd (2013) Functional characterization of core components of the *Bacillus subtilis* cyclic-di-GMP signaling pathway. *J Bacteriol* **195**: 4782-4792.

Hengge, R. (2009) Principles of c-di-GMP signalling in bacteria. *Nat Rev Microbiol* **7**: 263-273.

Hobley, L., Ostrowski, A., Rao, F.V., Bromley, K.M., Porter, M., Prescott, A.R. *et al.* (2013) BslA is a self-assembling bacterial hydrophobin that coats the *Bacillus subtilis* biofilm. *Proc Natl Acad Sci U S A* **110**: 13600-13605.

Jenal, U., and Malone, J. (2006) Mechanisms of cyclic-di-GMP signaling in bacteria. *Annu Rev Genet* **40**: 385-407.

Kobayashi, K., and Iwano, M. (2012) BslA(YuaB) forms a hydrophobic layer on the surface of *Bacillus subtilis* biofilms. *Mol Microbiol* **85**: 51-66.

Koseoglu, V.K., Heiss, C., Azadi, P., Topchiy, E., Guvener, Z.T., Lehmann, T.E. *et al.* (2015) *Listeria monocytogenes* exopolysaccharide: origin, structure, biosynthetic machinery and c-di-GMP-dependent regulation. *Mol Microbiol* **96**: 728-743.

Le Quere, B., and Ghigo, J.M. (2009) BcsQ is an essential component of the *Escherichia coli* cellulose biosynthesis apparatus that localizes at the bacterial cell pole. *Mol Microbiol* **72**: 724-740.

Lee, V.T., Matewish, J.M., Kessler, J.L., Hyodo, M., Hayakawa, Y., and Lory, S. (2007) A cyclic-di-GMP receptor required for bacterial exopolysaccharide production. *Mol Microbiol* **65**: 1474-1484.

Lewis, P.J., and Marston, A.L. (1999) GFP vectors for controlled expression and dual labelling of protein fusions in *Bacillus subtilis*. *Gene* **227**: 101-110.

Liang, Z.X. (2015) The expanding roles of c-di-GMP in the biosynthesis of exopolysaccharides and secondary metabolites. *Nat Prod Rep* **32**: 663-683.

Marvasi, M., Visscher, P.T., and Casillas Martinez, L. (2010) Exopolymeric substances (EPS) from *Bacillus subtilis*: polymers and genes encoding their synthesis. *FEMS Microbiol Lett* **313**: 1-9.

McLoon, A.L., Guttenplan, S.B., Kearns, D.B., Kolter, R., and Losick, R. (2011) Tracing the domestication of a biofilm-forming bacterium. *J Bacteriol* **193**: 2027-2034.

Merritt, J.H., Ha, D.G., Cowles, K.N., Lu, W., Morales, D.K., Rabinowitz, J. *et al.* (2010) Specific control of *Pseudomonas aeruginosa* surface-associated behaviors by two c-di-GMP diguanylate cyclases. *MBio* **1**.

Morikawa, M., Kagihiro, S., Haruki, M., Takano, K., Branda, S., Kolter, R., and Kanaya, S. (2006) Biofilm formation by a *Bacillus subtilis* strain that produces gamma-polyglutamate. *Microbiology* **152**: 2801-2807.

Nagorska, K., Ostrowski, A., Hinc, K., Holland, I.B., and Obuchowski, M. (2010) Importance of *eps* genes from *Bacillus subtilis* in biofilm formation and swarming. *J Appl Genet* **51**: 369-381.

Nicolas, P., Mader, U., Dervyn, E., Rochat, T., Leduc, A., Pigeonneau, N. *et al.* (2012) Condition-dependent transcriptome reveals high-level regulatory architecture in *Bacillus subtilis*. *Science* **335**: 1103-1106.

Robledo, M., Jimenez-Zurdo, J.I., Velazquez, E., Trujillo, M.E., Zurdo-Pineiro, J.L., Ramirez-Bahena, M.H. *et al.* (2008) *Rhizobium* cellulase CelC2 is essential for primary symbiotic infection of legume host roots. *Proc Natl Acad Sci U S A* **105**: 7064-7069.

Romero, D., Aguilar, C., Losick, R., and Kolter, R. (2010) Amyloid fibers provide structural integrity to *Bacillus subtilis* biofilms. *Proc Natl Acad Sci U S A* **107**: 2230-2234.

Roux, D., Cywes-Bentley, C., Zhang, Y.F., Pons, S., Konkol, M., Kearns, D.B. *et al.* (2015) Identification of poly-N-acetylglucosamine as a major polysaccharide component of the *Bacillus subtilis* biofilm matrix. *J Biol Chem* **290**: 19261-19272.

Scoffone, V., Dondi, D., Biino, G., Borghese, G., Pasini, D., Galizzi, A., and Calvio, C. (2013) Knockout of *pgdS* and *ggt* genes improves gamma-PGA yield in *B. subtilis*. *Biotechnol Bioeng* **110**: 2006-2012.

Shapiro, J.A. (1998) Thinking about bacterial populations as multicellular organisms. *Annu Rev Microbiol* **52**: 81-104.

Simm, R., Morr, M., Kader, A., Nimtz, M., and Romling, U. (2004) GGDEF and EAL domains inversely regulate cyclic di-GMP levels and transition from sessility to motility. *Mol Microbiol* **53**: 1123-1134.

Solano, C., Garcia, B., Latasa, C., Toledo-Arana, A., Zorraquino, V., Valle, J. *et al.* (2009) Genetic reductionist approach for dissecting individual roles of GGDEF proteins within the c-di-GMP signaling network in *Salmonella*. *Proc Natl Acad Sci U S A* **106**: 7997-8002.

Stewart, P.S., and Franklin, M.J. (2008) Physiological heterogeneity in biofilms. *Nat Rev Microbiol* **6**: 199-210.

Straight, P.D., Fischbach, M.A., Walsh, C.T., Rudner, D.Z., and Kolter, R. (2007) A singular enzymatic megacomplex from *Bacillus subtilis*. *Proc Natl Acad Sci U S A* **104**: 305-310.

Vlamakis, H., Chai, Y., Beauregard, P., Losick, R., and Kolter, R. (2013) Sticking together: building a biofilm the *Bacillus subtilis* way. *Nat Rev Microbiol* **11**: 157-168.
Xu, H., Chater, K.F., Deng, Z., and Tao, M. (2008) A cellulose synthase-like protein involved in hyphal tip growth and morphological differentiation in *Streptomyces*. *J Bacteriol* **190**: 4971-4978.
Xu, J., Kim, J., Koestler, B.J., Choi, J.H., Waters, C.M., and Fuqua, C. (2013) Genetic analysis of *Agrobacterium tumefaciens* unipolar polysaccharide production reveals complex integrated control of the motile-to-sessile switch. *Mol Microbiol* **89**: 929-948.
Zeigler, D.R., Pragai, Z., Rodriguez, S., Chevreux, B., Muffler, A., Albert, T. *et al.* (2008) The origins of 168, W23, and other *Bacillus subtilis* legacy strains. *J Bacteriol* **190**: 6983-6995.

2.1.7 Supplementary material

2.1.7.1 Bioinformatic analysis of components encoded within the *ydaJKLMN* operon (Text S1)

Based on sequence alignments, the first gene product YdaJ belongs to the six-hairpin glycosidase superfamily and is predicted to harbor a GH8 (glycosyl hydrolase) domain (**Fig. S2A**; NCBI). This domain is also present in already described extracellularly-acting endoglucanases such as BcsZ and PssZ from *E. coli* and *L. monocytogenes* respectively (Mazur and Zimmer, 2011; Koseoglu *et al.*, 2015) which are known to be involved in exopolysaccharide modification by cleaving β(1-4)-linked glycosidic bonds. Most likely, YdaJ performs its function outside the cytoplasm as its precursor appears to contain a signal peptide that is presumably cleaved off between position 20 and 21 aa, and the mature lipoprotein is apparently retained at the membrane by lipid modification via a cysteine residue (first residue in mature protein aa 21, as predicted by LipoP 1.0 server, Uniprot).

The second gene within the operon encodes for the transmembrane protein YdaK which we have described earlier in this article. The protein YdaL likely belongs to the carbohydrate esterase 4 superfamily (Phyr2), whose members include enzymes performing e.g. the deacetylation of peptidoglycan and chitin (CAZY, NCBI). Moreover, also the sequence of YdaL reveals a signal peptide for extracellular localization and contains a predicted C-terminally located transmembrane helix (**Fig. S2A**, SignalP 4.1, Uniprot, TMHMM 2.0). The function of YdaL is not obvious using biofinformatics, but the biological role of the proteins YdaM and YdaN is clearer: YdaM contains four predicted transmembrane helices and an enclosed predicted cytoplasmic glycosyltransferase domain (TMHMM 2.0, predicted dolichyl-phosphate beta-D-mannosyltransferase activity and lipid anchor for GDP-mannose by Uniprot). It belongs to the CESA-like cellulose synthase superfamily (CAZY, NCBI, **Fig. S2A**) comprising enzymes, among them a variety of glycosltransferase family 2 members (GT-A fold, DDG/DCD motif), as also

predicted for YdaM. Enzymes of this family catalyze the polymerization of activated sugar compounds using an inverting mechanism, like the bacterial cellulose synthase component BcsA for example (Morgan *et al.*, 2013; Morgan *et al.*, 2014). Among different other exopolysaccharides, bacterial cellulose-, alginate- and poly-β-N-acetylglucosamine- (PNAG) synthesizing mechanisms are classified as pathways belonging to the so-called synthase-dependent polysaccharide systems (reviewed in Whitney and Howell, 2013; Becker, 2015). In these systems, a membrane-embedded glycosyltransferase complex assembles and ensures the translocation of a growing polysaccharide chain across the inner membrane, in contrast to the so called Wzx/Wzy- and ATP-binding cassettes (ABC)-transporter-dependent pathways, which rely on flippases and efflux pump-like complexes, respectively, to guarantee the transfer across the inner membrane (reviewed in (Becker, 2015; Schmid *et al.*, 2015).

The last gene product, YdaN, belongs to the so-called BcsB superfamily (pfam03170). Sequence analysis of YdaN revealed a putative signal peptide for extracellular localization with a predicted cleavage site between residue 23 and 24 and a C-terminally located putative transmembrane helix (**Fig. S2A**, LipoP 1.0, TMHMM 2.0), indicating that YdaN might have a similar biological function as BcsB.

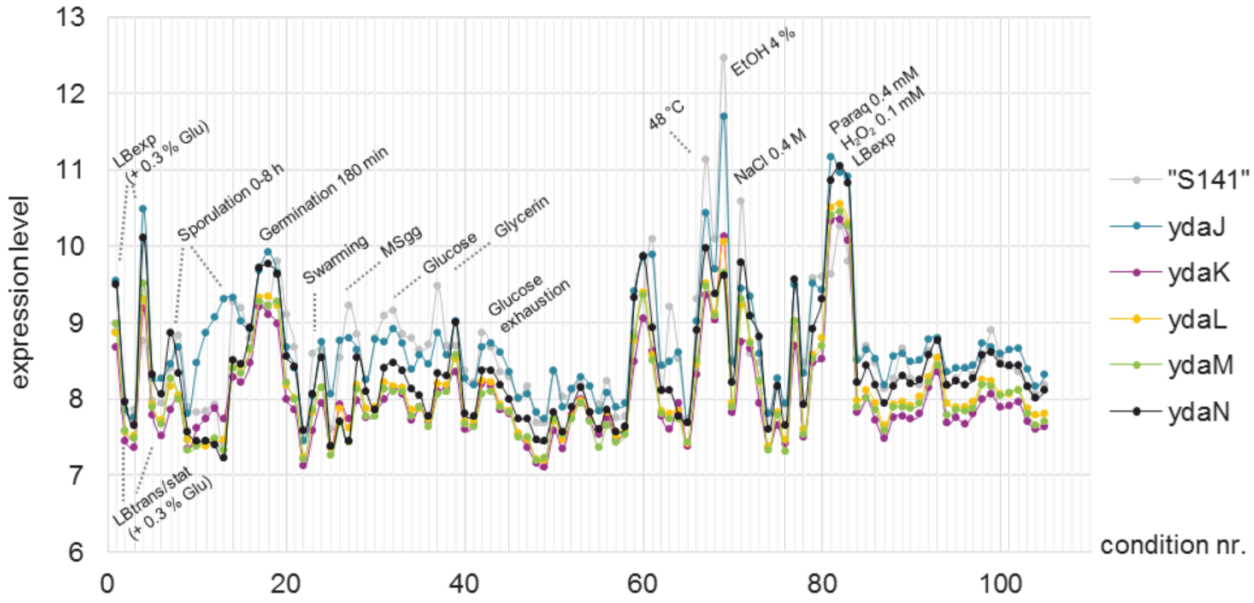

Fig. S1. Condition-dependent transcriptomes of *ydaJ* , *ydaK* (mangenta), *ydaL* (yellow), *ydaM* (green), *ydaN* (black) and of the 5´ upstream region "S141" (478812-478943, gray), as obtained by Nicolas *et al.*, 2012; http://subtiwiki.uni-goettingen.de/

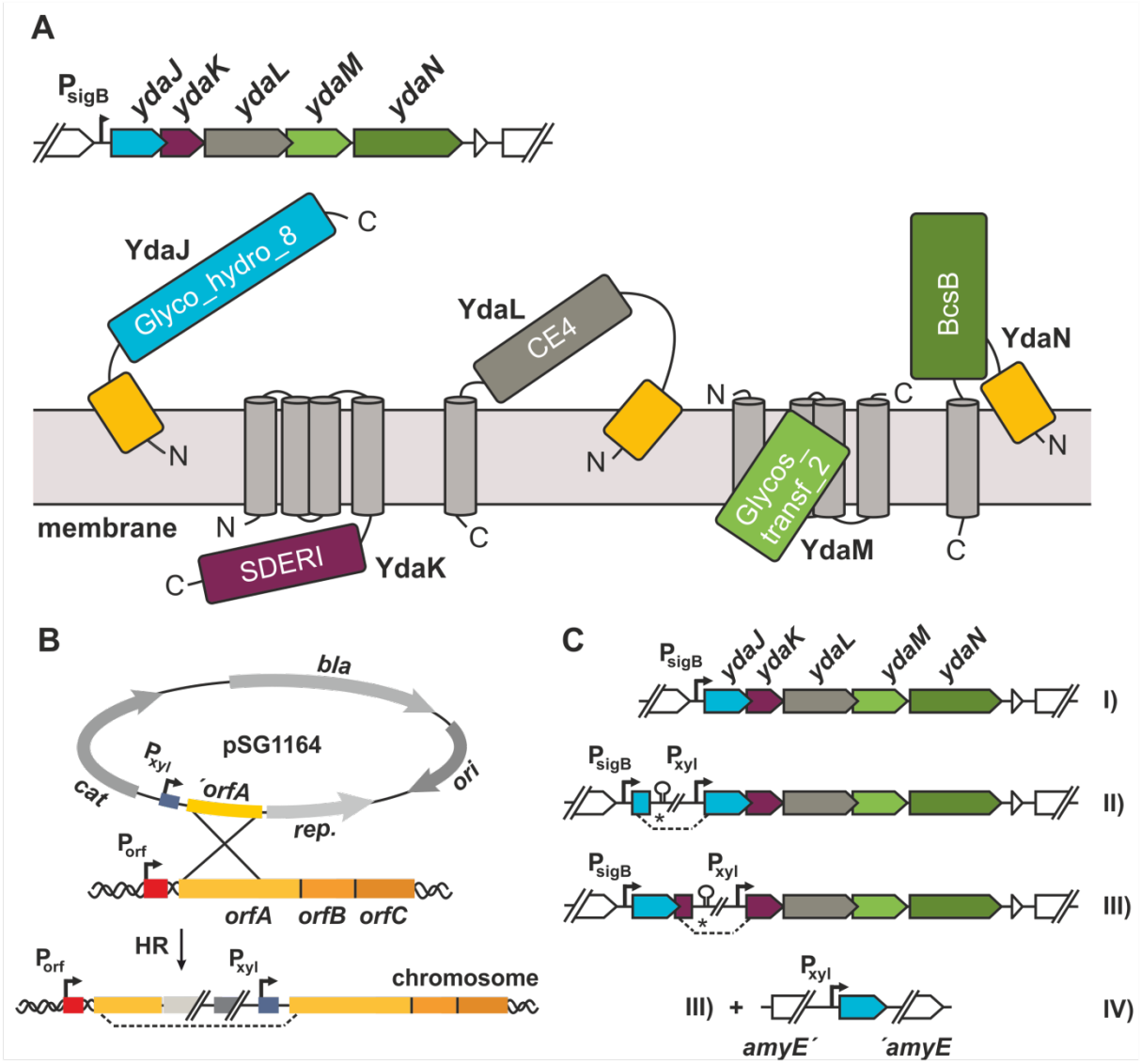

Fig. S2. Model for the putative *ydaJKLMN* encoded exopolysaccharide synthesis machinery

(**A**) Genomic organization of the *ydaJKLMN* operon in *B. subtilis* and predicted domain organization and topology of proteins encoded within the putative exopolysaccharide operon. Blue: GH8, Glycosyl hydrolase family 8, YdaJ/ *ydaJ*; Purple: degenerated GGDEF domain protein, c-di-GMP receptor YdaK/ *ydaK*; Grey: CE4, carbohydrate esterase 4 superfamily, YdaL/ *ydaL*; Lime: glycosltransferase family 2, YdaM/ *ydaM*; Green: BcsB superfamily, bacterial cellulose synthase subunit, YdaN/ *ydaN*. For a detailed description of domain and topology description see Text S1. (**B**) Integration of a representative recombinant pSG1164 plasmid, which allows the overexpression of a whole transcriptional unit, into the *B. subtilis* genome, adapted from (Dougherty et al., 2004) and (**C**) Genomic organization of the *ydaJKLMN* operon in WT strains *B. subtilis* 168 & NCIB3610 (P_{sigB}-*ydaJKLMN*) respectively (**I**) and the respective overexpression strains *B. subtilis* 168/NCIB3610-PB53 (P_{xyl}-*ydaJKLMN)* (**II**), *B. subtilis* 168/NCIB3610-PB55 (P_{xyl}-*ydaKLMN)* (**III**) and *B. subtilis* 168-PB55+PB15 (P_{xyl}-*ydaKLMN*; *amyE*::P_{xyl}-*ydaJ* (**IV**). * Indicates an insertional point mutation in the corresponding constructs; dashed lines represent the integrated plasmid into the genome.

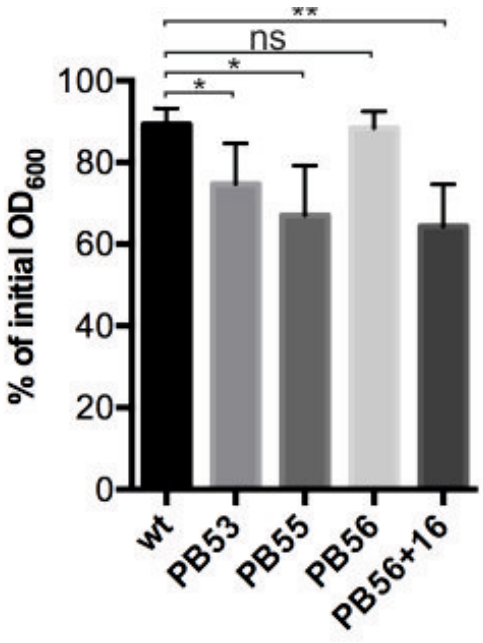

Fig. S3. EPS-dependent *B. subtilis* cell aggregation measured by spectrophotometry
Overnight cultures of *B. subtilis* 168 (wild type) and strains carrying integrated overexpression constructs pPB53 (P_{xyl}-*ydaJKLMN*), pPB55 (P_{xyl}-*ydaKLMN*), pPB56 (P_{xyl}-*ydaLMN*) and pPB56+pPB16 (P_{xyl}-*ydaLMN*; *amyE*::P_{xyl}-*ydaK*) were inoculated into LB supplemented with 0.1 % (w/v) xylose and grown to an OD_{600} of 1.0 at 37 °C. OD_{600} was determined before and 90 min after settling of cultures. Stars indicate significant differences from wild type (* < 0.05, ** < 0.005, two-sided independent T-test using GraphPadPrism V6). Expression of *ydaJKLMN* and *ydaKLMN* led to significant aggregation of strains 168-PB53, 168-PB55, 168-PB56+16 compared to aggregation of the wild type control.

2.1.7.2 Experimental procedures (Text S2)

Bacterial strains and growth conditions

Bacillus subtilis strains used in this study (**Table S3**) derived from the laboratory wild-type strain 168, the non-domesticated strain NCIB3610 and its derivative DK1042, a plasmid transformable *comI* mutant (Konkol *et al.*, 2013). *E. coli* DH5α was used for plasmid constructions and transformation using standard techniques (Mamiatis *et al.*, 1985).

E. coli strains were routinely cultivated at 37 °C and *B. subtilis* at 30 °C for overnight cultures and microscopy and at 37 °C previous to phenotypical tests in Luria-Bertani (LB) medium. The growth rate was determined by the optical density at 600 nm (OD_{600}). Prior to microscopy cells were washed twice in $S7_{50}$ minimal medium containing 1.0 % (w/v) fructose, 0.5 % (w/v) xylose, 0.1 % (w/v) glutamate, 0.004 % (w/v) casamino acids (Jaacks *et al.*, 1989).

When required, media were supplemented with the following antibiotics: ampicillin (100 μg ml^{-1}), chloramphenicol (5 μg ml^{-1}), spectinomycin (100 μg ml^{-1}), tetracycline (10 μg ml^{-1}) and kanamycin (5 μg ml^{-1}). For induction of the xylose promoter, glucose was exchanged for 0.1 % fructose, and xylose was added to 0.1 %. For induction of the hyperspank promoter, the culture medium was supplemented with 1 mM isopropyl-β-D-thiogalactopyranoside (IPTG).

Congo Red staining

For the determination of Congo Red binding in case of *B. subtilis* 168 derivatives, bacteria from overnight plates were restreaked on freshly prepared salt-free LB agar plates supplemented with Congo Red (40 μg ml^{-1}, Sigma), Coomassie Brilliant Blue (20 μg ml^{-1}, increases the color contrast of colonies on the agar, Sigma) and with or without 0.1 % (w/v) xylose or 1 mM IPTG. Otherwise plates were inoculated with 2 μl of an exponentially growing culture applied as small spots and incubated for 20 h at 30 °C. For photography of macro-colonies a conventional digital camera and a light screen were used.

Biofilm formation assay

B. subtilis NCIB3610 strains were picked from overnight growth on selective LB plates and cultured in LB containing appropriate antibiotics at 30 °C for 14 h. Daily cultures were prepared by diluting the overnight cultures 1:100 in LB followed by incubation at 37 °C to an OD_{600} of 1.0 without selective pressure. Subsequently LB was exchanged to MSgg [5 mM potassium phosphate (pH 7.0), 100 mM 3-(*N*-morpholino)propane-sulfonic acid (pH 7.0), 2 mM $MgCl_2$, 700 μM $CaCl_2$, 50 μM $MnCl_2$, 100 μM $FeCl_3$, 1 μM $ZnCl_2$, 2 μM thiamine, 0.5 % glycerol, 0.5 % glutamate] and cells were grown for additional 30 min at 37 °C before spotting 2 μl of cell

suspension on MSgg plates (solidified with 1.5 % Bacto agar, 6- or 12well plates, dried overnight at 30 °C) supplemented with Congo Red (40 μg ml^{-1}) and Coomassie Brilliant Blue (20 μg ml^{-1}) and with or without 0.1 % (w/v) xylose and or 1 mM IPTG (Branda *et al.*, 2001; Asally *et al.*, 2012). Plates were sealed and incubated up to 96 h at 25 °C. The colony morphology was analysed over time using the ChemiDocTM MP System (BIO-RAD).

Strain construction

***yda* overexpression mutants**

In order to generate strains overexpressing the *ydaJKLMN* operon or truncated versions of it, 3 overexpression constructs using the integrative vector pSG1164 (**Table S2**; **Fig. S2C**) were created: pSG1164-PB53, -PB55, -PB56. Approximately 500 bp of the 5´ region of the genes *ydaJ*, *ydaK* and *ydaL* were amplified first by PCR using the oligonucleotides (**Table S1**) PB15f/PB53r for ´*ydaJ*, PB16f/PB55r for ´*ydaK* and PB17f/PB56r for ´*ydaL* respectively and genomic DNA from *B. subtilis* NCIB3610 as a template. Resulting fragments were digested with *Apa*I/*Cla*I and ligated into the corresponding sites of pSG1164 downstream of a xylose-inducible promotor. Recombinant plasmids (**Table S2**) were introduced into *B. subtilis* strain 168 and *B. subtilis* NCIB3610 (DK1042, Konkol *et al.*, 2013) by genetic transformation as previously described (Zafra *et al.*, 2012). In order to verify correct single-crossover plasmid integration into the host genomes, PCR was performed allowing the amplification of the complete operon and the respective *ydaJ*/ *ydaK*-truncated overexpression version, by using a specific xylose promotor binding primer (PG5050f) and a primer complementary to the distal end of the operon (PB19r). For the integration of the corresponding constructs into the genome of a NCBI3610-derived *epsH* mutant DS9259 (Chan *et al.*, 2014), chromosomal DNA from the corresponding DK1042 strains was isolated first and subsequently 200-500 ng of DNA was transformed into the mutant.

Complementation strains

To generate strains which overexpress *ydaJ*, *ydaK* and a truncated version of *ydaK* (331-852 bp, *ggdef*) from the ectopic *amyE* locus under the control of a xylose promotor respectively, the corresponding coding sequences were amplified using the oligonucleotides (**Table S1**) PB15f/PB15r (*ydaJ*), PB16f/PB16r (*ydaK*), PB68f/PB16r (*ydaK*, 331-852 bp, *ggdef*) and chromosomal DNA of the *B. subtilis* wild type strain NCIB3610. The resulting fragments were further integrated in the expression vector pSG1193 by *Apa*I and *Spe*I giving rise to the plasmids pSG1193-PB15, -16, -68. The corresponding constructs were further integrated into the genomes of *B. subtilis* wild types 168 or NCIB3610 (DK1042) by plasmid transformation. A double-

crossover recombination of the DNA sequences at the *amyE* locus on the chromosomes was confirmed by screening loss of starch degradation.

Fusion proteins encoded at the original locus

To obtain C-terminal yellow fluorescent fusion proteins (Venus YFP with monomerizing A206K mutation), a minimum of 500 bp of the 3´ region of the respective genes were amplified first by PCR using the oligonucleotides PB10-PB14 listed in **Table S1** and chromosomal DNA of *B. subtilis* NCIB3610 as the template. The resulting fragments were cloned into plasmid pSG1164-NLMV by using isothermal "Gibson" assembly (Gibson *et al.*, 2009). Competent *B. subti4lis* 168 cells were transformed with plasmids pPB10, 13, 14, (**Table S2**) generating the strains listed in **Table S3**. In a similar way a xylose inducible N-terminal translational mCerulean-YdaM was generated. The 5' part of *ydaM (*about 500 bp) was amplified from chromosomal DNA and inserted between *Eco*RI and *Apa*I in pHJDS2 establishing pPB93 (**Table S2**).

Xylose-inducible translational fluorescent fusions

To generate inducible translational C-terminal fusions of YdaK and YdaN, the entire coding sequence missing the termination codon of the corresponding gene was amplified by PCR using NCIB3610 chromosomal DNA as a template and the following primer pairs: PB16f/PB24r and PB57f/PB57r for YdaK-CFP and YdaK-mV-YFP fusions respectively and PB96f/PB96r for YdaN-mV-YFP (**Table S1**). The resulting fragments were digested with *Eco*RI/*Apa*I and ligated into the corresponding sites of pSG1193-NLMV/ pSG1192 containing a spectinomycin resistance cassette, a polylinker downstream of the Pxylose promoter, and the gene encoding mV-YFP or CFP between the two arms of the *amyE* gene, to create pPB24/ pPB57 and pPB96 respectively. Recombinant plasmids were introduced into the *B. subtilis* strain 168 by genetic transformation.

Fluorescence microscopy

Cells were grown in LB rich medium under selective pressure to the exponential growth phase at 30 °C, 0.1 % (w/v) xylose was added to the growth media to induce expression of genes downstream of the encoded fusion protein at original locus or the encoded fusion protein itself at the *amyE* locus, and washed twice with $S7_{50}$ containing 1.0 % (w/v) fructose and 0.5 % (w/v) xylose prior to microscopy. For microscopy, 2 µl of cells were spotted on a coverslip and immobilized by a thin agarose pad [1 % (w/v) agarose in $S7_{50}$ minimal medium]. Total internal reflection fluorescence microscopy (TIRFM) was performed using a Zeiss Axio Observer A1 equipped with a 100 x TIRF objective (numerical aperture NA of 1.45) using the TIRF setup

from Visitron Systems (Munich, Germany). YFP fluorophores were excited by exposure to a 515 nm laser beam and CFP fluorophores to 445 nm. Images were acquired with an Evolve EM-CCD camera (Photometrix) and were processed with ImageJ (National Institutes of Health, Bethesda, MD).

Confocal microscopy was performed at a Leica SP8 LSM confocal microscope equipped with a 100x objective (NA 1.4). Fluorophores were excited with a pulsed white light laser source at 514 or 445 nm respectively. Photon emission was detected with gated hybrid detectors at the appropriate wavelength. Images were processed with the Leika LAS AF software and deconvolution was performed using the Huygens-algorithm. (200-400 Hz, 3x line average)

Bioinformatic analysis

The protein domain structures and topologies were analyzed using Pfam (http://www.sanger.ac.uk), SMART (http://www.smart.embl-heidelberg.de), UniProt (http://www.uniprot.org/), NCBI (http://www.ncbi.nlm.gov), TMHMM Server v. 2.0 (http://www.cbs.dtu.dk/services/TMHMM), SignalP Server v. 4.1 (http://www.cbs.dtu.dk /services/SignalP), LipoP 1.0 server (http://www.cbs.dtu.dk /services/LipoP) and CAZY (http://www.cazy.org).

Table S1. Oligonucleotides used in this study

Primer	Sequence 5´- 3´
PB10f	AAGGAGATTCCTAGGATGGGTACCGGAgcagagcttcggcgctca
PB10r	CCTCCCAGGCCAGATAGGCCGGGCCCtagttcattcatcatcatctcg
PB13f	AAGGAGATTCCTAGGATGGGTACCGGAgctatcacatccgctttttc
PB13r	CCTCCCAGGCCAGATAGGCCGGGCCCcccgcttttatgttgattgtat
PB14f	AAGGAGATTCCTAGGATGGGTACCGGAgacgttacagcaaatgatgcga
PB14r	CCTCCCAGGCCAGATAGGCCGGGCCCttctgtatctgtctttctttttt
PB15f	CATGGGCCCGTGAGGCATGTACTAATTG
PB15r	CCGACTAGTTCACTGAATGATATTT
PB16f	CATGGGCCCATGAAAATATCATTCAGTG
PB16r	ACGACTAGTTTATAGTTCATTCATCATC
PB17f	CATGGGCCCTTGCTATGCGTCATGATGC
PB19r	TCGACTAGTTTATTCTGTATCTGTCTTTC
PB24r	ATGAATTCTAGTTCATTCATCATCATC
PB53r	GCATCGATTCATATTGTATGTC
PB55r	GCATCGATTGAGCAGCAAAAACAC
PB56r	GCATCGATGAAAAGAATGCGTTGTG
PB57f	GCGAATTCATGAAAATATCATTCAG
PB57r	CATGGGCCCTAGTTCATTCATCATC
PB68f	CATGGGCCCATGCACGATATTACAG
PB93f	CATGGGCCCTTGGGTAATACGC
PB93r	CATGAATTCCGCATTGATGACG
PB96f	CATGAATTCTTGAAACAAATAATG
PB96r	CATGGGCCCTTCTGTATCTGTCTTTC
PG5050f	CAATTATTAGAGGTCATCGTTC

Table S2. Plasmids and vectors used in this study

Vector/plasmid	Relevant genotype	Source
pSG1164	*bla*, *cat*, *yfp*	Lewis and Marston, 1999
pSG1164-NLMV	*bla*, *cat*, *mVyfp*	Lab. stock
pSG1193	*bla*, *spec*, *yfp*	Lewis and Marston, 1999
pSG1192	*bla*, *spec*, *cfp*	Lewis and Marston, 1999
pSG1193-NLMV	*bla*, *spec*, *mVyfp*	Lab. stock
pHJDS2	*bla*, *cat*, *mCerulean*	Defeu Soufo and Graumann, 2006
pXG003	*amyE*::P_{IPTG}-*ydaK* (*spec*)	Gao et al., 2013
pSG1164-NLMV-PB10	*ydaK-mV-yfp* (*cat*)	This study
pSG1164-NLMV-PB13	*ydaM-mV-yfp* (*cat*)	This study
pSG1164-NLMV-PB14	*ydaN-mV-yfp* (*cat*)	This study
pSG1193-PB15	*amyE*::P_{xyl}-*ydaJ* (*spec*)	This study
pSG1193-PB16	*amyE*::P_{xyl}-*ydaK* (*spec*)	This study
pSG1193-PB68	*amyE*::P_{xyl}-$ydaK_{ggdef}$ (*spec*)	This study
pSG1192-CFP-PB24	*amyE*::P_{xyl}-*ydaK-cfp* (*spec*)	This study
pSG1164-PB53	P_{xyl}-*ydaJKLMN* (*cat*)	This study
pSG1164-PB55	P_{xyl}-*ydaKLMN* (*cat*)	This study
pSG1164-PB56	P_{xyl}-*ydaLMN* (*cat*)	This study
pSG1193-NLMV-PB57	*amyE*::P_{xyl}-*ydaK-mV-yfp* (*spec*)	This study
pHJDS2-PB93	P_{xyl}-*mcerulean-ydaM* (*cat*)	This study
pSG1193-NLMV-PB96	*amyE*::P_{xyl}-*ydaN-mV-yfp* (*spec*)	This study

Table S3. Strains used in this study

Strain	Relevant genotype	Source
B. subtilis 168	wild type, *trpC2*	Lab. stock
Derivatives of 168 (transformed with plasmid)		
168-PB10	*ydaK-mV-yfp* (*cat*), *trpC2*	This study
168-PB13	*ydaM-mV-yfp* (*cat*), *trpC2*	This study
168-PB14	*ydaN-mV-yfp* (*cat*), *trpC2*	This study
168-PB15	*amyE*::P_{xyl}-*ydaJ* (*spec*), *trpC2*	This study
168-PB16	*amyE*::P_{xyl}-*ydaK* (*spec*), *trpC2*	This study
168-PB24	*amyE*::P_{xyl}-*ydaK-cfp* (*spec*), *trpC2*	This study
168-PB53	P_{xyl}-*ydaJKLMN* (*cat*), *trpC2*	This study
168-PB55	P_{xyl}-*ydaKLMN* (*cat*), *trpC2*	This study
168-PB56	P_{xyl}-*ydaLMN* (*cat*), *trpC2*	This study
168-PB57	*amyE*::P_{xyl}-*ydaK-mV-yfp* (*spec*), *trpC2*	This study
168-PB68	*amyE*::P_{xyl}-$ydaK_{ggdef}$ (*spec*), *trpC2*	This study
168-PB93	P_{xyl}-*mCerulean-ydaM* (*cat*), *trpC2*	This study
168-PB96	*amyE*::P_{xyl}-*ydaN-mV-yfp* (*spec*), *trpC2*	This study
168-XG003	*amyE*::P_{IPTG}-*ydaK* (*spec*), *trpC2*	This study
168-PB13+PB24	*ydaM-mV-yfp* (*cat*), *amyE*::P_{xyl}-*ydaK-cfp* (*spec*), *trpC2*	pPB24→168-PB13
168-PB55+PB15	P_{xyl}-*ydaKLMN* (*cat*), *amyE*::P_{xyl}-*ydaJ* (*spec*), *trpC2*	pPB15→168-PB55 This study
168-PB56+PB16	P_{xyl}-*ydaLMN* (*cat*), *amyE*::P_{xyl}-*ydaK* (*spec*), *trpC2*	pPB16→168-PB56 This study
168-PB56+PB57	P_{xyl}-*ydaLMN* (*cat*), *amyE*::P_{xyl}-*ydaK-mV-yfp* (*spec*), *trpC2*	pPB57→168-PB56 This study
168-PB56+PB68	P_{xyl}-*ydaLMN* (*cat*), *amyE*:: P_{xyl}-$ydaK_{ggdef}$ (*spec*), *trpC2*	pPB68→168-PB56 This study
168-PB56+ pSG1193NLMV	P_{xyl}-*ydaLMN* (*cat*), *amyE*::P_{xyl}-*mV-yfp* (*spec*), *trpC2*	p1193→168-PB56 This study
168-PB56+XG003	P_{xyl}-*ydaLMN* (*cat*), *amyE*::P_{IPTG}-*ydaK* (*spec*), *trpC2*	pXG003→ 168-PB56 This study
168-PB93+PB57	P_{xyl}-*mcerulean-ydaM* (*cat*), *amyE*::P_{xyl}-*ydaK-mV-yfp* (*spec*), *trpC2*	pPB57→168-PB93 This study
168-PB93+PB96	P_{xyl}-*mcerulean-ydaM* (*cat*), *amyE*::P_{xyl}-*ydaN-mV-yfp* (*spec*), *trpC2*	pPB96→168-PB93 This study
B. subtilis NCIB3610	wild type, prototroph	BGSC
DK1042 (NCIB3610)	prototroph, *comI*^{Q12L}	BGSC, 3A38 Konkol *et al.*, 2013

Table S3. Strains used in this study (continued)

Strain	Relevant genotype	Source
Derivatives of DK1042 (transformed with plasmid DNA)		
NCIB3610-PB53	P_{xyl}-*ydaJKLMN* (*cat*), *comI*^{Q12L}	This study
NCIB3610-PB55	P_{xyl}-*ydaKLMN* (*cat*), *comI*^{Q12L}	This study
NCIB3610-PB56	P_{xyl}-*ydaLMN* (*cat*), *comI*^{Q12L}	This study
NCIB3610-PB56+PB16	P_{xyl}-*ydaLMN* (*cat*), *amyE*::P_{xyl}-*ydaK* (*spec*), *comI*^{Q12L}	pPB16→NCIB3610-PB56 This study
NCIB3610-PB56+ pSG1193NLMV	P_{xyl}-*ydaLMN* (*cat*), *amyE*::P_{xyl}-*mV-yfp* (*spec*), *comI*^{Q12L}	p1193→NCIB3610-PB56 This study
Derivatives of NCIB3610 (transformed with chromosomal DNA)		
DS9289	Δ*ydaK*	Gao *et al.*, 2013
DS859	*sinR*::*kan*	Blair et al., 2008
DS9259	*epsH*::*tet*	Chan *et al.*, 2014
DS9259-PB53	*epsH*::*tet*, P_{xyl}-*ydaJKLMN* (*cat*)	NCIB3610-PB53→DS9259 This study
DS9259-PB55	*epsH*::*tet*, P_{xyl}-*ydaKLMN* (*cat*)	NCIB3610-PB55→DS9259 This study

2.1.7.3 References supplementary material

Asally, M., Kittisopikul, M., Rue, P., Du, Y., Hu, Z., Cagatay, T. *et al.* (2012) Localized cell death focuses mechanical forces during 3D patterning in a biofilm. *Proc Natl Acad Sci U S A* **109**: 18891-18896.

Becker, A. (2015) Challenges and perspectives in combinatorial assembly of novel exopoly saccharide biosynthesis pathways. *Front Microbiol* **6**: 687.

Blair, K.M., Turner, L., Winkelman, J.T., Berg, H.C., and Kearns, D.B. (2008) A molecular clutch disables flagella in the Bacillus subtilis biofilm. *Science* **320**: 1636-1638.

Branda, S.S., Gonzalez-Pastor, J.E., Ben-Yehuda, S., Losick, R., and Kolter, R. (2001) Fruiting body formation by *Bacillus subtilis*. *Proc Natl Acad Sci U S A* **98**: 11621-11626.

Chan, J.M., Guttenplan, S.B., and Kearns, D.B. (2014) Defects in the flagellar motor increase synthesis of poly-gamma-glutamate in *Bacillus subtilis*. *J Bacteriol* **196**: 740-753.

Defeu Soufo, H.J., and Graumann, P.L. (2006) Dynamic localization and interaction with other *Bacillus subtilis* actin-like proteins are important for the function of MreB. *Molecular Microbiology* **62**: 1340-1356.

Dougherty, T.J., Barret, J.F., and Pucci, M.J. (2004) Genomics-Based Approaches to Novel Antimicrobial Target Discovery. In *Microbial Genomics and Drug Discovery* Dougherty, T.J., and Projan, S.J. (eds): Marcel Dekker, Inc. .

Gibson, D.G., Young, L., Chuang, R.Y., Venter, J.C., Hutchison, C.A., 3rd, and Smith, H.O. (2009) Enzymatic assembly of DNA molecules up to several hundred kilobases. *Nat Methods* **6**: 343-345.

Jaacks, K.J., Healy, J., Losick, R., and Grossman, A.D. (1989) Identification and characterization of genes controlled by the sporulation-regulatory gene spo0H in *Bacillus subtilis*. *J Bacteriol* **171**: 4121-4129.

Konkol, M.A., Blair, K.M., and Kearns, D.B. (2013) Plasmid-encoded ComI inhibits competence in the ancestral 3610 strain of *Bacillus subtilis*. *J Bacteriol* **195**: 4085-4093.

Koseoglu, V.K., Heiss, C., Azadi, P., Topchiy, E., Guvener, Z.T., Lehmann, T.E. *et al.* (2015) *Listeria monocytogenes* exopolysaccharide: origin, structure, biosynthetic machinery and c-di-GMP-dependent regulation. *Mol Microbiol* **96**: 728-743.

Lewis, P.J., and Marston, A.L. (1999) GFP vectors for controlled expression and dual labelling of protein fusions in *Bacillus subtilis*. *Gene* **227**: 101-110.

Mamiatis, T., Fritsch, E.F., Sambrook, J., and Engel, J. (1985) Molecular cloning–A laboratory manual. New York: Cold Spring Harbor Laboratory. 1982, 545 S., 42 $. *Acta Biotechnologica* **5**: 104-104.

Mazur, O., and Zimmer, J. (2011) Apo- and cellopentaose-bound structures of the bacterial cellulose synthase subunit BcsZ. *J Biol Chem* **286**: 17601-17606.

Morgan, J.L., Strumillo, J., and Zimmer, J. (2013) Crystallographic snapshot of cellulose synthesis and membrane translocation. *Nature* **493**: 181-186.

Morgan, J.L., McNamara, J.T., and Zimmer, J. (2014) Mechanism of activation of bacterial cellulose synthase by cyclic di-GMP. *Nat Struct Mol Biol* **21**: 489-496.

Schmid, J., Sieber, V., and Rehm, B. (2015) Bacterial exopolysaccharides: biosynthesis pathways and engineering strategies. *Front Microbiol* **6**: 496.

Whitney, J.C., and Howell, P.L. (2013) Synthase-dependent exopolysaccharide secretion in Gram-negative bacteria. *Trends Microbiol* **21**: 63-72.

Zafra, O., Lamprecht-Grandio, M., de Figueras, C.G., and Gonzalez-Pastor, J.E. (2012) Extracellular DNA release by undomesticated *Bacillus subtilis* is regulated by early competence. *PLoS One* **7**: e48716.

2.2 Article II

New functions and subcellular localization patterns of c-di-GMP components (GGDEF domain proteins) in *B. subtilis*.

2.2.1 Abstract

The universal and pleiotropic cyclic dinucleotide second messenger c-di-GMP is most prominently known to inversely regulate planktonic and sessile lifestyles of Gram-negative species. In the Gram-positive model organism *Bacillus subtilis*, intracellular c-di-GMP levels are modulated by a concise set of three diguanylate cylases (DgcK, DgcP, DgcW) and one phosphodiesterase (PdeH). Two recent studies have reported the negative influence of the c-di-GMP receptor DgrA (PilZ domain protein) on swarming motility indicating a conserved role of this second messenger across the bacterial domain. However, it has been suggested that the degenerated GGDEF protein YdaK and the inactive EAL domain protein YkuI may also function as c-di-GMP receptors regulating potentially other processes than motility. Here we describe a novel c-di-GMP dependent signaling network in *B. subtilis* regulating the production of an unknown exopolysaccharide (EPS) that leads to strongly altered colony morphologies upon overproduction. The network consists of the c-di-GMP receptor YdaK and the c-di-GMP synthetase DgcK. Both proteins establish a spatially close signal-effector cluster at the membrane. The cytoplasmic DgcP synthetase can complement for DgcK only upon overproduction, while the third c-di-GMP synthetase, DgcW, of *B. subtilis* is not part of the signaling pathway. Removal of the regulatory EAL domain from DgcW reveals a distinct function in biofilm formation. Therefore, our study is compatible with the "local pool signaling" hypothesis, but shows that in case of the *yda* operon, this can easily be overcome by overproduction of non-cognate DGCs, indicating that global pools can also confer signals to regulatory circuits in a Gram-positive bacterium.

2.2.2 Introduction

Bacteria utilize a multitude of regulatory processes to ensure the adaptation to environmental changes for the sake of growth- and survival optimization. Upon detection of diverse primary signals, transduction of these external stimuli into a cellular response can be ubiquitously realized by the production of purine nucleotide derivatives (Gomelsky, 2011; Hengge *et al.*, 2016). The dynamic synthesis- and degradation mechanisms of these so called second messengers have an enormous impact on corresponding cellular downstream effects as they determine and modulate the cellular levels and therefore, also (at least to some extent) the probability of interaction between second messengers and their specific effector molecules (effector proteins and/ or riboswitches, reviewed in Ryan *et al.*, 2012).

Bis-(3'–5')-cyclic dimeric guanosine monophosphate (c-di-GMP) is a well-established purine second messenger regulating most notably bacterial lifestyle orchestration. The consensus of numerous studies implies that an increase in c-di-GMP production correlates with a sessile lifestyle [biofilm (BF) formation], whereas low c-di-GMP levels favor planktonic cell behavior. Specific diguanylate cyclases (DGCs) harbor conserved GGDEF domains and synthesize c-di-GMP from two molecules of guanosine-5'-triphosphate (GTP), whereas specific phosphodiesterases (PDEs, containing either EAL or HD-GYP domains) mediate its degradation into the linear dinucleotide 5′-phosphoguanylyl-(3′,5′)-guanosine (pGpG) and/ or GMP (Romling *et al.*, 2013; Jenal *et al.*, 2017). Interestingly, these characteristic domains are frequently combined with diverse N-terminal soluble and/ or membrane-integrated domains which are primarily utilized for sensory purposes in order to modulate DGC and PDE activities respectively (Plate and Marletta, 2012; Zahringer *et al.*, 2013).

Another fundamental regulatory process of intracellular c-di-GMP homeostasis is the allosteric product inhibition of DGC activity (Christen *et al.*, 2006; De *et al.*, 2008; Schirmer and Jenal, 2009). This is achieved by the interaction of c-di-GMP with conserved auto-inhibitory I-site motifs (primary and secondary) in order to prevent over-consumption and excessive production of the substrate and the product respectively. Very recently, it was demonstrated that I-sites do not only contribute to the maintenance of c-di-GMP homeostasis as negative regulatory elements, but can also positively regulate the physical interaction of an active DGC with its specific c-di-GMP receptor (Dahlstrom *et al.*, 2016). I-site motifs can furthermore function as c-di-GMP "receptor sites" (activation motifs) of enzymatically inactive (degenerated) GGDEF domains to drive exopolysaccharide (EPS) synthesis for example (Chen *et al.*, 2014). By limiting the total amount of c-di-GMP available and additionally providing an interaction platform for corresponding effector molecules and interaction partners respectively, I-site motifs

of active and inactive GGDEF domains are thus able to modulate diverse levels of signal specificity.

Recently, we have proven the requirement of the potential c-di-GMP effector protein YdaK, a degenerated GGDEF-TM protein, for the synthesis of an extracellular matrix component generated by the products of the *yda*(*J*)*KLMN* (*ydaJ-N*) operon in *Bacillus subtilis* (Nicolas *et al.*, 2012; Bedrunka and Graumann, 2017). The unknown EPS strongly affects Congo Red (CR) binding and the characteristic morphology of *B. subtilis* macro colonies grown on BF-promoting medium, for example. Enhanced CR-binding can be likewise visualized in the absence of *epsH* belonging to the *epsA-O* cluster, which implies the production of an alternative EPS in case of *ydaJ-N* overexpression. Whether *ydaJ-N* overexpression has an effect on the expression of other matrix gene operons such as *epsA-O* and *tapA-sipW-tasA* remains to be clarified. In contrast to the *epsA-O* operon, which is essential for development of complex colony and pellicle BFs (Kearns *et al.*, 2005), deletions targeting the *ydaJ-N* operon have no influence on the establishment of such BFs (Gao *et al.*, 2013; Bedrunka and Graumann, 2017). Importantly, the influence of *ydaJ-N* on colony BF architecture can be recognized only upon overexpression (**Fig. S1**). Its potential significance on BF formation therefore requires further investigations using different experimental systems and conditions.

However, our previous findings provide a new tool to study the effect of c-di-GMP in *B. subtilis* with respect to EPS production via YdaK. For a while now, degenerated GGDEF domains have been known to function as positive regulators of EPS production most likely via their conserved I-site motifs (Liang, 2015), a mechanism that has been also proposed for YdaK. The TM-protein is not able to synthesize c-di-GMP, still it can bind the second messenger *in vitro* via its soluble degenerated GGDEF domain (Gao *et al.*, 2013).

In this study, we wanted to further investigate the potential c-di-GMP/ I-site dependent activation of EPS synthesis in *B. subtilis* and were especially interested whether a physiological relation between YdaK and *B. subtilis* DGCs does exist and whether this EPS promoting putative c-di-GMP effector can be genetically linked to the activity of one specific DGC.

Three different enzymes are capable of c-di-GMP synthesis in *B. subtilis*: the two GGDEF domain proteins DgcK and DgcP (formerly YhcK and YtrP) and the GGDEF-EAL domain protein DgcW (YkoW). The current knowledge on the cellular roles of c-di-GMP synthesizing enzymes in *B. subtilis* is limited to motility control, mediated by the interaction between DgrA (formerly YpfA, PilZ- domain protein) and the flagellar component MotA upon elevated intracellular c-di-GMP levels. However, the regulatory modes and physiological functions of these three DGCs with respect to EPS production/ BF formation and motility inhibition respectively remained unknown (Chen *et al.*, 2012; Gao *et al.*, 2013). Inactivation of *dgc* genes

(*dgcK*, *dgcP*, *dgcW*) in undomesticated *B. subtilis* strains, individually or in combination, results in no detectable phenotypes with respect to BF formation and motility (**Fig. 1AB**; Gao *et al.*, 2013; Chen *et al.*, 2012). However, overproduction of the GGDEF domain proteins DgcK and DgcP, as well as an overproduction of a DgcW variant lacking the adjacent EAL domain, respectively, causes a transient inhibition of swarming motility (Gao *et al.*, 2013). Under these circumstances, or upon deletion of the sole PDE gene *pdeH* (formerly *yuxH*), elevated intracellular c-di-GMP concentrations could be detected resulting in premature motility cessation via the "high affinity" c-di-GMP receptor DgrA [dissociation constant (K_D) 11 nM] but notably, in no observable alterations concerning BF formation (Gao *et al.*, 2013).

To approach the cellular functions of DGCs in *B. subtilis* with respect to EPS production/ colony BF formation, we generated diverse combinations of overexpression and deletion mutants. By examining their behavior towards BF formation, we are able to provide genetic and cell biological evidence for the existence of novel and distinct functions for DgcK, DgcP and DgcW. In order to extend our understanding of c-di-GMP signaling components in *B. subtilis*, a comparative fluorescence microscopy analysis of YdaK and its putative c-di-GMP delivering synthetases was carried out. Importantly, we show that both YdaK and DgcK fluorescent fusions form subcellular clusters and co-localize to the same cellular positions. Additionally, they exhibit similar dynamic behavior suggesting a physiological connection between YdaK and DgcK, as already implicated by our phenotypical analysis.

2.2.3 Results

2.2.3.1 Cell biological evidence for an implication of c-di-GMP in biofilm formation in *B. subtilis*

The "low affinity" c-di-GMP receptor YdaK (K_D 1 μM) does not serve as an effector protein to modulate swarming motility directly (Gao *et al.*, 2013), but instead affects BF formation by positively regulating the production of an unknown EPS synthesized by the products of the *ydaJ-N* operon (Bedrunka and Graumann, 2017).

We wanted to investigate the potential involvement of DGCs and thus c-di-GMP in EPS production via induction of YdaK. Deletion and overexpression of *ydaK* alone have not revealed any phenotypic effects so far. Therefore, we initially introduced two expression constructs pSG1164-PB53 (P_{xyl}-*ydaJ-N*) and pSG1164-PB55 (P_{xyl}-*ydaK-N*), steering the expression of the transcriptional units *ydaJ-N* and *ydaK-N* respectively, into the genome of wild type *B. subtilis* NCIB3610, and into that of a *dgc* triple mutant strain lacking the native c-di-GMP-synthesizing components (strain DS1809, Δ*dgcK* Δ*dgcW dgcP*::*tet*, **Fig. 1A**).

As shown in an earlier study (Bedrunka and Graumann, 2017), induction of *ydaJ-N* (strain NCIB3610-PB53, P_{xyl}-*ydaJ-N*) and overexpression of *ydaK-N* (strain NCIB3610-PB55, P_{xyl}-*ydaK-N*) respectively, lead to strongly altered and wrinkled colony morphologies and inhibited surface spreading behavior (**Fig. S1** and **Fig. 1A**, second and third row, respectively) of *B. subtilis* on solid BF medium (Branda *et al.*, 2001). These changes are indicative of EPS production as demonstrated for different bacterial species (Serra *et al.*, 2013).

Essentially, inactivation of all three *dgc* genes prevents the synthesis of this unknown EPS in both induction strains (Fig. 1A, fifth row: strain DS1809-PB53, Δ*dgcK*, -*P*, -*W*, P_{xyl}-*ydaJ-N*; sixth row: strain DS1809-PB55, Δ*dgcK*, -*P*, -*W*, P_{xyl}-*ydaK-N*). The morphology of these resembled that of the wild type supporting the c-di-GMP dependence of the *ydaJ-N*-related EPS machinery (**Fig. 1A**, first row).

We proceeded to test the effect of *ydaK-N* induction (construct pSG1164-PB55, P_{xyl}-*ydaK-N*) on BF-promoting medium in single *dgc* gene mutant backgrounds (**Fig. 1B**). Importantly, in strains in which the endogenous locus *dgcK* was deleted (strain DS9305-PB55, Δ*dgcK*, P_{xyl}-*ydaK-N*, **Fig. 1B**, third row) production of EPS by YdaK-N was completely abolished despite the presence of xylose, as respective colony architectures resembled wild type appearance (NCIB3610, P_{sigB}-*ydaJ-N*, **Fig. 1B**, first row). In contrast, disruption of *dgcP* did not impair EPS production via YdaK-N, reflected by the altered colony morphology in the case *ydaK-N* induction (strain DS9537-PB55, Δ*dgcP*, P_{xyl}-*ydaK-N*, **Fig. 1B**, right column, forth row), compared to the *dgcK*

background deletion strain (**Fig. 1B**, right column, third row). Similarly, deletion of *dgcW* also resulted in altered BF formation upon induction of *ydaK-N* (strain DS9883-PB55, Δ*dgcW*, P_{xyl}-*ydaK-N*, **Fig. 1B** right column, fifth row) implying that EPS production via YdaK-N is independent of DgcP and DgcW under our experimental conditions, but dependent of DgcK.

Thus, our experiments demonstrate that activation of EPS production via the degenerated GGDEF domain protein YdaK relies on the integrity of *dgc* genes and furthermore indicate that YdaK is activated via DgcK under BF-promoting conditions, which results in activation of EPS production in a c-di-GMP dependent manner. In order to further support the hypothesis of YdaK activation via c-di-GMP, we performed site directed replacement mutagenesis of conserved I-site (inhibitory site) residues in YdaK proposed to be involved in c-di-GMP binding (Gao *et al*., 2013, **Fig. 1C**). Based on sequence analysis, YdaK likely has a primary and secondary inhibitory site (Gao *et al*., 2013). The putative secondary I-site motif RxxR is found at residues R157 to R160, whereas the putative primary I-site motif RxxD (R202 to D205) locates five residues upstream of the degenerated active site motif SDERI (conserved motif GGDEF). To test the activity of the primary I-site variants, YdaK^{R202A} and YdaK^{D205A} (pXG003-PB80 & pXG003-PB81, respectively) were introduced at the ectopic *amyE* locus of strains that harbored a xylose-dependent promoter driving *ydaLMN* expression (pSG1164-PB56; **Fig. 1C**). Induction of *ydaLMN* alone (strain NCIB3610-PB56, P_{xyl}-*ydaL-N*, **Fig. 1C**, second row) did not result in EPS production as reflected by unaltered colony morphology of the correponding strain compared to *ydaK-N* overexpression (strain NCIB3610-PB55, P_{xyl}-*ydaK-N*; **Fig. 1C**, first row) in agreement with a previous study (Bedrunka and Graumann, 2017). Complementation with a wild type copy of *ydaK in trans* restored EPS production upon xylose and IPTG addition (strain NCIB3610-PB56-XG003, P_{xyl}-*ydaLMN*, *amyE*::P_{IPTG}-*ydaK*, **Fig 1C**, third row). However, when strain NCIB3610-PB56 (P_{xyl}-*ydaL-N*) was complemented with *ydaK* alleles encoding the R202A (NCIB3610-PB56-PB80, P_{xyl}-*ydaLMN, amyE*::P_{IPTG}-*ydaK*^{R202A}, **Fig. 1C**, forth row) or D205A point mutants (NCIB3610-PB56-PB81, P_{xyl}-*ydaLMN, amyE*::P_{IPTG}-*ydaK*^{D205A}, **Fig. 1C**, fifth row) respectively, EPS production was abolished. These observations suggest that an intact primary I-site motif of YdaK is required for c-di-GMP binding and thus YdaK activity.

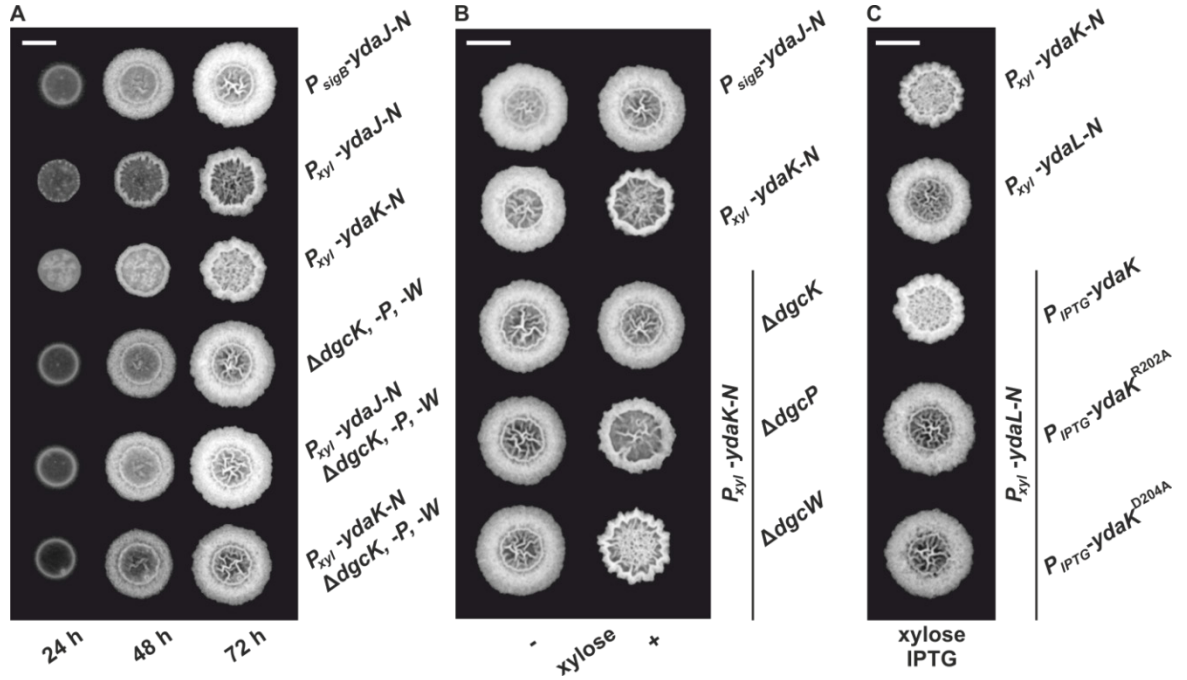

Fig. 1. Combinatorial deletions of *dgc* genes and particularly inactivation of *dgcK* and disruption of the putative YdaK I-site motif RxxD lead to an inhibition of Yda(J)KLMN-mediated EPS production in *B. subtilis*

(**A**) Top view of *B. subtilis* macro colony morphology and expansion on biofilm promoting medium (MSgg, Branda *et al.*, 2001) supplemented with 0.1 % (w/v) xylose, 40 μg/ml Congo Red (CR) and 20 μg/ml Coomassie Brilliant Blue (CB) at different timepoints for WT NCIB3610 (P_{sigB}-*ydaJ-N*), NCIB3610-PB53 (P_{xyl}-*ydaJ-N*), NCIB3610-PB55 (P_{xyl}-*ydaK-N*), DS1809 (Δ*dgcK*, -*P*, -*W*), DS1809-PB53 (Δ*dgcK*, -*P*, -*W*, P_{xyl}-*ydaJ-N*) and DS1809-PB55 (Δ*dgcK*, -*P*, -*W*, P_{xyl}-*ydaK-N*) at 25 °C. Reduced colony expansion and altered wrinkle patterns (*hyper-wrinkles*) indicate EPS production by the products of the *yda* operon. (**B**) *B. subtilis* biofilm morphology on MSgg (+ CR, CB) solid medium 72 h post-inoculation in the absence and presence of 0.1 % (w/v) xylose for wild type strain NCIB3610 (P_{sigB}-*ydaJ-N*), the overexpression strain NCIB3610-PB55 (P_{xyl}-*ydaK-N*) and combined overexpression and deletion mutants: DS9305-PB55 (Δ*dgcK*; P_{xyl}-*ydaK-N*), DS9537-PB55 (Δ*dgcP*; P_{xyl}-*ydaK-N*) and DS9883-PB55 (Δ*dgcW*; P_{xyl}-*ydaK-N*). (**C**) Colony morphology of the overproduction mutant strain NCIB3610-PB56 (P_{xyl}-*ydaL-N*) and the complementation strains NCIB3610-PB56-XG003 (P_{xyl}-*ydaL-N*; *amyE*::P_{IPTG}-*ydaK*), NCIB3610-PB56-PB80 (P_{xyl}-*ydaL-N, amyE*::P_{IPTG}-*ydaK*^{R202A}), NCIB3610-PB56-PB81 (P_{xyl}-*ydaL-N, amyE*::P_{IPTG}-*ydaK*^{D205A}) grown at 25 °C on MSgg (+ CR, CB) solid medium with 0.1 % (w/v) xylose and 1 mM IPTG after 72 h. Bars correspond to 5 mm.

2.2.3.2 DgcK, DgcP and truncated DgcW ("ΔEAL") can activate EPS production in *B. subtilis* via overproduced YdaK

Given that EPS production mediated by YdaK-N is suppressed in the absence of all three *dgc* genes and specifically upon disruption of *dgcK* (**Fig. 1AB**), we were interested whether the loss of the *ydaK-N* expression phenotype in a *dgc* triple mutant can be complemented only with *dgcK* or whether additional *dgc* genes (*dgcP*, *dgcW*) can positively influence the production of the unknown EPS, e.g. when they are overexpressed. Therefore, we introduced each *dgc* gene individually at the ectopic *amyE* locus under the control of an IPTG-inducible promoter, into the genome of the *dgc* triple mutant, which induces *ydaK-N* upon xylose addition, and tested BF formation in the presence or absence of xylose and IPTG, respectively (**Fig. 2A**). As expected, the overexpression of *dgcK* restored modified BF formation upon addition of xylose and IPTG (**Fig. 2A**, first column, first row, strain: DS1809-PB55-XG004, Δ*dgcK*, -*P*, -*W*, P_{xyl}-*ydaK-N*, *amyE*::P_{IPTG}-*dgcK*) as observed in wild type backgrounds (**Fig. 1B**, second column, second row, strain NCIB3610-PB55, P_{xyl}-*ydaK-N*). Interestingly, also an overexpression of *dgcP* restored hyper-wrinkle formation (**Fig. 2A**, second column, first row, strain: DS1809-PB55-XG002, Δ*dgcK*, -*P*, -*W*, P_{xyl}-*ydaK-N*, *amyE*::P_{IPTG}-*dgcP*).

In contrast to *dgcK* and *dgcP* (encoding GGDEF domain proteins), reintroduction of full length *dgcW* (coding for a GGDEF-EAL domain tandem protein) at the *amyE* site (**Fig. 2A**, third column, first row, strain: DS1809-PB55-XG001, Δ*dgcK*, -*P*, -*W*, P_{xyl}-*ydaK-N*, *amyE*::P_{IPTG}-*dgcW*) did not restore altered biofilm morphology of strain NCIB3610-PB55 (P_{xyl}-*ydaK-N*). However, colonies grown in the presence of IPTG/xylose (**Fig. 2A**, third column, first row) and IPTG (**Fig. 2A**, third column, third row) respectively, exhibited a distinct phenotype compared to the wild type (**Fig. 1A**, first column, first row). Overexpression of *dgcW* resulted in a visible reduction of thick wrinkle structures and in a loss of the associated central ring that usually marks the initial inoculation area, in a *dgc* triple mutant overexpressing *ydaK-N* (**Fig. 2A**, third column, first row) and also in wild type background (**Fig. 2B**, third column, first row).

This rather modest but reproducible BF-inhibiting phenotype became more severe when a DgcW variant was overproduced lacking the C-terminal EAL domain (**Fig. 2A**, forth column, third row; **Fig. 2B**, forth column, first row). Overexpression of *dgcW*-Δ*eal* caused an entire loss of wrinkle formation in the center of the macro colony in both genomic backgrounds, in DS1809-PB55 (**Fig. 2A**, forth column, third row, strain DS1809-PB55-XG086, Δ*dgcK*, -*P*, -*W*, P_{xyl}-*ydaK-N*, *amyE*::P_{IPTG}-*dgcW*Δ*eal*) and in NCIB3610 (**Fig. 2B**, forth column, first row, strain NCIB3610-XG086, *amyE*::P_{IPTG}-*dgcW*Δ*eal*). Furthermore, we found that induction of *ydaK-N* accompanied by an overexpression of *dgcW*-Δ*eal* lead to enhanced wrinkle formation and altered BF formation (**Fig. 2A**, forth column, first row, strain DS1809-PB55-XG086, Δ*dgcK*, -*P*, -*W*, P_{xyl}-*ydaK-N*,

amyE::P_{IPTG}-*dgcW*Δ*eal*). This suggests that a truncated version of DgcW is able to provide c-di-GMP to activate EPS production via YdaK.

In summary, our complementation analysis reveals that both DgcK and DgcP support EPS production when being overproduced, whereas DgcW is only able to do so upon deletion of the GGDEF-adjacent EAL domain. Therefore, we suggest that the activity of the EAL domain (potentially c-di-GMP hydrolysis) of DgcW masks the enzymatic activity of its neighboring (upstream) GGDEF domain (c-di-GMP synthesis). Because the overproduction of DgcW-ΔEAL by itself had a strong effect on BF morphology, our findings suggest that DgcW affects a pathway different from that of the *yda* operon, and that therefore, at least two independent c-di-GMP processes occur during BF formation in case of *ydaK-N* and *dgcW*Δ*eal* overexpression.

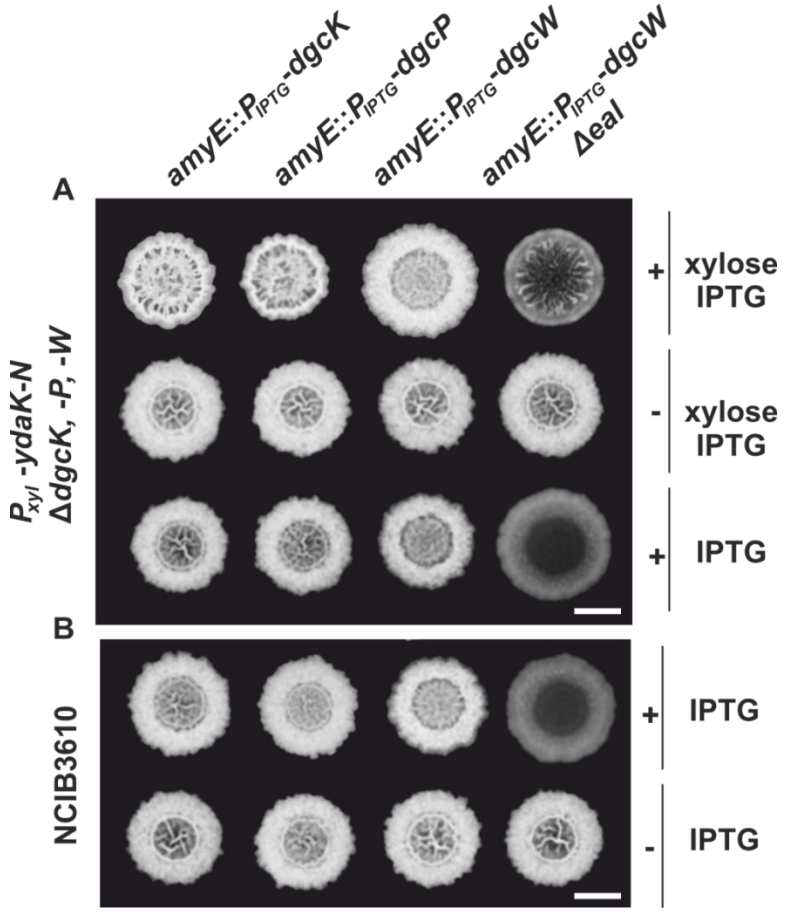

Fig. 2. Altered biofilm formation due to *ydaK-N* overexpression can be restored in a *dgc* triple mutant by providing *dgcK*, *dgcP* and *dgcW*Δ*eal in trans*
(**A**) Colony development on MSgg medium supplemented with CR 40 μg/ml, CB 20 μg/ml in the presence or absence of 0.1 % (w/v) xylose and/ or 1 mM IPTG, respectively, 72 h after incubation at 25 °C by strains: DS1809-PB55-XG004 (Δ*dgcK*, -*P*, -*W*, P_{xyl}-*ydaK-N*, *amyE*::P_{IPTG}-*dgcK*), DS1809-PB55-XG002 (Δ*dgcK*, -*P*, -*W*, P_{xyl}-*ydaK-N*, *amyE*::P_{IPTG}-*dgcP*), DS1809-PB55-XG001 (Δ*dgcK*, -*P*, -*W*, P_{xyl}-*ydaK-N*, *amyE*::P_{IPTG}-*dgcW*), DS1809-PB55-XG086 (Δ*dgcK*, -*P*, -*W*, P_{xyl}-*ydaK-N*, *amyE*::P_{IPTG}- *dgcW*Δ*eal*). Scale bar: 5 mm. (**B**) Biofilm colony morphology of *B. subtilis* NCIB3610

strains individually overexpressing *dgcK* (strain NCIB3610-XG004, *amyE*::P_{IPTG}-*dgcK*), *dgcP* (NCIB3610-XG002, *amyE*::P_{IPTG}-*dgcP*), *dgcW* (NCIB3610-XG001, *amyE*::P_{IPTG}-*dgcW*) and *dgcW*Δ*eal* (NCIB3610-XG086, *amyE*::P_{IPTG}-*dgcW*Δ*eal*) from the ectopic amylase locus. Scale bars: 5 mm.

2.2.3.3 Subcellular localization and dynamics of the c-di-GMP receptor YdaK and the DGCs DgcK and DgcP in *B. subtilis*

Several DGCs in different bacterial species have been reported to occur in complex with their effector proteins/ targets in order to maintain signal specificity within certain signaling cascades (Lindenberg *et al.*, 2013; Dahlstrom *et al.*, 2015). Additionally, it has been suggested that differential subcellular localization patterns of DGCs may affect their function and thus the interplay with its corresponding effectors (Merritt *et al.*, 2010; Zhu *et al.*, 2016). This prompted us to perform comparative localization studies of the c-di-GMP receptor YdaK and of the corresponding DGCs (DgcK and DgcP) that were able to restore EPS production mediated by YdaK-N in a *dgc* triple mutant (**Fig. 2A**).

In a recent study, we investigated the subcellular localization of YdaK and of its potential downstream targets, the putative glycosyltransferases YdaM and YdaN, by fluorescence microscopy (Bedrunka & Graumann, 2017). YdaK-, YdaM-, and YdaN-mV-YFP fusions (mV: monomeric Venus) expressed from their original promoter and at their native site on the chromosome, formed static subcellular clusters (usually one or two single foci per cell) at the membrane, predominantly at the septa and/ or at cell poles in exponentially growing *B. subtilis* cells. YdaM/YdaK and YdaM/ YdaN fluorescent fusions co-localized to the same cellular positions supporting the idea that specific protein localization at the cell membrane might be necessary to facilitate protein-protein interactions and EPS production.

Functional C-terminal mV-YFP fusions of full-length YdaK induced from the ectopic *amyE* site were able to support EPS activation in a mutant of undomesticated *B. subtilis* that induced *ydaL-N* upon xylose addition (strain NCIB3610-PB56-PB57, P_{xyl}-*ydaL-N*, *amyE*::P_{xyl}-*ydaK-mV-yfp*, **Fig. S2**) as depicted in **Fig. 3Aii** Ectopically induced YdaK-mV-YFP fusions primarily localized at the peripheries of cells as double foci at mid cell and/ or at the cell poles revealing high signal intensities but also as lateral patches with rather low signal intensities (**Fig. 3Aiii**). As an additional control, we included a C-terminal fluorescent fusion of YdaK lacking its 4 predicted TMHs (*transmembrane helices*, **Fig. 3Bi**) in this study.

The corresponding construct was introduced into the genome of NCIB3610-PB56 (resulting strain: NCIB-PB56-PB100, P_{xyl}-*ydaL-N, amyE*::P_{xyl}-*ydaK*Δ*4tmh-mV-yfp*; upper panel in **Fig. 3Bii**, **Fig. S2**). In contrast to YdaK-mV-YFP full length fusions (**Fig. 3A**) and wild type YdaK (NCIB3610-PB56-PB16, P_{xyl}-*ydaL-N, amyE*::P_{xyl}-*ydaK*; lower panel in **Fig. 3Bii**), the

truncated variants YdaKΔ4TMH-mV-YFP failed to restore altered BF formation upon overproduction resulting in unaffected colony morphologies. This is most likely due to the fact that removal of TMHs results in a cytoplasmic distribution of these fusion proteins (**Fig. 3Biii**), which is not due to degradation of the fusions as verified by Western blots of cell extracts using an antibody against GFP (**Fig. S2**). Thus, YdaK must localize in a complex with its downstream effector proteins YdaLMN at its native membrane position in order to activate EPS production at specific sites of the bacterial cell membrane, which we have already hypothesized earlier.

In view of these finding, we wondered whether DgcK, the specific c-di-GMP delivering DGC for YdaK (**Fig. 1B**), would resemble YdaK localization (**Fig. 3C**). Initially, we have examined the subcellular localization of C-terminal DgcK-mV-YFP produced from the original locus in *B. subtilis* NCIB3610 cells (strain NCIB3610-PB01, P_{dgcK}-*dgcK-mV-yfp*). Fusion proteins were hardly detectable suggesting low expression levels of *dgcK-mV-yfp* under our experimental conditions. Therefore, we visualized the subcellular localization of N- and C-terminal mV-YFP fusions of DgcK originated from the ectopic *amyE* locus upon xylose addition (strain NCIB3610-PB90, *amyE*::P_{xyl}-*dgcK-mV-yfp*). Only the translational C-terminal DgcK-mV-YFP proved to be functional (**Fig. 3Cii**, **Fig. S3**). The phenotypes of the *dgc* triple mutant strains, inducing *ydaK-N* from the original locus and *dgcK-mV-yfp* from the *amyE* locus (DS1809-PB55-PB90, Δ*dgcK*, -*P*, -*W*, P_{xyl}-*ydaK-N*, *amyE*::P_{xyl}-*dgcK-mV-yfp*), were similar to those of the Δ*dgcK*, -*P*, -*W* strains carrying the P_{xyl}-*ydaK-N* construct and the wild-type *dgcK* allele (DS1809-PB55-PB90, Δ*dgcK*, -*P*, -*W*, P_{xyl}-*ydaK-N*, *amyE*::P_{IPTG}-*dgcK*) in that both strains had altered BF morphologies and were comprised in colony spreading behavior (compare **Fig. 2A**, first column and **Fig. 3Cii**, first row). In contrast to this, overproduction of the fluorescent protein mV-YFP alone from the endogenous locus and induction of *ydaK-N* in a triple DGC mutant did not result in EPS production (DS1809-PB55-1193NLMV, Δ*dgcK*, -*P*, -*W*, P_{xyl}-*ydaK-N*, *amyE*::P_{xyl}-*mV-yfp*).

Similarly to our observation of YdaK-mV-YFP clustering (**Fig. 3Aiii**), DgcK-mV-YFP fusion proteins also formed assemblies that retained a preference of localization to the cell poles and septa in NCIB3610 (**Fig. 3Ciii**). This observation implies that DgcK and YdaK might be in spatial proximity at these cellular positions and might establish a spatially linked signal-effector cluster at the membrane. In addition to the comparable localization patterns of YdaK-mV-YFP and DgcK-mV-YFP (**Fig. 3**), both fusion proteins exhibited a similar movement behavior when overproduced. We performed time-lapse experiments with both fusion proteins produced from the *amyE* locus upon xylose addition in exponentially growing *B. subtilis* NCIB3610 wild type cells. Upon continuous illumination (515 nm) with 100 ms intervals, foci detected at the septa were predominantly static, displaying negligible movement within a time span of several hundred ms (**Fig. 4A**).

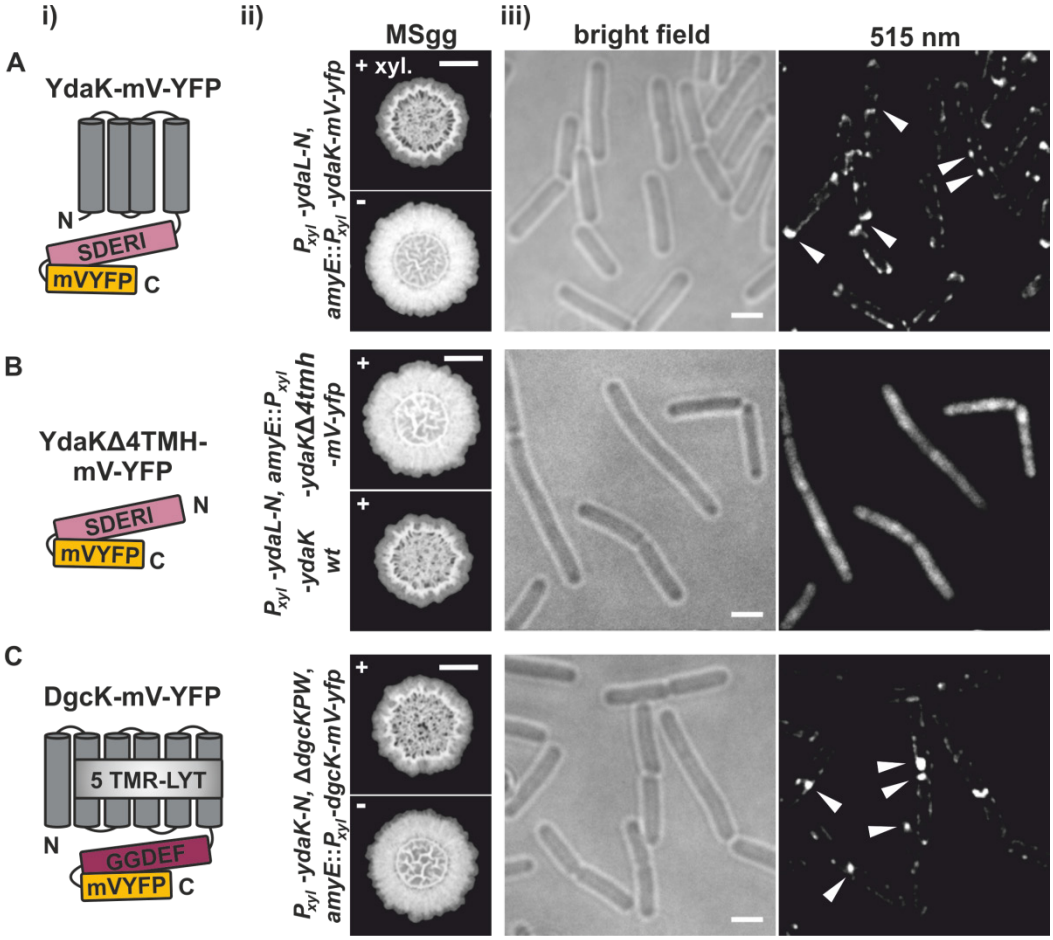

Fig. 3. Functional translational mV-YFP-fusions of the c-di-GMP receptor YdaK and of the synthase DgcK form subcellular assemblies at the cell poles and septa of exponentially growing *B. subtilis* NCIB3610

i) Schematic representation of (**A**) YdaK-mV-YFP-, (**B**) YdaKΔ4TMH-mV-YFP- and of (**C**) DgcK-mV-YFP- domain organization and topology (predicted by SMART). Grey: TM helices; light grey: predicted TM-receptor domain 5TMR–LYT; purple: GGDEF domain; light purple: GGDEF domain harboring the degenerated active site motif SDERI; yellow: C-terminal mV-YFP. **ii**) Verification of functionality of (**A**) YdaK-mV-YFP (strain: NCIB3610-PB56-PB57; P_{xyl}-*ydaL-N*, *amyE*::P_{xyl}-*ydaK-mV-yfp*) and of (**C**) DgcK-mV-YFP (strain: DS1809-PB55-PB90; Δ*dgcK*, -*P*, -*W*, P_{xyl}-*ydaK-N*, *amyE*::P_{xyl}-*dgcK-mV-yfp*). (**B**) Colony morphology of strain NCIB3610-PB56-PB100 (upper panel, P_{xyl}-*ydaL-N*, *amyE*::P_{xyl}-*ydaKΔ4tmh-mV-yfp*) and NCIB3610-PB56-PB16 (lower panel, P_{xyl}-*ydaL-N*, *amyE*::P_{xyl}-*ydaK*) in the presence of 0.1 % (w/v) xylose. Altered colony morphology in the presence of xylose reflects EPS production by the products of the *yda* operon and functionality of the corresponding fusion proteins. Unaltered colony morphology of strain NCIB3610-PB56-PB100 in contrast to strain NCIB3610-PB56-PB16 (lower panel, P_{xyl}-*ydaL-N*, *amyE*::P_{xyl}-*ydaK*) reflects inability of YdaKΔ4TMH-mV-YFP to stimulate EPS production Scale bars: 5 mm. **iii**) Mid-exponential-phase *B. subtilis* NCIB3610 cells expressing (**A**) *ydaK-mV-yfp* (strain: NCIB3610-PB56-PB57; P_{xyl}-*ydaL-N*, *amyE*::P_{xyl}-*ydaK-mV-yfp*), (**B**) *ydaKΔ4tmh-mV-yfp* (strain NCIB3610-PB56-PB100; P_{xyl}-*ydaL-N*, *amyE*::P_{xyl}-*ydaKΔ4tmh-mV-yfp*) and (**C**) *dgcK-mV-yfp* (strain NCIB3610-PB90, *amyE*::P_{xyl}-*dgcK-mV-yfp*) from the amylase locus, 45 min after induction with 0.1 % (w/v) xylose. Bars: 2 µm. White triangles indicate subcellular clustering of YdaK-mV-YFP and DgcK-mV-YFP respectively.

Polar foci were especially observed in case of YdaK-mV-YFP fusions and dynamic movement of both protein foci with lower "resting times" at the lateral cell periphery (**Movie S1**, **Movie S2**). Although we observed events of co-localization in only 30 % of total signals counted between DgcK-CFP (*amyE* locus) and YdaK-m-YFP (**Fig. 4B**, strain NCIB3610-PB37-PB10, *amyE*::P_{xyl}-*dgcK-cfp*, P_{ydaK}-*ydaK-mV-yfp*), our data strongly suggest that c-di-GMP signaling and YdaK activation by DgcK occurs at the cell membrane and employs close spatial proximity of the players involved.

In addition to the localization of YdaK and DgcK, we also monitored mV-YFP labeled DgcP fusions in *B. subtilis* NCIB3610 (**Fig. 5**, **Fig. S4**). DgcP is a c-di-GMP synthesizing protein containing N-terminal GAF domains (putative sensor domain) and a C-terminal GGDEF domain, hinting that it is most likely a soluble protein in contrast to YdaK, DgcK and DgcW. To test for the functionality of N- and C-terminal fusions, we applied the same complementation assay as described for DgcK (compare to **Fig. 3**). Overexpression of *mV-yfp-dgcP* and of *dgcP-mV-yfp* respectively, in a DGC triple mutant inducing YdaK-N (strains: DS1809-PB55-PB85, Δ*dgcK*, *-P*, *-W*, P_{xyl}-*ydaK-N*, *amyE*::P_{xyl}-*mV-yfp-dgcP*; DS1809-PB55-PB86, Δ*dgcK*, *-P*, *-W*, P_{xyl}-*ydaK-N*, *amyE*::P_{xyl}-*dgcP-mV-yfp*) caused altered BF colony morphologies (**Fig. 5AB**, "MSgg panel") in the same manner as seen for overexpression of *dgcK-mV-yfp* (**Fig. 3Bii**).

Interestingly, stable mV-YFP-DgcP (**Fig. 5A**, left panel, **Fig S4**) and DgcP-mV-YFP (**Fig. 5A**, right panel, **Fig. S4**) both assembled to subcellular clusters at the periphery of exponentially growing cells (produced from the ectopic *amyE* locus, strains NCIB3610-PB85, *amyE*::P_{xyl}-*mV-yfp-dgcP*; NCIB3610-PB86, *amyE*::P_{xyl}-*dgcP-mV-yfp*). Furthermore, both fusion proteins moved dynamically through the cell, but frequently arrested at the cell membrane for several 100 ms intervals (**Fig. 5B**, **Movie S3**, **Movie S4**). A similar behavior was observed for DgcP-mV-YFP whose synthesis was initiated by its native promoter at its original locus resulting in low amounts of fusion proteins (**Fig. 5C**, **Fig. S4**). Thus, we conclude that DgcP would be able to deliver c-di-GMP to YdaK potentially through spatial proximity at the cell membrane. However, it is equally possible that YdaK is activated simply by elevated cytosolic c-di-GMP levels following the overproduction of DgcP (see deltaEAL-DgcW).

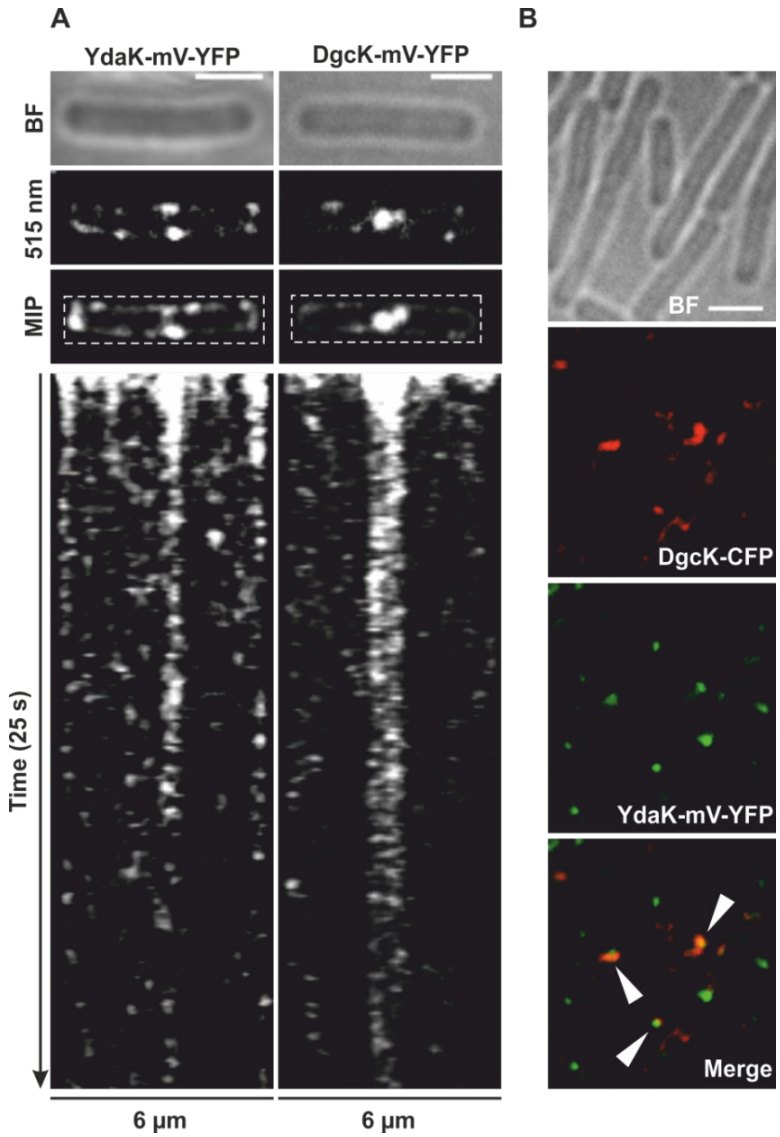

Fig. 4. Dynamics and simultaneous localization of YdaK and DgcK in *B. subtilis* NCIB3610

(**A**) Representative time-lapse kymographs of YdaK-mV-YFP (left panel, strain NCIB3610-PB57; *amyE*::P_{xyl}-*ydaK-mV-yfp*) and DgcK-mV-YFP (right panel, strain NCIB3610-PB90; *amyE*::P_{xyl}-*dgcK-mV-yfp*) 45 min after induction with 0.1 % xylose (w/v). BF: bright field (first row); snapshots (second row) and maximum intensity projection (MIP, third row) from time-lapse microscopy; fourth row: kymographs of fluorescence intensities along the rectangular selection depicted in the third row. Images were taken every 0.1 seconds upon continous illumination with 515 nm. (**B**) Co-localization of DgcK-CFP (445 nm, false colored red) originated from the ectopic *amyE* locus and YdaK-mV-YFP (515 nm, false-colored green) produced from the original locus, triangles indicate co-localization events (strain NCIB3610-PB37-PB10; *amyE*::P_{xyl}-*dgcK-cfp*, P_{ydaK}-*ydaK-mV-yfp*). Scale bars: 2 µm.

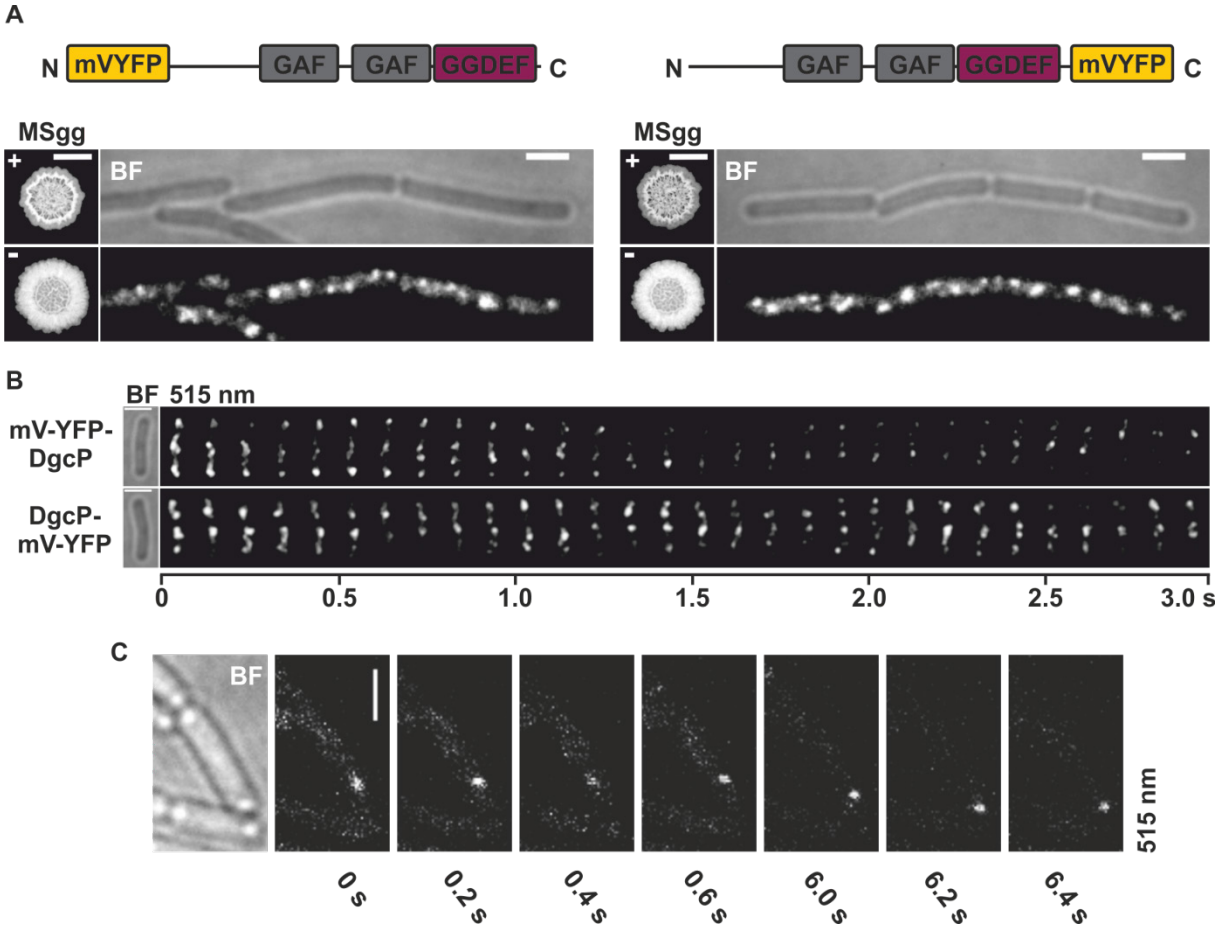

Fig. 5. Subcellular localization and dynamics of DgcP in *B. subtilis* NCIB3610
(**A**) Epifluorescence of cells overexpressing *mV-yfp-dgcP* (left panel, strain NCIB3610-PB85; *amyE*::P_{xyl}-*mV-yfp-dgcP*) and *dgcP-mV-yfp* (right panel, strain NCIB3610-PB86; *amyE*::P_{xyl}-*dgcP-mV-yfp*) 45 min after induction with 0.1 % (w/v) xylose (Scale bars: 2 μm). The "MSgg panel" depicts the functionality assay for the corresponding fusion protein/ strain in the presence and absence of 0.1 % (w/v) xylose (left: DS1809-PB55-PB85, Δ*dgcK*, *-P*, *-W*, P_{xyl}-*ydaK-N*, *amyE*::P_{xyl}-*mV-yfp-dgcP*; right: DS1809-PB55-PB86, Δ*dgcK*, *-P*, *-W*, P_{xyl}-*ydaK-N*, *amyE*::P_{xyl}-*dgcP-mV-yfp*). Scale bar: 5mm. Color code for schematic representation of corresponding fusion protein (domain organization predicted by SMART): grey: GAF (domain found in cGMP-specific phosphodiesterases, adenylyl and guanylyl cyclases and phytochromes which often serves as a cyclic nucleotide binding domain), purple: GGDEF domain (active site motif GGEEL), yellow: N- and C-terminal mV-YFP respectively. (**B**) Time-lapse fluorescence microscopy of DgcP fusions produced. Images were captured every 100 ms under continious illumination (515 nm). Bars: 2 μm. (**C**) Time-lapse microscopy of DgcP-mV-YFP produced from the original locus (strain NCIB3610-PB08). Images were captured at the time points (seconds) indicated next to the panels at time intervals of 200 ms. Bars: 2 μm.

2.2.4 Discussion

For Gram-positive bacteria, where the physiological role of c-di-GMP is not as well-characterized as in Gram-negative bacteria, c-di-GMP was demonstrated to influence, for example, swarming motility in the model organism *B. subtilis,* while it was not reported to have an effect on BF formation in this organism (Gao *et al.*, 2013). Our study reveals that EPS production and therefore also potentially BF formation, are regulated by c-di-GMP, most likely post-translationally, via the effector protein YdaK (degenerated GGDEF domain protein), encoded within the putative EPS-synthesis operon *ydaJ-N* (Nicolas *et al.*, 2012; Bedrunka and Graumann, 2017). The function of the unknown EPS in terms of BF formation, however, requires further examinations. Under our experimental conditions, YdaK is directed in its activity via DGC DgcK. We found that the presence of *dgc* genes and particularly the presence of *dgcK* and furthermore an intact conserved I-site motif (RxxD) of YdaK are indispensable for the production of an unknown EPS synthesized by YdaK-N on BF promoting medium, thereby revealing a new function for one of the three known DGC enzymes in *B. subtilis*.

DgcK was first mentioned in the course of comparative genomic analysis revealing novel families of putative membrane-associated receptors (Anantharaman and Aravind, 2003). In this context, DgcK (formerly YhcK) and LytS from *B. subtilis* were selected to be the eponyms for the 5TMR –LYT family (for 5 transmembrane receptors of the LytS-YhcK type, PF07694) sharing a conserved membrane-spanning domain encompassing 5 TM helices harboring distinctive sequence features (ligand binding). Its mode of activation remains to be clarified. Interestingly, orthologs of DgcK [DgcA (Lmo1911) and DgcB (Lmo1912)] have been demonstrated to control ManNAc-Gal EPS synthesis (a β-1,4-linked N-acetylmannosamine chain decorated with α-1,6-linked galactose) via a degenerated GGDEF domain protein (PssE, encoded in the *pssABCDE* operon) in *Listeria monocytogenes* suggesting that this signaling cascade might be conserved in Gram-positive species (Chen *et al.*, 2014; Koseoglu *et al.*, 2015). However, members of the *B. cereus* group contain the ortholog gene *cdgA* (Fagerlund *et al.*, 2016) but no operon similar to *ydaJ-M* of *B. subtilis*. Considering this, our study cannot exclude the possibility that DgcK affects other c-di-GMP signaling pathways even in *B. subtilis* via different effector proteins. The c-di-GMP receptor DgrA (PilZ domain protein) negatively influences swarming motility upon elevated intracellular c-di-GMP levels (Chen *et al.*, 2012; Gao *et al.*, 2013). However, the source of c-di-GMP "feeding" this receptor still needs to be elucidated. One could speculate that upon detection of an unknown signal (activation via 5TMR-LYT) DgcK activates both, DgrA and YdaK and thus swarming motility and EPS production respectively can be inversely regulated in order to mediate motile-to-sessile transition, the initial step of BF formation (Belas, 2014).

The direct regulation via DgcK notwithstanding, the activation of *B. subtilis* YdaK can also be accomplished by an overproduction of DgcP, which suggests that either DgcP has the potential to weakly activate the putative EPS machinery under normal conditions, or that globally elevated c-di-GMP concentrations due to the overproduction of the corresponding DGC are responsible for the activation of the machinery, i.e. that c-di-GMP signaling can be overcome by enhanced levels of a non-cognate DGC.

Moreover, overproduction of a truncated version of the third DGC, DgcW (a TM GGDEF-EAL tandem protein), lacking its C-terminal EAL domain also leads to an activation of YdaK. The construct mediated a transient cessation of swarming motility, when overexpressed in a GGDEF quadruple mutant, whereas overproduction of full length DgcW did not alter motility behavior via the PilZ domain protein DgrA (Gao *et al.*, 2013). Thus, we suggest that an elimination of the EAL domain leads to elevated c-di-GMP concentrations in comparison to the WT protein and consequently activation of the *yda* operon can occur. On the other hand, we can exclude that DgcW influences the putative EPS machinery under physiological conditions because an overexpression of full length DgcW could not restore EPS production. Intriguingly, we found a new c-di-GMP-associated phenotype concerning biofilm formation during overexpression of truncated DgcW, in that we observed a profound effect on BF formation, suggesting that unbalanced production of c-di-GMP through DgcW interferes with biofilm maturation. The GGDEF domain of DgcW harbors a degenerated I-site motif (instead of RxxD, PxxG). Therefore, we hypothesize that the BF defect is a result of elevated c-di-GMP concentrations and thus a secondary effect, as DgcW-ΔEAL may not be subjected allosteric product inhibition in contrast to DgcK/P, or an elimination of the EAL domain results in an "exposure" of interaction sides for potential interaction partners/ receptors of the GGDEF domain, thereby providing sufficient c-di-GMP concentrations that are limited in the WT protein by the adjacent EAL domain. It will be interesting to examine the potential involvement of the three proposed c-di-GMP receptors (DgrA, YdaK, YkuI) in the process of BF inhibition upon overproduction of DgcW-ΔEAL. Noteworthy, *dgcW* is assigned to the SigD regulon and co-expressed with various chemotaxis proteins (Nicolas *et al.*, 2012; SubtiWiki) suggesting that DgcW might be linked to chemotaxis regulation potentially even through the activity of a yet unidentified c-di-GMP receptor in *B. subtilis*.

Besides the investigation of functions of DGCs in *B. subtilis*, we wanted to expand our knowledge on the dynamic behavior of GGDEF proteins in living cells. The presence of numerous DGC, PDE and c-di-GMP receptor-encoding genes in various bacterial genomes raises questions regarding the mechanisms that establish specificity within these apparent diverse regulatory circuits (Hengge, 2009). One hypothesis proposes spatial proximity of c-di-GMP

metabolizing proteins, effectors and targets, producing small localized specific concentrations as suggested in several studies (Merritt *et al.*, 2010; Dahlstrom *et al.*, 2015). We provide evidence that in *B. subtilis*, such a module shows subcellular clustering within the cell membrane. YdaK and DgcK co-localized to the same subcellular positions in the cell membrane establishing a potential c-di-GMP source-target network, which possibly ensures discrete c-di-GMP pools that are not utilized by other working modules, as already suggested for different other bacterial organisms (Guvener and Harwood, 2007; Ryan *et al.*, 2010; Tan *et al.*, 2014). Furthermore, both fusion proteins localized preferentially to the septa of exponentially growing cells where they exhibited high fluorescence intensities, indicating that both fusion might form higher oligomeric structures.

However, activation of EPS production can be also accomplished by potential non-cognate DGCs. Thus it remains unclear whether c-di-GMP routes in *B. subtilis* do depend on central c-di-GMP hubs or whether they can be locally administrated (Valentini *et al.*, 2016). For DgcP, we found diffusive movement within the cytosol, which contrasts the membrane-integral localization of DgcK, but interestingly, DgcP also arrested at many sites along the cell membrane, indicating that it may interact with a membrane-bound receptor. Enhanced levels of DgcP may thereby provide c-di-GMP directly to YdaK, but it is also possible that elevated cellular c-di-GMP levels activate YdaK in a non-specific manner. This idea is supported by the finding that overproduced DgcW lacking the EAL domain can also lead to an activation of the *yda* operon. Therefore, both local and global c-di-GMP pools appear to play important roles in signaling pathways in *B. subtilis*.

It will be interesting to further investigate *in vivo* dynamics of DGCs, or their receptors and of their regulated proteins, in order to obtain a more detailed view of the molecular mechanism operating based on local and/ or global c-di-GMP signaling.

2.2.5 Materials & methods

General methods and bacterial growth conditions

DNA manipulation and *Escherichia coli* DH5α transformations were carried out using standard techniques (Mamiatis *et al.*, 1985; Gibson *et al.*, 2009). *E. coli* strains were routinely cultivated at 37 °C in Lysogeny Broth (LB) medium supplemented with 100 μg ml^{-1} ampicillin. Lists of utilized plasmids and oligonucleotides are provided in Supplementary **Table S2** and **S3** respectively. All constructs were verified by DNA sequencing.

Bacillus subtilis strains used in this study derived from the non-domesticated strain NCIB3610 (BGSC) or its transformable derivative DK1042 (Gift from D. Kearns). For transformation of both classes of derivatives, *B. subtilis* overnight cultures were grown in liquid LB at 30 °C and were diluted to OD_{600} 0.08 in 10 ml of a modified competence medium (Zafra *et al.*, 2012). Inoculated cells were further incubated at 37 °C and 200 rpm. Upon entry into stationary phase (OD_{600} 1.4-1.6), 300-500 ng of purified genomic DNA were added to 1 ml culture of NCIB3610 derivatives and 0.5-1 μg of plasmid DNA to 1 ml culture of DK1042 derivatives respectively. Cells were further incubated at 37 °C and 200 rpm for 2 h followed by selection on solid medium with the appropriate antibiotic. Final antibiotic concentrations were: 5 μg ml^{-1} chloramphenicol, 50-100 μg ml^{-1} spectinomycin and 10 μg ml^{-1} tetracycline. Supplementary **Table S1** provides a detailed description of strains and whether they were generated by plasmid- or by chromosomal DNA-transformation.

For routine growth, *B. subtilis* cells were streaked from frozen stocks onto LB agar plates and incubated overnight at 37 °C. Overnight cultures were grown at 30°C and 200 rpm in LB under antibiotic selective pressure and at 37 °C previous to phenotypical tests and fluorescence microscopy. Prior to microscopy cells were washed twice in $S7_{50}$ minimal medium containing 1.0 % (w/v) fructose, 0.5 % (w/v) xylose, 0.1 % (w/v) glutamate, 0.004 % (w/v) casamino acids (Jaacks *et al.*, 1989). For induction of the xylose promoter, xylose was added up to 0.1 % (w/v). For induction of the hyperspank promoter, the culture medium was supplemented with 1 mM isopropyl-β-D-thiogalactopyranoside (IPTG).

Strain construction

yda expression constructs

To generate strains overexpressing the transcriptional unit *ydaJ-N* or truncated variants of it (*ydaK-N*, *ydaL-N*), we used three overexpression constructs: pSG1164-PB53, -PB55, -PB56 (Bedrunka and Graumann, 2017). Recombinant plasmids were introduced into *B. subtilis*

NCIB3610 (DK1042) by genetic transformation (Zafra *et al*., 2012). Correct single-crossover plasmid integration into the host genome was verified by PCR using a specific xylose promoter binding primer (PG5050f) and a primer complementary to the distal end of the operon (PB19r) as already described in Bedrunka and Graumann (2017). For integration of the corresponding constructs into the genomes of NCBI3610 derived *dgc* mutants, which were kindly provided by Charles Dann III and Daniel Kearns (Indiana), first chromosomal DNA from the corresponding DK1042 strains was isolated and subsequently 300-500 ng of purified DNA was transformed into the corresponding *dgc* mutant backgrounds. The maintenance of gene deletions was verified via PCR using the oligonucleotides (2928-3040) listed in **Table S3**.

Complementation strains

Overexpression constructs of *ydaK*, *dgcK*, *dgcP*, *dgcW* and of *dgcW*Δ*eal* under the control of a hyperspank promotor at the *amyE* site respectively (pXG003, pXG004, pXG002, pXG001, pXG086) were kindly provided by the Labs of Charles Dann III and Daniel Kearns (Indiana). The corresponding constructs were integrated first into the genomes of *B. subtilis* NCIB3610 (DK1042) by plasmid transformation. A double-crossover recombination of the DNA sequences at the *amyE* locus on the chromosomes was confirmed by screening loss of starch degradation. To overexpress the corresponding genes in the NCIB3610 derived *dgc* mutant strains which also overexpress the *ydaK-N* operon (strain DS1809-PB55), chromosomal DNA was isolated from DK1042 derivatives and further transformed into the corresponding mutant strains (300-500 ng). Mutations R202A and D204A in YdaK were created using a PCR-based site-directed mutagenesis kit (Q5 Site-Directed Mutagenesis Kit, NEB). Mutagenesis was performed on plasmid pXG003 carrying the *ydaK* gene using primer pairs PB80f/PB80r for R202A and PB81f/PB81r for D204A, respectively. Mutant alleles were fully sequenced to verify mutations.

Xylose-inducible translational fluorescent fusions (at *amyE*)

To generate inducible translational C-terminal fusions of YdaK, YdaKΔ4TMH, DgcK, DgcP and DgcW to mVenus-YFP (Venus YFP with monomerizing A206K mutation) or CFP, the corresponding coding sequences missing the stop codon, were amplified by PCR using NCIB3610 chromosomal DNA as a template and primer pairs PB57f/PB57r for *ydaK-mV-yfp*, PB100f/PB57r for *ydaK*Δ4*tmh-mV-yfp*, PB90f/PB90r for *dgcK-mV-yfp* and PB21f/PB37r *dgcK-cfp*, PB86f/PB86r for *dgcP-mV-yfp* and PB88f/PB88r for *dgcW-mV-yfp*, respectively (Table S3). The resulting fragments were digested and ligated into the corresponding sites of pSG1193-NLMV containing a spectinomycin resistance cassette, a polylinker downstream of the xylose promoter, and the gene encoding mV-YFP between the two arms of the *amyE* gene. For C-terminal CFP

fusions, *dgcK* was cloned into pSG1192 (Lewis and Marston, 1999). The resulting recombinant plasmids are listed in Table S2. Constructs for N-terminal YFP fusions of DgcK, DgcP and DgcW were generated in a similar manner using oligonucleotides PB21f/PB79r for *dgcK*, PB20f/PB85r for *dgcP* and PB87f/PB87r for *dgcW* and plasmid pSG1729-MVYFP. Recombinant plasmids were introduced into the *B. subtilis* strain DK1042 by genetic transformation. A double-crossover recombination of the DNA sequences at the *amyE* locus on the chromosomes was confirmed by screening loss of starch degradation and stability of fusion proteins was verified by immune-detection using anti-GFP serum (see below). To overexpress fusion genes in NCIB3610 derived *dgc* mutant strains which also overexpress the truncated *ydaKLMN* operon (strain DS1809-PB55) and to test for their functionality, chromosomal DNA was isolated from DK1042 derivatives and further transformed into the corresponding mutants (300-500 ng).

Fusion proteins encoded at the original locus

To obtain *mV-yfp* gene fusions of *dgcK*, *ydaK*, and *dgcP*, which are encoded at the endogenous locus and expression is driven by the respective original promotor, a minimum of 500 bp of the 3´ region of the genes was amplified first by PCR using the oligonucleotides, PB01/f/PB01r, PB10f/PB10r and PB08f/PB08r respectively. The resulting fragments were cloned into plasmid pSG1164-NLMV using overlapping sequences [isothermal "Gibson" assembly (ITA), Gibson *et al.*, 2009]. Competent cells of DK1042 were transformed with the plasmids pSG1164-NLMV-PB01, pSG1164-NLMV-PB10 and pSG1164-NLMV-PB08 generating the strains listed in Table S1. For Co-localization studies of YdaK-mV-YFP and DgcK-CFP, plasmid pSG1164-NLMV-PB10 was transformed into NCIB3610-PB37 (*amyE*::P_{xyl}-*dgcK-cfp*) resulting in strain NCIB3610-PB37-PB10.

Biofilm formation assay

Undomesticated *B. subtilis* NCIB3610 strains were cultured in LB containing appropriate antibiotics at 30 °C for 14 h. Daily cultures were grown in LB at 37 °C to an OD_{600} of 1.0 without antibiotics. For biofilm growth, bacteria from a liquid LB culture were collected and transferred to liquid MSgg medium [5 mM potassium phosphate (pH 7.0), 100 mM 3-(*N*-morpholino) propane-sulfonic acid (pH 7.0), 2 mM $MgCl_2$, 700 μM $CaCl_2$, 50 μM $MnCl_2$, 100 μM $FeCl_3$, 1 μM $ZnCl_2$, 2 μM thiamine, 0.5 % glycerol, 0.5 % glutamate]. Cells were incubated for additional 30 min at 37°C and 200 rpm before inoculation (2 μl) on MSgg plates (MSgg medium fortified with 1.5 % Bacto agar, 6- well plates, dried overnight) supplemented with Congo Red (40 μg ml^{-1}) and Coomassie Brilliant Blue (20 μg ml^{-1}) and with or without 0.1 % (w/v) xylose and or 1 mM IPTG (Branda *et al.*, 2001; Asally *et al.*, 2012). Plates were sealed and incubated up to 72 h at 25 °C.

Colony morphology was documented over time using the ChemiDocTM MP System (BIO-RAD). For each strain, we analyzed 3 biological replicates in at least two independent experiments.

Fluorescence microscopy

Cells were grown in LB rich medium under selective pressure to the exponential growth phase at 37 °C. D-xylose was added in different concentrations [0.001 %, 0.01 % and 0.1 % (v/v)] to the growth media to induce expression of genes downstream of the encoded fusion protein at original locus or the encoded fusion protein itself at the *amyE* locus for 45 min at 37 °C. For microscopy, 2 µl of washed cells were spotted on a coverslip and immobilized by a thin agarose pad [1% (w/v) agarose in $S7_{50}$ minimal medium]. Fluorescence microscopy was performed using a Zeiss Axio Observer A1 equipped with a 100 x TIRF objective (numerical aperture NA of 1.45) using the setup from Visitron Systems (Munich, Germany). YFP fluorophores were excited by exposure to a 515 nm laser beam and CFP fluorophores to 445 nm. Images were acquired with an Evolve EM-CCD camera (Photometrix) and were processed with ImageJ (National Institutes of Health, Bethesda, MD).

Immunoblotting

To validate expression levels of fusion genes and stability of fusion proteins respectively, cells were grown in LB medium at 37 °C until exponential phase and gene expression was artificially induced with different xylose concentrations in case of *amyE* encoded gene fusions. 45 min after induction and incubation at 37 °C and 200 rpm, equal amounts of cells were resuspended in lysis buffer (50 mM EDTA, 100 mM NaCl, 2.5 mg ml^{-1} lysozyme, 0.1 mg ml^{-1} RNase, 0.01 mg ml^{-1} DNase, pH 7.5) and incubated for 20 min at 37 °C. SDS sample buffer (final concentration, 1 X) was added to the cell lysate and boiled at 95 °C for 10 min, except for lysates which derived from strain NCIB3610-PB90 (*amyE*::P_{xyl}-*dgcK-mV-yfp*). These samples were incubated at RT for 1 h prior to SDS-PAGE on 4-20 % (v/v) Tris/ Glycin gradient gels which have been also used for separation of YdaK fusion proteins. DgcP fusion proteins were separated via SDS-PAGE on 12 % (v/v) gels. The proteins were transferred to a nitrocellulose membrane, applying the semidry Western blotting method for 1 h and 45 mA and YFP-fused proteins were visualized by a primary polyclonal α-GFP antiserum (dilution, 1:500) and a secondary goat α-rabbit antiserum coupled to a horseradish peroxidase.

2.2.6 Acknowledgments

We would like to thank Daniel Kearns and Charles Dann III (University of Indiana, USA) for kindly providing us with strains and plasmids, and Nina El Najjar, Thomas Rösch and Gert Bange (SYNMIKRO, Marburg) for helpful comments on the manuscript. This work was supported through funding from the LOEWE program of the state of Hessen for the Centre of Synthetic Microbiology (SYNMIKRO) and by the University of Marburg.

2.2.7 References

Anantharaman, V., and Aravind, L. (2003). Application of comparative genomics in the identification and analysis of novel families of membrane-associated receptors in bacteria. *BMC Genomics* 4(1), 34. doi: 10.1186/1471-2164-4-34.

Asally, M., Kittisopikul, M., Rue, P., Du, Y., Hu, Z., Cagatay, T., *et al.* (2012). Localized cell death focuses mechanical forces during 3D patterning in a biofilm. *Proc Natl Acad Sci U S A* 109(46), 18891-18896. doi: 10.1073/pnas.1212429109.

Bedrunka, P., and Graumann, P.L. (2017). Subcellular clustering of a putative c-di-GMP-dependent exopolysaccharide machinery affecting macro colony architecture in *Bacillus subtilis*. *Environ Microbiol Rep* in press. doi: 10.1111/1758-2229.12496.

Belas, R. (2014). Biofilms, flagella, and mechanosensing of surfaces by bacteria. *Trends Microbiol* 22(9), 517-527. doi: 10.1016/j.tim.2014.05.002.

Branda, S.S., Gonzalez-Pastor, J.E., Ben-Yehuda, S., Losick, R., and Kolter, R. (2001). Fruiting body formation by *Bacillus subtilis*. *Proc Natl Acad Sci U S A* 98(20), 11621-11626. doi: 10.1073/pnas.191384198.

Chen, L.H., Koseoglu, V.K., Guvener, Z.T., Myers-Morales, T., Reed, J.M., D'Orazio, S.E., *et al.* (2014). Cyclic di-GMP-dependent signaling pathways in the pathogenic Firmicute *Listeria monocytogenes*. *PLoS Pathog* 10(8), e1004301. doi: 10.1371/journal.ppat.1004301.

Chen, Y., Chai, Y., Guo, J.H., and Losick, R. (2012). Evidence for cyclic Di-GMP-mediated signaling in *Bacillus subtilis*. *J Bacteriol* 194(18), 5080-5090. doi: 10.1128/JB.01092-12.

Christen, B., Christen, M., Paul, R., Schmid, F., Folcher, M., Jenoe, P., *et al.* (2006). Allosteric control of cyclic di-GMP signaling. *J Biol Chem* 281(42), 32015-32024. doi: 10.1074/jbc.M603589200.

Dahlstrom, K.M., Giglio, K.M., Collins, A.J., Sondermann, H., and O'Toole, G.A. (2015). Contribution of physical interactions to signaling specificity between a diguanylate cyclase and its effector. *MBio* 6(6), e01978-01915. doi: 10.1128/mBio.01978-15.

Dahlstrom, K.M., Giglio, K.M., Sondermann, H., and O'Toole, G.A. (2016). The inhibitory site of a diguanylate cyclase is a necessary element for interaction and signaling with an effector protein. *J Bacteriol* 198(11), 1595-1603. doi: 10.1128/JB.00090-16.

De, N., Pirruccello, M., Krasteva, P.V., Bae, N., Raghavan, R.V., and Sondermann, H. (2008). Phosphorylation-independent regulation of the diguanylate cyclase WspR. *PLoS Biol* 6(3), e67. doi: 10.1371/journal.pbio.0060067.

Fagerlund, A., Smith, V., Rohr, A.K., Lindback, T., Parmer, M.P., Andersson, K.K., *et al.* (2016). Cyclic diguanylate regulation of *Bacillus cereus* group biofilm formation. *Mol Microbiol* 101(3), 471-494. doi: 10.1111/mmi.13405.

Gao, X., Mukherjee, S., Matthews, P.M., Hammad, L.A., Kearns, D.B., and Dann, C.E., 3rd (2013). Functional characterization of core components of the *Bacillus subtilis* cyclic-di-GMP signaling pathway. *J Bacteriol* 195(21)**,** 4782-4792. doi: 10.1128/JB.00373-13.

Gibson, D.G., Young, L., Chuang, R.Y., Venter, J.C., Hutchison, C.A., 3rd, and Smith, H.O. (2009). Enzymatic assembly of DNA molecules up to several hundred kilobases. *Nat Methods* 6(5)**,** 343-345. doi: 10.1038/nmeth.1318.

Gomelsky, M. (2011). cAMP, c-di-GMP, c-di-AMP and now cGMP: bacteria use them all! *Mol Microbiol* 79(3)**,** 562-565.

Guvener, Z.T., and Harwood, C.S. (2007). Subcellular location characteristics of the *Pseudomonas aeruginosa* GGDEF protein, WspR, indicate that it produces cyclic-di-GMP in response to growth on surfaces. *Mol Microbiol* 66(6)**,** 1459-1473. doi: 10.1111/j.1365-2958.2007.06008.x.

Hengge, R. (2009). Principles of c-di-GMP signalling in bacteria. *Nat Rev Microbiol* 7(4)**,** 263-273. doi: 10.1038/nrmicro2109.

Hengge, R., Grundling, A., Jenal, U., Ryan, R., and Yildiz, F. (2016). Bacterial signal transduction by cyclic di-GMP and other nucleotide second messengers. *J Bacteriol* 198(1)**,** 15-26. doi: 10.1128/JB.00331-15.

Jaacks, K.J., Healy, J., Losick, R., and Grossman, A.D. (1989). Identification and characterization of genes controlled by the sporulation-regulatory gene spo0H in *Bacillus subtilis*. *J Bacteriol* 171(8)**,** 4121-4129.

Jenal, U., Reinders, A., and Lori, C. (2017). Cyclic di-GMP: second messenger extraordinaire. *Nat Rev Microbiol*. doi: 10.1038/nrmicro.2016.190.

Kearns, D.B., Chu, F., Branda, S.S., Kolter, R., and Losick, R. (2005). A master regulator for biofilm formation by *Bacillus subtilis*. *Mol Microbiol* 55(3)**,** 739-749. doi: 10.1111/j.1365-2958.2004.04440.x.

Koseoglu, V.K., Heiss, C., Azadi, P., Topchiy, E., Guvener, Z.T., Lehmann, T.E., *et al.* (2015). *Listeria monocytogenes* exopolysaccharide: origin, structure, biosynthetic machinery and c-di-GMP-dependent regulation. *Mol Microbiol* 96(4)**,** 728-743. doi: 10.1111/mmi.12966.

Lewis, P.J., and Marston, A.L. (1999). GFP vectors for controlled expression and dual labelling of protein fusions in *Bacillus subtilis*. *Gene* 227(1)**,** 101-110.

Liang, Z.X. (2015). The expanding roles of c-di-GMP in the biosynthesis of exopolysaccharides and secondary metabolites. *Nat Prod Rep* 32(5)**,** 663-683. doi: 10.1039/c4np00086b.

Lindenberg, S., Klauck, G., Pesavento, C., Klauck, E., and Hengge, R. (2013). The EAL domain protein YciR acts as a trigger enzyme in a c-di-GMP signalling cascade in *E. coli* biofilm control. *The EMBO journal* 32(14)**,** 2001-2014.

Mamiatis, T., Fritsch, E.F., Sambrook, J., and Engel, J. (1985). Molecular cloning–A laboratory manual. New York: Cold Spring Harbor Laboratory. 1982, 545 S., . *Acta Biotechnologica* 5(1)**,** 104-104. doi: 10.1002/abio.370050118.

Merritt, J.H., Ha, D.G., Cowles, K.N., Lu, W., Morales, D.K., Rabinowitz, J., *et al.* (2010). Specific control of *Pseudomonas aeruginosa* surface-associated behaviors by two c-di-GMP diguanylate cyclases. *MBio* 1(4). doi: 10.1128/mBio.00183-10.

Nicolas, P., Mader, U., Dervyn, E., Rochat, T., Leduc, A., Pigeonneau, N., *et al.* (2012). Condition-dependent transcriptome reveals high-level regulatory architecture in *Bacillus subtilis*. *Science* 335(6072)**,** 1103-1106. doi: 10.1126/science.1206848.

Plate, L., and Marletta, M.A. (2012). Nitric oxide modulates bacterial biofilm formation through a multicomponent cyclic-di-GMP signaling network. *Mol Cell* 46(4)**,** 449-460. doi: 10.1016/j.molcel.2012.03.023.

Romling, U., Galperin, M.Y., and Gomelsky, M. (2013). Cyclic di-GMP: the first 25 years of a universal bacterial second messenger. *Microbiol Mol Biol Rev* 77(1)**,** 1-52. doi: 10.1128/MMBR.00043-12.

Ryan, R.P., McCarthy, Y., Andrade, M., Farah, C.S., Armitage, J.P., and Dow, J.M. (2010). Cell-cell signal-dependent dynamic interactions between HD-GYP and GGDEF domain proteins mediate virulence in *Xanthomonas campestris*. *Proc Natl Acad Sci U S A* 107(13), 5989-5994. doi: 10.1073/pnas.0912839107.

Ryan, R.P., Tolker-Nielsen, T., and Dow, J.M. (2012). When the PilZ don't work: effectors for cyclic di-GMP action in bacteria. *Trends Microbiol* 20(5), 235-242. doi: 10.1016/j.tim.2012.02.008.

Schirmer, T., and Jenal, U. (2009). Structural and mechanistic determinants of c-di-GMP signalling. *Nat Rev Microbiol* 7(10), 724-735. doi: 10.1038/nrmicro2203.

Serra, D.O., Richter, A.M., and Hengge, R. (2013). Cellulose as an architectural element in spatially structured *Escherichia coli* biofilms. *J Bacteriol* 195(24), 5540-5554. doi: 10.1128/Jb.00946-13.

Tan, H., West, J.A., Ramsay, J.P., Monson, R.E., Griffin, J.L., Toth, I.K., *et al.* (2014). Comprehensive overexpression analysis of cyclic-di-GMP signalling proteins in the phytopathogen *Pectobacterium atrosepticum* reveals diverse effects on motility and virulence phenotypes. *Microbiology* 160(Pt7), 1427-1439. doi: 10.1099/mic.0.076828-0.

Valentini, M., Laventie, B.J., Moscoso, J., Jenal, U., and Filloux, A. (2016). The diguanylate cyclase HsbD intersects with the HptB regulatory cascade to control *Pseudomonas aeruginosa* biofilm and motility. *Plos Genetics* 12(10), e1006354. doi: ARTN e100635410.1371/journal.pgen.1006354.

Zafra, O., Lamprecht-Grandio, M., de Figueras, C.G., and Gonzalez-Pastor, J.E. (2012). Extracellular DNA release by undomesticated *Bacillus subtilis* is regulated by early competence. *PLoS One* 7(11), e48716. doi: 10.1371/journal.pone.0048716.

Zahringer, F., Lacanna, E., Jenal, U., Schirmer, T., and Boehm, A. (2013). Structure and signaling mechanism of a zinc-sensory diguanylate cyclase. *Structure* 21(7), 1149-1157. doi: 10.1016/j.str.2013.04.026.

Zhu, B., Liu, C., Liu, S., Cong, H., Chen, Y., Gu, L., *et al.* (2016). Membrane association of SadC enhances its diguanylate cyclase activity to control exopolysaccharides synthesis and biofilm formation in *Pseudomonas aeruginosa*. *Environ Microbiol* 18(10), 3440-3452. doi: 10.1111/1462-2920.13263.

2.2.8 Supplementary material

Movie S1: Fluorescence microscopy of *B. subtilis* NCIB3610 producing YdaK-mV-YFP
Movie S2: Exponential *B. subtilis* NCIB3610 producing DgcK-mV-YFP
Movie S3: Exponential *B. subtilis* NCIB3610 expressing *mV-yfp-dgcP*
Movie S4: Exponential *B. subtilis* NCIB3610 expressing *dgcP-mV-yfp*
Time intervals: 100 ms upon continuous illumination with 515 nm
All movies are played at 15 fps (frames per second)
Movies are provided on attached CD-ROM (appendix A8.1)

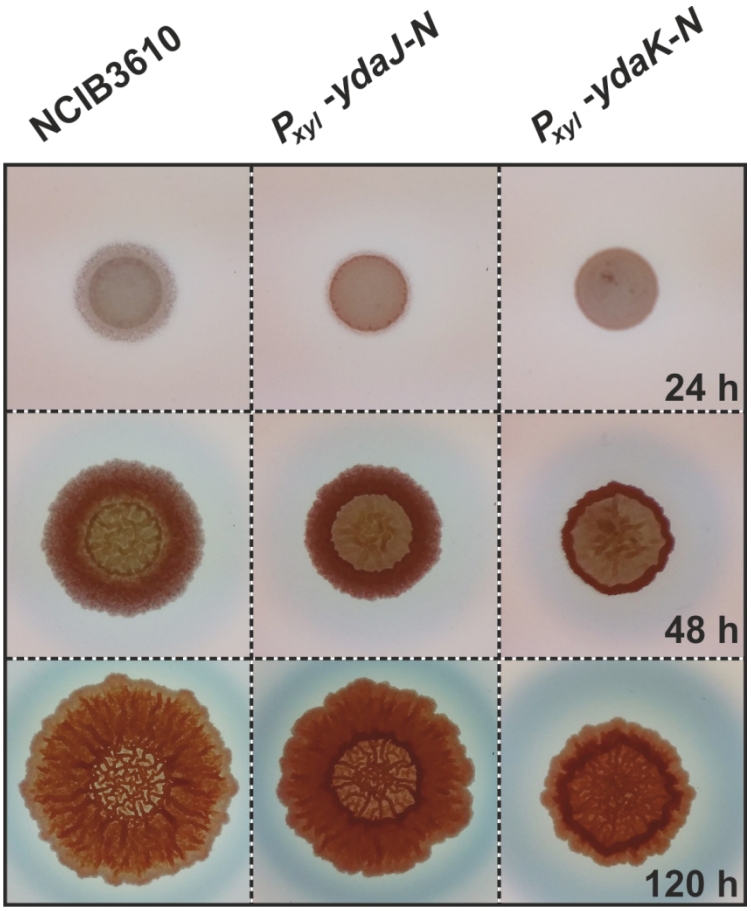

Fig. S1. Overexpression of the *ydaJ-N*- and *ydaK-N*- operon variants results in increased Congo Red staining and altered BF colony morphologies of *B. subtilis* NCIB3610
Individual clones of the indicated strains (WT NCIB3610; NCIB3610-PB53: P_{xyl}-*ydaJ-N*; NCIB3610-PB55: P_{xyl}-*ydaK-N*) were grown in LB at 37 °C. An aliquot of mid-log cultures was spotted on MSgg agar plates supplemented with 0.1 % (w/v) xylose, CR 40 µg/ml, CB 20 µg/ml, following incubation at 28 °C. Imaging of colonies was carried out at the indicated time points using a light screen.

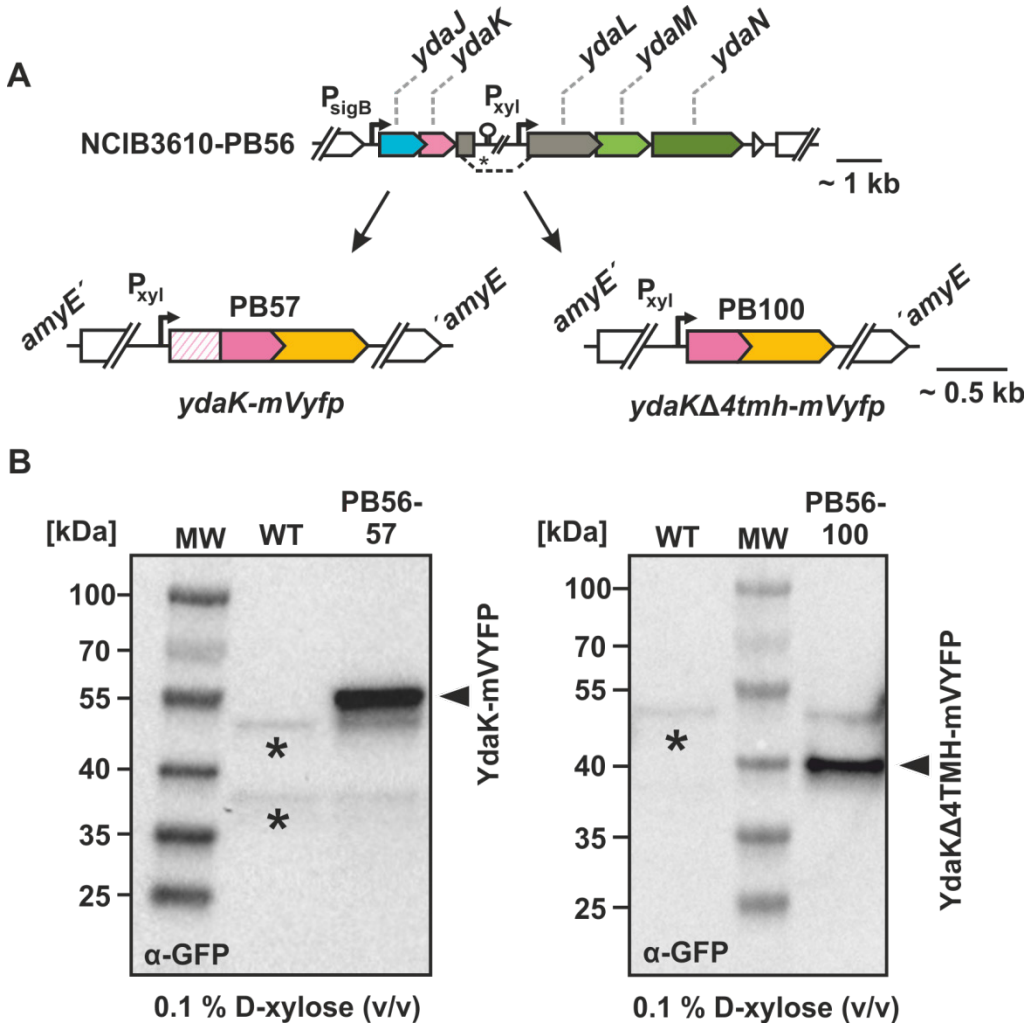

Fig. S2. Verification of YdaK-fusion proteins by Western Blotting
(**A**) Schematic representation of the *ydaJ-N* and *amyE* genomic locus in strains overexpressing *ydaLMN/ ydaK-mV-yfp* (left, strain: NCIB3610-PB56-PB57; P_{xyl}-*ydaL-N*, *amyE*::P_{xyl}-*ydaK-mV-yfp)* and *ydaLMN/ ydaKΔ4tmh-mV-yfp* (right, strain: NCIB3610-PB56-PB100, P_{xyl}-*ydaL-N*, *amyE*::P_{xyl}-*ydaKΔ4tmh-mV-yfp)* respectively. Dashed line represents the integrated plasmid pSG1164-PB56 into the genome of NCIB3610. Star indicates an insertional point mutation in the construct resulting in Δ*ydaJK*. (**B**) Immuno-detection of YdaK-mV-YFP (left) and of the truncation mutant YdaKΔ4TMH-mV-YFP (right) in total cell extracts of the indicated strains WT (wild type NCIB3610), NCIB3610-PB56-PB57 and NCIB-PB56-PB100 respectively, using anti-GFP antiserum. Gene expression was induced at OD_{600} 0.45 for 45 min at 37 °C with 0.1 % xylose (w/v). All lanes are normalized to optical cell density. Separation of proteins via SDS-PAGE was performed on 4-20 % (v/v) polyacrylamide gels prior to transfer on a nitrocellulose membrane by the semidry Western blotting method. The asterisks in the wild type control indicate cross-reacting species present in all lanes. The calculated sizes of the two fusion proteins are 59 kDa, for YdaK-mV-YFP and 42 kDa for YdaKΔ4TMH-mV-YFP.

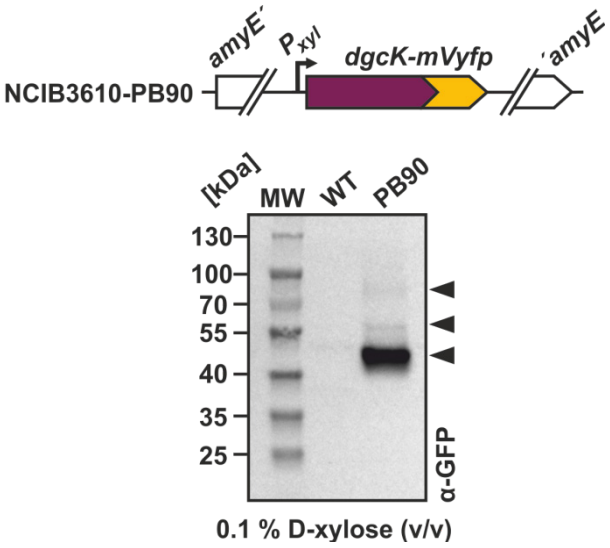

Fig. S3. Immunodetection of DgcK-mV-YFP using α-GFP antiserum
Scheme of a*myE* gene locus in strain NCIB3610-PB90 overexpressing *dgcK-mV-yfp* and detection of C-terminal mV-YFP fusions of DgcK. Expression was induced at OD_{600} 0.5 for 45 min at 37 °C. Lysed cells were incubated with SDS sample buffer for 45 min at RT. Separation of proteins from equal amounts of cells via SDS-PAGE was performed on 4-20 % (v/v) polyacrylamide gels prior to Western blotting. Arrows indicate position of DgcK-mV-YFP fusions (estimated size 67 kDa). Note that DgcK-mV-YFP runs aberrantly during SDS-PAGE.

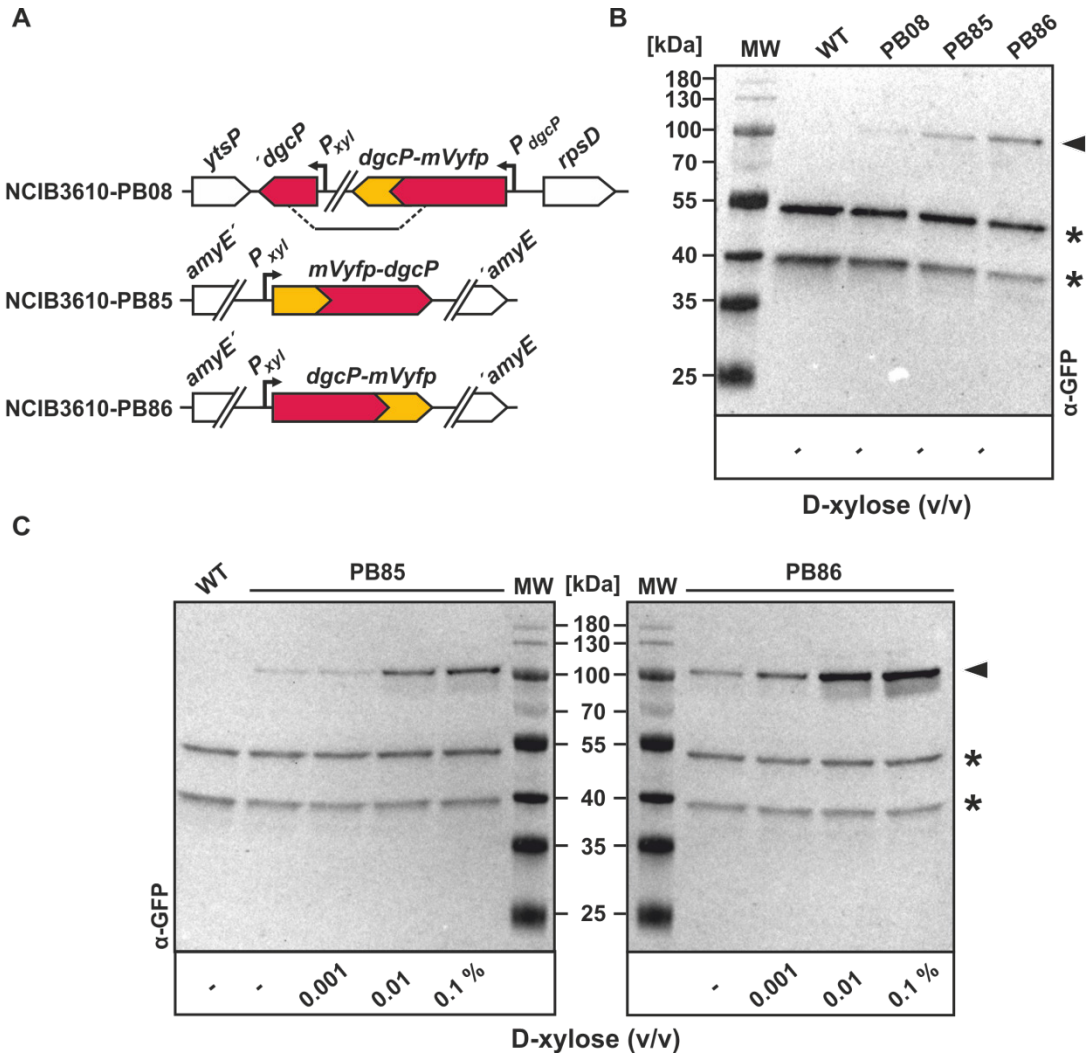

Fig S4. Analysis of DgcP fusion proteins via immunodetection with α-GFP antiserum
(**A**) Schematic representation of *mV-yfp* gene fusions for strains NCIB3610-PB08 (original locus, P_{dgcP}-*dgcP-mV-yfp*), NCIB3610-PB85 (*amyE*::P_{xyl}-*mV-yfp-dgcP*) and NCIB3610-PB86 (*amyE*::P_{xyl}-*dgcP-mV-yfp*). (**B**) Comparison of *dgcP* gene fusion expression levels without xylose, expressed from its native locus and *amyE* loci respectively. (**C**) Comparative analysis of *mV-yfp-dgcP* and *dgcP-mV-yfp* expression levels by detection of the corresponding fusion protein using α-GFP antiserum upon addition of different inducer concentrations. Estimated size of all fusion proteins: 92 kDa as depicted by arrows. Asterisks indicate unspecific cross-reacting species.

Table S1. Strains used in this study

Strain	Relevant genotype	Source
B. subtilis NCIB3610	Wild type, prototroph	BGSC
DK1042 (NCIB3610)	prototroph, *comI*^{Q12L}	BGSC, 3A38 Gift from D. Kearns
Derivatives of NCIB3610 (DK1042, transformed with plasmid DNA)		
NCIB3610-PB01	P_{dgcK}-*dgcK-mV-yfp* (*cat*)	This study
NCIB3610-PB08	P_{dgcP}-*dgcP-mV-yfp* (*cat*)	This study
NCIB3610-PB37	*amyE*::P_{xyl}-*dgcK-cfp* (*spec*), *comI*^{Q12L}	This study
NCIB3610-PB53	P_{xyl}-*ydaJKLMN* (*cat*), *comI*^{Q12L}	Bedrunka and Graumann, 2017
NCIB3610-PB55	P_{xyl}-*ydaKLMN* (*cat*), *comI*^{Q12L}	Bedrunka and Graumann, 2017
NCIB3610-PB56	P_{xyl}-*ydaLMN* (*cat*), *comI*^{Q12L}	Bedrunka and Graumann, 2017
NCIB3610-PB57	*amyE*::P_{xyl}-*ydaK-mV-yfp* (*spec*), *comI*^{Q12L}	This study
NCIB3610-PB79	*amyE*::P_{xyl}-*mV-yfp-dgcK* (*spec*), *comI*^{Q12L}	This study
NCIB3610-PB85	*amyE*::P_{xyl}-*mV-yfp-dgcP* (*spec*), *comI*^{Q12L}	This study
NCIB3610-PB86	*amyE*::P_{xyl}-*dgcP-mV-yfp* (*spec*), *comI*^{Q12L}	This study
NCIB3610-PB87	*amyE*::P_{xyl}-*mV-yfp-dgcW* (*spec*), *comI*^{Q12L}	This study
NCIB3610-PB88	*amyE*::P_{xyl}-*dgcW-mV-yfp* (*spec*), *comI*^{Q12L}	This study
NCIB3610-PB90	*amyE*::P_{xyl}-*dgcK-mV-yfp* (*spec*), *comI*^{Q12L}	This study
NCIB3610-PB100	*amyE*::P_{xyl}-*ydaK⌴4tmh-mV-yfp* (*spec*), *comI*^{Q12L}	This study
NCIB3610-1193	*amyE*::P_{xyl}-*mV-yfp* (*spec*), *comI*^{Q12L}	This study
NCIB3610-XG001	*amyE*::P_{IPTG}-*dgcW* (*spec*), *comI*^{Q12L}	This study
NCIB3610-XG002	*amyE*::P_{IPTG}-*dgcP* (*spec*), *comI*^{Q12L}	This study
NCIB3610-XG003	*amyE*::P_{IPTG}-*ydaK* (*spec*), *comI*^{Q12L}	This study
NCIB3610-XG004	*amyE*::P_{IPTG}-*dgcK* (*spec*), *comI*^{Q12L}	This study
NCIB3610-XG086	*amyE*::P_{IPTG}-*dgcW*Δ*eal* (*spec*), *comI*^{Q12L}	This study
NCIB3610-PB37-PB10	*amyE*::P_{xyl}-*dgcK-cfp* (*spec*), *ydaK-mV-yfp* (*cat*), *comI*^{Q12L}	pPB10 → NCIB3610-PB37 This study
NCIB3610-PB56-PB57	P_{xyl}-*ydaLMN* (*cat*), *amyE*::P_{xyl}-*ydaK-mV-yfp* (*spec*), *comI*^{Q12L}	pPB57→ NCIB3610-PB56 This study

Table S1. Strains used in this study (continued)

Strain	Relevant genotype	Source
NCIB3610-PB56-pSG1193NLMV	P_{xyl}-*ydaLMN* (*cat*), *amyE*::P_{xyl}-*mV-yfp* (*spec*), *comI*^{Q12L}	Bedrunka and Graumann, 2017
NCIB3610-PB56-PB80	P_{xyl}-*ydaLMN* (*cat*), *amyE*::P_{IPTG}-*ydaK*^{R202A} (*spec*), *comI*^{Q12L}	pPB80 → NCIB3610-PB56 This study
NCIB3610-PB56-PB81	P_{xyl}-*ydaLMN* (*cat*), *amyE*::P_{IPTG}-*ydaK*^{D205A} (*spec*), *comI*^{Q12L}	pPB81 → NCIB3610-PB56 This study
NCIB3610-PB56-PB100	P_{xyl}-*ydaLMN* (*cat*), *amyE*::P_{xyl}-*ydaK⊥4tmh-mV-yfp* (*spec*), *comI*^{Q12L}	pPB100→ NCIB3610-PB56 This study
NCIB3610-PB56-XG003	P_{xyl}-*ydaLMN* (*cat*), *amyE*::P_{IPTG}-*ydaK* (*spec*), *comI*^{Q12L}	pXG003→ NCIB3610-PB56 This study
Derivatives of NCIB3610 wild type (transformed with chromosomal DNA)		
DS9305	Δ*dgcK*	Gao *et al*., 2013
DS9305-PB55	Δ*dgcK*, P_{xyl}-*ydaKLMN* (*cat*)	NCIB3610-PB55 →DS9305 This study
DS9537	*dgcP*::*tet*	Gao *et al*., 2013
DS9537-PB55	*dgcP*::*tet*, P_{xyl}-*ydaKLMN* (*cat*)	NCIB3610-PB55 →DS9537 This study
DS9883	Δ*dgcW*	Gao *et al*., 2013
DS9883-PB55	Δ*dgcW*, P_{xyl}-*ydaKLMN* (*cat*)	NCIB3610-PB55 →DS9883 This study
DS1809	Δ*dgcK* Δ*dgcW dgcP*::*tet*	Gift from D. Kearns Lab.
DS1809-PB53	Δ*dgcK* Δ*dgcW dgcP*::*tet*, P_{xyl}-*ydaJKLMN* (*cat*)	NCIB3610-PB53 →DS1809 This study
DS1809-PB55	Δ*dgcK* Δ*dgcW dgcP*::*tet*, P_{xyl}-*ydaKLMN* (*cat*)	NCIB3610-PB55 →DS1809 This study
DS1809-PB55-XG001	Δ*dgcK* Δ*dgcW dgcP*::*tet*, P_{xyl}-*ydaKLMN* (*cat*), *amyE*::P_{IPTG}-*dgcW* (*spec*)	NCIB3610-XG001 →DS1809-PB55 This study
DS1809-PB55-XG002	Δ*dgcK* Δ*dgcW dgcP*::*tet*, P_{xyl}-*ydaKLMN* (*cat*), *amyE*::P_{IPTG}-*dgcP* (*spec*)	NCIB3610-XG002 →DS1809-PB55 This study
DS1809-PB55-XG004	Δ*dgcK* Δ*dgcW dgcP*::*tet*, P_{xyl}-*ydaKLMN* (*cat*), *amyE*::P_{IPTG}-*dgcK* (*spec*)	NCIB3610-XG004 →DS1809-PB55 This study
DS1809-PB55-XG086	Δ*dgcK* Δ*dgcW dgcP*::*tet*, P_{xyl}-*ydaKLMN* (*cat*), *amyE*::P_{IPTG}-*dgcW*Δ*eal* (*spec*)	NCIB3610-XG086 →DS1809-PB55 This study

Table S1. Strains used in this study (continued)

Strain	Relevant genotype	Source
DS1809-PB55-PB79	Δ*dgcK* Δ*dgcW dgcP*::*tet*, P_{xyl}-*ydaKLMN* (*cat*), *amyE*::P_{xyl}-*mV-yfp-dgcK* (*spec*)	NCIB3610-PB79 →DS1809-PB55 This study
DS1809-PB55-PB85	Δ*dgcK* Δ*dgcW dgcP*::*tet*, P_{xyl}-*ydaKLMN* (*cat*), *amyE*::P_{xyl}-*mV-yfp-dgcP* (*spec*)	NCIB3610-PB85 →DS1809-PB55 This study
DS1809-PB55-PB86	Δ*dgcK* Δ*dgcW dgcP*::*tet*, P_{xyl}-*ydaKLMN* (*cat*), *amyE*::P_{xyl}-*dgcP-mV-yfp* (*spec*)	NCIB3610-PB86 →DS1809-PB55 This study
DS1809-PB55-PB90	Δ*dgcK* Δ*dgcW dgcP*::*tet*, P_{xyl}-*ydaKLMN* (*cat*), *amyE*::P_{xyl}-*dgcK-mV-yfp* (*spec*)	NCIB3610-PB90 →DS1809-PB55 This study
DS1809-PB55-pSG1193NLMV	Δ*dgcK* Δ*dgcW dgcP*::*tet*, P_{xyl}-*ydaKLMN* (*cat*), *amyE*::P_{xyl}-*mV-yfp* (*spec*)	NCIB3610-1193 →DS1809-PB55 This study

Table S2. Plasmids and vectors used in this study

Vector/ plasmid	Relevant genotype	Source
pSG1164	*bla*, *cat*, *yfp*	Lewis, Martson, 1999
pSG1164-NLMV	*bla*, *cat*, *mVyfp*	Lab. stock
pSG1192	*bla*, *spec*, *cfp*	Lewis, Martson, 1999
pSG1193-NLMV	*bla*, *spec*, *mVyfp*	Lab. stock
pSG1729-MVYFP	*bla*, *spec*, *mVyfp*	Lab. stock
pSG1164-NLMV-PB01	P_{dgcK}-*dgcK-mV-yfp* (*cat*)	This study
pSG1164-NLMV-PB08	P_{dgcP}-*dgcP-mV-yfp* (*cat*)	This study
pSG1164-NLMV-PB10	P_{ydaK}-*ydaK-mV-yfp* (*cat*)	Bedrunka and Graumann, 2017
pSG1192-CFP-PB37	*amyE*::P_{xyl}-*dgcK-cfp* (*spec*)	This study
pSG1164-PB53	P_{xyl}-*ydaJKLMN* (*cat*)	Bedrunka and Graumann, 2017
pSG1164-PB55	P_{xyl}-*ydaKLMN* (*cat*)	Bedrunka and Graumann, 2017
pSG1164-PB56	P_{xyl}-*ydaLMN* (*cat*)	Bedrunka and Graumann, 2017
pSG1193-NLMV-PB57	*amyE*::P_{xyl}-*ydaK-mV-yfp* (*spec*)	Bedrunka and Graumann, 2017
pSG1729-MVYFP-PB79	*amyE*::P_{xyl}-*mV-yfp-dgcK* (*spec*)	This study
pXG003	*amyE*::P_{IPTG}-*ydaK* (*spec*)	Gao *et al.*, 2013
pXG003-PB80	*amyE*::P_{IPTG}-*ydaK*^{R202A} (*spec*)	This study
pXG003-PB81	*amyE*::P_{IPTG}-*ydaK*^{D205A} (*spec*)	This study
pSG1193-NLMV-PB90	*amyE*::P_{xyl}-*dgcK-mV-yfp* (*spec*)	This study
pSG1729-MVYFP-PB85	*amyE*::P_{xyl}-*mV-yfp-dgcP* (*spec*)	This study
pSG1193-NLMV-PB86	*amyE*::P_{xyl}-*dgcP-mV-yfp* (*spec*)	This study
pSG1729-MVYFP-PB87	*amyE*::P_{xyl}-*mV-yfp-dgcW* (*spec*)	This study
pSG1193-NLMV-PB88	*amyE*::P_{xyl}-*dgcW-mV-yfp* (*spec*)	This study
pSG1193-NLMV-PB100	*amyE*::P_{xyl}-*ydaK*⊥*4tmh-mV-yfp* (*spec*)	This study

Table S2. Plasmids and vectors used in this study (continued)

Vector/ plasmid	Relevant genotype	Source
pXG001	*amyE*::P_{IPTG}-*dgcW* (*spec*)	Gao *et al.*, 2013
pXG002	*amyE*::P_{IPTG}-*dgcP* (*spec*)	Gao *et al.*, 2013
pXG004	*amyE*::P_{IPTG}-*dgcK* (*spec*)	Gao *et al.*, 2013
pXG086	*amyE*::P_{IPTG}-*dgcW*Δ*eal* (*spec*)	Gao *et al.*, 2013

Table S3. Oligonucleotides used in this study

Primer	Sequence 5´- 3´
PB01f	AAGGAGATTCCTAGGATGGGTACCGGAggcgtgtataaccgaagaaaat
PB01f	CCTCCCAGGCCAGATAGGCCGGGCCCttctttttttctgaaaaacacac
PB08f	AAGGAGATTCCTAGGATGGGTACCGGAgctgtaaccaattcaatgcttc
PB08r	CCTCCCAGGCCAGATAGGCCGGGCCCttttattgagtcatgaatcatcaa
PB16f	CATGGGCCCATGAAAATATCATTCAGTG
PB16r	ACGACTAGTTTATAGTTCATTCATCATC
PB19r	TCGACTAGTTTATTCTGTATCTGTCTTTC
PB20f	CATGGGCCCATGGTAGAACAAAC
PB21f	CATGGGCCCTTGCTGAAAGAACTG
PB37r	ACGGAATTCTTCTTTTTTTTCTG
PB57r	CATGGGCCCTAGTTCATTCATCATC
PB79r	CATGAATTCTCATTCTTTTTTTTCTGAAAAAC
PB80f	GACAAGCGTTGCGGAAACGGATAAG
PB80r	CTGATTTGCTGACCGACATATTG
PB81f	GGGACGGAATTTCTTAGCCGTTTCCCGAACGCT
PB81r	AGCGTTCGGGAAACGGCTAAGAAATTCCGTCCC
PB85r	CATGAATTCTTATTTTATTGAGTCATG
PB86f	CATGAATTCATGGTAGAACAAACTAAAG
PB86r	CATGGGCCCTTTTATTGAGTCATGAATC
PB87f	CATGGGCCCATGGGATTCGGTATTTGG
PB87r	CATCTCGAGTTATTGCGACGGCTGTTC
PB88r	CATGGTACCATGGGATTCGGTATTTG
PB88f	CATGGGCCCTTGCGACGGCTGTTCAATAATG
PB90f	CATGAATTCTTGCTGAAAGAACTGTTTG
PB90r	CATGGGCCCTTCTTTTTTTTTCTGAAAAAC
PB100f	CATGAATTCATGCACGATATTACAGCAG
PB103f	CATGAATTCATGATCATGAAACAAATG
PG5050f	CAATTATTAGAGGTCATCGTTC
2928 *dgcW*f	AGGAGGAATTCATCCTGCCAAAACAACGCCA
2931 *dgcW*r	CTCCTGGATCCCAGGGTATAGGCCTTCGT
2932 *ydaK*f	AGGAGGAATTCGTCTTTGAAGACATACAATATG
2935 *ydaK*r	CTCCTGGATCCCTCTGAGCTGTTTCGCCAC
2936 *dgcK*f	AGGAGGAATTCTCGTTGAAGTCGGTCTAGCTC
2939 *dgcK*r	CTCCTGGATCCTCGGGATTGCTGAGTCTGAC
3037 *dgcP*f	AGGAGGGATCCGTCTGCTCTATTCGACCATG
3040 *dgcP*r	CTCCTCTCGAGCAGAAATTGTGCTTCCG

3 UNPUBLISHED RESULTS

3.1 Inhibition of motility via DgrA and the influence of *dgc* genes

As described earlier (see section **1.4.1**), the PilZ-domain protein DgrA has a negative influence on swarming motility in *B. subtilis*. Inhibition of swarming motility by DgrA was recognized upon elevated intracellular c-di-GMP levels as a consequence of *pdeH* deletion or of *dgcK*-, *dgcP*-, and *dgcW*Δ*eal* overexpression respectively. The transient reduction of motility in *pdeH* mutants could be substantially rescued by the presence of an ectopic P_{pdeH}-*pdeH* complementation construct or by a second mutation in *dgrA* or by the simultaneous disruption of all GGDEF proteins (YdaK, DgcK, DgcP, DgcW) coding genes (Chen *et al.*, 2012; Gao *et al.*, 2013). Nonetheless, it remained unknown which DGCs contribute to motility inhibition through c-di-GMP synthesis via DgrA.

To answer this question, *pdeH* was deleted in all three *dgc* single mutants and in the *dgc* triple mutant (single mutant strains and triple mutant strain were kindly provided by D. Kearns). Whereas Gao and coauthors (2013) did investigate a GGDEF quadruple mutant including *ydaK* in their study, this gene deletion was not included herein as disruption of *ydaK* has been reported to have no influence on motility inhibition in a *pdeH* mutant in contrast to a *dgrA* disruption (Gao *et al.*, 2013). In order to generate combinatorial mutants of *pdeH* and *dgcK*, *dgcP* and *dgcW*, genomic DNA from strain DK391 (Δ*pdeH*) was isolated and transformed into the *dgcK*- (DS9305), *dgcP*- (DS9537) and *dgcW*- (DS9883) single mutants and the *dgc* triple mutant (DS1809, Δ*dgcK* Δ*dgcW* *dgcP*::*tet*). Gene disruptions and the presence of the kanamycin resistance marker *kan* inserted into *pdeH* were verified by PCR (**5.3.3**). For quantitative swarm expansion assays (**5.2.4**) of the resulting double/ quadruple mutant strains (**Fig. 3.1**), cells were grown to mid-exponential phase without selective pressure, harvested and subsequently resuspended into 1 x PBS buffer to an optical density (OD_{600}) of 10. Soft LB agar [0.7 % (w/v)] plates were centrally inoculated with equal amounts of the corresponding cell suspension and placed into larger petri dishes (14 cm diameter) containing 5 ml of water in order to ensure constant humidity in all samples at 37 °C. The colony diameter was measured at three different time points after inoculation (T1: 1 h, T2: 2

h, T3: 3 h) along a drawn transect on the bottom of plate as an indicator of swarming motility. Strains NCIB3610 (WT) and DK391 (*pdeH*::*kan*) served as control strains.

In good agreement with the aforementioned studies (Chen *et al.*, 2012; Gao *et al.*, 2013), the *pdeH*-deficient strain DK391 did show a clear defect in motility revealing an approximate 60 %, 67 % and 50 % reduction in the diameter of the colony compared to that of the WT at 1 h, 2 h and 3 h post-inoculum, respectively (**Fig. 3.1**). As expected, the motility defect of the *pdeH* mutant could be rescued by deleting all genes encoding active DGCs (strain DS1809-DK391: Δ*dgcK*-, *P*-, *W*, Δ*pdeH*). Both strains, WT and DS1809-DK391, exhibited comparable colony diameters at all time points measured. Again, these results are consistent with the previous observations that wild type motility can be restored to cells lacking *pdeH* when either DgrA or c-di-GMP production is abolished. Also the participation of YdaK during that particular process can be excluded (Chen *et al.*, 2012; Gao *et al.*, 2013).

Surprisingly, none of the *dgc* single mutants harboring a *pdeH* deletion (DS9305-DK391: Δ*dgcK*, Δ*pdeH*; DS9537-DK391: Δ*dgcP*, Δ*pdeH*; DS9883-DK391: Δ*dgcW*, Δ*pdeH*) was able to restore swarming motility to WT behavior after 1 h of incubation as observed for strain DS1809-DK391 lacking all *dgc* genes. The colony diameter of the generated double mutants was indistinguishable from that of the *pdeH* mutant at this particular time point. However, all double mutants showed a slight increase in colony diameter size compared to the *pdeH* single mutant (DK391) at time points T_2 and T_3. In comparison to strain DK391, an increase of approximately 38 % in colony diameter was observed when *dgcK* and *pdeH* (DS9305-DK391) were absent from the genome, whereas disruption of *dgcP* (DS9537-DK391: Δ*dgcP*, Δ*pdeH*) and *dgcW* (DS9883-DK391: Δ*dgcW*, Δ*pdeH*) lead to 28 % and 25 % of increase in colony expansion respectively (3 h of incubation). Nevertheless, also at T_2 and T_3, single deletions of the corresponding *dgc* genes were unable to counteract the effect of *pdeH* disruption. This observation is in contrast to the triple deletion (DS1809-DK391) and indicates that removal of one particular DGC results in only moderate alterations in intracellular c-di-GMP levels, and therefore c-di-GMP dependent motility inhibition via DgrA can still occur. Based on these results, the question *which DGCs contribute to motility inhibition through c-di-GMP synthesis via DgrA* cannot be clearly answered. Alternatively, our data suggest that all three DGCs might cooperate in inhibition of motility. It is furthermore possible that deletion of a certain *dgc* gene affects the expression or activity of the corresponding other two *dgc* genes/ gene products masking the effect of single *dgc* deletions. Furthermore, all three DGCs are predicted to harbor N-terminal sensor domains potentially involved in signaling. It is plausible that for c-di-GMP dependent inhibition of motility, integration of different environmental/- cellular signals may be required, which is potentially only managed by a subset of two distinct DGCs.

In order to further elucidate the involvement of DGCs in motility inhibition, a set of *dgc* double mutants combined with a *pdeH* deletion has been already generated in the course of this study and swarming motility will be investigated in the future.

Although deletion of single *dgc* genes in a *pdeH* mutant did not result in WT motility behavior, deletion of *dgcK* caused more pronounced effects in comparison to the other *dgc* gene mutations because the Δ*dgcK* Δ*pdeH* strains swarmed slightly faster compared to strain Δ*dgcP* Δ*pdeH* and strain Δ*dgcW* Δ*pdeH*. On the one hand, these results imply that DgcK may be the major DGC involved in swarming motility, while on the other hand it plays an important role in EPS production via YdaK-N (section **2.2**). Thus, DgcK may activate both, DgrA and YdaK upon detection of an unknown signal, resulting in swarming inhibition and EPS production respectively as discussed in section **2.2.4**.

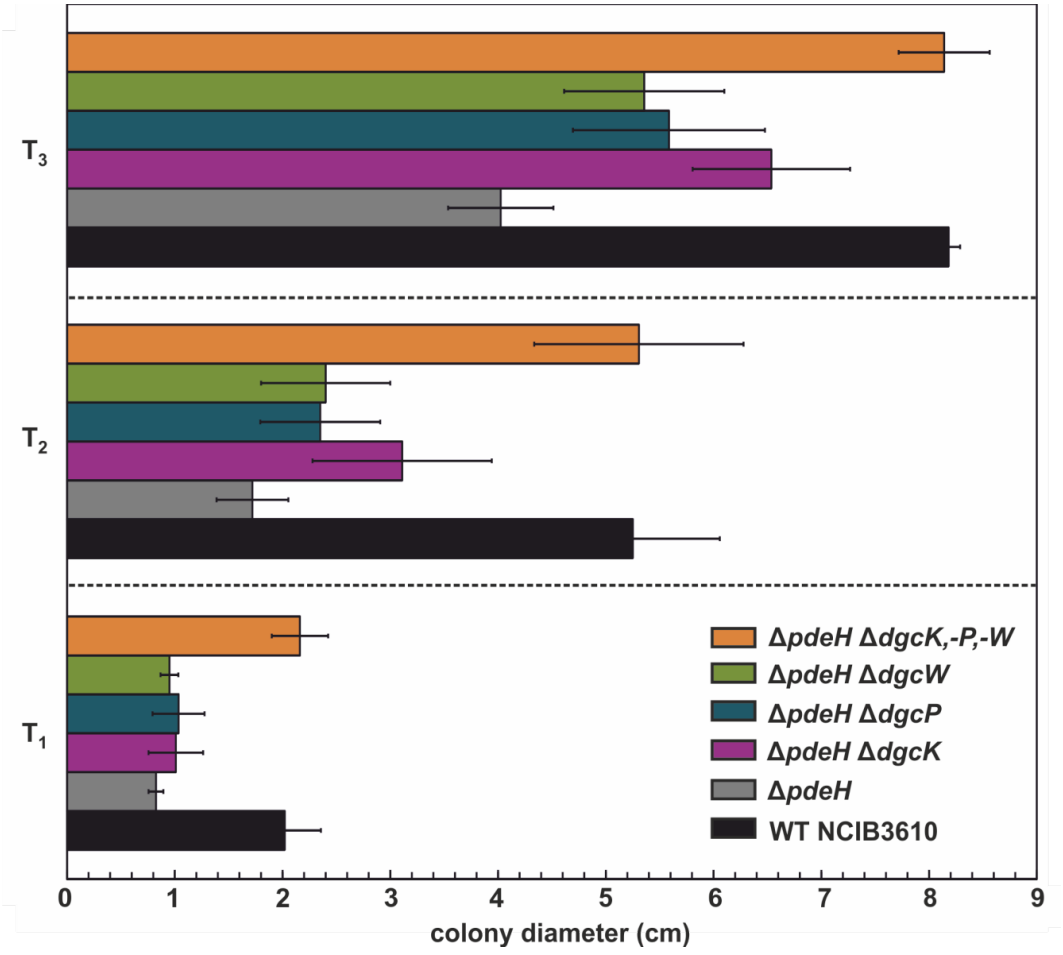

Fig. 3.1. Swarm expansion assays of *pdeH* mutant strains harboring additional *dgc* gene deletions in *B. subtilis* NCIB3610

The defect in swarming motility of the *pdeH* mutant can only be rescued by deleting all three *dgc* genes. Semi-quantitative colony expansion assay of WT *B. subtilis* NCIB3610 and of strains mutated in *pdeH* combined with deletions of the indicated *dgc* genes (DK391: Δ*pdeH*; DS9305-DK391: Δ*dgcK*, Δ*pdeH*; DS9537-DK391: Δ*dgcP*, Δ*pdeH*; DS9883-DK391: Δ*dgcW*, Δ*pdeH*; DS1809-

DK391: Δ*dgcK*-, *P*-, *W*, Δ*pdeH*) on 0.7 % (w/v) LB agar, one hour (T_1), two hours (T_2) and three hours (T_3) after incubation at 37 °C. All values are the averages of at least four experiments, which included three biological replicates. The colony diameter of all strains ranged between 0.8 and 0.9 cm at time point T_0.

3.2 Characterization of the GGDEF domain protein DgcP

The DGC protein DgcP encompasses an enzymatically active C-terminal GGDEF domain and moreover two putative GAF domains at its N-terminus (predicted by SMART server). The signaling function and mode of action of these GAF domains are unknown. Both domain classes are expected to be soluble. Strikingly, a major fraction of fluorescent DgcP fusion proteins localized dynamically to the cell periphery of *B. subtilis* as observed by conventional epifluorescence microscopy (section **2.2.3**, **Fig. 5**). This observation suggests that DgcP may localize to subcellular clusters underneath the cytoplasmic membrane rather than being homogenously distributed throughout the cytoplasm. Imaging localization of DgcP fusions and subcellular cluster formation using total internal reflection microscopy (TIRFM) further supports this idea (**Fig. 3.2**). TIRFM is a method that is particularly well suited for the analysis of localization and dynamics of molecules near the plasma membrane (Ambrose, 1956; Axelrode, 1981).

Earlier studies showed that DgcP is an active c-di-GMP synthetase *in vivo* and *in vitro* (Gao *et al.*, 2013). However, it remained unknown in which cellular processes DgcP might be involved. DgcP is the only described soluble DGC in *B. subtilis* and therefore an attractive bait protein for *in vitro* pull-down studies in order to identify potential interaction partners. Purification of DgcP would also allow studies on DgcP oligomerization *in vitro* inspired by the observation of DgcP-mV-YFP clustering *in vivo*.

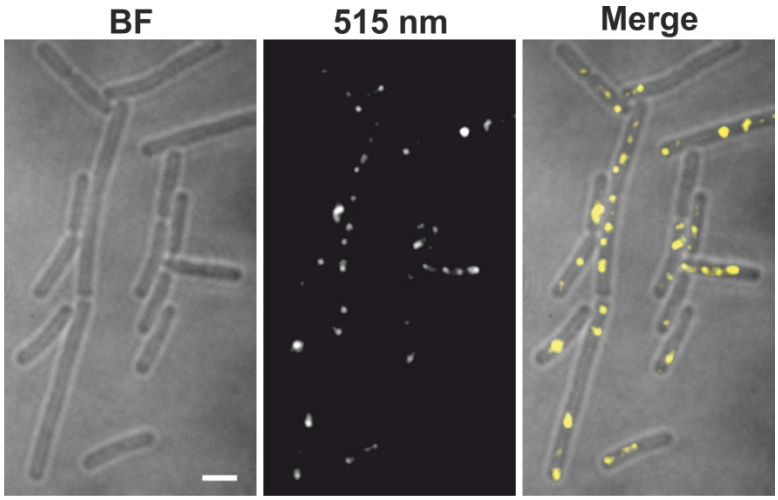

Fig. 3.2. DgcP-mV-YFP visualized by TIRFM reveals distinct foci formation
TIRF microscopy of mid-exponential-phase *B. subtilis* NCIB3610 cells expressing *dgcP-mV-yfp* from the amylase locus (strain: NCIB3610-PB86; *amyE*::P_{xyl}-*dgcP-mV-yfp*), 45 min after induction with 0.01 % (w/v) xylose. BF: bright field. Bar: 2 μm.

3.2.1 Purification of DgcP from *B. subtilis* and verification of co-eluting proteins by MS

In order to identify potential DgcP interaction partners by mass spectrometry (MS), a *B. subtilis* strain was constructed that overexpresses a *dgcP-strepII* fusion gene from a xylose-inducible promoter at the ectopic *amyE* locus (strain NCIB3610-PB29; *amyE*::P_{xyl}-*dgcP-strepII*), as it was not possible to obtain the corresponding fusion protein produced under the control of the native promoter from the original gene locus (strain NCIB3610-PB28). During purification of DgcP-StrepII via affinity chromatography the fusion protein served as a bait protein to enrich co-eluting proteins, which might represent putative interaction partners *in vivo*.

The resulting gene fusion, located between the two arms of *amyE*, was functional (**Fig. 3.3A**). This was verified by an introduction of *dgcP-strepII* at the *amyE* locus of a *dgc* triple mutant that overproduces *ydaK-N* (strain DK1809-PB55-PB29, Δ*dgcK*, *-P*, *-W*, P_{xyl}-*ydaK-N*, *amyE*::P_{xyl}-*dgcP-strepII*), followed by BF formation assays of the resulting strain on MSgg solid medium (see also chapter **3.2.3.3**). Overexpression of *dgcP-strepII* in a DGC triple mutant inducing YdaK-N caused altered BF colony morphologies in the same manner as observed for overexpression of wild type *dgcP* (strain DK1809-PB55-PB20, Δ*dgcK*, *-P*, *-W*, P_{xyl}-*ydaK-N*, *amyE*::P_{xyl}-*dgcP*; **Fig. 3.3Aii**), which indicates that DgcP-StrepII is able to synthesize and to provide YdaK with c-di-GMP resulting in EPS production upon YdaK-N induction.

Cultures of *B. subtilis* wild type NCIB3610, which served as an initial control strain and of the engineered strain NCIB3610-PB29 were grown to exponential phase (OD_{600} 0.6) and gene expression was induced with 0.5 % (w/v) xylose. After two hours of growth at 37 °C, protein lysates were prepared from both strains and subsequently incubated with Strep-Tactin-Sepharose using two separate gravity flow columns (**5.4.2**). The obtained elution factions from both affinity purification steps were analyzed by SDS-PAGE (**5.4.5**). Coomassie-Brilliant-Blue (CB) staining of the corresponding gels (**Fig. 3.3B**) revealed almost no protein signals in elution fractions obtained from wild type cell lysates, whereas a prominent signal corresponding to the size of DgcP-StrepII (69 kDa) was detected in the majority of elution fractions obtained from strain NCIB3610-PB29. The presence and identity of DgcP-StrepII fusion proteins was furthermore confirmed by Western blot analysis using a Strep-tag specific monoclonal antibody conjugated to horseradish peroxidase (**Fig. 3.3C**; **5.4.8**). Besides DgcP-StrepII, the Strep-tag antibody could detect an additional protein with an approximate size of 130 kDa, which was especially prominent in elution fractions obtained from wild type lysates.

For further analysis of present proteins, fractions containing purified DgcP-StrepII and their corresponding controls from wild type lysates were pooled, concentrated and loaded on a

SDS-PAGE gradient gel [4-20 % (v/v)]. To improve detection of low-abundant proteins, colloidal Coomassie staining was applied (**5.4.6**). Because of the high abundance of different protein signals in the corresponding samples only selected protein bands as presented were subjected to mass spectrometric analysis following tryptic digestion (**Fig. 3.3D**).

A majority of proteins identified in the DgcP-StrepII samples were also detected in the corresponding control samples (see also appendix **A8.2**) including the ABC-transporter protein SufC (Hirabayashi *et al.*, 2015), the chaperone GroEL (Mogk *et al.*, 1997) and the metabolic enzyme PdhC (Dihydrolipoyllysine-residue acetyltransferase component of pyruvate dehydrogenase complex; Lowe *et al.*, 1983). These proteins belong to the one hundred most abundant proteins in *B. subtilis* (Eymann *et al.*, 2004, Halbedel *et al.*, 2014) and were considered as non-relevant catches. Additionally, a known biotin-harboring protein could be identified in high amounts throughout all analyzed samples. The pyruvate carboxylase PycA is known to bind to Strep-Tactin and to co-purify with Strep-tagged proteins (Herzberg *et al.*, 2007; SubtiWiki database). Considering this, the unknown protein with an approximate size of 130 kDa, which was detected in the above-described Western blot analysis, most likely represents PycA. However, among the several by-catches that co-purified with DgcP-StrepII, the most abundant peptides not detected in the control sample belonged to the non-ribosomal peptide synthetases SrfAA and SrfAB (**Fig. 3.3D**; **A8.2**). Furthermore, peptides assigned to three other non-ribosomal peptide synthetases proposed to produce plipastatin, could be detected (PpsA, PpsB and PpsC). The co-purification of non-ribosomal peptide synthetases with DgcP-StrepII was confirmed by two additional independent experiments suggesting that DgcP might be involved in the process of non-ribosomal peptide synthesis through an interaction with the corresponding components. Nevertheless, additional controls have to be included in order to exclude artificial aggregates such as unspecific interactions of those large proteins with the Strep-tag itself. In addition to that, further expression and purification optimizations of the DgcP fusion are required in order to eliminate the high abundance of unspecific by-catches. Strikingly, not a single peptide assigned to DgcP-StrepII could be detected by MS analysis in all three experiments, an issue that has to be also addressed in the future.

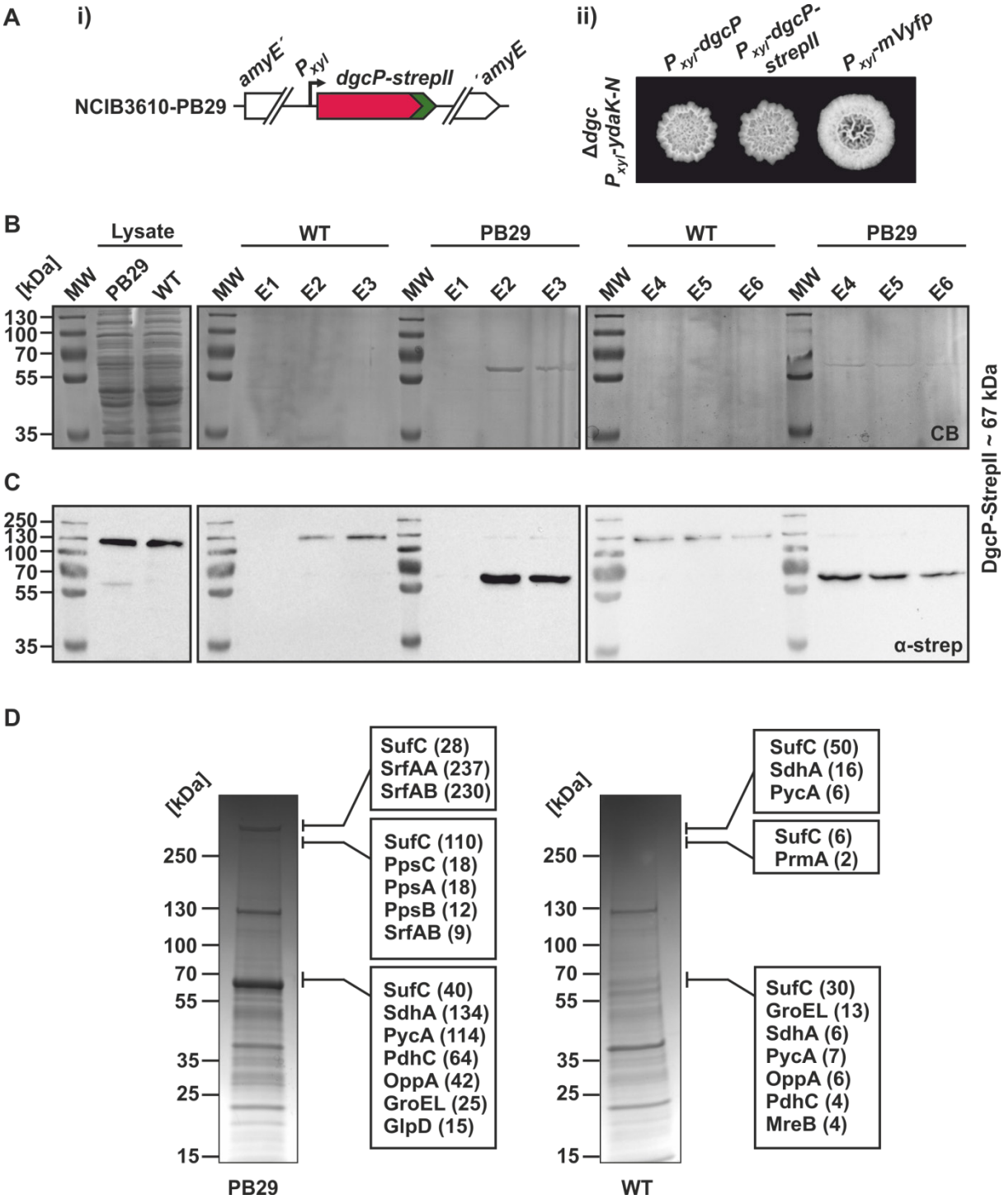

Fig. 3.3. Isolation of DgcP-StrepII from *B. subtilis* cell extracts via Strep-Tactin affinity chromatography and identification of prey proteins by mass spectrometry

(**A**) Scheme of *amyE* gene locus in strain NCIB3610-PB29 overexpressing *dgcP-strepII* upon addition of the inducer xylose **i**) and verification of DgcP-StrepII functionality by phenotypical complementation assays as described in chapter 2.2 **ii**). Overexpression of *dgcP-strepII* in a DGC triple mutant background, which overproduces YdaK-N (strain DK1809-PB55-PB29, Δ*dgcK*, *-P*, *-W*, P_{xyl}*-ydaK-N*, *amyE*::P_{xyl}*-dgcP-strepII*), results in altered BF morphologies on MSgg solid medium supplemented with 0.2 % (w/v) xylose in the same manner as observed for the wild type gene (strain DK1809-PB55-PB20, Δ*dgcK*, *-P*, *-W*, P_{xyl}*-ydaK-N*, *amyE*::P_{xyl}*-dgcP*). Strain DK1809-PB55-pSG1193NLMV (Δ*dgcK*, *-P*, *-W*, P_{xyl}*-ydaK-N*, *amyE*::P_{xyl}*-mV-yfp*) resembles wild type (NCIB3610)

appearance and served as control strain in this experiment. (**B**) Seperation by SDS-PAGE and Coomassie-staining (CB) of elution fractions (E1-E6) obtained after Strep-Tactin affinity chromatography performed with *B. subtilis* NCIB3610 and NCIB3610-PB29 originated cell extracts respectively. MW: molecular weight standards. (**C**) Corresponding Western blot analysis using a Strep-tag antibody. The estimated size of DgcP-StrepII is ~ 67 kDa. (**D**) SDS-PAGE of concentrated pull-down fractions on a 4–20 % (v/v) polyacrylamide gel following Colloidal Coomassie-staining and identity of proteins present in the depicted areas by MS. Brackets indicate total score values of the protein identifications (see also appendix **A8.2**).

3.2.2 Pull-down assays with recombinant DgcP-Strep and cell fractions from *B. subtilis*

In a second approach, I opted to capture putative DgcP interaction partners from extracts of *B. subtilis* using purified heterologously produced DgcP-Strep fusion proteins (**5.4.1**). Therefore, plasmid encoded *dgcP-strep* was overexpressed using the T7 promoter-based expression system of the corresponding pPR-IBA101 vector in *E. coli* BL21 (DE3). Purification of recombinant DgcP-Strep fusion proteins was performed by a two-step protocol including Strep-Tactin affinity chromatography followed by size exclusion chromatography (SEC; **5.4.3**). Recombinant DgcP-Strep was purified in relatively high amounts from *E. coli* BL21 (DE3) lysates and SEC yielded sufficient amounts of apparently pure protein for subsequent pull-down assays with *B. subtilis* lysate. Representative results of such tandem purification are depicted in **Fig. 3.4**.

The analysis of the corresponding elution profile revealed the presence of DgcP-Strep in three distinct peak fractions (**Fig. 3.4BC**). A high amount of DgcP-Strep was detected in fractions, which overlapped with the exclusion volume of the column. However, a small fraction of protein eluting between 120 and 140 ml, was found in two independent purifications, suggesting that DgcP-Strep either forms artificial aggregates and/- or is able to self-assemble into higher multimeric structures. The second scenario is supported by the fact that His_6-DgcP (see **A8.3**) and GST-His_6-DgcP (data not shown) fusions revealed similar SEC profiles and a high tendency to oligomerize as observed for DgcP-Strep. Thus, different affinity tags seem to have no influence on the observed DgcP oligomerization *in vitro*. DgcP fusion proteins formed furthermore subcellular clusters *in vivo* (compare to: chapter **2.2**). Taken together, these data suggest that DgcP oligomerization could be an important feature of this protein.

In addition to the two high-molecular weight fractions, DgcP-Strep eluted as an additional peak at an elution volume of approximately 158 ml, which would correspond to dimeric DgcP-Strep (apparent molecular weight of 134 kDa; assuming globular particles). This observation is in good agreement with previous biochemical studies of different DGCs showing

that homo-dimerization of these enzyme is required for their correct enzymatic function (Paul *et al.*, 2007; De *et al.*, 2008; Schirmer, 2016). If not specified differently, all further experiments were performed with proteins obtained from fractions corresponding to the ‘158 ml-peak, likely representing the homodimeric state of DgcP.

For pull-down assays, purified DgcP-Strep was immobilized on Strep-Tactin Sepharose beads (**5.4.2**). The so-prepared protein was incubated in cell fractionates of *B. subtilis* NCIB3610 cultures grown to exponential phase. After stringent washing, DgcP-Strep and proteins, which remained bound to the fusion protein were eluted from the affinity matrix and subjected to silver-stained, gradient SDS-PAGE [4-12 % (v/v)]. Two high-molecular weight bands were clearly visible in the experimental lane and absent in the control samples (elution fractions obtained from columns which were incubated solely with DgcP-Strep and lysate respectively, **Fig. 3.4D**). MS analysis revealed the presence of peptides assigned to the non-ribosomal peptide synthetase SrfAA from *B. subtilis*, which is consistent with the previous observation (**3.2.1**). Nevertheless, also this pull-down assay needs to include an additional control in order to validate whether DgcP or the Strep-tag pulls down non-ribosomale peptide synthetases.

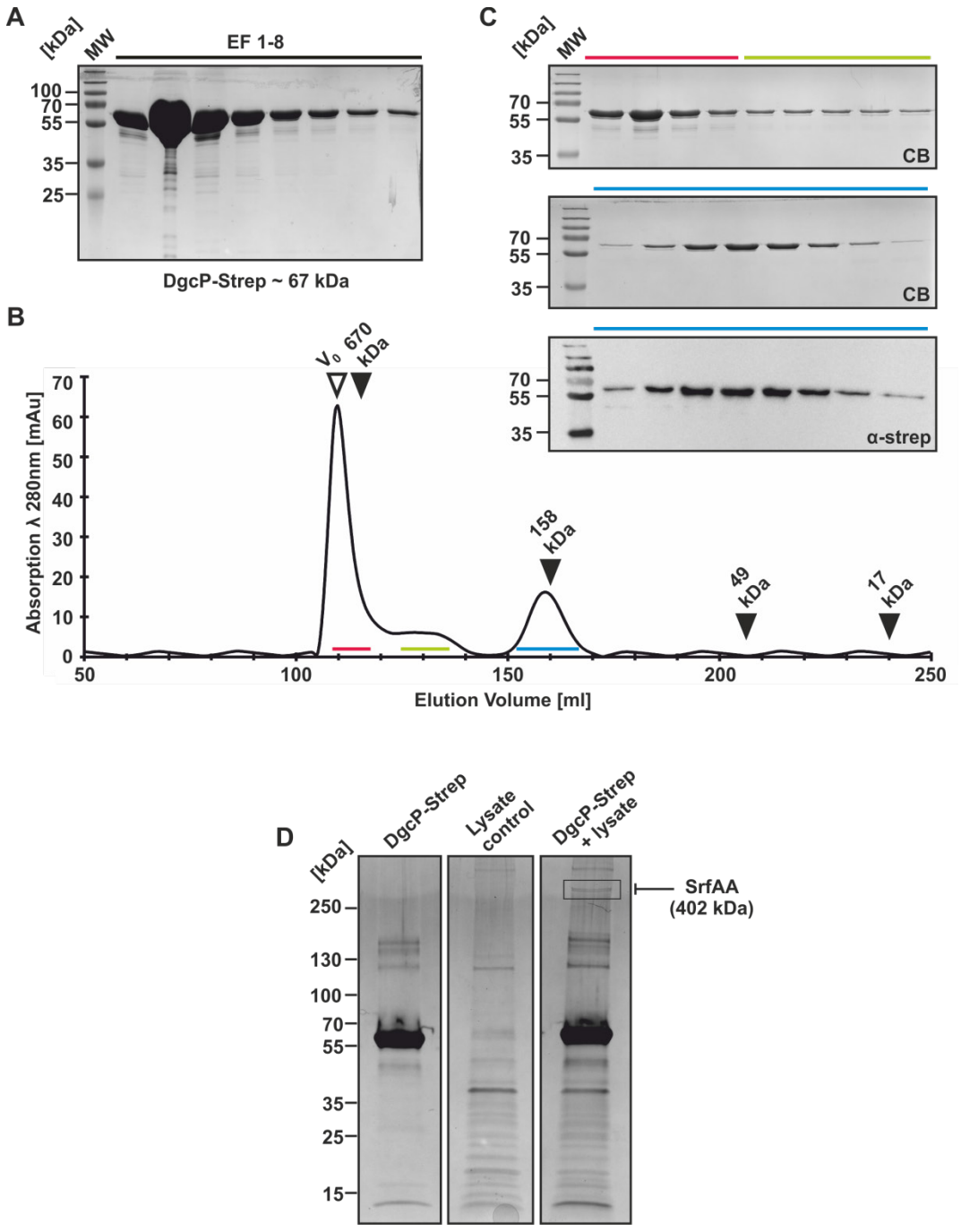

Fig. 3.4. Two-step purification of recombinant DgcP-Strep for pull-down assays with *B. subtilis* cell extracts

(A) Coomassie-stained SDS-PAGE of the affinity purification of DgcP-Strep using Strep-Tactin sepharose. EF: elution fraction. MW: molecular weight standards. (**B**) The size exclusion chromatogram showing the UV absorbance at 280 nm, reveals three peaks. Black triangles indicate positions of standard proteins with different molecular weights, separated on the same column. The void volume (110 ml) of the Superdex 200 column is marked with a white triangle. Differently colored bars indicate the corresponding fractions and their elution positions. (**C**) Coomassie-stained SDS-PAGE (CB) and Western blot analysis (α-strep) of the indicated elution fractions confirming that DgcP-Strep is the major protein component. (**D**) Shows a silver-stained SDS-PAGE of a pull-down assay with DgcP-Strep and cell lysate from *B. subtilis* NCIB3610. Lane 1 & 2 (controls): staining of proteins obtained from samples, which were incubated solely

with DgcP-Strep and Lysate respectively. Lane 3: DgcP-Strep pulls down the high-molecular-weight protein SrfAA as verified by mass spectrometry.

3.2.3 *In vivo* analysis of truncated DgcP mutant variants

Different full length variants of recombinant DgcP (His_6-, Strep-, GST-His_6-tag) accumulated in relatively high amounts in the void fraction during SEC in this study, which indicates the formation of artificial aggregates and/ or of higher multimeric structures (**3.2.2**; appendix **A8.3**). Likely for these reasons, Gao and co-workers (2013) performed *in vitro* analysis of DgcP activity using truncated protein mutants lacking the foremost 116 aa (N-terminal His-tag variants). This lead to the question of whether the N-terminal region of DgcP could be crucial for the establishment of oligomeric structures/- aggregates *in vitro* and also for its accurate function *in vivo*, the latter including activation of the c-di-GMP receptor YdaK through protein cluster formation at the membrane, for instance (see chapter **2.2**).

In addition to the conserved GAF- and GGDEF-domains, DgcP contains an approximately 142 aa long N-terminus revealing no architectural similarities to any known protein domains. The predicted secondary structure consensus generated from PROFsec and PSIPred indicates the presence of three helices and two short β-sheet structures with intervals of loop structures within this region (**Fig. 3.5A**; see also **A8.4**, low confidence scores ignored). The amino acid sequence of DgcP was further examined using the Disorder Prediction Meta-Server (DisMeta), which analyzes a protein sequence using eight disorder prediction algorithms (DISEMBL, DISOPRED2, DISpro, FoldIndex, GlobPlot2, IUPred, RONN, VSL2). Three out of eight algorithms estimated a specific region within the domain lacking N-terminus of DgcP to be disordered (depending on the algorithm between residue 50 and 68). This area locates in a proposed extended loop covering residues 44-76 (PSIPred, **Fig. 3.5A**) and represents an attractive target to study potential protein-protein interactions. Noteworthy, the aforementioned region contains a PxxS motif (aa 53-56), which is highly conserved in various DgcP homologs of the *B. subtilis* lineage including *B. amyloliquefaciens* and *B. velezensis* (BlastP). Intrinsically disordered protein regions frequently function as hubs in protein interaction networks (Dunker *et al.*, 2008; Glover *et al.*, 2016). Considering the bioinformatics predictions, it is therefore plausible that the predicted disordered areas within the N-terminus of DgcP might be also crucial for protein oligomerization and/ or membrane localization and potentially also for an interaction with YdaK, with non-ribosomale peptide synthetases and/- or with yet unknown interaction partners, respectively.

To evaluate the effect of N-terminal truncational DgcP mutants on the subcellular localization and on the ability of these variants to activate EPS production via YdaK *in vivo*, two initial constructs were generated. The coding regions of DgcPΔN116 (Gao *et al.*, 2013; construct pSG1193NLMV-PB101) and of DgcPΔN52 (including the conserved PxxS motif; construct pSG1193NLMV-PB102) were fused to *mV-yfp* and expression was driven by a xylose promotor from the ectopic *amy*E locus. Both plasmids were transformed individually into WT *B. subtilis* NCBI3610 (strain DK1042) for Western blot and fluorescence microscopy analysis (resulting strains: NCIB3610-PB101, *amyE*:: P_{xyl}-*dgcP*ΔN116-*mV-yfp*; NCIB3610-PB102, *amyE*::P_{xyl}-*dgcP* ΔN52-*mV-yfp*). In order to test activity of the corresponding fusion proteins towards YdaK, complementation assays on MSgg solid medium were performed as described for full length DgcP-mV-YFP fusions in chapter **2.2**.

Gao *et al.* (2013) have demonstrated enzymatic activity of His-DgcP fusion protein variants lacking the N-terminal 116 aa *in vitro*. However, truncation of the first 116 aa in this study resulted in poor production of the corresponding fusion proteins following full induction (**Fig. 3.5B**). Moreover, this mutant failed to activate EPS production in a DGC deletion strain overexpressing *ydaK-N* (VI in **Fig. 3.5C**; strain: DS1809-PB55-PB101, Δ*dgcK*, *-P*, *-W*, P_{xyl}-*ydaK-N*, *amyE*:: P_{xyl}-*dgcP*ΔN116-*mV-yfp*) and revealed different subcellular localization patterns compared to DgcP-mV-YFP (**Fig. 3.5E**). For comparable microscopy analysis of full length DgcP-mV-YFP and truncated DgcPΔN116-mV-YFP in WT backgrounds, production of DgcP-mV-YFP was not artificially induced (in contrast to DgcPΔN116-mV-YFP) resulting in low protein levels due to the leakiness of the corresponding xylose-dependent promoter (see also **Fig. S4** and **2.2.8**). Comparative time-lapse fluorescence microscopy of individual cells expressing *dgcP-mV-yfp* (**Fig. 3.5E**, upper panel) and *dgcP*ΔN116-*mV-yfp* (**Fig. 3.5E**, lower panel) from the *amyE* locus, revealed two distinct behaviors for the corresponding fusion protein. Whereas DgcP-mV-YFP underwent various arresting moments at the cell peripheries and furthermore dynamic assembly and disassembly of subcellular clusters potentially at the plasma membrane, the truncated DgcPΔN116-mV-YFP variants poorly localized as distinct foci within the analyzed cells and failed to restore the dynamic localization pattern of DgcP-mV-YFP. However, when foci were observed, the corresponding signals accumulated predominantly at the cell poles for several seconds. These experiments suggest that the N-terminal region of DgcP plays an important role in the membrane-associated dynamics of DgcP *in vivo,* and may also be important to prevent aggregation of the protein.

Interestingly, the truncated variant DgcPΔN52-mV-YFP (strain: DS1809-PB55-PB102, Δ*dgcK*, *-P*, *-W*, P_{xyl}-*ydaK-N*, *amyE*:: P_{xyl}-*dgcP*ΔN52-*mV-yfp*) was also unable to compensate for the loss of DGCs in a DGC triple mutant overexpressing *ydaK-N* (compare to: IV and V in **Fig.**

3.5C), despite relatively high protein levels. Comparative Western blot analysis of both fusion proteins (DgcP-mV-YFP and DgcPΔN52-mV-YFP) revealed a stable and comparable protein production (**Fig. 3.5B**), although *dgcP*Δ52-*mV-yfp* expression was approximately 1.4 fold decreased in comparison to *dgcP-mV-yfp* (comparison of measured Intensity-Volumes using Image Lab 4.0.1 software). However, expression of *dgcP-mV-yfp* [0.01 % (w/v) xylose] resulted in protein amounts comparable to full induction of *dgcP*Δ52-*mV-yfp* expression [0.1 % (w/v) xylose]. Under these induction conditions the full length fusion protein was able to activate EPS production via YdaK-N (data not shown), in contrast to full induction of *dgcP*Δ52-*mV-yfp* expression (**Fig. 3.5C**). Additionally, DgcPΔN52-mV-YFP localized dynamically to subcellular clusters at the cell periphery in a similar manner as observed for DgcP-mV-YFP fusions (**Fig. 3.5D**). Thus and in contrast to DgcPΔN116-mV-YFP, the inability of DgcPΔN52-mV-YFP to induce EPS production cannot be attributed to insufficient protein production and/ or protein aggregation.

In summary, these observations imply an involvement of the foremost 52 aa of DgcP in YdaK activation, but a rather minor role in correct localization/- oligomerisation of fusion proteins at the membrane. A possible motif for membrane localization and/ or cluster formation might encompass the two proline residues (at position 53 aa and 55 aa respectively) localized in the predicted unstructured region (see above), which have been included in the herein described construct. Although DgcPΔN52-mV-YFP behaved similiarly to DgcP-mV-YFP during fluorescence microscopy analysis, it is equally possible that YdaK activation is disturbed due to an unphysiological dynamic behavior of DgcPΔN52-mV-YFP, which cannot be resolved within time intervals of 100 ms and classical epifluorescence. Therefore, it remains to be clarified whether DgcPΔN52-mV-YFP indeed fails to activate YdaK due to disturbed protein dynamics resulting in defective putative DgcP-YdaK interactions and/- or as a consequence of alterations in its enzymatic activity.

Nevertheless, these initial experiments propose the first 52 aa to be an attractive target to study potential interactions between DgcP and YdaK *in vivo* and *in vitro* and furthermore reveal a reasonable starting point for further truncation analysis of DgcP in order to narrow down distinct residues, which enable subcellular clustering of DgcP *in vivo*.

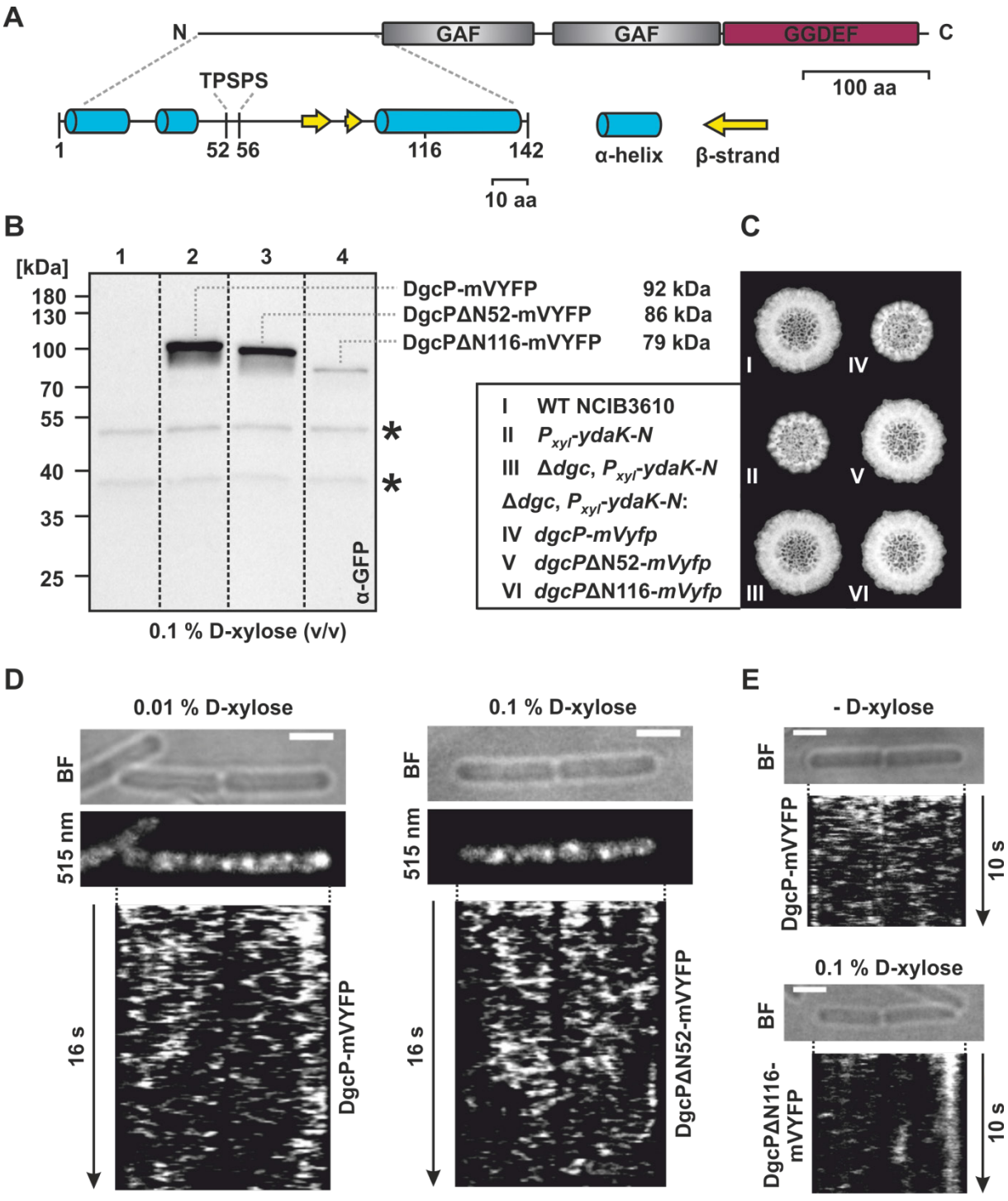

Fig 3.5 The N-terminus of DgcP is crucial for activation of EPS production mediated by YdaK-N

(**A**) Scheme of DgcP domain organization predicted by SMART and secondary structure prediction of the amino-terminal 142 residues generated by PSIPred. Grey: GAF (domain found in cGMP-specific phosphodiesterases, adenylyl and guanylyl cyclases and phytochromes which often serves as a cyclic nucleotide binding domain), purple: GGDEF domain, blue: alpha-helix, yellow: beta-strand. The highlighted PxxS motif can be found in various DgcP homologs and may potentially contribute to DgcP-mV-YFP cluster formation. (**B**) Immuno-detection of DgcP-mV-YFP and truncated mutant proteins using anti-GFP antiserum in total cell extracts obtained from the following strains: WT NCIB3610 (lane 1), NCIB3610-PB86 (lane 2, *amyE*::P_{xyl}-*dgcP*Δ-

mV-yfp), NCIB3610-PB102 (lane 3, *amyE*:: P_{xyl}-*dgcP*ΔN52-*mV-yfp*), and NCIB3610-PB101 (lane 4, *amyE*:: P_{xyl}-*dgcP*ΔN116-*mV-yfp*). Gene expression was induced at OD_{600} 0.45 for 45 min at 37 °C with 0.1 % xylose (w/v). All lanes are normalized to optical cell density. The calculated sizes of the corresponding fusion proteins are indicated. Asterisks indicate cross-reacting species present in all lanes. (**C**) Biofilm colony morphology of WT NCIB3610 (**I**); NCIB3610-PB55, P_{xyl}-*ydaK-N* (**II**); DS1809-PB55, Δ*dgcK*, -*P*, -*W*, P_{xyl}-*ydaK-N* (**III**); DS1809-PB55-PB86, Δ*dgcK*, -*P*, -*W*, P_{xyl}-*ydaK-N*, *amyE*::P_{xyl}-*dgcP-mV-yfp* (**IV**); DS1809-PB55-PB102, Δ*dgcK*, -*P*, -*W*, P_{xyl}-*ydaK-N*, *amyE*:: P_{xyl}-*dgcP*ΔN52-*mV-yfp* (**V**); DS1809-PB55-PB101, Δ*dgcK*, -*P*, -*W*, P_{xyl}-*ydaK-N*, *amyE*::P_{xyl}-*dgcP*ΔN116-*mV-yfp* (**V**). Unaltered colony morphologies of strains **V** and **VI** in contrast to strain **IV** reflect the inability of truncated DgcP mutants to stimulate EPS production. (**D, E**) Time-lapse epifluorescence microscopy of full length DgcP-mV-YFP and the truncated mutant proteins DgcPΔN52-mV-YFP and DgcPΔN116-mV-YFP produced from the *amyE* locus upon addition of different inducer concentrations. Images were captured every 100 ms under continious illumination with 515 nm. Kymographs of fluorescence intensities were genereated along the whole cell body. Bars: 2 μm.

4 GENERAL DISCUSSION

Cyclic diguanylate (c-di-GMP) plays a key integral role in regulating microbial adaptation to changing environmental conditions. Mainly studied in Gram-negative bacteria, the second messenger is prominently known to mediate the motile to sessile lifestyle transition and vice versa. Commonly, high intracellular c-di-GMP concentrations negatively interfere with motility-based processes, while positively affecting ECM production, which eventually favors bacterial BF formation. Conversely, low levels promote BF dispersal and the planktonic mode of bacterial life (Römling *et al.*, 2013; Purcell & Tamayo, 2016; Jenal *et al.*, 2017).

Besides different c-di-GMP receptors, a given bacterial genome typically encodes several paralogous copies of c-di-GMP synthesizing (DGCs) and hydrolyzing (PDEs) enzymes, which together constitute one of the largest families of bacterial signaling proteins (Hengge, 2009; Reinders *et al.*, 2016). Their activities are frequently combined with sensory functions, ensuring rapid integration of numerous external and internal signals and allowing fast cellular responses through the coupled determination of intracellular c-di-GMP concentrations (Mills *et al.*, 2011).

Defining how and under which conditions c-di-GMP levels and their outcomes are modulated is of primary importance, especially with respect to BF formation and dispersal, in order to understand microbial adaptation to environmental cues. However, the multiplicity and the diversity of DGCs/ PDEs signaling functions frequently hinder a full comprehension of corresponding signaling pathways. In many examples single-gene mutations of *dgc* and *pde* genes do not result in observable phenotypic alterations with regard to motility and/- or BF formation. On the other hand, an apparent lack of correlation between global c-di-GMP levels and observed phenotypes has been recognized in some bacterial species, which contrasts the c-di-GMP signaling dogma described above. This means that elevating or reducing c-di-GMP levels does not necessarily lead to sessile and motile bacterial behavior respectively. For example, individual deletions of the DGC genes *sadC* and *roeA* in *P. aeruginosa* result in mutant strains with similar c-di-GMP levels but distinct phenotypes (Merrit *et al.*, 2010).

Several explanations exist, which might contribute to the lack of detectable phenotypic changes and/- or to the missing correlation between intracellular c-di-GMP concentrations and phenotypic outputs (Tamayo, 2013; Valentini and Filloux, 2016). These include redundancy and compensatory effects among the corresponding metabolic enzymes, for instance. Furthermore,

some of these proteins are catalytically inactive and have acquired adaptor and/- or c-di-GMP effector functions. Lack of gene expression and/- or the absence of appropriate stimuli under laboratory conditions often prevents the corresponding signaling components to become operative, which impedes their characterization *in vivo*. Additionally, functional sequestration of signaling components (temporal and spatial) can also contribute to the masking of phenotypic outputs examined in the laboratory.

This work investigates the role of c-di-GMP and its players in the Gram-positive model organism *B. subtilis*. Importantly and in contrast to other bacterial species such as *E. coli* and *P. aeuruginosa*, *B. subtilis* possesses a relatively small *c-di-GMP equipment* (compare to: **1.4**), and provides therefore a suitable model system to study c-di-GMP signaling in Gram-positive bacteria at apparently low complexity. At the beginning of this study, it was already known that c-di-GMP participates in motility control in this organism via the PilZ-domain protein DgrA upon elevated c-di-GMP levels (Chen *et al.*, 2012; Gao *et al.*, 2013), but the role of another c-di-GMP receptor, YdaK, has not been characterized so far. Also the regulatory modes and physiological functions of c-di-GMP building enzymes (DGCs) remained unknown. The lack of observable DGC gene mutant (deletion and overexpression) phenotypes concerning motility and BF formation apparently hampered further analysis in the past.

In the course of my studies, I was able to define a novel c-di-GMP-dependent regulatory pathway and to unravel the cellular function of components encoded in the previously undescribed *ydaJKLMN* operon in *B. subtilis*. These new insights could be gained due to the employment of a relatively simple synthetic construct (compare to: **2.1.7**). The construct mediates the overexpression of the entire transcriptional *ydaJ-N* unit and thus an overproduction of all encoding components upon integration into the genome can be achieved. Importantly, overproduction of YdaJ-N led to the discovery of a novel c-di-GMP-dependent and EPS-associated phenotype. This could not be accomplished in former genetic studies likely for reasons of stoichiometry since Gao and co-workers (2013) investigated the effect of a single gene overexpression of *ydaK* on BF formation. Consequently, a solely overproduction of YdaK cannot enhance or reveal its cognate cellular output since its corresponding downstream targets (YdaLMN) remain shorthanded.

The newly discovered pathway described herein, includes the c-di-GMP synthesizing enzyme DgcK, the c-di-GMP receptor YdaK and its associated EPS synthesizing components (YdaLMN). However, the soluble DGC DgcP and a truncated variant of DgcW (ΔEAL) have also the potential to influence YdaK in its activity upon overproduction.

In addition to genetic studies coupled with phenotypic analysis, comparative fluorescence microscopy analysis of the corresponding protein components was carried out. This revealed that distinct patterns of localization of involved components exit, which can lead to spatial signal specificity. Therefore, this study sets up a new framework to investigate the subcellular localization and dynamic behavior of the three GGDEF domain proteins YdaK, DgcK and DgcP and their interactions with each other in detail. This chapter discusses the findings obtained in this study in detail and future perspectives are given.

4.1 Functional analysis of the EPS operon *ydaJKLMN*

The gene encoding the c-di-GMP receptor YdaK resides within a co-directional gene cluster (*ydaJKLMN*), providing direct evidence and a genetic link for the function of YdaK as a c-di-GMP sensor to potentially exert control over the products of its gene neighbors. Tiling microarray expression data obtained by Nicolas and co-workers (2012) further supported an operonal structure of this gene cluster, which is apparently under the control of the general stress sigma factor σ^B (Petersohn *et al.*, 1999). Based on bioinformatics analysis of the corresponding elements, we hypothesized that components encoded within this region are most likely involved in EPS synthesis. To test this hypothesis, I generated diverse overexpression mutants of the operon, which were subjected to phenotypical analysis allowing for indirect evidence of EPS production. Indeed, induction of *ydaJ-N* led to cell clumping during exponential growth in liquid culture, increased Congo Red staining of colony BFs and strongly altered BF architectures. Following the investigation of *ydaK-N* overexpression in different DGC mutant backgrounds, we were able to assign a new function for c-di-GMP in *B. subtilis* involving the regulation of EPS production.

The most similar c-di-GMP-dependent mechanism to that operating in *B. subtilis* involves the recently characterized listerial *pssE-A* EPS operon (Chen *et al.*, 2014; Koseoglu *et al.*, 2015) and the *pel* operon from *P. aeruginosa* (Lee *et al.*, 2007). These machineries are also post-translationally controlled via an I-site c-di-GMP receptor protein. In the following, the function of each *ydaJ-N* encoded component is described and parallels to other bacterial EPS synthesizing machineries are drawn.

4.1.1 YdaJ´s function likely involves EPS modification

YdaJ is a predicted extracellularly-acting GH8 (glycosyl hydrolase family 8) domain protein belonging to the class of β-1,4 linkage-specific glycosidases. The protein sequence reveals 28 % identity (80 % coverage) to PssZ from *L. monocytogenes* EDG-e, both sharing conserved motifs proposed to reconstitute active sites of GH8 family proteins (Alzari *et al.*, 1996; Koseoglu *et al.*, 2015).

This study provides genetic evidence (compare **3.1.3**) that YdaJ by itself is not involved in polysaccharide polymerization but rather counterbalances the putative polysaccharide synthase-complex YdaM/YdaN, consistent with the proposed GH function of PssZ (Koseoglu *et al.*, 2015). YdaJ can prevent cell aggregation and disperse cell aggregates. Both, overexpression of *ydaJ-N* and induction of the truncated operon variant *ydaK-N* lacking *ydaJ*, lead to CR binding of colonies, wrinkle formation, reduced surface spreading behavior and importantly to cell aggregation events in liquid medium, which suggests that at least some EPS is retained at the cell surface. However, the observed phenotypes were invariably more pronounced in the absence of *ydaJ* independent of the strain background. Additionally, overexpression of *ydaJ* from an ectopic locus with a concomitant induction of *ydaK-N* abolished wrinkled patterns of colonies and cell aggregation events in liquid completely. Nevertheless, CR binding was still detectable under these conditions indicating that EPS synthesis was not abolished. Thus, it seems that YdaJ determines chain length and/or hydrolyses of improperly synthesized polysaccharides through post-synthetic EPS processing.

Koseoglu and co-workers (2015) observed comparable effects in terms of CR binding and cell aggregation during their genetic analysis of *pssZ*. Their study revealed a distinct function for PssZ, which involves specific glycosyl hydrolase activity towards the listerial EPS ManNAcGal synthesized by the products of the *pssA-E* operon. Noteworthy and in contrast to *ydaJ*, *pssZ* does not locate in the gene cluster responsible for EPS synthesis, but is part of another putative operon including the two DGC genes *dgcA* and *dgcB* and furthermore the PDE gene *pdeC*. The appearance of *pssZ* within this gene locus, whose encoding components regulate the post-translational activation of the PssA-E machinery via c-di-GMP, supports the view of PssZ as an EPS modifying component rather than being involved in the biosynthesis process *per se*, because production of the corresponding components seems to be at least at the transcriptional level uncoupled. However, further examinations are required in order to evaluate the necessity of PssZ directly in EPS synthesis. Furthermore, biochemical approaches revealed the potential of a heterologously produced variant of PssZ to inhibit cell aggregation effects of *L. monocytogenes* cultures (caused by a c-di-GMP-dependent activation of the PssA-E machinery) in a dose-

dependent manner. After treatment reducing sugars could be detected in culture supernatants.

Likewise, this approach could be applied for further analysis of YdaJ. More importantly, it appears to be a promising *in vitro* tool to induce the release of carbohydrate subunits from aggregating cell cultures that overproduce the putative EPS through addition of YdaJ. This would potentially allow isolation and chemical characterization of the unknown EPS sugar content.

As counterintuitive as it may seem at first glance, glycosylhydrolases are commonly involved in the process of EPS synthesis and/- or modification. In case of cellulose synthesis for instance, cellulases represent important regulatory elements, which also interfere with the production yield of the polysaccharide (Vain *et al.*, 2014). In *G. xylinus* and in *Rhizobium leguminosarum* for example, disruption of endoglucanase-encoding genes deregulates cellulose production resulting in extended and irregularly packed cellulose micro-fibrils (Robledo *et al.*, 2012). It will be interesting to examine the influence of apparently deregulated EPS synthesis through loss of YdaJ, on the function and structure/ composition of this EPS, which is not clear yet (**4.1.6**).

4.1.2 YdaK is an essential activator of EPS production

The YdaK-GGDEF domain represents a class of c-di-GMP receptors, including the PssE- and PelD-GGDEF domains from *L. monocytogenes* and *P. aeruginosa* respectively, that harbor a degenerated active site and a conserved I-site motif. Both, PssE and PelD are essential membrane integral activation components of their corresponding EPS machineries mediating their function through c-di-GMP binding to conserved I-site motifs (Lee *et al.*, 2007; Li *et al.*, 2012; Whitney *et al.*, 2012; Chen *et al.*, 2014).

In the course of genetic studies, I was able to assign a similar function for YdaK in *B. subtilis*. Particularly, I could demonstrate that an artificial induction of the proposed EPS-operon *ydaJ-N* requires the presence of *ydaK* in order to obtain detectable phenotypes such as CR binding and cell aggregation. The occurrence of these phenotypes was furthermore dependent on the presence of *dgc* genes, more precisely on *dgcK*. As such, it is conceivably to speculate that YdaK is an essential component in this context performing its function through a c-di-GMP-dependent, post-translational control mechanism. Similar to PssE and PelD, the soluble YdaK-GGDEF domain binds c-di-GMP with moderate activity *in vitro* (Gao *et al.*, 2013). However, an involvement of the conserved I-site residues has not been investigated so far for this protein. Despite the lack of biochemical evidence, the current study supports the view of the RxxD motif (R202, D205) as a target for c-di-GMP binding. Generated *ydaK* alleles encoding the R202A and

D205A point mutants were not able to induce the EPS-related phenotypes in contrast to the wild type allele, which implies that these mutations likely abrogate c-di-GMP binding to the receptor thereby preventing polysaccharide production.

How does YdaK mediate c-di-GMP signal transfer to activate synthesis of the unknown EPS? Considering recent studies on c-di-GMP receptors, two scenarios are conceivable. Binding of c-di-GMP to YdaK may either link the protein to an unknown binding partner, presumably YdaM (see below), or may instead favor an interruption of protein-protein interactions. To illuminate the underlying mechanism, further genetic and biochemical analysis are required. Those could include suppressor mutant screens combined with biochemical and structural analysis of the soluble part of YdaK (112 aa-283 aa; TMHMM server) and *in vivo* and *in vitro* protein-protein interaction studies.

In the course of my investigations, I have recognized a relative frequent emergence of suppressor mutants (originating from *ydaK-N* overexpression mutant colonies for example) on CR plates after prolonged incubation. These mutants did not exhibit the characteristic CR staining and reduced colony size, despite presence of the corresponding integrated plasmid (data not shown). It is tempting to speculate that these suppressors might accumulate mutations targeting the *ydaJ-N* operon and specifically *ydaK*. Therefore, sequencing of the corresponding alleles might potentially reveal further residues crucial for c-di-GMP binding and consequently YdaK activity. Mutations occurring in other *ydaJ-N* genes could provide further insights into essential components/ activation residues.

In a variety of characterized c-di-GMP receptors, binding of the ligand usually induces large conformational changes that propagate signal transduction. Binding of c-di-GMP to the PilZ-domain of the bacterial cellulose synthase for example displaces a gating loop from the active site that blocks the entrance of the substrate UDP-glucose in the absence of c-di-GMP resulting in an allosteric activation of BscA (Morgan *et al.*, 2014).

Strikingly, c-di-GMP binding to the soluble part of the degenerated GGDEF domain protein PelD (*pel* operon) does not result in any structural rearrangements of the truncated variant as demonstrated by two independent studies (Li *et al.*, 2012; Whitney *et al.*, 2012). Furthermore and in apparent contrast to active GGDEF domains, the degenerated GGDEF domain of PelD has been demonstrated to behave monomeric *in vitro*. However, Whitney and co-workers recognized the presence of a helical *juxtamembrane region* harboring a predicted coiled-coil motif that could not be assessed structurally. It was speculated that this motif might convey homodimerization of PelD *in vivo* upon c-di-GMP binding to the conserved I-site motif of the GGDEF domain, resulting in signal transduction (Whitney *et al.*, 2012).

For YdaK, interdomain cross-linking might be also considered as a plausible model of activation. Coiled-coil prediction programs such as MARCOIL (Alva *et al.*, 2016), COILS (Lupas *et al.*, 1991) and COILS/ PCOILS (Alva *et al.*, 2016) suggest the presence of coiled-coil motifs located downstream of the last predicted TMH of YdaK (residues 92-111, TMHMM server). As predicted by COILS/ PCOILS for example, residues 115- 130 and 145-159 reveal high confidence levels to form coiled-coil structures (97 % and 89 % respectively). Thus, it is possible that binding of c-di-GMP to the YdaK I-site motif results in conformational changes thereby inducing dimerization via the formation of coiled-coil structures, which could influence potential protein-protein interactions of YdaK with YdaL, YdaM and/- or YdaN.

In the course of this study, I have also investigated a truncated *ydaK* gene variant encoding residues 111-283, which represent the soluble part of YdaK demonstrated to bind c-di-GMP *in vitro* (Gao *et al.*, 2013). Despite the presence of putative coiled-coil motifs, overproduction of this truncated (Δ4TMH) version was not able to support CR binding and altered BF morphology of bacterial colonies. Additionally, mV-YFP tagged proteins were found diffused in the cytoplasm in contrast to the full length version that localizes to specific membrane sites together with its potential downstream targets YdaM and YdaN, respectively. Hence, YdaK activity does apparently not only dependent on ligand binding, but furthermore on membrane localization via its TM domain in order to activate EPS production.

4.1.3 The putative deacetylase YdaL

The concrete role of YdaL has not been elucidated so far. Nevertheless, preliminary data obtained from this study suggest an essential requirement of its activity with regard to EPS production mediated by the YdaK-N proteins. Overexpression of *ydaMN* induced from the original locus along with an artificial induction of *ydaK* from the *amyE* locus did not result in detectable CR binding or altered colony morphologies (data not shown) in contrast to overexpression including the *ydaL* allele.

YdaL is a predicted single-pass type I membrane protein (Uniprot) and structurally similar to members of the carbohydrate esterase 4 superfamily (CE4, Phyre2), which mediate the deacetylation of peptidoglycan and chitin, for example. In a variety of bacterial organisms the degree of EPS deacetylation, particularly the de-N-acetylation of hexosamine sugars, has been reported to be crucial for BF formation (Lee *et al.*, 2016; Colvin *et al.*, 2013). For instance, the extracellular CE4 domain-containing deacetylases IcaB and PelA from *S. epidermidis* and *P. aeruginosa* are required for the biosynthesis of the adhesive polysaccharides PIA (polysaccharide

intercellular adhesin) and Pel respectively (Pokrovskaya *et al.*, 2013; Colvin *et al.*, 2013). Partial de-N-acetylation of the corresponding hexosamine sugar units (N-acetylglucosamine and N-acetylgalactosamine) results in a positive net charge of the mature EPS under neutral and acidic conditions due to the protonation of the corresponding amino groups (Lee *et al.* 2016). Positive charges facilitate EPS secretion through the outer membrane of Gram-negative bacteria (Itoh *et al.*, 2008; Berne *et al.*, 2015), but mainly they seem to be required for the structural maintenance of the polymer, its potential retention on the cell surface and the adherence of the organism to (negatively charged) surfaces (Vuong *et al.*, 2004). Likewise, the predicted CE4 protein PssB is necessary for the production of the listerial cell-surface bound EPS (Koseoglu *et al.*, 2015). Given that deacetylation appears to be a common modification process/ mode of bacterial EPS production (Lee *et al.*, 2016), YdaL could exhibit similar extracellular functions. The lack of EPS deacetylation due to the absence of *ydaL* (see above) may prevent an association of the unknown EPS to the negatively charged cell wall thereby abolishing cell-cell and/ or cell-surface contacts, for instance.

4.1.4 The putative EPS-synthase complex YdaMN

Consolidating recent literature and bioinformatics predictions, it seems that YdaM and YdaN reconstitute the core components of this presumably synthase-dependent EPS machinery similar to PssC and PssD from *L. monocytogenes*. I expect that YdaM is responsible for the polymerization reaction, whereas YdaN likely assists in EPS extrusion. Despite their genetic linkage, YdaM co-localized with YdaN to the same cellular positions supporting the functional connection between these two components.

In my view, the most promising interaction candidate for YdaK is indeed YdaM, a predicted TM protein belonging to the glycosltransferase (GT) family 2. In contrast to YdaL and YdaN, whose catalytic domains are predicted to localize extracellularly, YdaM exposes its GT domain to the cytoplasm, which might interact with the cytoplasmic GGDEF domain of YdaK. Analogous to the PilZ-domain of the cellulose synthase subunit BscA for example, one could speculate that YdaK prevents the access of sugar units to the active site of YdaM in its apo-state through direct protein-protein interactions. Binding of c-di-GMP would then resolve this interaction or blocking mechanism allowing the entrance of activated sugar compounds. Alternatively, different ligand binding states of YdaK may influence the stability of the putative YdaMN synthase complex. For example, binding of c-di-GMP to YdaK may result in an

interruption of YdaM-YdaK interaction, thereby favoring the assembly of a catalytically active YdaMN (sub)-complex leading to EPS synthesis activation.

Notably, YdaM reveals high sequence homology to PssC from *L. monocytogenes* (47 % sequence identity and 97 % coverage). Among the PssA-E proteins, PssC has been proposed to catalyze the polymerization of N-acetylmannosamine through the formation of β-1,4-linkages (Koseoglu *et al.*, 2015). Due to their high sequence homology, it stands to reason that YdaM may use a similar substrate for EPS synthesis, potentially a hexosamine sugar. On the contrary, the BcsB-domain proteins YdaN and PssD proposed to function as EPS extrusion scaffolds, do not share high sequence similarities, which points towards differences in the sugar composition of the corresponding EPSs. The listerial EPS consists of β-1,4-linked N-acetylmannosamine chains with terminal α-1,6-linked galactose molecules. The enzyme catalyzing the galactosyl transfer has not been identified so far (Koseoglu *et al.*, 2015).

It is not possible to predict the composition of the newly identified EPS in *B. subtilis* based on sequence analysis of the YdaJ-N proteins and on our phenotypic studies. The ECM-dependent CR-binding of colony BFs served as a useful proxy for the assessment of EPS production in this study. Nevertheless, this does not enable detailed suggestions concerning EPS-composition as CR-binding has been demonstrated to correlate with the synthesis of diverse ECM components including polysaccharides but also amyloids (Reichhardt *et al.*, 2016).

4.1.5 Model for c-di-GMP-dependent EPS production in *B. subtilis*

However, parallels to the listerial EPS production mechanism can be certainly drawn, especially because phylogenetic analysis of the *L. monocytogenes* proteins PssC (homolog to YdaM), PssD (YdaN) and PssZ (YdaJ) revealed clustering of homologous proteins within a branch of firmicutes including members of the *Bacillus*-, *Clostridium*- and *Lactobacillus* genus (Koseoglu *et al.*, 2015). This suggests that certain members of these genera might produce similar EPSs by analogous mechanisms representing a potentially important adaptation process for these Gram-positive species.

Based on my genetic and cell biological studies and considering the bioinformatics predictions of YdaJ-N proteins and their similarities to the listerial EPS machinery, I would like to propose the following model for EPS production mediated by the YdaJ-N machinery in *B. subtilis* (**Fig. 4.1**). The second messenger c-di-GMP is synthesized in close proximity to its integral membrane receptor YdaK through the activity of the potentially physically associated DGC DgcK upon detection of an unknown signal. Binding of c-di-GMP to the conserved I-site

motif of the cytoplasmic YdaK-GGDEF domain may lead to conformational changes, thereby allowing synthesis and export of the unknown polysaccharide. These two presumably coupled processes are mediated by the putative glycosyltransferase complex, which is composed of YdaM and YdaN and likely interacts with YdaK. Similar to the bacterial cellulose synthase complex BcsAB, YdaMN potentially also constitutes a channel in order to couple polysaccharide synthesis with its translocation across the membrane (Morgan *et al.*, 2013; Römling and Galperin, 2015).

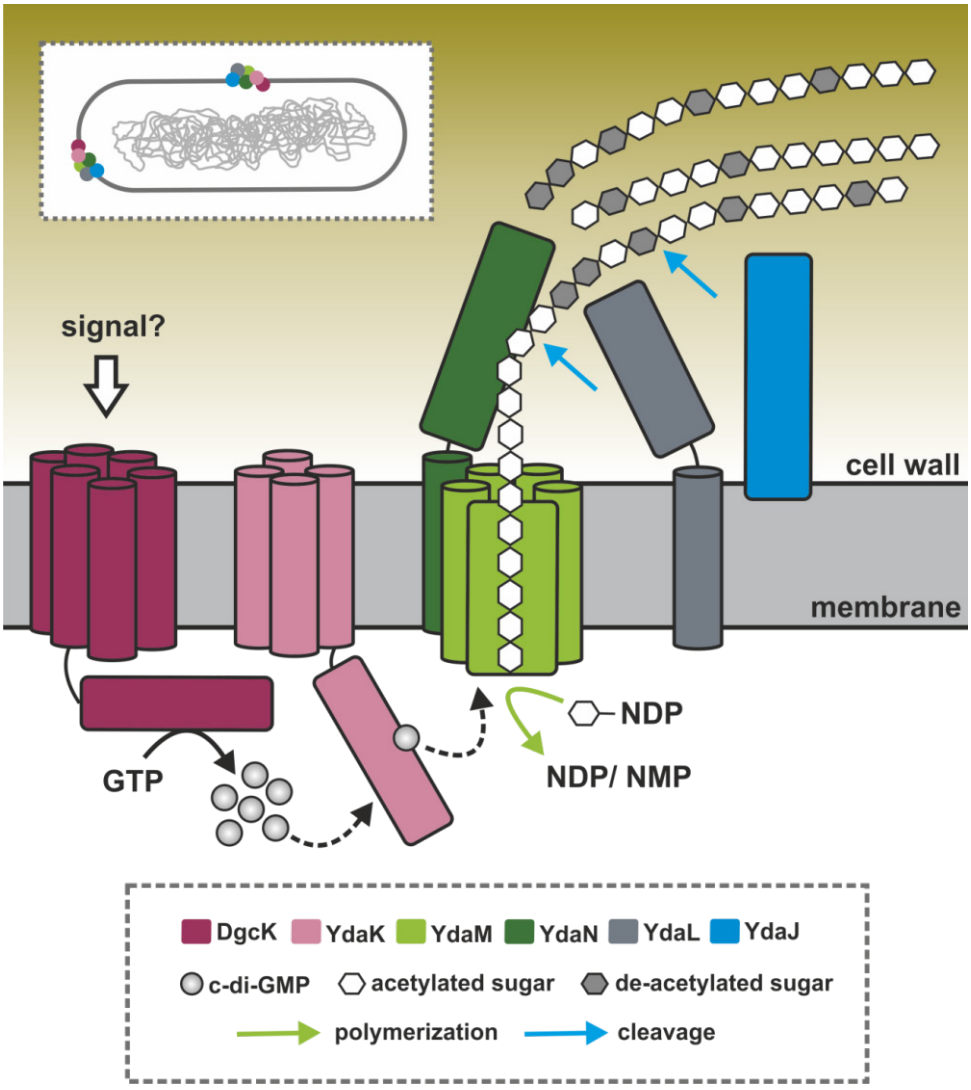

Fig. 4.1. Model for spatially restricted and c-di-GMP-regulated EPS production mediated by the operon encoded YdaJ-N proteins in *B. subtilis*
EPS production via YdaJ-N takes place at distinct sites of the bacterial membrane including polar and mid cell/- septal regions. The second messenger c-di-GMP is synthesized from GTP by the DGC DgcK upon perception of an unknown signal generating presumably local pools of c-di-GMP. The spatially close c-di-GMP receptor YdaK (degenerated GGDEF domain protein) binds c-di-GMP via its conserved I-site motif and activates the EPS synthase components (YdaMN) through an unknown mechanism. The polysaccharide produced by YdaMN is potentially further

modified by the action of YdaJ and YdaL. For detailed information refer to section **4.1**. Barrels represent TM helices and dashed arrows indicate c-di-GMP binding to YdaK and a putative interaction of c-di-GMP-bound YdaK with YdaMN, respectively. NDP/ NMP: Nucleoside-diphosphate/- monophosphate.

Whereas YdaM is predicted to catalyze polysaccharide synthesis through an incorporation of relevant carbohydrates into the growing chain, YdaN may operate as a translocation unit during synthesis in order to guarantee polysaccharide export onto the cell surface. The nascent EPS is presumably further subjected to post-synthetic polymer modifications mediated by the predicted extracellular-acting proteins YdaL and YdaJ. While YdaL may modify the polymer through deacetylation, YdaJ most probably hydrolyzes β-1,4-linkages within the carbohydrate chain in a periodic manner. The hydrolytic activity of this putative enzyme might play an important role in maturation and/- or export of the EPS across or on the top of the cell wall. For example, it is possible that YdaJ is required for a controlled alignment of individual polysaccharide chains to form higher order structures. An additional or alternative function of YdaJ could also include the cleavage of lipid-linked intermediates during translocation in order to facilitate an unhampered extrusion of the polymer.

4.1.6 Function of the newly identified EPS

Bacterial exopolysaccharides have been demonstrated to serve a plethora of functions. For example, they can have a role in water retention and serve as nutrient sources and energy sinks respectively, and furthermore offer protection against extracellular stress factors by providing a physical barrier (Nwodo *et al.*, 2012). The previously described listerial EPS, for instance, conveys protection against several disinfectants and long-term desiccation (Chen *et al.*, 2014). During initiation of BF formation EPSs are involved in the reversible and irreversible attachment of cells to a surface and are furthermore indispensable for the maturation of a BF.

The physiological role of the EPS synthesized by YdaJ-N could not be determined so far. As mentioned earlier (compare to: **2.1.3.1**), the *ydaJ-N* operon is assigned to the σ^B-regulon, which is reflected in the upregulated transcription of corresponding elements upon stress treatment including ethanol stress, known to be is a strong inducer of this regulon in *B. subtilis* (Boylan *et al.*, 1993). This suggests that the unknown EPS might convey some stress resistance. Ethanol-stressed *ydaK* mutants [10 % (v/v)] did not reveal significant differences in their survival rates compared to the wild type in this work. However, such survival experiments were performed in liquid rich medium, in contrast to the transcriptome studies performed by Nicolas

et al., 2012. Therefore, additional experiments using different media compositions and also different stress factors/ conditions are required.

Besides conveying stress resistance, the unknown EPS could be potentially also involved in BF formation, more precisely in the initial steps involving reversible attachment to surfaces. Deletion mutant strains of *ydaK* have so far only been investigated using the widely applied colony BF formation assay (Gao *et al.*, 2013; this study) and have not revealed any visible changes in their morphologies compared to the wild type. However, this assay is likely unsuitable to study BF initiation because cells are artificially applied on a surface (agar), which is subsequently dried to inhibit swarming and therefore cells are forced to some extent to settle down. Thus, alternative methods should be applied such as flow cell advices or *in situ* plant root colonization assays.

In addition to altered colony morphologies, induction of YdaJ-N also lead to the formation of cell aggregates in liquid media during exponential phase, indicating that the unknown EPS mediates cell-to-cell adhesion of proliferating cells. Distinct localization patterns of the YdaJ-N components (cell poles and mid cell) further support the view of locally administrated EPS synthesis, whose product remains attached to the cell wall and provides cell-to-cell and/- or cell-to-surface contacts, similar to the listerial ManNAc-Gal EPS (**Fig. 4.2**). The observed cell aggregates could be easily resolved through vortexing, suggesting that only weak physical interactions are established. In my view, such weak interactions represent an appropriate prerequisite for an EPS that might mediate reversible attachment of cells to a surface and/- or reversible cell aggregation in the early stages of BF formation on a surface. Contrarily, a constitutive derepression of the major EPS synthesis operon *epsA-O* (*sinR* deletion mutant, compare to: **1.2.3**) results in *hyper-aggregated* cells (Winkelman *et al.*, 2009). Notably an induction of YdaJ-N cannot compensate for the loss of the BF essential EPS. The corresponding EPS does apparently convey stronger interactions in comparison to YdaJ-N´s EPS, which are eventually not compatible with a reversible settlement of cells. Thus it is possible that *B. subtilis* synthesizes distinct EPSs during different stages of BF formation.

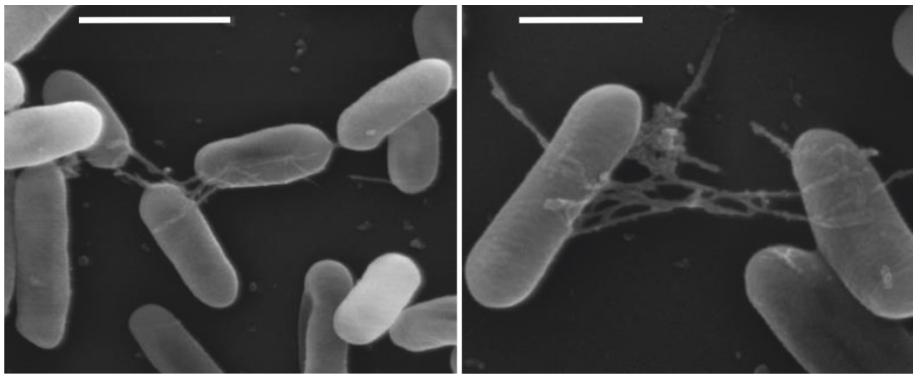

Fig. 4.2. SEM micrographs of *L. monocytogenes* cells and cell-bound intercellular EPS
Upon deletion of all encoding PDE genes, *L. monocytogenes* produces the EPS ManNAc-Gal at distinct sites of the membrane via PssA-E, which results in visible cell-to-cell contacts. Micrograph adapted from: Koseoglu *et al.*, 2015: Scale bars: 1 μm (left panel), 0.5 μm (right panel).

4.2 Low and high c-di-GMP signaling specificity models

C-di-GMP regulates different processes with specific readouts by binding to diverse target molecules thereby exerting control on processes at multiple levels including transcriptional, translational and post-translational control mechanisms (Römling *et al.*, 2013). Although c-di-GMP signaling components and their underlying molecular mechanisms have been intensively studied during the last three decades (particularly in Gram-negative model organisms), the major challenge is now to understand how a bacterial cell is able to integrate a signal and to specify the cognate cellular output under the apparent complexity of this second messenger system (Hengge, 2009; Merrit *et al.*, 2011). In other words: how is pathway signaling specificity achieved?

Based on genetic studies using different bacterial species, functional sequestration of c-di-GMP signaling components has been proposed to ensure specific targeting of certain c-di-GMP-dependent processes by individual DGCs and/ or PDEs (Hengge, 2009; Jenal, 2013). But how can sequestration be achieved, especially in scenarios where different DGCs and/ or PDEs with discrete outputs are not temporally separated but have to operate in parallel without affecting non-cognate effector molecules or with only minimal cross-talk?

In the following sections current hypotheses are discussed and further applied on the c-di-GMP signaling system in *B. subtilis*.

4.2.1 Spatial sequestration of c-di-GMP signaling components

One hypothesis suggests that signaling specificity must, in part, involve spatial sequestration of metabolizing enzymes and of effector molecules into subcellular units allowing the separation of discrete control modules through the establishment of multi-protein-complexes at the bacterial membrane, for example (Ryan *et al.*, 2010; Merrit *et al.*, 2011; Lindenberg *et al.*, 2013). Thereby, DGCs and PDEs are thought to generate and maintain so-called *local c-di-GMP pools*, which target only locally associated effector molecules and might therefore convey high signal specificity (Hengge, 2009; Valentini and Filloux, 2016). However, small molecules such as c-di-GMP and cAMP presumably diffuse freely and rapidly in the cytoplasm (270-780 μm s^{-1} for cAMP; Zaccolo *et al.*, 2006; Mills *et al.*, 2011). In the absence of compartmentalizing structures in the bacterial cell, an equilibrium concentration of these second messengers would be reached within a timeframe of few milliseconds (Mills *et al.*, 2011). Therefore, it is unlikely that signal specificity is achieved through spatially separated c-di-GMP concentrations but rather through the establishment of local c-di-GMP gradients (Richter, 2015). Diffusion of the second messenger would then be limited through the action of effector proteins, which efficiently bind and/ or degrade c-di-GMP in the aforementioned multi-protein-complexes (Merrit *et al*, 2011). However, depending on the affinity of these effectors it is possible that upon synthesis a portion of such local pools subsequently interacts with associated effector proteins whereas the remaining pool fraction rapidly diffuses away from the complex and becomes freely accessible for other effector molecules. In such scenarios, local c-di-GMP gradients may therefore also have the potential to activate high affinity c-di-GMP effector molecules, which are distributed and diffuse throughout the cytoplasm and are not part of multi-protein-complexes in their ligand-free state.

4.2.2 The global pool hypothesis

C-di-GMP receptor affinities are known to vary considerably (Römling *et al.*, 2013). For example, the cellulose synthase harbors a PilZ domain with a 43-fold lower affinity for c-di-GMP compared to the PilZ domain of the motility inhibitor YcgR (Pultz *et al.*, 2012). Based on such observations, an alternative, but not mutually exclusive, mechanism by which signaling specificity could be achieved has been proposed. Selective activation of different DGCs and PDEs could affect the global/ common c-di-GMP concentration within the cell and the response degree would be simply determined through the binding affinities of different effectors for c-di-GMP and through the corresponding kinetics of DGCs/ PDEs (Mills *et al.*, 2011; Römling *et al.*, 2013). Consistent with the signal integrating function of DGCs and PDEs, this could potentially lead to

a graded response that regulates a series of downstream effectors in a defined order at particular cytoplasmic c-di-GMP levels (Pultz *et al.*, 2012; Jenal, 2013; Reinders *et al.*, 2016). Indeed, a global c-di-GMP pool might convey low signaling specificity and is therefore more likely to allow the coordination and cross-talking between multiple pathways. Cross-talks are for example crucial for the overall development of a bacterial BF, where c-di-GMP levels are known to gradually increase (Valentini and Filloux, 2016).

In summary, two general models for signal specificity through functional sequestration can be distinguished. Spatially sequestering the signal (pool) in multi-protein complexes at distinct cellular site may result in highly specific signaling despite a potential leakiness of the corresponding modules. Temporal and/ or conditional separation through differential expression and activation of DGCs/ PDEs/ output systems respectively, could have a distinct impact on the global c-di-GMP pool and could under certain conditions grant cross-talk between different c-di-GMP-dependent processes. Importantly, both regulatory scenarios seem to play important roles in the course of BF development and are likely to be far away from being mutually exclusive.

4.2.3 C-di-GMP signaling in *B. subtilis* - local and global hubs

In this study, we provide evidence that both, local and global c-di-GMP pools might operate in *B. subtilis* (**Fig. 4.3**).

Comparative genomics of c-di-GMP signaling components revealed that over half of all GGDEF- and EAL-domain proteins contain localization signals such as TMHs (Seshasavee *et al.*, 2010). This argues for a predominant signaling and enzymatic activity of these proteins at the bacterial membrane. Consistent with this observation, localization studies performed in this work, revealed distinct subcellular localization patterns for the three DGCs at the membrane of *B. subtilis*. Therefore, we propose that they could form independent signaling clusters in distinct segments of the membrane, potentially together with their corresponding effector proteins. In particular, we could demonstrate that the DGC DgcK and the c-di-GMP receptor YdaK both form subcellular, mostly static clusters, which co-localized to a certain extent, at the membrane of cell poles and at mid-cell during division (**Fig. 4.3**). Importantly, under our experimental conditions DgcK has been shown to activate EPS synthesis via YdaK. Thus, DgcK and the YdaJ-N proteins likely form a c-di-GMP signaling module. Especially in the context of this localized structural machinery, it is reasonable to assume that the maintenance of a local c-di-GMP pool or gradient would allow the achievement of a rapid and efficient physiological

response (EPS synthesis) with a minimal absolute change in the intracellular c-di-GMP concentration (Jenal, 2013).

However, we recognized that DgcP is also able to activate the YdaJ-N machinery upon overproduction. DgcP forms dynamic subcellular clusters, potentially at the membrane *in vivo* and furthermore tends to form multimeric structures *in vitro*. Thus, it is likely that DgcP interacts with YdaK, potentially via its foremost 52 aa (compare to: **3.2.3**) upon integration of an unknown signal and subsequent cluster formation at the membrane resulting in activation of EPS synthesis (**Fig. 4.3**). Nevertheless, it seems that local signaling in case of YdaK activation can be overcome by elevated global concentration of intracellular c-di-GMP as discussed earlier (**2.2.4**), because overproduction of DgcW-ΔEAL also resulted in EPS synthesis. Different fluorescent fusion proteins of DgcW localized to distinct sites of the membrane (data not shown), but a conclusive statement concerning their functionality could not be drawn in the course of this study. Removal of the c-di-GMP degrading EAL domain apparently dysregulates the activity of DgcW and results in globally elevated c-di-GMP concentration, which in turn revealed a new BF-associated phenotype. Therefore, the EAL domain of DgcW might be important to regulate local c-di-GMP gradients in motile cells (*dgcW* belongs to the σ^D-regulon, compare to: **1.4.2**).

Spatially sequestered c-di-GMP modules have been proposed to contain DGCs, c-di-GMP receptors and furthermore PDEs, the later proposed to minimize cross-talks between certain modules (Hengge, 2009). However, in contrast to GGDEF domain proteins, only a small minority of EAL domain proteins, which are furthermore few in number in most genomes, contain signal-sensing partner domains (Seshasavee *et al.*, 2010). This indicates that most EAL proteins lacking signaling domains, including PdeH from *B. subtilis*, are regulated at the transcriptional level and might act on the overall intracellular c-di-GMP pool without direct responses to environmental cues. In *B. subtilis*, PdeH seems to have a central role in maintaining cell motility by keeping c-di-GMP concentrations below a threshold, which activates the motility inhibitor DgrA similar to *E. coli* PdeH. Importantly, motility inhibition via DgrA has been recognized so far only upon elevated c-di-GMP levels (*pdeH* deletion) and none of the examined single *dgc* gene deletions was able to rescue this effect (compare to: **3.1**). These observations indicate that removal of one particular DGC results in only moderate alterations in intracellular c-di-GMP levels and further suggest that DgrA depends on global hubs of c-di-GMP, despite its lower K_D compared to YdaK, generated by more than one DGC (**Fig. 4.3**).

Despite best efforts, I was not able to generate functional fluorescent fusion proteins for PdeH and DgrA. However, corresponding stable fusions localized predominatly diffusive in the cytoplasm (data not shown).

Therefore, cytosolic PdeH and DgrA might act or respond to global c-di-GMP levels. However, it is equally possible that PdeH is indeed also part of the local DgcK/ YdaK signaling module at the membrane and that DgrA establishes together with its cognate DGCs a module close to flagella. Detailed *in vivo* and *in vitro* protein-protein interactions studies will certainly provide a more detailed view of the corresponding mechanisms.

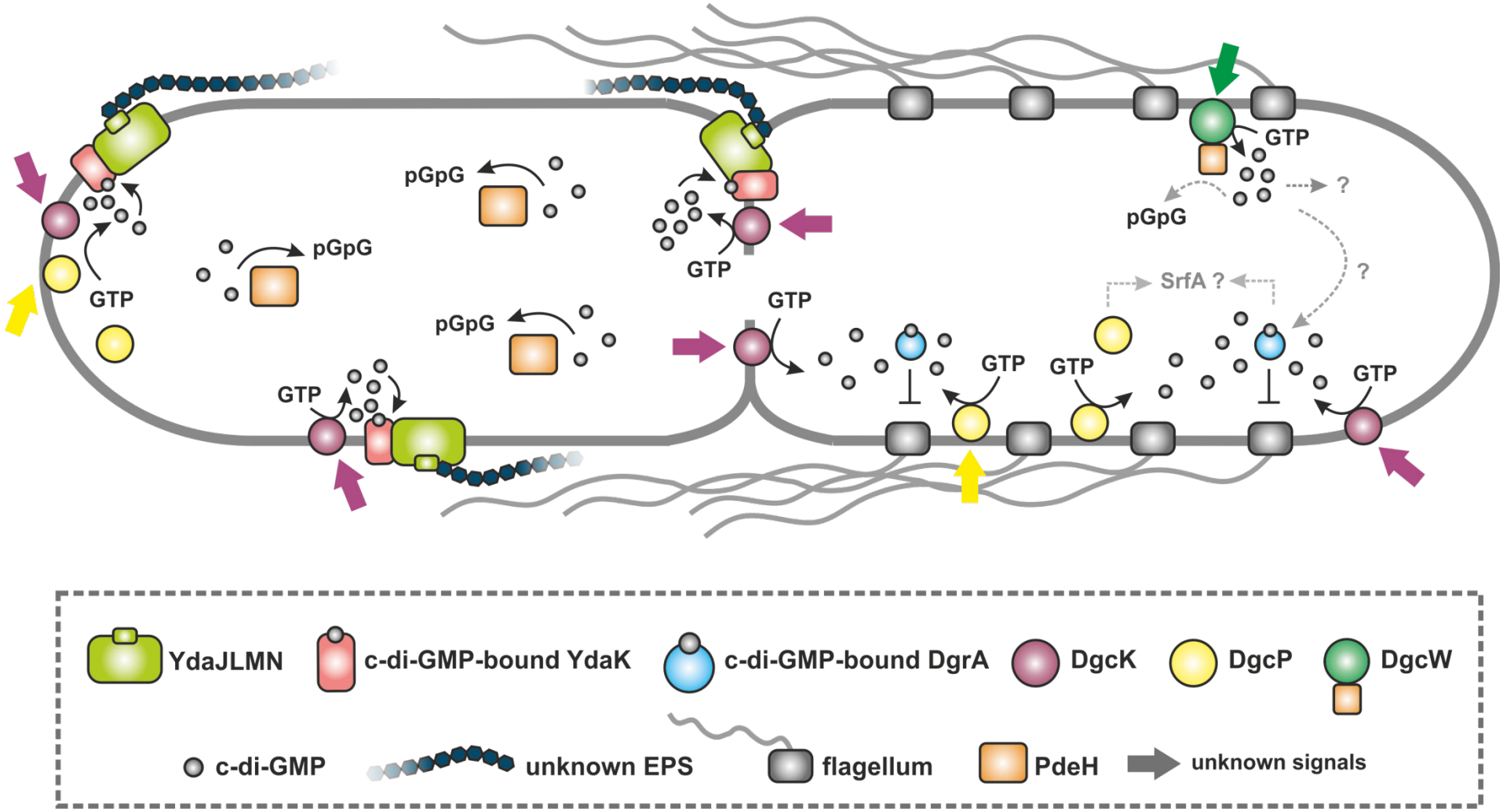

Fig. 4.3. Model for local and global c-di-GMP signaling modules in *B. subtilis*

5 GENERAL MATERIAL & METHODS

5.1 Material

5.1.1 Reagents and kits

Standard chemicals used in this work were purchased from Carl Roth (Karlsruhe, Germany), Sigma-Aldrich (Steinheim, Germany), AppliChem (Darmstadt, Germany) or GE Healthcare (Munich, Germany). DNA modifying enzymes, DNA polymerases and further reagents (dNTPs, reaction buffers) for molecular cloning and genetic manipulations were supplied by New England Biolabs (Frankfurt a. M., Germany). Size standards for DNA and proteins were obtained from New England Biolabs and from Thermo Fischer Scientific (Schwerte, Germany) respectively. Kits for plasmid extraction were manufactured by VWR (Darmstadt, Germany). PCR purification and gel extraction were performed using kits from Qiagen (Hilden, Germany).

5.1.2 Oligonucleotides

Oligonucleotides were ordered from Metabion (Planegg/Steinkirchen, Germany) or Sigma-Aldrich (Steinheim, Germany) adjusted to 100 pmol μl^{-1} with ddH_2O and stored at -20 °C. Used oligonucleotides are listed in sections **2.1.7**, **2.2.8** and in the appendix (**A8.5**).

5.1.3 Vectors

In the scope of this work various vectors were used for different purposes (listed in sections **2.1.7**, **2.2.8** and in the appendix **A8.6**). For recombinant protein overproduction in *E. coli*, the commercial expression vectors pET24d(+) (Novagen/ Merck, Darmstadt, Germany) and pPR-IBA101 (IBA, Göttingen, Germany) served as vectors for the production of $(His)_6$- and Strep-tagged (Twin-Strep-tag®) proteins respectively. N-terminal GST (Glutathione S-transferase)-$(His)_6$ fusion proteins were generated using pGAT3 (J. Peränen and M. Hyvönen, unpublished). All vectors provide an IPTG (isopropyl-β-D-thiogalactopyranoside) inducible expression, based on the T7 bacteriophage system (West *et al.*, 1980). Expression of corresponding fusion genes

was induced by providing a source of T7 RNA polymerase in the host cell [*E. coli* BL21 (DE3)]. In case of N-terminal $(His)_6$- and GST-$(His)_6$-tagged proteins, the coding sequence for the $(His)_6$-tag was implemented in the corresponding oligonucleotides. Cloning of genes into the pPR-IBA101 gave rise to C-terminal tagged fusion proteins.

To monitor protein localization or to overexpress untagged genes and/-or entire transcriptional units in *B. subtilis* (see also **2.1.8**), vectors of the pSG series were employed (Lewis and Martson, 1999; Feucht and Lewis, 2001). These allow the generation of C- or N-terminal fusions with different variants of fluorescent proteins. Corresponding genes/ gene fragments and/- or gene fusions were integrated into the chromosome by homologous recombination via a single Campbell-type integration at the original locus, or via a double crossing over reaction at the ectopic *amyE* site, coding for α-amylase. In case of *amyE* site targeting, successful integration was confirmed by screening loss of starch degradation. Gene expression was either controlled by the corresponding native promoter or by an artificial xylose-inducible P_{xyl} promoter.

The *amyE* site vector pDR111 (provided by David Rudner, Harvard Medical School, Boston, Massachusetts, USA) served to overexpress genes under the control of an IPTG inducible promoter ($P_{hyper\text{-}spank}$) after chromosomal integration.

The threonine site vector pDG1664 (Guerout-Fleury *et al.*, 1996) was used to integrate genes under the control of their native promoter at the ectopic *thrC* locus. Transformants were screened for MLS- (Macrolide-Lincosamide-Streptogramin) resistance and spectinomycin sensitivity, the later indicating a double-crossover recombination has occurred.

The resistance change vector pCm::Tet was used to exchange a chloramphenicol (Cm) resistance to a tetracycline (Tet) resistance mediated by a double-crossover recombination event *in vivo* (Steinmetz *et al.*, 1994). Successful integration was confirmed by gain of a Tet resistance and by simultaneous loss of Cm resistance.

5.1.4 Bacterial strains

E. coli strain DH5α (Woodcock *et al.*, 1989) was used for the construction and propagation of plasmids, and *E. coli* strain BL21 (DE3) (Thermo Fischer Scientific, Schwerte, Germany) for heterologous gene overexpression.

B. subtilis strains constructed in this work are derivatives of the laboratory domesticated strains PY79 (Youngman *et al.*, 1983; Schroeder and Simmons, 2013), 168 (Burkholder and Giles, 1974; Albertini and Galizzi, 1999) and the undomesticated strains NCIB3610 (Branda *et al.*, 2001; Srivatsan *et al.*, 2008) and DK1042 (Konkol *et al.*, 2013; Nye *et al.*, 2017). Details on the

construction of strains are described in the corresponding articles (see section 3), and a list of all bacterial strains constructed in the course of this study is given in the appendix (**A8.7**).

5.2 Microbiological and cell biological methods

5.2.1 Bacterial growth and supplements

For cloning purposes and propagation of vectors and plasmids respectively, *E. coli* DH5a strains were aerobically cultivated overnight at 37 °C in LB (lysogeny broth, Miller; **Table 5.1**) medium and on LB agar purchased from Carl Roth (Karlsruhe, Germany). Solid and liquid media were prepared according to manufacturer instructions and sterilized by autoclaving for 30 min at 121 °C and 2 bar. In case of recombinant gene expression and subsequent protein purification, derivatives of *E. coli* BL21 (DE3) were grown first to an OD_{600} of 0.6-0.7 (**5.2.3**) and gene expression was induced with 0.5 mM IPTG followed by incubation at 25 °C for 4 h.

B. subtilis strains were routinely cultivated at 30 °C to 37 °C in LB medium under constant shaking at 200 rpm or on LB agar plates. Prior to inoculation in liquid media from a frozen stock, *B. subtilis* strains were streaked on LB 1.5 % (w/v) agar plates. Strains that were subsequently used for fluorescence microscopy were either cultured in LB liquid medium or in $S7_{50}$ (**Table 5.1**). Sterilization of $S7_{50}$ components was accomplished by using sterile filtration (pore size 0.2 μm). In case of cell cultivation in LB, cells were washed two to three times with $S7_{50}$ prior to microscopy. Media were supplemented with the appropriate additives and antibiotics in final concentrations as listed in **Table 5.2**. Selection of *B. subtilis* transformants carrying spectinomycin resistance markers was performed on agar plates using Difco Sporulation Medium (DSM, refer to **Table 5.1**). For induction of the xylose promoter, xylose was added up to 0.5 % (w/v). Induction of the *hyper-spank* promoter was accomplished by medium supplementation with 1 mM IPTG. For colony BF formation assays cells were grown on solid MSgg medium as described earlier (section **2.1.8**).

5.2.2 Storage of bacteria

For long-term storage, strains were grown to late log phase, subsequently supplemented with glycerol to a final concentration of 20 % (v/v) and stored at -80 °C.

5.2.3 Determination of cell density

Optical densities of bacterial cultures were measured in a cuvette (Sarstedt, Nümbrecht, Germany) with 1 cm thickness using the Ultrospec™ 10 cell density meter (Amersham Pharmacia Biotech) at a wave length of 600 nm (OD_{600}) against sterile medium. A value of 0.1 corresponds to a cell density of approximately $1x10^8$ cells ml^{-1}.

Table 5.1: Bacterial growth media

Medium	Composition	Final concentration
LB medium	Trypton	10 g l^{-1}
	Yeast extract	5 g l^{-1}
	NaCl	10 g l^{-1}
	Agar-Agar	15 g l^{-1}
	pH 7.0 ± 0.2	
DSM medium	Nutrient broth	0.8 % (w/v)
	$MgSO_4$	0.1 mM
	KCl	1.3 mM
	NaOH	0.5 mM
	Bacto® Agar	1.5 % (w/v)
	$Ca(NO_3)_2$ *	10 mM
	$MnCl_2$ *	0.1 mM
	$FeSO_4$ *	0.01 mM
	* Addition after sterilization	
$S7_{50}$ medium	10 x $S7_{50}$ salts	1 x
	100 x $S7_{50}$ metals	1 x
	D-glucose *	1 % (w/v)
	Glutamic acid	0.5 mM
	Casamino acids	0.004 % (w/v)

* D-glucose was substituted by D-fructose if induction of a xylose inducible promoter was desired.

10 x $S7_{50}$ salts	MOPS	500 mM
	$(NH_4)_2SO_4$	100 mM
	KH_2PO_4	50 mM
	adjusted pH to 7.0 (KOH)	
100 x $S7_{50}$ metals	$MgCl_2$	0.2 M
	$CaCl_2$	70 mM
	$MnCl_2$	5 mM
	$ZnCl_2$	0.1 mM
	Thiamine-HCL	0.01 % (w/v)
	HCl	2 mM
	$FeCl_3$	0.5 mM

MSgg medium	Potassium phosphate Stock solution 0.5 M pH 7.0	5 mM
	K_2HPO_4	54.4 g l^{-1}
	KH_2PO_4	25.5 g l^{-1}
	MOPS	100 mM
	$MgCl_2$	2 mM
	$CaCl_2$	0.7 mM
	$MnCl_2$	0.05 mM
	$FeCl_3$	0.1 mM
	$ZnCl_2$	0.001 mM
	Thiamine-HCl	0.002 mM
	Glycerol	0.5 % (w/v)
	Sodium glutamic acid	0.5 % (w/v)
	Trypton	2 % (w/v)
SOC medium	Yeast extract	0.5 % (w/v)
	NaCl	0.05 % (w/v)
	KCl	2.5 mM
	pH 7.0	
	$MgCl_2$ *	10 mM
	D-glucose *	20 mM
	* Addition after sterilization	
10x MCM medium * **(250 ml, pH 7.0)**	K_2HPO_4 x 3 H_2O	35.1 g
	KH_2PO_4	13.1 g
	D-Glucose	50 g
	Potassium glutamate	5 g
	Casein hydrolysate	2.5 g
	300 mM Sodium citrate	25 ml
	22 mg ml^{-1} ferric ammonium citrate	2.5 ml

* sterile filtration of mixed components and storage at -20 °C. Competent cultures were grown in diluted 1x MCM medium supplemented with 3.33 % (w/v) of 1 M $MgSO_4$.

Table 5.2: Media supplements

Antibiotic/ supplement	Final concentration
Ampicillin (Amp)	100 μg ml^{-1}
Kanamycin (Kan)	50 μg ml^{-1} (*E .coli*)
	10 μg ml^{-1} (*B. subtilis*)
Chloramphenicol (Cm)	5 μg ml^{-1}
Spectinomycin (Spec)	100 μg ml^{-1}
Tetracyclin (Tet)	20 μg ml^{-1}
Lincomycin (Lin)	25 μg ml^{-1}
Erythromycin (Ery)	1 μg ml^{-1}
Congo Red (CR)	40 μg ml^{-1}
Coomassie Brilliant Blue (CB)	20 μg ml^{-1}
IPTG	0.5-1 mM
D-xylose (Xyl)	up to 0.5 % (w/v)

5.2.4 Motility assay

Swarming motility of different *B. subtilis* mutants was analyzed on soft agar plates as previously described (Patrick & Kearns, 2009). Swarm plates contained 25 ml of LB medium fortified with 0.7 % (w/v) Bacto® Agar and were prepared one day prior to use. To minimize water content on the agar, plates were dried for 20 min open-faced in a laminar flow hood prior to inoculation and for 15 min postinoculation. 1 ml of cells grown to mid-exponential phase (OD_{600} 0.6-0.8) was resuspended in PBS buffer (8 g l^{-1} NaCl, 0.2 g l^{-1} KCl, 1.44 g l^{-1} Na_2HPO_4, 0.24 g l^{-1} KH_2PO_4, pH 7.0) to an OD_{600} of 10 and centrally spotted on the soft agar plate. Each plate was placed separately into larger petri dishes (14 cm diameter) containing 5 ml of water in order to ensure constant humidity in all samples. Plates were incubated at 37 °C and motility expansion was measured at one hour intervals along a drawn transect on the plate.

5.3 Molecular biological methods

5.3.1 Isolation of chromosomal DNA

In order to isolate chromosomal DNA from *B. subtilis*, cells were grown over night in LB at 30 °C. 2 ml of culture was pelleted by centrifugation (2 min, 13000 rpm, Eppendorf 5424R) and harvested cells were either stored at -20 °C or subsequently resuspended in 500 μl lysis buffer (50 mM EDTA, 100 mM NaCl, pH 7.5). Lysozyme was added to a final concentration of 2 mg ml^{-1} and the suspension was incubated at 37 °C for 15-30 min followed by an additional incubation

step with 20 µl of cooled 15 % (w/v) N-lauryl-sarcosine solution for 5 min on ice. After addition of 500 µl phenol (Roti-Phenol, Roth) samples were gently mixed by inversion and were centrifuged at 13000 rpm for 5-10 min. The upper (aqueous) phase was transferred to a fresh reaction tube using a clipped pipette tip. After addition of one volume of phenol: chloroform:isoamyl alcohol [25:24:1 (v/v/v), Roth] and a subsequent centrifugation step (10-15 min, 13000 rpm), the upper phase was again transferred into a new reaction cup containing 40 µl of sodium acetate (stock solution 3 M). After these two extraction steps, DNA was precipitated by adding 1 ml of ethanol (99.8 %) and gentle inversion. After pooling of DNA with a Pasteur pipette into a new reaction tube containing 70 % ethanol (v/v), the DNA was dried at room temperature and dissolved in 70-100 µl ddH_2O. Prior to storage at -20 °C, the concentration of extracted DNA was determined using a NanoDrop Lite ND-100 (Thermo Fischer Scientific).

5.3.2 Plasmid isolation by alkaline cell lysis

For plasmid preparation from *E. coli* DH5α (Birnboim and Doly 1979), overnight cultures (3-4 ml) carrying the desired plasmid were first centrifuged at 13000 rpm and RT for 1 min (Eppendorf 5424R). After removal of residual medium, cells were resuspended in 300 µl P1 buffer and lysed by addition of 300 µl P2 buffer. The lysate was neutralized through addition of 300 µl P3 buffer, kept on ice for further 10 min and cleared by centrifugation (15 min, 13000 rpm, 4 °C). Plasmid DNA in the supernatant was precipitated by addition of 600 µl isopropanol and subsequent centrifugation (45 min, 13000 rpm, RT). After removal of isopropanol, extracted plasmid DNA was washed in 500 µl of 70 % ethanol (v/v), dried at 37° C and dissolved in 30 µl ddH_2O.

Preparation of plasmid DNA with higher purity for sequencing purposes has been performed using the QIAprep Spin Miniprep Kit (Qiagen, Germany) or the Omega E.Z.N.A R Plasmid DNA Mini Kit I (VWR, Germany) according to the manufacturers' instructions

Buffer P1	Tris-HCl (pH 8.0)	50 mM
	EDTA	10 mM
	RNase A	100 µg ml^{-1}
Buffer P2	NaOH	200 mM
	Sodium dodecyl sulfate (SDS)	1 % (w/v)
Buffer P3	Potassium acetat	0.3 M
	Acetic acid	11.5 % (v/v)

5.3.3 Polymerase chain reaction - PCR

For amplification of specific DNA fragments (for analytical and preparative purposes), polymerase chain reaction (PCR) was performed (Mullis *et al.*, 1986). A standard PCR reaction contained 1x reaction buffer (5x Phusion® High-Fidelity reaction buffer, NEB), 50-100 ng chromosomal DNA (10-30 ng plasmid DNA), 200 µM dNTPs, 0.5 µM of each oligonucleotide (primer), 3 % (v/v) DMSO (dimethyl sulfoxide) and 0.02 U/µl polymerase (Phusion® High-Fidelity DNA Polymerase, NEB). Each PCR reaction was performed using a thermocycler (Biometra) applying the protocol shown below (**Table 5.3**). The duration for the elongation step was chosen according to the synthesis rate of the polymerase (1000 bps min^{-1}) and the length of the desired DNA fragment. To estimate the optimal annealing temperature for each oligonucleotide pair, an online Tm calculator was used (https://www.neb.com/tools-and-resources/interactive-tools/tm-calculator).

Following analysis by agarose gel electrophoresis (**5.2.2.4**), DNA fragments were purified from enzymes, nucleotides and salts using the QIAquick® PCR Purification Kit (Qiagen) according to the manufacturer's instruction.

Table 5.3: Thermocycling conditions for a routine PCR

Step	Temperature	Time	
Initial denaturation	98 °C	30 sec	
Denaturation	98 °C	10 sec	30 cycles
Annealing	55-65 °C	20-30 sec	
Extension	72 °C	60 sec/ kb	
Final extension	72 °C	10 min	
Hold	4-10 °C	∞	

5.3.4 Agarose gel electrophoresis

Size analysis and quality control of generated DNA fragments and plasmids respectively were assessed by horizontal agarose gel electrophoresis, which enables separation of DNA according to their size. Depending on the estimated size of analyzed molecules, gels were prepared in 1x TAE-buffer (see below) with an agarose percentage ranging from 0.8 to 1.2 % (w/v). Agarose was dissolved in TAE-buffer by heating and poured into horizontal gel casts. To stain DNA

molecules, 0.01 % (v/v) Midori Green (Nippon Genetics Europe GmbH) was added to the agarose mixture. Prior to loading of DNA probes on the agarose gel, samples were supplemented with 6x loading dye (NEB). Electrophoresis was carried out at 80-120 V (Electrophoresis power supply, Consort EV243) and DNA was visualized using a UV-Transilluminator.

50x TAE-Buffer	Tris-Acetat pH 8.2-8.4	2 M
	EDTA	0.05 M

5.3.5 Molecular cloning

The construction of plasmids and related procedures (extraction of plasmid/ chromosomal DNA, PCR reactions, specific digestion and ligation of DNA fragments) were performed according to standard protocols (Sambrook *et al.*, 1989). Besides conventional cloning procedures using restriction endonucleases, a variety of constructs has been constructed applying the so-called *Gibson Assembly* technique (Gibson *et al.*, 2009).

5.3.6 Site-directed mutagenesis

Site-directed mutagenesis, using a PCR-based kit (Q5® Site-Directed Mutagenesis Kit, NEB), was performed to create specific, targeted point mutations in a plasmid encoded gene. For this purpose, two oligonucleotides were designed using an online tool provided by NEB (http://nebasechanger.neb.com/). Nucleotide substitutions were created by incorporating the desired mismatch in the center of the forward (mutagenic) primer, which included at least ten complementary nucleotides to the template at the 3´ end of the mutation. The 5´ end of the reverse primer was designed in such way that it begins at the nucleotide base next to the 5´ end of the mutagenic primer, and proceeds in the opposite direction on the complementary DNA strand (back-to-back annealing of primers). After exponential amplification via PCR (**5.3.2**), the amplified material was incubated with an enzyme mix containing a Kinase, Ligase and the restriction enzyme *Dpn*I for plasmid circularization and template removal respectively.

5.3.7 DNA sequencing

To verify correct cloning and mutagenesis of genes or gene fragments, DNA sequencing was performed by the following companies: GATC Biotech (Konstanz, Germany) or by Eurofins Genomics (Ebersberg, Germany). Purified plasmids (**5.2.2.2**) were provided in a concentration of 50-100 ng μl^{-1} and oligonucleotides according to the corresponding companies´ instructions.

5.3.8 Preparation of chemically competent *E. coli* cells and transformation

Chemically competent *E. coli* cells, either DH5α for cloning or BL21 (DE3) for overexpression, were prepared following a slow growth protocol as described by Inoue *et al.*, (1990). To this end, an overnight pre-culture was diluted to an OD_{600} of 0.005 in 125 ml of SOB medium and incubated at 18 °C and 200 rpm for approximately 48 h until an OD_{600} of 0.6 was reached. Following an incubation of the culture on ice for 10 min, cells were harvested by centrifugation (10 min, 3000 rpm, 4 °C; rotor: JLA-16.250, centrifuge: Avanti® J-E, Beckman Coulter) and subsequently resuspended in 80 ml of cold TB buffer. After an additional incubation period (10 min) on ice, the culture was again centrifuged for 10 min at 3000 rpm and 4 °C (rotor: SX4750, centrifuge AllegraR X-15R, Beckman Coulter) and the pellet was resuspended in 20 ml of TB supplemented with 7 % (v/v) DMSO. Following a finale 10 min-long incubation on ice, the cell suspension was aliquoted (100 µl), shock frozen in liquid nitrogen and competent cells were stored at -80 °C.

For transformation, an aliquot of competent cells was thawed on ice and DNA was added to the cells. In case of ligation reactions, the total ligation volume (20 µl) was added and in case of closed plasmids up to 100 ng of DNA. After incubation for 20-30 min on ice, cells were exposed to a heat shock at 42 °C for 90 sec, cooled on ice for 2-5 min and in a final step supplemented with 700 µl of SOB medium (**Table 5.1**). Following incubation at 37 °C and 200 rpm for 1 h, cells were streaked on LB agar plates (**Table 5.1**) containing appropriate antibiotics for selection (**Table 5.2**), and grown for 16 h at 37 °C.

TB Buffer	HEPES pH 6.7	10 mM
	$CaCl_2$	15 mM
	KCl	250 mM
	$MnCl_2$	55 mM

5.3.9 Preparation and transformation of competent *B. subtilis* cells

At the transition from exponential to stationary phase, a small subpopulation of *B. subtilis* cultures develops a state of natural competence. These competent cells are characterized by their ability to uptake exogenous DNA via a membrane-associated machinery in order to integrate this DNA into their genome, for instance. Laboratory strains of *B. subtilis* such as strain PY79 and strain 168, are renowned for high-frequency natural transformation (Zafra *et al.*, 2012; Konkol *et al.*, 2013). However, the ancestral *B. subtilis* strain NCIB3610 has been shown to be poorly competent in laboratory conditions due to the plasmid-encoded competence inhibitor ComI. To circumvent this, a *comI*^{Q12L} mutant strain (DK1042, Konkol *et al.*, 2013) was used in the course of this study. For transformation of different *B. subtilis* derivatives (including NCIB3610, DK1042, PY79 and 168), corresponding cultures were grown overnight in liquid LB at 30 °C and were diluted to an OD_{600} of 0.08 in 10 ml of Modified Competence Medium (MCM, Spizizen, 1958; **Table 5.1**), followed by incubation at 37 °C and 200 rpm. Using this competence medium, strain NCIB3610 has been demonstrated to develop low competence efficiencies (Zafra *et al.*, 2012). When cultures reached an OD_{600} of 1.3-1.5, up to 500 ng of plasmid or genomic DNA were added to 1 ml of cell suspension. After further incubation at 37 °C and constant shaking for at least 2 hours, cells were plated with appropriate antibiotics (**Table 5.2**).

5.4 Biochemical methods

5.4.1 Purification of recombinant produced proteins from *E. coli* BL21 (DE3)

For protein purification via affinity chromatography [immobilized metal affinity chromatography (IMAC, Nickel affinity chromatography) and Strep-Tactin affinity chromatography] and subsequent size exclusion chromatography (SEC), 2 l of the corresponding overexpression culture (**5.2.1**) were harvested 4 hours after induction (4000 rpm, 15 min, 4 °C; rotor: JA-12, centrifuge: Avanti® J-E, Beckman Coulter) and stored at -20 °C for 16 h.

For protein extraction, cells were washed twice in 1/50 sample volume of buffer W (see below) and resuspended with equal amounts of buffer W prior to cell lysis using the M-110L Microfluidizer (Microfluidics, AG Bange, Synmikro). Obtained lysates were cleared by centrifugation for 45 min at 13000 rpm and 4 °C (rotor: JLA-16.250, centrifuge: Avanti® J-E, Beckman Coulter). The clear supernatant was loaded on a 1 ml HisTrap™ FF or a 1 ml StrepTrap™ HP column (GE Healthcare), depending on the protein to be purified (His_6- and

Strep-tagged proteins respectively). Columns were equilibrated with 10 column volumes (CV) of the corresponding buffer W prior to use. After lysate loading and washing of columns with the respective buffer W (30-40 CV), bound proteins were eluted with 10 ml of the corresponding elution buffer E. The obtained elution fractions were analyzed by SDS-PAGE (**5.4.4**) and SEC (Gelfiltration, **5.4.3**).

Buffer W (His-tag)	HEPES	20 mM
	NaCl	250 mM
	KCl	20 mM
	$MgCl_2$	20 mM
	Imidazole	40 mM
	pH 8.0	
Buffer E (His-tag)	HEPES	20 mM
	NaCl	250 mM
	KCl	20 mM
	$MgCl_2$	20 mM
	Imidazole	500 mM
	pH 8.0	
Buffer W (Strep-tag)	Tris-HCl pH 8.0	100 mM
	NaCl	150 mM
Buffer E (Strep-tag)	Tris-HCl pH 8.0	100 mM
	NaCl	150 mM
	Desthiobiotin	2.5 mM

5.4.2 Purification of DgcP-StrepII from *B. subtilis* NCIB3610

A culture (1 l) of the engineered strain NCIB3610-PB29 was grown to exponential phase without selective pressure in LB medium (37 °C) and gene expression was induced with 0.5 % (w/v) xylose. After two hours of growth at 37 °C, cells were harvested (**5.4.1**), washed with buffer W (see above) and resuspended in 20 ml of buffer W complemented with protease inhibitors (cOmplete™, Roche). Resuspended cells were lysed by two passages through a French press cell at approximately 20000 psi (Amicon). To clarify the lysate from cell debris, samples were centrifuged (**5.4.1**) and the supernatant subsequently incubated with Strep-Tactin-Sepharose (1 ml, IBA) using a gravity flow column (BIO-RAD). The column was washed with 15 ml buffer W and bound DgcP-StrepII proteins were eluted in fractions of 0.5 ml by addition of buffer E (see above), followed by concentration of pooled fractions using Amicon® Ultra-15 centrifugal filter units (Merck Millipore), and subsequent analysis via SDS-PAGE (**5.4.5**).

5.4.3 Gelfiltration

Gelfiltration was performed using an ÄKTA FPLC (GE Healthare) and a Superdex 200 (10/300 GL), which was equilibrated with running buffer, prior to injection of pooled and concentrated elution fractions (using Amicon® Ultra-15 centrifugal filter units, 50 K molecular weight cut-off, Merck Millipore) obtained after affinity chromatography. Separation of proteins was performed at a constant flow rate of 0.5 ml min^{-1} at 4 °C. The absorption profile of protein samples was measured at 260 nm and proteins from different absorption maxima were analyzed by SDS-PAGE (**5.4.5**).

Running buffer	HEPES	20 mM
	NaCl	200 mM
	KCl	20 mM
	$MgCl_2$	20 mM
	pH 7.5	

5.4.4 Determination of protein concentration

The concentration c [mol l^{-1}] of a purified protein was calculated from the measured absorbance at 280 nm with a spectrophotometer and the specific extinction coefficient ε (l mol^{-1} cm^{-1}) of the protein, applying the equation of Lambert and Beer ($c = A\ \varepsilon^{-1}\ d^{-1}$; d: path length of used quartz cuvette: 1 cm). Theoretical extinction coefficients were determined using the online tool ProtParam (web.expasy.org/protparam; Gasteiger *et al.*, 2005).

5.4.5 Sodium-dodecylsulfate polyacrylamide gel electrophoresis (SDS-PAGE)

SDS-PAGE was performed to separate proteins according to their molecular mass under denaturating conditions. The visualization of protein samples was carried out with self-prepared polyacrylamide gels of 12.5 % (v/v) or with 4–20% (v/v) polyacrylamide gels obtained from BIO-RAD (Mini-PROTEAN® TGX™ Precast Protein Gels).

Gels were prepared according to Laemmli (1970) using the Mini-PROTEAN® system (BIO-RAD). Protein samples were mixed with 4x SDS loading buffer (refer to **2.2.5**), boiled for 10 minutes at 95 °C and loaded on the gel. Electrophoresis was carried out in a Mini-PROTEAN® Tetra Cell with 80-140 V (Electrophoresis power supply, Consort EV243). PageRuler™ Plus from Thermo Scientific was used as protein ladder.

5.4.6 Coomassie staining of polyacrylamide gels

Following SDS-PAGE, polyacrylamide gels were either stained with Coomassie Brilliant Blue (CB) or subjected to Silver-staining (**5.4.7**) or to Western blotting (**5.4.8**). For CB staining, gels were soaked for 30-60 min in CB staining solution [25 % (v/v) ethanol, 20 % (v/v) acetic acid, 0.25 % (w/v) Coomassie Brilliant Blue R-250]. A mixture of ddH_2O [60 % (v/v)], ethanol [30 % (v/v)] and acetic acid [10 % (v/v)] served as destaining solution to remove excess stain. Colloidal Coomassie staining was performed following manufacturer's recommendations (Roti®-Blue, Roth).

5.4.7 Silver staining of polyacrylamide gels

To visualize low-abundant proteins after SDS-PAGE, gels were stained with silver nitrate. First, the gel was fixed over night or for 1 h in solution 1. After three washing steps with 50 % (v/v) ethanol, the gel was incubated for 30 min in solution 2. Following three short washing steps with ddH_2O (20 sec), the gel was stained for 30 min with solution 3. After three additional washing steps with ddH_2O, developing solution 4 was added until a sufficient stain was accomplished. The reaction was stopped by addition of solution 5 and the gel stored in solution 6.

Solution 1	25 ml	methanol
	6 ml	acetic acid
	0.027 ml	formaldehyde solution [37 % (v/v)]
	ad 50 ml	ddH_2O
Solution 2	0.250 ml	thiosulfate solution (40 mg ml^{-1})
	ad 50 ml	ddH_2O
Solution 3	0.200 g	$AgNO_3$
	0.094 ml	formaldehyde solution [37 % (v/v)]
	ad 50 ml	ddH_2O
Solution 4	3 g	Na_2CO_3
	0.075 ml	formaldehyde solution [37 % (v/v)]
	0.15 ml	thiosulfate solution (40 mg ml^{-1})
	ad 50 ml	ddH_2O
Solution 5	25 ml	methanol
	6 ml	acetic acid
	ad 50 ml	ddH_2O
Solution 6	10 % (v/v)	glycerol
	5 % (v/v)	ethanol

5.4.8 Western blotting and immunodetection of fusion proteins

In order to transfer proteins after SDS-PAGE (**5.4.5**) onto a nitrocellulose membrane (pore size 2 µm; 82 mm thick; Protran BA83, Whatman™, GE Healthcare), the semi-dry Western blotting protocol (Harlow and Lane, 1988) was applied using either the Trans-Blot® Turbo™ Transfer System (BIO-RAD) or the PerfectBlue™ Semi-Dry-Blotter Sedec™ (VWR Peqlab). To this end, three layers of Rotilabo® blotting paper (Roth, 0.35 mm thick) soaked in transfer buffer, a nitrocellulose membrane soaked in ddH_2O, the SDS-PAGE gel and another three layers of blotting paper were placed on the top of each other inside the blotting apparatus. The electro-transfer was conducted for 90 min at 0.8 mA per cm^2 of gel area.

Fluorescent protein fusions covalently bound to the nitrocellulose membrane after transfer, were subsequently detected using a specific α-GFP antiserum (dilution 1:500, produced by Gramsch Laboratories, Schwabhausen) and a secondary antibody conjugated with horseradish peroxidase (mouse-α-rabbit-HRP, dilution 1:10.000, Sigma). Prior to detection, the nitrocellulose membrane was incubated in blocking solution over night at 4 °C under constant shaking, followed by an additional incubation period of 1 h (RT). The membrane was then incubated for 1 h with the α-GFP antiserum (diluted in blocking solution), followed by three washing steps with PBST (3 x 10 min), incubation with the secondary antibody for 1 h and final washing (3 x 10 min) with PBST. Fusion proteins were visualized by chemiluminescence, as a consequence of enzymatic luminol oxidation by the IgG coupled horseradish peroxidase. In order to start this reaction, the membrane was incubated for 1 min in a mixture of solution 1 and solution 2 prior to signal detection using the ChemiDoc™ MP Imaging System (BIO-RAD). Proteins fused to a Strep-tag were detected using a Strep-Tactin® HRP Conjugate (Strep-Tactin® labeled with horseradish peroxidase) according to the manufacturer's recommendations (IBA).

PBST	Na_2HPO_4	0.8 mM
	NaH_2PO_4	2 mM
	NaCl	10 mM
	Tween 20	0.1 % (v/v)
Blocking solution	PBST with 5 % (w/v) skim milk powder	
Solution 1	Luminol	2.5 mM
	Coumaric acid	0.4 mM
	Tris-HCl pH 8.5	100 mM
Solution 2	H_2O_2	0.018 % (v/v)
	Tris-HCl pH 8.5	100 mM

5.5 Software

Protein domain structures and topologies were analyzed using Pfam (http://www.sanger.ac.uk), SMART (http://www.smart.embl-heidelberg.de), UniProt (http://www.uniprot.org/), NCBI (http://www.ncbi.nlm.gov), TMHMM Server v. 2.0 (http://www.cbs.dtu.dk/services/TMHMM), SignalP Server v. 4.1 (http://www.cbs.dtu.dk /services/SignalP), LipoP 1.0 server (http://www.cbs.dtu.dk/services/LipoP), CAZY (http://www.cazy.org), DisMeta (http://www-nmr.cabm.rutgers.edu/bioinformatics/disorder/), PsiPred (http://bioinf.cs.ucl.ac.uk/psipred/), COILS/PCOILS (https://omictools.com/coils-pcoils-tool), MARCOIL (https://toolkit.Tuebingen.mpg.de/#/tools/marcoil). Protein characteristics, like the extinction coefficient, were calculated using the ProtParam software (www.expasy.ch/tools/protparam.html). DNA and amino acid sequences from *B. subtilis* were obtained from the SubtiWiki server (http://subtiwiki.uni-goettingen.de/). The Basic Local Alignment Search Tool (BLAST, http://blast.ncbi.nlm.nih.gov/Blast.cgi) and ClustalW (http://www.genome.jp/tools/clustalw/) were used for comparison of DNA or amino acid sequences. Data of protein purification obtained during SEC were analyzed with PrimeView software (GE Healthcare). Microscope images were analyzed using Fiji ImageJ or MetaMorph 6.3-Software (Meta Imaging Software). For statistical analysis and to visualize experimental data, Excel 2010 (Microsoft) was used. To assemble and draw figures, CorelDRAW Graphics Suite X5 was utilized.

6 BIBLIOGRAPHY

Albertini, A.M., and Galizzi, A. (1999). The sequence of the *trp* operon of *Bacillus subtilis* 168 (*trpC2*) revisited. *Microbiology* 145(12), 3319-3320.

Allard-Massicotte, R., Tessier, L., Lécuyer, F., Lakshmanan, V., Lucier, J.-F., Garneau, D., *et al.* (2016). *Bacillus subtilis* early colonization of *Arabidopsis thaliana* roots involves multiple chemotaxis receptors. *mBio* 7(6), e01664-01616.

Alva, V., Nam, S.-Z., Söding, J., and Lupas, A.N. (2016). The MPI bioinformatics Toolkit as an integrative platform for advanced protein sequence and structure analysis. *Nucleic acids research* 44(W1), W410-W415.

Alzari, P.M., ne Souchon, H., and Dominguez, R. (1996). The crystal structure of endoglucanase CelA, a family 8 glycosyl hydrolase from *Clostridium thermocellum*. *Structure* 4(3), 265-275.

Ambrose, E. (1956). A surface contact microscope for the study of cell movements. *Nature* 178, 1194.

Amikam, D., and Benziman, M. (1989). Cyclic diguanylic acid and cellulose synthesis in *Agrobacterium tumefaciens*. *J Bacteriol* 171(12), 6649-6655.

Amikam, D., and Galperin, M.Y. (2006). PilZ domain is part of the bacterial c-di-GMP binding protein. *Bioinformatics* 22(1), 3-6. doi: 10.1093/bioinformatics/bti739.

Anantharaman, V., and Aravind, L. (2003). Application of comparative genomics in the identification and analysis of novel families of membrane-associated receptors in bacteria. *BMC Genomics* 4(1), 34. doi: 10.1186/1471-2164-4-34.

Anantharaman, V., Aravind, L., and Koonin, E.V. (2003). Emergence of diverse biochemical activities in evolutionarily conserved structural scaffolds of proteins. *Curr Opin Chem Biol* 7(1), 12-20.

Anderson, G., and O'toole, G. (2008). Innate and induced resistance mechanisms of bacterial biofilms, in *Bacterial biofilms*. Springer, 85-105.

Anwar, N., Rouf, S.F., Römling, U., and Rhen, M. (2014). Modulation of biofilm-formation in *Salmonella enterica serovar Typhimurium* by the periplasmic DsbA/DsbB oxidoreductase system requires the GGDEF-EAL domain protein STM3615. *PloS one* 9(8), e106095.

Aravind, L., and Koonin, E.V. (1998). The HD domain defines a new superfamily of metal-dependent phosphohydrolases. *Trends in biochemical sciences* 23(12), 469-472.

Arora, S.K., Ritchings, B.W., Almira, E.C., Lory, S., and Ramphal, R. (1997). A transcriptional activator, FleQ, regulates mucin adhesion and flagellar gene expression in *Pseudomonas aeruginosa* in a cascade manner. *Journal of bacteriology* 179(17), 5574-5581.

Artsimovitch, I. (2010). A processive riboantiterminator seeks a switch to make biofilms. *Molecular microbiology* 76(3), 535-539.

Asally, M., Kittisopikul, M., Rue, P., Du, Y., Hu, Z., Cagatay, T., *et al.* (2012). Localized cell death focuses mechanical forces during 3D patterning in a biofilm. *Proc Natl Acad Sci U S A* 109(46), 18891-18896. doi: 10.1073/pnas.1212429109.

Ashman, D.F., Lipton, R., Melicow, M.M., and Price, T.D. (1963). Isolation of adenosine 3', 5'-monophosphate and guanosine 3', 5'-monophosphate from rat urine. *Biochem Biophys Res Commun* 11, 330-334.

Ausmees, N., Mayer, R., Weinhouse, H., Volman, G., Amikam, D., Benziman, M., *et al.* (2001). Genetic data indicate that proteins containing the GGDEF domain possess diguanylate cyclase activity. *FEMS Microbiology Letters* 204(1), 163-167.

Axelrod, D. (1981). Cell-substrate contacts illuminated by total internal reflection fluorescence. *The Journal of cell biology* 89(1), 141-145.

Baker, P., Whitfield, G.B., Hill, P.J., Little, D.J., Pestrak, M.J., Robinson, H., *et al.* (2015). Characterization of the *Pseudomonas aeruginosa* glycoside hydrolase PslG reveals that its levels are critical for Psl polysaccharide biosynthesis and biofilm formation. *Journal of Biological Chemistry* 290(47), 28374-28387.

Banin, E., Vasil, M.L., and Greenberg, E.P. (2005). Iron and *Pseudomonas aeruginosa* biofilm formation. *Proceedings of the National Academy of Sciences of the United States of America* 102(31), 11076-11081.

Baraquet, C., and Harwood, C.S. (2013). Cyclic diguanosine monophosphate represses bacterial flagella synthesis by interacting with the Walker A motif of the enhancer-binding protein FleQ. *Proceedings of the National Academy of Sciences* 110(46), 18478-18483.

Baraquet, C., Murakami, K., Parsek, M.R., and Harwood, C.S. (2012). The FleQ protein from *Pseudomonas aeruginosa* functions as both a repressor and an activator to control gene expression from the pel operon promoter in response to c-di-GMP. *Nucleic acids research*, gks384.

Barzu, O., and Danchin, A. (1994). Adenylyl cyclases: a heterogeneous class of ATP-utilizing enzymes. *Prog Nucleic Acid Res Mol Biol* 49, 241-283.

Beavo, J.A., and Brunton, L.L. (2002). Cyclic nucleotide research - still expanding after half a century. *Nat Rev Mol Cell Biol* 3(9), 710-718. doi: 10.1038/nrm911.

Becker, A. (2015) Challenges and perspectives in combinatorial assembly of novel exopoly saccharide biosynthesis pathways. *Front Microbiol* **6**: 687.

Bellini, D., Caly, D.L., McCarthy, Y., Bumann, M., An, S.Q., Dow, J.M., *et al.* (2014). Crystal structure of an HD-GYP domain cyclic-di-GMP phosphodiesterase reveals an enzyme with a novel trinuclear catalytic iron centre. *Molecular microbiology* 91(1), 26-38.

Benigar, E., Dogsa, I., Stopar, D., Jamnik, A., Cigić, I.K., and Tomšič, M. (2014). Structure and dynamics of a polysaccharide matrix: aqueous solutions of bacterial levan. *Langmuir* 30(14), 4172-4182.

Berne, C., Ducret, A., Hardy, G.G., and Brun, Y.V. (2015). Adhesins involved in attachment to abiotic surfaces by Gram-negative bacteria. *Microbiology spectrum* 3(4).

Birnboim, H., and Doly, J. (1979). Nucleic Acid Res. 7, 1513–1523.

Biswas, K.H., Badireddy, S., Rajendran, A., Anand, G.S., and Visweswariah, S.S. (2015). Cyclic nucleotide binding and structural changes in the isolated GAF domain of *Anabaena* adenylyl cyclase, CyaB2. *PeerJ* 3, e882.

Boehm, A., Kaiser, M., Li, H., Spangler, C., Kasper, C.A., Ackermann, M., *et al.* (2010). Second messenger-mediated adjustment of bacterial swimming velocity. *Cell* 141(1), 107-116.

Boehm, A., Steiner, S., Zaehringer, F., Casanova, A., Hamburger, F., Ritz, D., *et al.* (2009). Second messenger signalling governs *Escherichia coli* biofilm induction upon ribosomal stress. *Molecular microbiology* 72(6), 1500-1516.

Bordeleau, E., Purcell, E.B., Lafontaine, D.A., Fortier, L.-C., Tamayo, R., and Burrus, V. (2015). Cyclic di-GMP riboswitch-regulated type IV pili contribute to aggregation of *Clostridium difficile*. *Journal of bacteriology* 197(5), 819-832.

Boylan, S.A., Redfield, A.R., Brody, M.S., and Price, C.W. (1993). Stress-induced activation of the sigma B transcription factor of *Bacillus subtilis*. *Journal of bacteriology* 175(24), 7931-7937.

Branda, S.S., Chu, F., Kearns, D.B., Losick, R., and Kolter, R. (2006). A major protein component of the *Bacillus subtilis* biofilm matrix. *Mol Microbiol* 59(4), 1229-1238. doi: 10.1111/j.1365-2958.2005.05020.x.

Branda, S.S., Gonzalez-Pastor, J.E., Ben-Yehuda, S., Losick, R., and Kolter, R. (2001). Fruiting body formation by *Bacillus subtilis*. *Proc Natl Acad Sci U S A* 98(20), 11621-11626. doi: 10.1073/pnas.191384198.

Branda, S.S., González-Pastor, J.E., Dervyn, E., Ehrlich, S.D., Losick, R., and Kolter, R. (2004). Genes involved in formation of structured multicellular communities by *Bacillus subtilis*. *Journal of bacteriology* 186(12), 3970-3979.

Branda, S.S., Vik, Å., Friedman, L., and Kolter, R. (2005). Biofilms: the matrix revisited. *Trends in microbiology* 13(1), 20-26.

Burbulys, D., Trach, K.A., and Hoch, J.A. (1991). Initiation of sporulation in *B. subtilis* is controlled by a multicomponent phosphorelay. *Cell* 64(3), 545-552.

Cairns, L.S., Hobley, L., and Stanley-Wall, N.R. (2014). Biofilm formation by *Bacillus subtilis*: new insights into regulatory strategies and assembly mechanisms. *Mol Microbiol* 93(4), 587-598. doi: 10.1111/mmi.12697.

Cairns, L.S., Marlow, V.L., Bissett, E., Ostrowski, A., and Stanley-Wall, N.R. (2013). A mechanical signal transmitted by the flagellum controls signalling in *Bacillus subtilis*. *Molecular microbiology* 90(1), 6-21.

Candela, T., and Fouet, A. (2006). Poly-gamma-glutamate in bacteria. *Molecular microbiology* 60(5), 1091-1098.

Chai, L., Romero, D., Kayatekin, C., Akabayov, B., Vlamakis, H., Losick, R., *et al.* (2013). Isolation, characterization, and aggregation of a structured bacterial matrix precursor. *Journal of Biological Chemistry* 288(24), 17559-17568.

Chai, Y., Kolter, R., and Losick, R. (2010). Reversal of an epigenetic switch governing cell chaining in *Bacillus subtilis* by protein instability. *Molecular microbiology* 78(1), 218-229.

Chandrangsu, P., and Helmann, J.D. (2016). Intracellular Zn (II) Intoxication Leads to Dysregulation of the PerR Regulon Resulting in Heme Toxicity in *Bacillus subtilis*. *PLoS genetics* 12(12), e1006515.

Charbonneau, H., Prusti, R.K., LeTrong, H., Sonnenburg, W.K., Mullaney, P.J., Walsh, K.A., *et al.* (1990). Identification of a noncatalytic cGMP-binding domain conserved in both the cGMP-stimulated and photoreceptor cyclic nucleotide phosphodiesterases. *Proceedings of the National Academy of Sciences* 87(1), 288-292.

Chen, L.H., Koseoglu, V.K., Guvener, Z.T., Myers-Morales, T., Reed, J.M., D'Orazio, S.E., *et al.* (2014). Cyclic di-GMP-dependent signaling pathways in the pathogenic Firmicute *Listeria monocytogenes*. *PLoS Pathog* 10(8), e1004301. doi: 10.1371/journal.ppat.1004301.

Chen, Y., Chai, Y., Guo, J.H., and Losick, R. (2012). Evidence for cyclic Di-GMP-mediated signaling in *Bacillus subtilis*. *J Bacteriol* 194(18), 5080-5090. doi: 10.1128/JB.01092-12.

Christen, B., Christen, M., Paul, R., Schmid, F., Folcher, M., Jenoe, P., *et al.* (2006). Allosteric control of cyclic di-GMP signaling. *J Biol Chem* 281(42), 32015-32024. doi: 10.1074/jbc.M603589200.

Christen, M., Christen, B., Allan, M.G., Folcher, M., Jeno, P., Grzesiek, S., *et al.* (2007). DgrA is a member of a new family of cyclic diguanosine monophosphate receptors and controls flagellar motor function in *Caulobacter crescentus*. *Proc Natl Acad Sci U S A* 104(10), 4112-4117. doi: 10.1073/pnas.0607738104.

Christen, M., Christen, B., Folcher, M., Schauerte, A., and Jenal, U. (2005). Identification and characterization of a cyclic di-GMP-specific phosphodiesterase and its allosteric control by GTP. *Journal of Biological Chemistry* 280(35), 30829-30837.

Chu, F., Kearns, D.B., McLoon, A., Chai, Y., Kolter, R., and Losick, R. (2008). A novel regulatory protein governing biofilm formation in *Bacillus subtilis*. *Molecular microbiology* 68(5), 1117-1127.

Civril, F., Deimling, T., de Oliveira Mann, C.C., Ablasser, A., Moldt, M., Witte, G., *et al.* (2013). Structural mechanism of cytosolic DNA sensing by cGAS. *Nature* 498(7454), 332-337. doi: 10.1038/nature12305.

Colvin, K.M., Alnabelseya, N., Baker, P., Whitney, J.C., Howell, P.L., and Parsek, M.R. (2013). PelA deacetylase activity is required for Pel polysaccharide synthesis in *Pseudomonas aeruginosa*. *Journal of bacteriology* 195(10), 2329-2339.

Conner, J.G., Zamorano-Sánchez, D., Park, J.H., Sondermann, H., and Yildiz, F.H. (2017). The ins and outs of cyclic di-GMP signaling in *Vibrio cholerae*. *Current Opinion in Microbiology* 36, 20-29.

Cooper, D.M., and Tabbasum, V.G. (2014). Adenylate cyclase-centred microdomains. *Biochemical Journal* 462(2), 199-213.

Corrigan, R.M., and Gründling, A. (2013). Cyclic di-AMP: another second messenger enters the fray. *Nature Reviews Microbiology* 11(8), 513-524.

Costerton, J.W., Cheng, K., Geesey, G.G., Ladd, T.I., Nickel, J.C., Dasgupta, M., *et al.* (1987). Bacterial biofilms in nature and disease. *Annual Reviews in Microbiology* 41(1), 435-464.

Costerton, J.W., Lewandowski, Z., Caldwell, D.E., Korber, D.R., and Lappin-Scott, H.M. (1995). Microbial biofilms. *Annu Rev Microbiol* 49, 711-745. doi: 10.1146/annurev.mi.49.100195.003431.

Dahl, M.K., Msadek, T., Kunst, F., and Rapoport, G. (1991). Mutational analysis of the *Bacillus subtilis* DegU regulator and its phosphorylation by the DegS protein kinase. *Journal of bacteriology* 173(8), 2539-2547.

Dahlstrom, K.M. (2016). Specificity in Signaling: Bacterial Decision-Making through the Cyclic Diguanylate Second Messenger. Dartmouth College.

Dahlstrom, K.M., Giglio, K.M., Collins, A.J., Sondermann, H., and O'Toole, G.A. (2015). Contribution of physical interactions to signaling specificity between a diguanylate cyclase and its Effector. *MBio* 6(6), e01978-01915. doi: 10.1128/mBio.01978-15.

Dahlstrom, K.M., Giglio, K.M., Sondermann, H., and O'Toole, G.A. (2016). The Inhibitory Site of a Diguanylate Cyclase Is a Necessary Element for Interaction and Signaling with an Effector Protein. *Journal of bacteriology* 198(11), 1595-1603.

Davey, M.E., and O'toole, G.A. (2000). Microbial biofilms: from ecology to molecular genetics. *Microbiology and molecular biology reviews* 64(4), 847-867.

Davies, B.W., Bogard, R.W., Young, T.S., and Mekalanos, J.J. (2012). Coordinated regulation of accessory genetic elements produces cyclic di-nucleotides for *V. cholerae* virulence. *Cell* 149(2), 358-370.

De, N., Navarro, M.V., Raghavan, R.V., and Sondermann, H. (2009). Determinants for the activation and autoinhibition of the diguanylate cyclase response regulator WspR. *Journal of molecular biology* 393(3), 619-633.

Dennis, P.G., Miller, A.J., and Hirsch, P.R. (2010). Are root exudates more important than other sources of rhizodeposits in structuring rhizosphere bacterial communities? *FEMS microbiology ecology* 72(3), 313-327.

Diethmaier, C., Newman, J.A., Kovács, Á.T., Kaever, V., Herzberg, C., Rodrigues, C., *et al.* (2014). The YmdB phosphodiesterase is a global regulator of late adaptive responses in *Bacillus subtilis*. *Journal of bacteriology* 196(2), 265-275.

Dietrich, L.E., Okegbe, C., Price-Whelan, A., Sakhtah, H., Hunter, R.C., and Newman, D.K. (2013). Bacterial community morphogenesis is intimately linked to the intracellular redox state. *Journal of bacteriology* 195(7), 1371-1380.

Dobell (1960). *Antony van Leeuwenhoek and his 'Little animals'*. Dover Publications, New York, NY.

Dogsa, I., Brloznik, M., Stopar, D., and Mandic-Mulec, I. (2013). Exopolymer diversity and the role of levan in *Bacillus subtilis* biofilms. *PLoS One* 8(4), e62044. doi: 10.1371/journal.pone.0062044.

Dubey, G.P., Mohan, G.B.M., Dubrovsky, A., Amen, T., Tsipshtein, S., Rouvinski, A., *et al.* (2016). Architecture and characteristics of bacterial nanotubes. *Developmental cell* 36(4), 453-461.

Dubnau, D., Hahn, J., Roggiani, M., Piazza, F., and Weinrauch, Y. (1994). Two-component regulators and genetic competence in *Bacillus subtilis*. *Research in microbiology* 145(5-6), 403-411.

Dunker, A.K., Oldfield, C.J., Meng, J., Romero, P., Yang, J.Y., Chen, J.W., *et al.* (2008). The unfoldomics decade: an update on intrinsically disordered proteins. *BMC genomics* 9(2), S1.

Elsholz, A.K., Wacker, S.A., and Losick, R. (2014). Self-regulation of exopolysaccharide production in *Bacillus subtilis* by a tyrosine kinase. *Genes & development* 28(15), 1710-1720.

Eymann, C., Dreisbach, A., Albrecht, D., Bernhardt, J., Becher, D., Gentner, S., et al. (2004). A comprehensive proteome map of growing *Bacillus subtilis* cells. *Proteomics* 4(10), 2849-2876.

Fabret, C., Feher, V.A., and Hoch, J.A. (1999). Two-component signal transduction in *Bacillus subtilis*: how one organism sees its world. *Journal of Bacteriology* 181(7), 1975-1983.

Fagerlund, A., Smith, V., Rohr, A.K., Lindback, T., Parmer, M.P., Andersson, K.K., et al. (2016). Cyclic diguanylate regulation of *Bacillus cereus* group biofilm formation. *Mol Microbiol* 101(3), 471-494. doi: 10.1111/mmi.13405.

Farrar, K., Bryant, D., and Cope-Selby, N. (2014). Understanding and engineering beneficial plant–microbe interactions: plant growth promotion in energy crops. *Plant biotechnology journal* 12(9), 1193-1206.

Feucht, A., and Lewis, P.J. (2001). Improved plasmid vectors for the production of multiple fluorescent protein fusions in *Bacillus subtilis*. *Gene* 264(2), 289-297.

Flemming, H.C., and Wingender, J. (2010). The biofilm matrix. *Nat Rev Microbiol* 8(9), 623-633. doi: 10.1038/nrmicro2415.

Fowler, D.M., Koulov, A.V., Balch, W.E., and Kelly, J.W. (2007). Functional amyloid–from bacteria to humans. *Trends in biochemical sciences* 32(5), 217-224.

Franklin, M.J., Chang, C., Akiyama, T., and Bothner, B. (2015). New Technologies for Studying Biofilms. *Microbiology spectrum* 3(4).

Friedman, L., and Kolter, R. (2004). Genes involved in matrix formation in *Pseudomonas aeruginosa* PA14 biofilms. *Mol Microbiol* 51(3), 675-690.

Fujita, M., González-Pastor, J.E., and Losick, R. (2005). High-and low-threshold genes in the Spo0A regulon of *Bacillus subtilis*. *Journal of bacteriology* 187(4), 1357-1368.

Galperin, M.Y. (2004). Bacterial signal transduction network in a genomic perspective. *Environ Microbiol* 6(6), 552-567. doi: 10.1111/j.1462-2920.2004.00633.x.

Galperin, M.Y., Gaidenko, T.A., Mulkidjanian, A.Y., Nakano, M., and Price, C.W. (2001a). MHYT, a new integral membrane sensor domain. *FEMS Microbiol Lett* 205(1), 17-23.

Galperin, M.Y., Nikolskaya, A.N., and Koonin, E.V. (2001b). Novel domains of the prokaryotic two-component signal transduction systems. *FEMS Microbiol Lett* 203(1), 11-21.

Gao, X., Mukherjee, S., Matthews, P.M., Hammad, L.A., Kearns, D.B., and Dann, C.E., 3rd (2013). Functional characterization of core components of the *Bacillus subtilis* cyclic-di-GMP signaling pathway. *J Bacteriol* 195(21), 4782-4792. doi: 10.1128/JB.00373-13.

Gasteiger, E., Hoogland, C., Gattiker, A., Duvaud, S.e., Wilkins, M.R., Appel, R.D., *et al.* (2005). *Protein identification and analysis tools on the ExPASy server*. Springer.

Gerwig, J. (2014). Control of biofilm formation in *Bacillus subtilis*. PhD thesis. Georg-August-Universität Göttingen.

Gerwig, J., Kiley, T.B., Gunka, K., Stanley-Wall, N., and Stülke, J. (2014). The protein tyrosine kinases EpsB and PtkA differentially affect biofilm formation in *Bacillus subtilis*. *Microbiology* 160(4), 682-691.

Gerwig, J., and Stülke, J. (2014). Far from being well understood: multiple protein phosphorylation events control cell differentiation in *Bacillus subtilis* at different levels. *Frontiers in Microbiology* 5(704). doi: 10.3389/fmicb.2014.00704.

Glover, K., Mei, Y., and Sinha, S.C. (2016). Identifying intrinsically disordered protein regions likely to undergo binding-induced helical transitions. *Biochimica et Biophysica Acta (BBA)-Proteins and Proteomics* 1864(10), 1455-1463.

Goldman, S.R., Sharp, J.S., Vvedenskaya, I.O., Livny, J., Dove, S.L., and Nickels, B.E. (2011). NanoRNAs prime transcription initiation *in vivo*. *Mol Cell* 42(6), 817-825. doi: 10.1016/j.molcel.2011.06.005.

Grau, R.R., de Oña, P., Kunert, M., Leñini, C., Gallegos-Monterrosa, R., Mhatre, E., *et al.* (2015). A duo of potassium-responsive histidine kinases govern the multicellular destiny of *Bacillus subtilis*. *MBio* 6(4), e00581-00515.

Guérout-Fleury, A.-M., Frandsen, N., and Stragier, P. (1996). Plasmids for ectopic integration in *Bacillus subtilis*. *Gene* 180(1), 57-61.

Guttenplan, S.B., Blair, K.M., and Kearns, D.B. (2010). The EpsE flagellar clutch is bifunctional and synergizes with EPS biosynthesis to promote *Bacillus subtilis* biofilm formation. *PLoS Genet* 6(12), e1001243.

Habazettl, J., Allan, M.G., Jenal, U., and Grzesiek, S. (2011). Solution structure of the PilZ domain protein PA4608 complex with cyclic di-GMP identifies charge clustering as molecular readout. *Journal of biological chemistry* 286(16), 14304-14314.

Halbedel, S., Kawai, M., Breitling, R., and Hamoen, L.W. (2014). SecA is required for membrane targeting of the cell division protein DivIVA *in vivo*. *Frontiers in microbiology* 5, 58.

Hamon, M.A., and Lazazzera, B.A. (2001). The sporulation transcription factor Spo0A is required for biofilm development in Bacillus subtilis. *Molecular microbiology* 42(5), 1199-1209.

Hamon, M.A., Stanley, N.R., Britton, R.A., Grossman, A.D., and Lazazzera, B.A. (2004). Identification of AbrB-regulated genes involved in biofilm formation by *Bacillus subtilis*. *Molecular microbiology* 52(3), 847-860.

Harlow, E., and Lane, D. (1988). A laboratory manual. *New York: Cold Spring Harbor Laboratory* 579.

Haussler, S., and Fuqua, C. (2013). Biofilms 2012: new discoveries and significant wrinkles in a dynamic field. *Journal of bacteriology* 195(13), 2947-2958.

Hay, I.D., Remminghorst, U., and Rehm, B.H. (2009). MucR, a novel membrane-associated regulator of alginate biosynthesis in *Pseudomonas aeruginosa*. *Applied and environmental microbiology* 75(4), 1110-1120.

Hengge, R. (2009). Principles of c-di-GMP signalling in bacteria. *Nat Rev Microbiol* 7(4), 263-273. doi: 10.1038/nrmicro2109.

Herzberg, C., Weidinger, L.A.F., Dörrbecker, B., Hübner, S., Stülke, J., and Commichau, F.M. (2007). SPINE: a method for the rapid detection and analysis of protein–protein interactions in vivo. *Proteomics* 7(22), 4032-4035.

Hickman, J.W., and Harwood, C.S. (2008). Identification of FleQ from *Pseudomonas aeruginosa* as ac-di-GMP-responsive transcription factor. *Molecular microbiology* 69(2), 376-389.

Hiltner, L.t. (1904). Über neuere Erfahrungen und Probleme auf dem Gebiete der Bodenbakteriologie unter besonderer Berücksichtigung der Gründüngung und Brache. *Arbeiten der Deutschen Landwirtschaftlichen Gesellschaft* 98, 59-78.

Hirabayashi, K., Yuda, E., Tanaka, N., Katayama, S., Iwasaki, K., Matsumoto, T., *et al.* (2015). Functional dynamics revealed by the structure of the SufBCD complex, a novel ATP-binding cassette (ABC) protein that serves as a scaffold for iron-sulfur cluster biogenesis. *Journal of Biological Chemistry* 290(50), 29717-29731.

Hobley, L., Ostrowski, A., Rao, F.V., Bromley, K.M., Porter, M., Prescott, A.R., *et al.* (2013). BslA is a self-assembling bacterial hydrophobin that coats the *Bacillus subtilis* biofilm. *Proc Natl Acad Sci U S A* 110(33), 13600-13605. doi: 10.1073/pnas.1306390110.

Høiby, N. (2014). A personal history of research on microbial biofilms and biofilm infections. *Pathogens and disease* 70(3), 205-211.

Høiby, N., Bjarnsholt, T., Givskov, M., Molin, S., and Ciofu, O. (2010). Antibiotic resistance of bacterial biofilms. *International journal of antimicrobial agents* 35(4), 322-332.

Hölscher, T., Bartels, B., Lin, Y.-C., Gallegos-Monterrosa, R., Price-Whelan, A., Kolter, R., *et al.* (2015). Motility, chemotaxis and aerotaxis contribute to competitiveness during bacterial pellicle biofilm development. *Journal of Molecular Biology* 427(23), 3695-3708.

Hubbard, C., McNamara, J.T., Azumaya, C., Patel, M.S., and Zimmer, J. (2012). The hyaluronan synthase catalyzes the synthesis and membrane translocation of hyaluronan. *Journal of molecular biology* 418(1), 21-31.

Hull, T.D., Ryu, M.-H., Sullivan, M.J., Johnson, R.C., Klena, N.T., Geiger, R.M., *et al.* (2012). Cyclic Di-GMP phosphodiesterases RmdA and RmdB are involved in regulating colony morphology and development in *Streptomyces coelicolor*. *Journal of bacteriology* 194(17), 4642-4651.

Humphries, J., Xiong, L., Liu, J., Prindle, A., Yuan, F., Arjes, H.A., *et al.* (2017). Species-Independent Attraction to Biofilms through Electrical Signaling. *Cell* 168(1), 200-209. e212.

Inoue, H., Nojima, H., and Okayama, H. (1990). High efficiency transformation of **Escherichia coli** with plasmids. *Gene* 96(1), 23-28.

Irnov, I., and Winkler, W.C. (2010). A regulatory RNA required for antitermination of biofilm and capsular polysaccharide operons in Bacillales. *Molecular microbiology* 76(3), 559-575.

Itoh, Y., Rice, J.D., Goller, C., Pannuri, A., Taylor, J., Meisner, J., *et al.* (2008). Roles of pgaABCD genes in synthesis, modification, and export of the *Escherichia coli* biofilm adhesin poly-β-1, 6-N-acetyl-D-glucosamine. *Journal of bacteriology* 190(10), 3670-3680.

Jenal, U. (2013). Think globally, act locally: How bacteria integrate local decisions with their global cellular programme. *The EMBO journal* 32(14), 1972-1974.

Jenal, U., Reinders, A., and Lori, C. (2017). Cyclic di-GMP: second messenger extraordinaire. *Nat Rev Microbiol*. doi: 10.1038/nrmicro.2016.190.

Jennings, L.K., Storek, K.M., Ledvina, H.E., Coulon, C., Marmont, L.S., Sadovskaya, I., *et al.* (2015). Pel is a cationic exopolysaccharide that cross-links extracellular DNA in the *Pseudomonas aeruginosa* biofilm matrix. *Proceedings of the National Academy of Sciences* 112(36), 11353-11358.

Johnston, E.B., Lewis, P.J., and Griffith, R. (2009). The interaction of *Bacillus subtilis* σA with RNA polymerase. *Protein Science* 18(11), 2287-2297.

Joo, H.-S., and Otto, M. (2012). Molecular basis of *in vivo* biofilm formation by bacterial pathogens. *Chemistry & biology* 19(12), 1503-1513.

Kaplan, J.á. (2010). Biofilm dispersal: mechanisms, clinical implications, and potential therapeutic uses. *Journal of dental research* 89(3), 205-218.

Kaufmann, S.H., and Schaible, U.E. (2005). 100th anniversary of Robert Koch's Nobel Prize for the discovery of the tubercle *bacillus*. *Trends in microbiology* 13(10), 469-475.

Kobayashi, K. (2007). Gradual activation of the response regulator DegU controls serial expression of genes for flagellum formation and biofilm formation in *Bacillus subtilis*. *Molecular microbiology* 66(2), 395-409.

Kobayashi, K., and Iwano, M. (2012). BslA (YuaB) forms a hydrophobic layer on the surface of *Bacillus subtilis* biofilms. *Molecular microbiology* 85(1), 51-66.

Kolodkin-Gal, I., Elsholz, A.K., Muth, C., Girguis, P.R., Kolter, R., and Losick, R. (2013). Respiration control of multicellularity in *Bacillus subtilis* by a complex of the cytochrome chain with a membrane-embedded histidine kinase. *Genes & development* 27(8), 887-899.

Konkol, M.A., Blair, K.M., and Kearns, D.B. (2013). Plasmid-encoded ComI inhibits competence in the ancestral 3610 strain of *Bacillus subtilis*. *J Bacteriol* 195(18), 4085-4093. doi: 10.1128/jb.00696-13.

Koseoglu, V.K., Heiss, C., Azadi, P., Topchiy, E., Guvener, Z.T., Lehmann, T.E., *et al.* (2015). *Listeria monocytogenes* exopolysaccharide: origin, structure, biosynthetic machinery and c-di-GMP-dependent regulation. *Mol Microbiol* 96(4), 728-743. doi: 10.1111/mmi.12966.

Kovács, Á.T. (2016). Bacterial differentiation via gradual activation of global regulators. *Current genetics* 62(1), 125-128.

Krasteva, P.V., Giglio, K.M., and Sondermann, H. (2012). Sensing the messenger: The diverse ways that bacteria signal through c-di-GMP. *Protein Science* 21(7), 929-948.

Kulasakara, H., Lee, V., Brencic, A., Liberati, N., Urbach, J., Miyata, S., *et al.* (2006). Analysis of *Pseudomonas aeruginosa* diguanylate cyclases and phosphodiesterases reveals a role for bis-(3'-5')-cyclic-GMP in virulence. *Proc Natl Acad Sci U S A* 103(8), 2839-2844. doi: 10.1073/pnas.0511090103.

Kulshina, N., Baird, N.J., and Ferré-D'Amaré, A.R. (2009). Recognition of the bacterial second messenger cyclic diguanylate by its cognate riboswitch. *Nature structural & molecular biology* 16(12), 1212-1217.

Lee, M.J., Geller, A.M., Bamford, N.C., Liu, H., Gravelat, F.N., Snarr, B.D., *et al.* (2016). Deacetylation of fungal exopolysaccharide mediates adhesion and biofilm formation. *MBio* 7(2), e00252-00216.

Lee, V.T., Matewish, J.M., Kessler, J.L., Hyodo, M., Hayakawa, Y., and Lory, S. (2007). A cyclic-di-GMP receptor required for bacterial exopolysaccharide production. *Mol Microbiol* 65(6), 1474-1484. doi: 10.1111/j.1365-2958.2007.05879.x.

Lemon, K., Earl, A., Vlamakis, H., Aguilar, C., and Kolter, R. (2008). Biofilm development with an emphasis on *Bacillus subtilis*, in *Bacterial Biofilms*. Springer, 1-16.

Lewis, P.J., and Marston, A.L. (1999). GFP vectors for controlled expression and dual labelling of protein fusions in *Bacillus subtilis*. *Gene* 227(1), 101-110.

Li, Y., Heine, S., Entian, M., Sauer, K., and Frankenberg-Dinkel, N. (2013). NO-induced biofilm dispersion in *Pseudomonas aeruginosa* is mediated by an MHYT domain-coupled phosphodiesterase. *J Bacteriol* 195(16), 3531-3542. doi: 10.1128/JB.01156-12.

Liang, Z.X. (2015). The expanding roles of c-di-GMP in the biosynthesis of exopolysaccharides and secondary metabolites. *Nat Prod Rep* 32(5), 663-683. doi: 10.1039/c4np00086b.

Limoli, D.H., Jones, C.J., and Wozniak, D.J. (2015). Bacterial extracellular polysaccharides in biofilm formation and function. *Microbiology spectrum* 3(3).

Lindenberg, S., Klauck, G., Pesavento, C., Klauck, E., and Hengge, R. (2013). The EAL domain protein YciR acts as a trigger enzyme in ac-di-GMP signalling cascade in *E. coli* biofilm control. *The EMBO journal* 32(14), 2001-2014.

Linder, J.U., and Schultz, J.E. (2003). The class III adenylyl cyclases: multi-purpose signalling modules. *Cell Signal* 15(12), 1081-1089.

Lodish, H., Berk, A., Zipursky, S.L., Matsudaira, P., Baltimore, D., and Darnell, J. (2000). Second Messengers. *Molecular cell biology*, *Scientific American Books New York,* 3

López, D., Vlamakis, H., and Kolter, R. (2010). Biofilms. *Cold Spring Harbor perspectives in biology* 2(7), a000398.

Lori, C., Ozaki, S., Steiner, S., Böhm, R., Abel, S., Dubey, B.N., *et al.* (2015). Cyclic di-GMP acts as a cell cycle oscillator to drive chromosome replication. *Nature* 523(7559), 236-239.

Lowe, P., Hodgson, J., and Perham, R. (1983). Dual role of a single multienzyme complex in the oxidative decarboxylation of pyruvate and branched-chain 2-oxo acids in *Bacillus subtilis*. *Biochemical Journal* 215(1), 133-140.

Luo, Y., and Helmann, J.D. (2012). Analysis of the role of *Bacillus subtilis* sigma(M) in beta-lactam resistance reveals an essential role for c-di-AMP in peptidoglycan homeostasis. *Mol Microbiol* 83(3), 623-639. doi: 10.1111/j.1365-2958.2011.07953.x.

Lupas, A., Van Dyke, M., and Stock, J. (1991). Predicting coiled coils from protein sequences. *Science* 252(5009), 1162.

Maharaj, R., May, T.B., Shang-Kwei, W., and Chakrabarty, A.M. (1993). Sequence of the *alg8* and *alg44* genes involved in the synthesis of alginate by *Pseudomonas aeruginosa*. *Gene* 136(1), 267-269.

Makman, R.S., and Sutherland, E.W. (1965). Adenosine 3', 5'-phosphate in Escherichia coli. *Journal of Biological Chemistry* 240(3), 1309-1314.

Mamou, G., Mohan, G.B.M., Rouvinski, A., Rosenberg, A., and Ben-Yehuda, S. (2016). Early developmental program shapes colony morphology in bacteria. *Cell reports* 14(8), 1850-1857.

Marczak, M., Dźwierzyńska, M., and Skorupska, A. (2013). Homo-and heterotypic interactions between Pss proteins involved in the exopolysaccharide transport system in *Rhizobium leguminosarum bv. trifolii*. *Biological chemistry* 394(4), 541-559.

Marlow, V.L., Porter, M., Hobley, L., Kiley, T.B., Swedlow, J.R., Davidson, F.A., *et al.* (2014). Phosphorylated DegU manipulates cell fate differentiation in the *Bacillus subtilis* biofilm. *Journal of bacteriology* 196(1), 16-27.

Marvasi, M., Visscher, P.T., and Casillas Martinez, L. (2010). Exopolymeric substances (EPS) from *Bacillus subtilis*: polymers and genes encoding their synthesis. *FEMS Microbiol Lett* 313(1), 1-9. doi: 10.1111/j.1574-6968.2010.02085.x.

Matsuyama, B.Y., Krasteva, P.V., Baraquet, C., Harwood, C.S., Sondermann, H., and Navarro, M.V. (2016). Mechanistic insights into c-di-GMP–dependent control of the biofilm regulator FleQ from *Pseudomonas aeruginosa*. *Proceedings of the National Academy of Sciences* 113(2), E209-E218.

McKew, B.A., Taylor, J.D., McGenity, T.J., and Underwood, G.J. (2011). Resistance and resilience of benthic biofilm communities from a temperate saltmarsh to desiccation and rewetting. *The ISME journal* 5(1), 30-41.

McLoon, A.L., Guttenplan, S.B., Kearns, D.B., Kolter, R., and Losick, R. (2011). Tracing the domestication of a biofilm-forming bacterium. *J Bacteriol* 193(8), 2027-2034. doi: 10.1128/jb.01542-10.

Méndez-Lorenzo, L., Porras-Domínguez, J.R., Raga-Carbajal, E., Olvera, C., Rodríguez-Alegría, M.E., Carrillo-Nava, E., *et al.* (2015). Intrinsic levanase activity of *Bacillus subtilis* 168 levansucrase (SacB). *PloS one* 10(11), e0143394.

Merritt, J.H., Ha, D.G., Cowles, K.N., Lu, W., Morales, D.K., Rabinowitz, J., *et al.* (2010). Specific control of *Pseudomonas aeruginosa* surface-associated behaviors by two c-di-GMP diguanylate cyclases. *MBio* 1(4). doi: 10.1128/mBio.00183-10.

Mielich-Süss, B., and Lopez, D. (2015). Molecular mechanisms involved in *Bacillus subtilis* biofilm formation. *Environmental microbiology* 17(3), 555-565.

Mills, E., Pultz, I.S., Kulasekara, H.D., and Miller, S.I. (2011). The bacterial second messenger c-di-GMP: mechanisms of signalling. *Cellular microbiology* 13(8), 1122-1129.

Minasov, G., Padavattan, S., Shuvalova, L., Brunzelle, J.S., Miller, D.J., Basle, A., *et al.* (2009). Crystal structures of YkuI and its complex with second messenger cyclic Di-GMP suggest catalytic mechanism of phosphodiester bond cleavage by EAL domains. *J Biol Chem* 284(19), 13174-13184. doi: 10.1074/jbc.M808221200.

Mogk, A., Homuth, G., Scholz, C., Kim, L., Schmid, F.X., and Schumann, W. (1997). The GroE chaperonin machine is a major modulator of the CIRCE heat shock regulon of *Bacillus subtilis*. *The EMBO Journal* 16(15), 4579-4590.

Molle, V., Fujita, M., Jensen, S.T., Eichenberger, P., González-Pastor, J.E., Liu, J.S., *et al.* (2003). The Spo0A regulon of Bacillus subtilis. *Molecular microbiology* 50(5), 1683-1701.

Monds, R.D., and O'Toole, G.A. (2009). The developmental model of microbial biofilms: ten years of a paradigm up for review. *Trends in microbiology* 17(2), 73-87.

Moradali, M.F., Donati, I., Sims, I.M., Ghods, S., and Rehm, B.H. (2015). Alginate polymerization and modification are linked in *Pseudomonas aeruginosa*. *MBio* 6(3), e00453-00415.

Moradali, M.F., Ghods, S., and Rehm, B.H. (2017). Activation Mechanism and Cellular Localization of Membrane-Anchored Alginate Polymerase in *Pseudomonas aeruginosa*. *Applied and Environmental Microbiology* 83(9), e03499-03416.

Morgan, J.L., McNamara, J.T., and Zimmer, J. (2014). Mechanism of activation of bacterial cellulose synthase by cyclic di-GMP. *Nat Struct Mol Biol* 21(5), 489-496. doi: 10.1038/nsmb.2803.

Morgan, J.L., Strumillo, J., and Zimmer, J. (2013). Crystallographic snapshot of cellulose synthesis and membrane translocation. *Nature* 493(7431), 181-186. doi: 10.1038/nature11744.

Morikawa, M. (2006). Beneficial biofilm formation by industrial bacteria *Bacillus subtilis* and related species. *Journal of bioscience and bioengineering* 101(1), 1-8.

Mullis, K., Faloona, F., Scharf, S., Saiki, R., Horn, G., and Erlich, H. (1986). Specific enzymatic amplification of DNA *in vitro*: the polymerase chain reaction, in: *Cold Spring Harbor symposia on quantitative biology*: Cold Spring Harbor Laboratory Press, 263-273.

Murray, E.J., Kiley, T.B., and Stanley-Wall, N.R. (2009). A pivotal role for the response regulator DegU in controlling multicellular behaviour. *Microbiology* 155(1), 1-8.

Navarro, M.V., De, N., Bae, N., Wang, Q., and Sondermann, H. (2009). Structural analysis of the GGDEF-EAL domain-containing c-di-GMP receptor FimX. *Structure* 17(8), 1104-1116.

Nelson, J.W., Sudarsan, N., Phillips, G.E., Stav, S., Lunse, C.E., McCown, P.J., et al. (2015). Control of bacterial exoelectrogenesis by c-AMP-GMP. *Proc Natl Acad Sci U S A* 112(17), 5389-5394. doi: 10.1073/pnas.1419264112.

Newell, P.D., Monds, R.D., and O'Toole, G.A. (2009). LapD is a bis-(3', 5')-cyclic dimeric GMP-binding protein that regulates surface attachment by *Pseudomonas fluorescens* Pf0–1. *Proceedings of the National Academy of Sciences* 106(9), 3461-3466.

Newman, J.A., Rodrigues, C., and Lewis, R.J. (2013). Molecular basis of the activity of SinR protein, the master regulator of biofilm formation in *Bacillus subtilis*. *Journal of Biological Chemistry* 288(15), 10766-10778.

Nicolas, P., Mader, U., Dervyn, E., Rochat, T., Leduc, A., Pigeonneau, N., *et al.* (2012). Condition-dependent transcriptome reveals high-level regulatory architecture in *Bacillus subtilis*. *Science* 335(6072), 1103-1106. doi: 10.1126/science.1206848.

Norman, T.M., Lord, N.D., Paulsson, J., and Losick, R. (2013). Memory and modularity in cell-fate decision making. *Nature* 503(7477), 481-486.

Nwodo, U.U., Green, E., and Okoh, A.I. (2012). Bacterial exopolysaccharides: functionality and prospects. *International journal of molecular sciences* 13(11), 14002-14015.

Ohlsen, K.L., Grimsley, J.K., and Hoch, J.A. (1994). Deactivation of the sporulation transcription factor Spo0A by the Spo0E protein phosphatase. *Proceedings of the National Academy of Sciences* 91(5)**,** 1756-1760.

Omoike, A., and Chorover, J. (2004). Spectroscopic study of extracellular polymeric substances from *Bacillus subtilis*: Aqueous chemistry and adsorption effects. *Biomacromolecules* 5(4)**,** 1219-1230.

Orr, M.W., Donaldson, G.P., Severin, G.B., Wang, J., Sintim, H.O., Waters, C.M., *et al.* (2015). Oligoribonuclease is the primary degradative enzyme for pGpG in *Pseudomonas aeruginosa* that is required for cyclic-di-GMP turnover. *Proc Natl Acad Sci U S A* 112(36)**,** E5048-5057. doi: 10.1073/pnas.1507245112.

Ostrowski, A., Mehert, A., Prescott, A., Kiley, T.B., and Stanley-Wall, N.R. (2011). YuaB functions synergistically with the exopolysaccharide and TasA amyloid fibers to allow biofilm formation by *Bacillus subtilis*. *Journal of bacteriology* 193(18)**,** 4821-4831.

Ozaki, S., Schalch-Moser, A., Zumthor, L., Manfredi, P., Ebbensgaard, A., Schirmer, T., *et al.* (2014). Activation and polar sequestration of PopA, ac-di-GMP effector protein involved in *Caulobacter crescentus* cell cycle control. *Molecular microbiology* 94(3)**,** 580-594.

Patrick, J.E., and Kearns, D.B. (2009). Laboratory strains of *Bacillus subtilis* do not exhibit swarming motility. *Journal of bacteriology* 191(22)**,** 7129-7133.

Paul, E., and Clark, F. (1989). Transformation of nitrogen between the organic and inorganic phase and to nitrate. *Soil microbiology and biochemistry. Academic Press, San Diego, CA. USA***,** 131-146.

Paul, K., Nieto, V., Carlquist, W.C., Blair, D.F., and Harshey, R.M. (2010). The c-di-GMP binding protein YcgR controls flagellar motor direction and speed to affect chemotaxis by a "backstop brake" mechanism. *Molecular cell* 38(1)**,** 128-139.

Paul, R., Abel, S., Wassmann, P., Beck, A., Heerklotz, H., and Jenal, U. (2007). Activation of the diguanylate cyclase PleD by phosphorylation-mediated dimerization. *Journal of biological chemistry* 282(40)**,** 29170-29177.

Perego, M., Glaser, P., and Hoch, J.A. (1996). Aspartyl-phosphate phosphatases deactivate the response regulator components of the sporulation signal transduction system in Bacillus subtilis. *Molecular microbiology* 19(6)**,** 1151-1157.

Pérez-Mendoza, D., and Sanjuán, J. (2016). Exploiting the commons: cyclic diguanylate regulation of bacterial exopolysaccharide production. *Current opinion in microbiology* 30**,** 36-43.

Petersohn, A., Bernhardt, J., Gerth, U., Höper, D., Koburger, T., Völker, U., *et al.* (1999). Identification of σB-dependent genes in *Bacillus subtilis* using a promoter consensus-directed search and oligonucleotide hybridization. *Journal of bacteriology* 181(18)**,** 5718-5724.

Pokrovskaya, V., Poloczek, J., Little, D.J., Griffiths, H., Howell, P.L., and Nitz, M. (2013). Functional characterization of *Staphylococcus epidermidis* IcaB, a de-N-acetylase important for biofilm formation. *Biochemistry* 52(32)**,** 5463-5471.

Pratt, J.T., Tamayo, R., Tischler, A.D., and Camilli, A. (2007). PilZ domain proteins bind cyclic diguanylate and regulate diverse processes in *Vibrio cholerae*. *J Biol Chem* 282(17)**,** 12860-12870. doi: 10.1074/jbc.M611593200.

Pultz, I.S., Christen, M., Kulasekara, H.D., Kennard, A., Kulasekara, B., and Miller, S.I. (2012). The response threshold of Salmonella PilZ domain proteins is determined by their binding affinities for c-di-GMP. *Molecular microbiology* 86(6)**,** 1424-1440.

Rall, T.W., and Sutherland, E.W. (1958). Formation of a cyclic adenine ribonucleotide by tissue particles. *J Biol Chem* 232(2)**,** 1065-1076.

Rao, F., Qi, Y., Chong, H.S., Kotaka, M., Li, B., Li, J., *et al.* (2009). The functional role of a conserved loop in EAL domain-based cyclic di-GMP-specific phosphodiesterase. *Journal of bacteriology* 191(15)**,** 4722-4731.

Reichhardt, C., McCrate, O.A., Zhou, X., Lee, J., Thongsomboon, W., and Cegelski, L. (2016). Influence of the amyloid dye Congo red on curli, cellulose, and the extracellular matrix in *E. coli* during growth and matrix purification. *Analytical and bioanalytical chemistry* 408(27)**,** 7709-7717.

Reinders, A., Hee, C.-S., Ozaki, S., Mazur, A., Boehm, A., Schirmer, T., *et al.* (2016). Expression and genetic activation of cyclic di-GMP-specific phosphodiesterases in *Escherichia coli*. *Journal of bacteriology* 198(3)**,** 448-462.

Remminghorst, U., and Rehm, B.H. (2006). Bacterial alginates: from biosynthesis to applications. *Biotechnology letters* 28(21)**,** 1701-1712.

Richter, A. (2016). c-di-GMP-abhängige Signal-transduktion bei der Kontrolle der Cellulose-Synthese in *Escherichia coli* Biofilmen. PhD thesis. Humboldt-Universität zu Berlin, Lebenswissenschaftliche Fakultät.

Richter, A.M., Povolotsky, T.L., Wieler, L.H., and Hengge, R. (2014). Cyclic-di-GMP signalling and biofilm-related properties of the Shiga toxin-producing 2011 German outbreak *Escherichia coli* O104: H4. *EMBO molecular medicine***,** e201404309.

Robledo, M., Rivera, L., Jiménez-Zurdo, J.I., Rivas, R., Dazzo, F., Velázquez, E., *et al.* (2012). Role of *Rhizobium* endoglucanase CelC2 in cellulose biosynthesis and biofilm formation on plant roots and abiotic surfaces. *Microbial cell factories* 11(1)**,** 125.

Romero, D., Aguilar, C., Losick, R., and Kolter, R. (2010). Amyloid fibers provide structural integrity to *Bacillus subtilis* biofilms. *Proc Natl Acad Sci U S A* 107(5)**,** 2230-2234. doi: 10.1073/pnas.0910560107.

Romero, D., and Kolter, R. (2014). Functional amyloids in bacteria. *International Microbiology* 17(2)**,** 65-73.

Römling, U., and Galperin, M.Y. (2015). Bacterial cellulose biosynthesis: diversity of operons, subunits, products, and functions. *Trends in microbiology* 23(9), 545-557.

Romling, U., Galperin, M.Y., and Gomelsky, M. (2013). Cyclic di-GMP: the first 25 years of a universal bacterial second messenger. *Microbiol Mol Biol Rev* 77(1), 1-52. doi: 10.1128/MMBR.00043-12.

Ross, P., Mayer, R., and Benziman, M. (1991). Cellulose biosynthesis and function in bacteria. *Microbiol Rev* 55(1), 35-58.

Ross, P., Weinhouse, H., Aloni, Y., Michaeli, D., Weinberger-Ohana, P., Mayer, R., *et al.* (1987). Regulation of cellulose synthesis in *Acetobacter xylinum* by cyclic diguanylic acid. *Nature* 325(6101), 279-281.

Roux, D., Cywes-Bentley, C., Zhang, Y.F., Pons, S., Konkol, M., Kearns, D.B., *et al.* (2015). Identification of Poly-N-acetylglucosamine as a Major Polysaccharide Component of the *Bacillus subtilis* Biofilm Matrix. *J Biol Chem* 290(31), 19261-19272. doi: 10.1074/jbc.M115.648709.

Rubinstein, S.M., Kolodkin-Gal, I., Mcloon, A., Chai, L., Kolter, R., Losick, R., *et al.* (2012). Osmotic pressure can regulate matrix gene expression in *Bacillus subtilis*. *Molecular microbiology* 86(2), 426-436.

Ryan, R.P., McCarthy, Y., Andrade, M., Farah, C.S., Armitage, J.P., and Dow, J.M. (2010). Cell-cell signal-dependent dynamic interactions between HD-GYP and GGDEF domain proteins mediate virulence in *Xanthomonas campestris*. *Proc Natl Acad Sci U S A* 107(13), 5989-5994. doi: 10.1073/pnas.0912839107.

Ryjenkov, D.A., Simm, R., Römling, U., and Gomelsky, M. (2006). The PilZ domain is a receptor for the second messenger c-di-GMP: The PilZ domain protein Ycgr controls motility in enterobacteria. *Journal of Biological Chemistry* 281(41), 30310-30314.

Sambrook, J., Fritsch, E.F., and Maniatis, T. (1989). Molecular cloning: a laboratory manual. Cold spring harbor laboratory press.

Sauer, K., Rickard, A.H., and Davies, D.G. (2007). Biofilms and biocomplexity. *Microbe-American Society for Microbiology* 2(7), 347.

Schirmer, T. (2016). C-di-GMP Synthesis: Structural Aspects of Evolution, Catalysis and Regulation. *Journal of molecular biology* 428(19), 3683-3701.

Schmid, J., Sieber, V., and Rehm, B. (2015). Bacterial exopolysaccharides: biosynthesis pathways and engineering strategies. *Front Microbiol* 6, 496. doi: 10.3389/fmicb.2015.00496.

Schmidt, A., Hammerbacher, A.S., Bastian, M., Nieken, K.J., Klockgether, J., Merighi, M., *et al.* (2016). Oxygen-dependent regulation of c-di-GMP synthesis by SadC controls alginate production in *Pseudomonas aeruginosa*. *Environmental microbiology*.

Schroeder, J.W., and Simmons, L.A. (2013). Complete genome sequence of *Bacillus subtilis* strain PY79. *Genome announcements* 1(6), e01085-01013.

Serra, D.O., Richter, A.M., and Hengge, R. (2013). Cellulose as an architectural element in spatially structured *Escherichia coli* biofilms. *J Bacteriol* 195(24), 5540-5554. doi: 10.1128/Jb.00946-13.

Seshasayee, A.S., Fraser, G.M., and Luscombe, N.M. (2010). Comparative genomics of cyclic-di-GMP signalling in bacteria: post-translational regulation and catalytic activity. *Nucleic acids research* 38(18), 5970-5981.

Shemesh, M., and Chai, Y. (2013). A combination of glycerol and manganese promotes biofilm formation in *Bacillus subtilis* via histidine kinase KinD signaling. *Journal of bacteriology* 195(12), 2747-2754.

Shimotsu, H., and Henner, D.J. (1986). Modulation of *Bacillus subtilis* levansucrase gene expression by sucrose and regulation of the steady-state mRNA level by *sacU* and *sacQ* genes. *Journal of bacteriology* 168(1), 380-388.

Shin, J.S., Ryu, K.S., Ko, J., Lee, A., and Choi, B.S. (2011). Structural characterization reveals that a PilZ domain protein undergoes substantial conformational change upon binding to cyclic dimeric guanosine monophosphate. *Protein Sci* 20(2), 270-277.

Simm, R., Morr, M., Kader, A., Nimtz, M., and Römling, U. (2004). GGDEF and EAL domains inversely regulate cyclic di-GMP levels and transition from sessility to motility. *Molecular microbiology* 53(4), 1123-1134.

Solano, C., García, B., Valle, J., Berasain, C., Ghigo, J.M., Gamazo, C., *et al.* (2002). Genetic analysis of *Salmonella enteritidis* biofilm formation: critical role of cellulose. *Molecular microbiology* 43(3), 793-808.

Sommerfeldt, N., Possling, A., Becker, G., Pesavento, C., Tschowri, N., and Hengge, R. (2009). Gene expression patterns and differential input into curli fimbriae regulation of all GGDEF/EAL domain proteins in *Escherichia coli*. *Microbiology* 155(4), 1318-1331.

Stanley, N.R., and Lazazzera, B.A. (2005). Defining the genetic differences between wild and domestic strains of *Bacillus subtilis* that affect poly-γ-DL-glutamic acid production and biofilm formation. *Molecular microbiology* 57(4), 1143-1158.

Steinmetz, M., and Richter, R. (1994). Plasmids designed to alter the antibiotic resistance expressed by insertion mutations in *Bacillus subtilis*, through *in vivo* recombination. *Gene* 142(1), 79-83.

Stoodley, P., Sauer, K., Davies, D., and Costerton, J.W. (2002). Biofilms as complex differentiated communities. *Annual Reviews in Microbiology* 56(1), 187-209.

Stöver, A.G., and Driks, A. (1999a). Regulation of synthesis of the Bacillus subtilis transition-phase, spore-associated antibacterial protein TasA. *Journal of bacteriology* 181(17), 5476-5481.

Stöver, A.G., and Driks, A. (1999b). Secretion, localization, and antibacterial activity of TasA, a *Bacillus subtilis* spore-associated protein. *Journal of bacteriology* 181(5), 1664-1672.

Suchanek, V.M. (2016). Role of Motility and its Regulation in *Escherichia coli* Biofilm formation. PhD thesis. University Heidelberg.

Sudarsan, N., Lee, E., Weinberg, Z., Moy, R., Kim, J., Link, K., et al. (2008). Riboswitches in eubacteria sense the second messenger cyclic di-GMP. *Science* 321(5887), 411-413.

Sutherland, E.W., and Rall, T.W. (1958). Fractionation and characterization of a cyclic adenine ribonucleotide formed by tissue particles. *Journal of Biological Chemistry* 232(2), 1077-1092.

Tamayo, R. (2013). The characterization of a cyclic-di-GMP (c-di-GMP) pathway leads to a new tool for studying c-di-GMP metabolic genes. *Journal of bacteriology* 195(21), 4779-4781.

Tarutina, M., Ryjenkov, D.A., and Gomelsky, M. (2006). An unorthodox bacteriophytochrome from *Rhodobacter sphaeroides* involved in turnover of the second messenger c-di-GMP. *Journal of Biological Chemistry* 281(46), 34751-34758.

Tischler, A.D., and Camilli, A. (2004). Cyclic diguanylate (c-di-GMP) regulates *Vibrio cholerae* biofilm formation. *Mol Microbiol* 53(3), 857-869. doi: 10.1111/j.1365-2958.2004.04155.x.

Tschowri, N., Schumacher, M.A., Schlimpert, S., babu Chinnam, N., Findlay, K.C., Brennan, R.G., et al. (2014). Tetrameric c-di-GMP mediates effective transcription factor dimerization to control *Streptomyces* development. *Cell* 158(5), 1136-1147.

Ullmann, A., and Monod, J. (1968). Cyclic AMP as an antagonist of catabolite repression in *Escherichia coli*. *FEBS letters* 2(1), 57-60.

Vain, T., Crowell, E.F., Timpano, H., Biot, E., Desprez, T., Mansoori, N., et al. (2014). The cellulase KORRIGAN is part of the cellulose synthase complex. *Plant physiology* 165(4), 1521-1532.

Valentini, M., and Filloux, A. (2016). Biofilms and cyclic di-GMP (c-di-GMP) signaling: lessons from *Pseudomonas aeruginosa* and other bacteria. *Journal of Biological Chemistry* 291(24), 12547-12555.

Valentini, M., Laventie, B.-J., Moscoso, J., Jenal, U., and Filloux, A. (2016). The Diguanylate Cyclase HsbD Intersects with the HptB Regulatory Cascade to Control *Pseudomonas aeruginosa* Biofilm and Motility. *PLoS Genet* 12(10), e1006354.

Verhamme, D.T., Kiley, T.B., and Stanley-Wall, N.R. (2007). DegU co-ordinates multicellular behaviour exhibited by *Bacillus subtilis*. *Molecular microbiology* 65(2), 554-568.

Vlamakis, H., Aguilar, C., Losick, R., and Kolter, R. (2008). Control of cell fate by the formation of an architecturally complex bacterial community. *Genes & development* 22(7), 945-953.

Vlamakis, H., Chai, Y., Beauregard, P., Losick, R., and Kolter, R. (2013). Sticking together: building a biofilm the *Bacillus subtilis* way. *Nat Rev Microbiol* 11(3), 157-168. doi: 10.1038/nrmicro2960.

Vuong, C., Voyich, J.M., Fischer, E.R., Braughton, K.R., Whitney, A.R., DeLeo, F.R., et al. (2004). Polysaccharide intercellular adhesin (PIA) protects *Staphylococcus epidermidis* against major components of the human innate immune system. *Cellular microbiology* 6(3), 269-275.

Wang, Y., Hay, I.D., Rehman, Z.U., and Rehm, B.H. (2015). Membrane-anchored MucR mediates nitrate-dependent regulation of alginate production in *Pseudomonas aeruginosa*. *Applied microbiology and biotechnology* 99(17), 7253-7265.

Wassmann, P., Chan, C., Paul, R., Beck, A., Heerklotz, H., Jenal, U., *et al.* (2007). Structure of BeF 3−-modified response regulator PleD: implications for diguanylate cyclase activation, catalysis, and feedback inhibition. *Structure* 15(8), 915-927.

Watnick, P., and Kolter, R. (2000). Biofilm, city of microbes. *Journal of bacteriology* 182(10), 2675-2679.

Weber, H., Pesavento, C., Possling, A., Tischendorf, G., and Hengge, R. (2006). Cyclic-di-GMP-mediated signalling within the sigma network of *Escherichia coli*. *Mol Microbiol* 62(4), 1014-1034. doi: 10.1111/j.1365-2958.2006.05440.x.

Weinrauch, Y., Guillen, N., and Dubnau, D. (1989). Sequence and transcription mapping of *Bacillus subtilis* competence genes *comB* and *comA*, one of which is related to a family of bacterial regulatory determinants. *Journal of bacteriology* 171(10), 5362-5375.

Wessel, J., Chu, A.Y., Willems, S.M., Wang, S., Yaghootkar, H., Brody, J.A., et al. (2015). Low-frequency and rare exome chip variants associate with fasting glucose and type 2 diabetes susceptibility. *Nat Commun* 6, 5897. doi: 10.1038/ncomms6897.

West, R.W., McConnell, D., and Rodriguez, R.L. (1980). Isolation of *E. coli* promoters from the late region of bacteriophage T7 DNA. *Molecular and General Genetics MGG* 180(2), 439-447.

Whitney, J.C., Colvin, K.M., Marmont, L.S., Robinson, H., Parsek, M.R., and Howell, P.L. (2012). Structure of the cytoplasmic region of PelD, a degenerate diguanylate cyclase receptor that regulates exopolysaccharide production in *Pseudomonas aeruginosa*. *Journal of Biological Chemistry* 287(28), 23582-23593.

Whitney, J.C., and Howell, P.L. (2013). Synthase-dependent exopolysaccharide secretion in Gram-negative bacteria. *Trends Microbiol* 21(2), 63-72. doi: 10.1016/j.tim.2012.10.001.

Wilking, J.N., Zaburdaev, V., De Volder, M., Losick, R., Brenner, M.P., and Weitz, D.A. (2013). Liquid transport facilitated by channels in *Bacillus subtilis* biofilms. *Proceedings of the National Academy of Sciences* 110(3), 848-852.

Williams, S. (1985). Oligotrophy in soil: Fact or fiction? Special Publications of the Society for General Microbiology (SPEC. PUBL. SOC. GEN. MICROBIOL.). 1985.

Willis, L.M., and Whitfield, C. (2013). Structure, biosynthesis, and function of bacterial capsular polysaccharides synthesized by ABC transporter-dependent pathways. *Carbohydrate research* 378**,** 35-44.

Wolfe, A.J., and Visick, K.L. (2010). The second messenger cyclic di-GMP. American Society for Microbiology Press.

Wolska, K.I., Grudniak, A.M., Rudnicka, Z., and Markowska, K. (2016). Genetic control of bacterial biofilms. *Journal of applied genetics* 57(2)**,** 225-238.

Xu, L., Venkataramani, P., Ding, Y., Liu, Y., Deng, Y., Yong, G.L., et al. (2016). A cyclic di-GMP-binding adaptor protein interacts with histidine kinase to regulate two-component signaling. *Journal of Biological Chemistry* 291(31)**,** 16112-16123.

York, L.M., Carminati, A., Mooney, S.J., Ritz, K., and Bennett, M.J. (2016). The holistic rhizosphere: integrating zones, processes, and semantics in the soil influenced by roots. *Journal of experimental botany***,** erw108.

Youngman, P., Perkins, J.B., and Losick, R. (1984). A novel method for the rapid cloning in *Escherichia coli* of *Bacillus subtilis* chromosomal DNA adjacent to Tn917 insertions. *Mol Gen Genet* 195(3)**,** 424-433.

Zaccolo, M., Di Benedetto, G., Lissandron, V., Mancuso, L., Terrin, A., and Zamparo, I. (2006). Restricted diffusion of a freely diffusible second messenger: mechanisms underlying compartmentalized cAMP signalling. Portland Press Limited.

Zafra, O., Lamprecht-Grandio, M., de Figueras, C.G., and Gonzalez-Pastor, J.E. (2012). Extracellular DNA release by undomesticated *Bacillus subtilis* is regulated by early competence. *PLoS One* 7(11)**,** e48716. doi: 10.1371/journal.pone.0048716.

Zhang, C., Li, B., Huang, X., Ni, Y., and Feng, X.-Q. (2016). Morphomechanics of bacterial biofilms undergoing anisotropic differential growth. *Applied Physics Letters* 109(14)**,** 143701.

7 ABBREVIATIONS

3-D	three-dimensional
aa	amino acid
AC	adenylate cyclase
ADP	adenosine diphosphate
Alg	alginate
amp	ampicillin
A-site	active site
ATP	adenosine triphosphate
Au	absorption unit
BF	biofilm
BLAST	basic local alignment search tool
Bp	base pair
BSA	bovine serum albumin
cAMP	cyclic adenosine monophosphate
cat/ cm	chloramphenicol
c-di-AMP	cyclic dimeric adenosine monophosphate
c-di-GMP	cyclic dimeric guanosine monophosphate
CFP	cyan fluorescent protein
cGMP	cyclic guanosine monophosphate
CSLM	confocal scanning laser microscopy
Da	Dalton
DGC	diguanylate cyclase
DSM	Difco sporulation medium
ECM	extracellular matrix
EPS	exopolysaccharide
GAF	domain found in cGMP-specific phosphodiesterases, adenylyl cyclases and FhlA
GMP	guanosine monophosphate
GST	glutathione S-transferase
GTP	guanosine triphosphate
h	hours
IPTG	isopropyl β-D-1-thiogalactopyranoside
kan	kanamycin
LB	lysogeny broth
MCPs	methyl-accepting chemotaxis proteins
MCS	multiple cloning site
min	minute
MS	mass spectrometry
ms	millisecond

NA	numeric aperature
NDP	nucleoside diphosphate
NMP	nucleoside monophosphate
NTA	nitrilotiracetic acid
OD	optical density
ORF	open reading frame
PAS	protein domain named after the proteins Per/Arnt/Sim
PBS	phosphate-buffered saline
PCR	polymerase chain reaction
PDE	(c-di-GMP-specific) phosphodiesterase
PEG	polyethylene glycol
PGA	poly-γ-glutamic acid
pGpG	5′-phosphoguanylyl-(3′,5′)-guanosine
psi	pound per square inch (pressure)
rdar	for red, dry and rough
rpm	revolutions per minute
RT	room temperature
SDS-PAGE	Sodium dodecylsulfate polyacrylamide gel electrophoresis
sec	second
SEC	size exclusion chromatography
SEM	scanning electron microscopy
TIRFM	Total internal reflection fluorescence microscopy
TM	trans membrane
TMH	trans membrane helix
TMR	trans membrane receptor
wt	wild type
xyl	xylose
YFP	yellow fluorescent protein

8 APPENDIX

A8.1 Movies

Movie S1: Fluorescence microscopy of *B. subtilis* NCIB3610 producing YdaK-mV-YFP

Movie S2: Exponential *B. subtilis* NCIB3610 producing DgcK-mV-YFP

Movie S3: Exponential *B. subtilis* NCIB3610 expressing *mV-yfp-dgcP*

Movie S4: Exponential *B. subtilis* NCIB3610 expressing *dgcP-mV-yfp*

Time intervals: 100 ms upon continuous illumination with 515 nm

Scale bars: 2 μm

All movies are played at 15 fps (frames per second) and are provided on the attached DVD.

A8.2 Mass spectrometry

Mass spectrometry-based identification of proteins was performed by the SYNMIKRO Mass Spectrometric Core Facility, Marburg (Dept. of Chemistry). Data analysis was performed using Proteome Discoverer (ThermoScientific) with SEQUEST and MASCOT (version 2.2; Matrix science). Original data sets are provided as Excel files on the attached DVD.

A8.3 Purification of His_6-DgcP

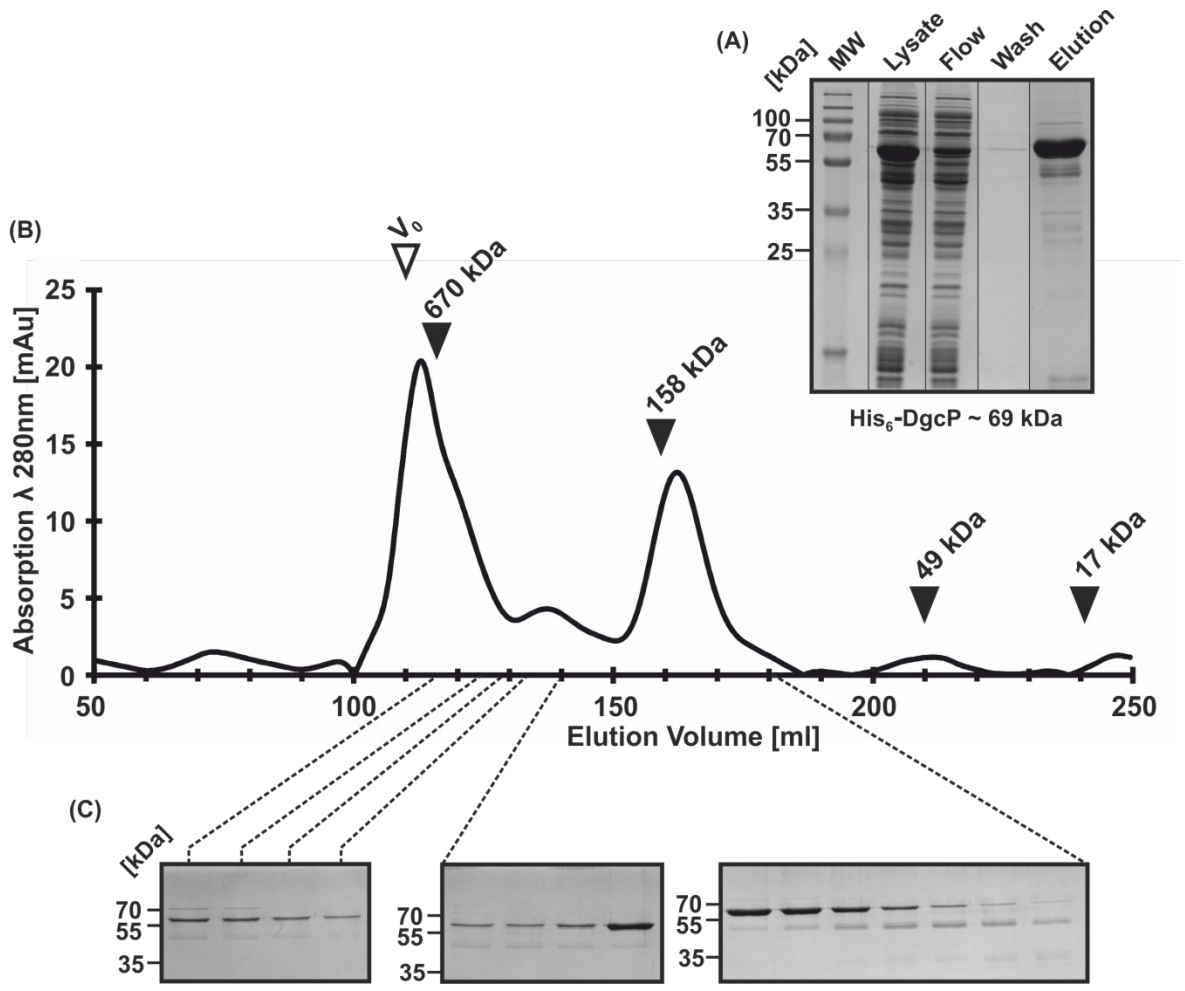

Fig. A8.3 Tandem purification of recombinant His_6-DgcP via IMAC and SEC
(A) Coomassie-stained SDS-PAGE of samples obtained during Ni-NTA affinity purification of -His_6-DgcP from soluble *E. coli* BL21 (DE3) cell extracts. MW: molecular weight standard. (**B**) Size exclusion chromatography of the elution fraction obtained by affinity chromatography and (**C**) visualization of purified His_6-DgcP via SDS-PAGE and Coomassie-staining. Black triangles indicate positions of standard proteins with different molecular weights, separated on the same column. The exclusion volume of the column is marked with a white triangle. His_6-DgcP eluted in a similar manner as observed for DgcP-Strep (section **3.2.2**).

A8.4 Disorder Prediction MetaServer Results for DgcP

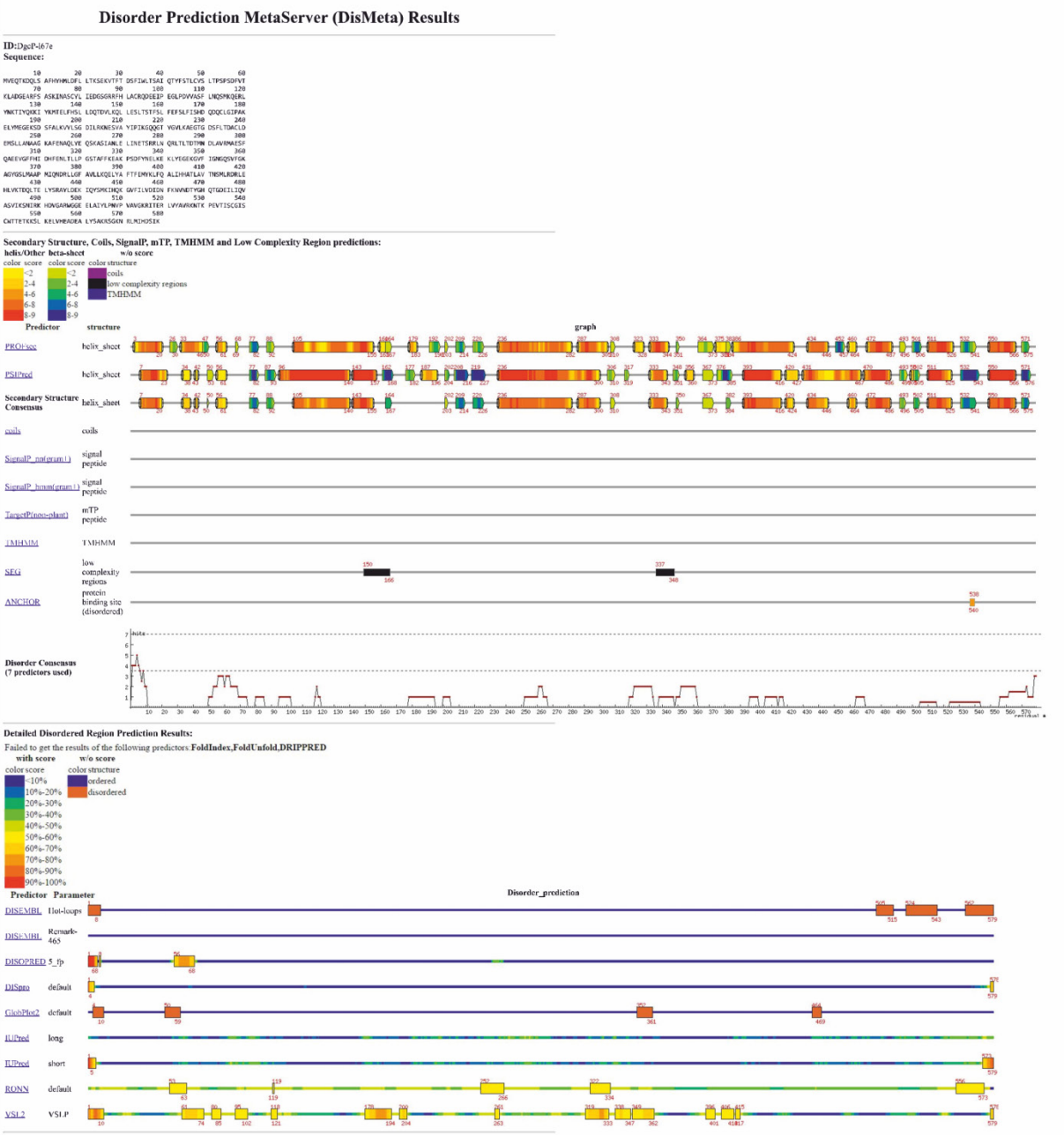

A8.5 List of oligonucleotides

A8.6 List of plasmids

A8.7 List of strains

Lists are provided as MS word files on the attached DVD.

CURRICULUM VITAE

Patricia Bedrunka
Date of birth: March 9th, 1986
Place of birth: Kłodzko (Glatz, Polen)

Oct 2012 - Jun 2017	Philipps-Universität-Marburg PhD thesis in Biology/ Microbiology under the supervision of Prof. Peter L. Graumann Titel: "The role of the second messenger cyclic di-GMP in *Bacillus subtilis*" LOEWE-Zentrum für Synthetische Mikrobiologie and Department of Chemistry
Feb 2012 - Sept 2012	Ruhr-Universität-Bochum Scientific assistant Department: Microbial Biology Supervisor: Prof. Dr. Nicole Frankenberg-Dinkel
Oct 2006 - Sept 2011	Studies in Biology, Ruhr-Universität-Bochum
2009 - 2011	Master of Science Thesis: „Untersuchungen zum sekundären Botenstoff c-di-GMP in *Dinoroseobacter shibae* DFL12^T" Department: Microbial Biology Supervisor: Prof. Dr. Nicole Frankenberg-Dinkel
2006 - 2009	Bachelor of Science Thesis: „Untersuchungen zur Oligomerisierung von Lipoxygenase 2, Allenoxid-Synthase und Allenoxid-Cyclase aus *A. thaliana* (L.) HEYNH " Department: Plant Physiology Supervisor: Dr. Stephan Pollmann
Jun 2006	Abitur, Anne-Frank-Gymnasium, Werne a. d. Lippe

ACKNOWLEDGMENTS

balanced

[redacted]
[redacted]
[redacted]
[redacted]
[redacted] ob nah oder fern
[redacted]